INDEX NO. : 95/19/E

MODELING AND ANALYSIS OF CARDIOVASCULAR SIGNALS

Thesis

Submitted by

Anumita Mitra

Doctor of Philosophy (Engineering)

Department of Electrical Engineering

Faculty Council of Engineering & Technology

Jadavpur University

Kolkata, India

2025

INDEX NO. : 95/19/E

1. **Title of the thesis: MODELING AND ANALYSIS OF CARDIOVASCULAR SIGNALS**

2. **Name, Designation**: **(a) Dr. Palash Kumar Kundu**
   Institution of Supervisors
   Professor
   Department of Electrical Engineering
   Jadavpur University, Kolkata-700032, India

   (b) Dr. Gautam Sarkar
   Professor
   Department of Electrical Engineering
   Jadavpur University, Kolkata-700032, India

3. List of Publication :

Journal Publication:

1) Anumita Mitra, Palash Kumar Kundu, Rajarshi Gupta, Jayanta Saha, & A. Talukdar, "CardioSim: a PC-based cardiac signal simulator using segmental modeling of electrocardiogram", Computer Methods in Biomechanics and Biomedical Engineering, 26(13), pg.1532–1548., 2022.

Conference Publications:

1) Anumita Mitra, Palash Kumar Kundu, Rajarshi Gupta, "Segment Specific Modeling of Electrocardiogram for Improved Reconstruction Error," 2020 IEEE Applied Signal Processing Conference (ASPCON), Kolkata, India, 2020, pp. 16-20.
2) Anumita Mitra, Palash Kumar Kundu, Rajarshi Gupta, "Hyperparameter Optimization of AutoRegressive Integrated Moving Average (ARIMA) Model-based Synthesis of Electrocardiogram," 2022 International Conference for Advancement in Technology (ICONAT), Goa, India, 2022, pp. 1-6.
3) Anumita Mitra and Palash Kumar Kundu, "Deep Learning-based Multiclass ECG Classification with Error-controlled ARIMA Model," *2024 IEEE Calcutta Conference (CALCON)*, Kolkata, India, 2024, pp. 1-5, doi: 10.1109/CALCON63337.2024.10914057.

4. List of Patents : NIL

5. List of Presentations in National/International/Conferences/Workshops :

1) Anumita Mitra, Palash Kumar Kundu, Rajarshi Gupta, "Segment Specific Modeling of Electrocardiogram for Improved Reconstruction Error," 2020 IEEE Applied Signal Processing Conference (ASPCON), Kolkata, India, 2020, pp. 16-20.
2) Anumita Mitra, Palash Kumar Kundu, Rajarshi Gupta, "Hyperparameter Optimization of AutoRegressive Integrated Moving Average (ARIMA) Model-based Synthesis of Electrocardiogram," 2022 International Conference for Advancement in Technology (ICONAT), Goa, India, 2022, pp. 1-6.
3) Anumita Mitra and Palash Kumar Kundu, "Deep Learning-based Multiclass ECG Classification with Error-controlled ARIMA Model," *2024 IEEE Calcutta Conference (CALCON)*, Kolkata, India, 2024, pp. 1-5, doi: 10.1109/CALCON63337.2024.10914057.

6. Communicated Journal

1) "Deep Learning based Approach for Lossless ECG Compression", to Cardiovascular Engineering and Technology.

Statement of Originality

I Anumita Mitra registered on 3rd June, 2019 do hereby declare that this thesis entitled "MODELING AND ANALYSIS OF CARDIOVASCULAR SIGNALS" contains literature survey and original research work done by the undersigned candidate as part of Doctoral studies.

All information in this thesis have been obtained and presented in accordance with existing academic rules and ethical conduct. I declare that, as required by these rules and conduct, I have fully cited and referred all materials and results that are not original to this work.

I also declare that I have checked this thesis as per the "Policy on Anti Plagiarism, Jadavpur University, 2019", and the level of similarity as checked by iThenticate software is 04 (four)%.

Anumita Mitra.

Signature of Candidate:

Date: 10.12.2025

Certified by Supervisor(s):
(Signature with date, seal)

1. 10/12/2025

Professor
Electrical Engg. Deptt.
Jadavpur University
Kolkata - 700 032

2.

Professor
Electrical Engg. Deptt.
Jadavpur University
Kolkata - 700 032

CERTIFICATE OF SUPERVISORS

This is to certify that the thesis entitled "MODELING AND ANALYSIS OF CARDIOVASCULAR SIGNALS" submitted by Smt. Anumita Mitra, who got her name registered on 3rd June 2019 for the award of Ph.D. (Engineering) degree of Jadavpur University is absolutely based upon her own work under the supervision of Dr. Palash Kumar Kundu and Dr. Gautam Sarkar and that neither her thesis nor any part of the thesis has been submitted for any degree / diploma or any other academic award anywhere before.

1.....

Signature of the Supervisor
and date with office seal

10/12/2025

Professor
Electrical Engg. Deptt.
Jadavpur University
Kolkata - 700 032

2.....

Signature of the Supervisor
and date with office seal

Professor
Electrical Engg. Deptt.
Jadavpur University
Kolkata - 700 032

ACKNOWLEDGEMENT

First and foremost, I am extremely grateful to my supervisors, Dr. Palash Kumar Kundu and Dr. Gautam Sarkar (Professor Electrical Engineering Department, Jadavpur University) for their invaluable advice, continuous support, and patience during my PhD study. Their immense knowledge and plentiful experience have encouraged me in all the time of my academic research. Without their invaluable guidance, this work would never have been a successful one. This work is a result of their encouragement, support, ideas, and constructive criticism.

I would like to thank Dr. Rajarshi Gupta, Professor, Applied Physics Department, University of Calcutta, India, for the support received from him to carry out this research work.

I express my sincere gratitude to my parents Mr. Samir Kumar Mitra and Mrs. Snigdha Mitra for their continuous encouragement, tireless motivation and taking enormous pains during my tenure of work. Without them, nothing would have been possible. I would especially thanks to my husband Mr. Surajit Sen and my loving son Sheyank Mitra Sen for their continuous encouragement to completion of my Ph.D. to endwith, I acknowledge all my well-wishers whom I could not mention and have contributed directly and indirectly towards the completion of my work. I also thank the almighty God for giving me mental patience and physical perseverance for completion of the research work in the present form.

Anumita Mitra,
10.12.25

Anumita Mitra
Department of Electrical Engineering
Jadavpur University
Kolkata, India

Dedicated to…
My Parents
My Husband
&
My Son

Who have always supported me in all my endeavors…

Contents

List of Figures

List of Tables

List of Abbreviations

a	Aberrated atrial premature beat
Adam	Adaptive moment estimation optimizer
AWN	Adaptive wavelet network
ARYTH	Arrhythmia
ANN	Artificial neural network
APC	Atrial premature beat
AV	Atrioventricular
AR	Auto regressive
ARIMA	Auto regressive integrated moving average
ARMA	Auto regressive moving average
BiLSTM	Bidirectional LSTM
BMI	Basic mass index
BIA	Bioelectrical impedance analysis
BSL	Biopac Student Lab
BW	Baseline wander
CO2	Carbon-di-oxide
MRI	Cardiac magnetic resonance imaging
CVD	Cardiovascular disease
CR	Compression ratio
CR	Compression ratio
DAC	Data acquisition card
1D-DCNN	1D-deep convolution neural network
Db	Daubechis
DAE	Deep auto encoder
DNN	Deep neural network
DPCM	Differential Pulse Code Modulation
DSO	Digital Storage Oscilloscope
DCM	Dilated cardiomyopathy
DDC	Direct data compression methods
DAST	Discrete Anamorphic Stretch Transform
DWT	Discrete wavelet Transform
DB-LSTM	Dynamically biased long short term memory
ECG	Electrocardiogram
EMG	Electromyography
EEC	Electroencephalogram
EMD	Empirical mode decomposition
FM	Feature matrix
F	Fusion of ventricular and normal beat
f	Fusion of ventricular and normal beat
GCM	Gaussian combination model

GMM	Gaussian mixture model
GA	Genetic algorithm
GUI	Graphical user interface
GSO	Grid search optimization
HRV	Heart rate variability
HT	Hilbert-transform
HPM	Hyperparameters prediction model
HYPER	Hypertension
ICA	Independent component analysis
ICU	Intensive care unit
IMFs	Intrinsic mode functions
KNN	K-nearest neighbor
LBBB	Left bundle branch block
VLL	Left leg
LWT	Lifting wavelet transform
LD	Linear discriminant model
RC	Logistic regression model
MCG	Magnetocardiogram
MEG	Magnetoencephalogram
MAE	Maximum absolute error
ME	Maximum error
m	Mean
MIMIC III	Medical Information Mart for Intensive Care III database
mitdb	MIT-BIH arrhythmia database
MA	Moving average
MLPNN	Multi layer perceptron neural network
MLP	Multilayer perceptron
MOPSO	Multi-objective particle swarm optimization
MOPSO	Multi-objective particle swarm optimization
AMI	Myocardial infarction anterior
IMI	Myocardial infarction inferior
NN	Neural network
J	Junctional Nodal premature beat
NSR	Normal sinus rhythm
O2	Oxygen
P	Paced
PE	Parameter extraction methods
PSO	Particle swarm optimization
PRD	Percentage root mean square difference
PRDN	Percentage root mean squared difference normalized
VLA	Potential between left arm
PVC	Premature ventricular contraction
PCA	Principal component analysis

PNN	Probabilistic neural network
ptbdb	PTB Diagnostic ECG database
QS	Quality score
RBF	Radial basic function
VRA	Potential at Right arm
RBBB	Right bundle branch block
RMSE	Root mean square error
seq	Sequential array
SE	Shannon energy
SNR	Signal-to-noise ratio
SVD	Singular value decomposition
SA	Sinoatrial
SD	Standard deviation
SVM	Support vector machine
SVEB	Supraventricular ectopic beat
TM	Target matrix
TD	Transformation domain-based methods
USB	Universal serial interface
Q	Unknown beat
VEB	Ventricular ectopic beat
WEDD	Wavelet energy based diagnostic distortion
WCT	Wilson Chest Terminal
WHO	World Health Organization
ZCP	Zero-crossing point

List of Symbols

.	Normal beat
[	Start of ventricular flutter/fibrillation
!	Ventricular flutter wave
]	End of ventricular flutter/fibrillation
/	Paced beat
|	Isolated QRS like artifact
ω_0	Angular frequency of fundamental component
a_0	Average value of zone potential signal
θ_n	Model Parameter
m	Mean
s	Standard deviation
v	ECG segment
x	Original ECG signal and
x_r	Reconstructed ECG signal
ε_t	Random error
c	Constant
θ	Model parameter
v_i	Velocity of particle in PSO
φ_1	Input biased vector of DAE
φ_2	Output biased vector of DAE
$g_{\theta 1}$	Activation function for hidden layer of DAE
$g_{\theta 2}$	Activation function for output layer of DAE
h	Observation status of PSO
U	Global search space in PSO
ω	Direction of normal vector to the hyperplane in SVM

Abstract

As per World Health Organization (WHO) cardiovascular diseases (CVD) is one of the most prominent causes of mortality rates all over the world. It is a main cause of death for 17.9 million lives each year. CVDs encompass a variety of cardiac conditions inclusive of rheumatic heart disease, coronary heart diseases, cardiomyopathy, arrhythmia, peripheral arterial disease and others. Many CVDs can be prevented by addressing the risk factors like diabetes, obesity, unhealthy diet, consumption of tobacco, harmful alcohol use.

CVDs can be treated effectively by early diagnosis. The proper diagnosis is possible by detecting the cardiac disease. It can be detected by recording the cardiovascular signal using Electrocardiography (ECG), Echocardiography, Chest X-ray, Heart CT Scan, Doppler Ultrasound etc. They provided valuable information regarding the electrical activity of heart. Cardiovascular signal represents the cardiac activity going on inside our body. For instance, pathologic Q waves, ST elevation, negative T waves etc. indicate acute myocardial infarction, the time interval between two consecutive R peak reveal the automatic regulation of patient which gives information regarding severity of illness. Pulse wave analysis also used for detection of many CVDs such as coronary artery disease, hypertension etc. Non-invasive measurement tool like ECG is very useful for critical care of hemodynamically unstable patients.

Computerized analysis and interpretation of cardiovascular signals has been one of the focused areas of research for electrical and electronics engineering. Analysis of cardiovascular signals has following advantages: non-invasive, cost effective, suitable for real-time monitoring, diagnosis from remote location and the parameters of analyzed signal are useful for clinical use. Due to its potentiality and advantages, the improvement in methodology and application of cardiovascular signal analysis and modeling will be promising in future. Modeling of cardiovascular signals can lead to diseases classification, compression for effective data storage and generation of synthetic waveforms for medical and engineering R&D applications. The proposed research aims to develop new methods for cardiovascular signal modeling and analysis to enable automated detection and interpretation of cardiac abnormalities. Advanced computational intelligence techniques, including deep learning, are employed to extract highly relevant features from cardiovascular signals. These features are then used to build robust and accurate models for cardiac assessment.

Chapter 1

Introduction

1.1 Introduction to Biomedical Signal:

Human body consisting of different physiological system like nervous system, digestive system, cardiovascular system, human skeleton system and many other systems [1], [2], [3]. Each system has different function and they generates different types of biomedical or physiological signals. These signals are used to extract clinical information for clinical analysis to understand the condition of the subject and for proper diagnosis. Biomedical signal can be classified into seven classes on the basis of there orgin. The biomedical signals are classified as bioelectrical, biomechanical, biochemical, bio-optical, biomagnetic signal, bioacoustic, bio-impedance.

a) Bioelectric Signal: These types of signals are generated by muscel cell and nervous system. The cell membrane generate action potential under a certain condition. The bioelectric signals are generated due to the action of many cells. Electrocardiogram (ECG), Electroencephalogram (EEC) signals are bioelectric signal.

b) Biomechanical Signal: These signals are generated by the mechanical activity of physiological system like pressure, flow, motion, displacement etc. For example, due to chest movement a meachnical signal is generated which can be measure and analysed for diagnosis purpose.

c) Biochemical Signal: These types of signal can be generated from living tissue or in the pathology at the time of sample analysis. For example, partial pressure of oxygen (O_2), partial pressure of carbon-di-oxide (CO_2) etc.

d) Bio-optical Signal: These signals are results of optical function of physiological system. These signals generated by fetching a light source the body part and the reflected rays are captured by camera or detector. These signals have variety of application like pulse oximetry to measure heart rate and oxygen saturation in red blood cell, cancer cell study etc.

e) Biomagnetic Signal: These are weak magnetic field produced by different organs of physiological system like heart, brain, lungs. The magnetic field is extremly weaker than earth magnetic field hence a strong detector is required to detect the signal. For example, Magnetocardiogram (MCG) which is obtained by recording magnetic field of heart, Magnetoencephalogram (MEG) is obtained from magnetic field of brain.

f) Bioacoustic Signal: These signals are captured from the sound of biological system like heart, lungs, bowel etc. These signals are usually captured from animal to understand animal ecology and to motior animal communication for analysising the effect of human noise on animal.

g) Bio-impedance Signal: These signal are used to measure the resistance capacity of body against a flow of electrical current. Thus these signals are also known as bioelectrical impedance analysis (BIA) signals. The most prominent factors which affect these type of signals are sex, weight, height, skin type etc. They are used for measuring blood flow and composition of human body.

Different types of biomedical signal represents different type of energy which carries most important information to understand the condition of different organs of human body. The computerized analysis and interpretation of biomedical signals becomes a focused area of research for electrical, electronics and computer engineering. In this work we have focused on ECG signal.

As per World Health Organization (WHO) cardiovascular disease (CVD) is a most prominent cause of mortality. In 2019, 17.9 million peopole died worldwide due CVDs which is 32% of global death. Out of 17.9 million death, the main cause of 85% death was heart attack and stroke. The rate of death due to CVDs can be decreased by constant motoring of cardiac activity and proper diagnosis. ECG signal modeling and analysis plays a vital role for monitoring and detection of cardiac diseases.

1.2 Relation of Biomedical signal with time-series:

The biomedical signal are time–series signal [4]. It can be classified into two types depending on its statistical properties namely stationary and non-stationary. The time series signal can be classified into two types on basis of its behavioral properties namely, time variant and time invarient.

1.2.1. Stationary time-series:

In stationary time series the statistical charateristics of data points are independent of time. The statistical characteristic like mean, variance, autocorrelation are remain constant over time. Staionary time series has a great importance for forcasting of future data. Thus signal are transformed into stationary time series for future value prediction. Random white noise are example of stationary time series.

1.2.2. Non-stationary time-series:

In non-stationary time sries, the statistical characteristics of data points are changes over time. It is a time dependent series where the characteristics of data points are different for each instant. Non-stationary time-series exhibits seasonality, trend and pattern as it continuously changed with time. ECG signal, PPG signal etc. are non-stationary time series.

1.2.3. Time invariant time-series:

In the time invarient time-series, the behavioral charcteristics like mean, spectral, variance etc. of the data are not changed over time.

1.2.4. Time variant time series:

In time varient time-series, the data point in the sequence are changed over time. The underlying relationship within the data like behavioural characteristics and parameters are not constant. In practical case most of the data are time invariant. Few example of Time series data are sales data, stock pattern, biomedical signal etc.

1.3 Mechanism of heart and its functioning

Heart is a muscular organ of cardiovascular system which pumps and circulates blood throughout the body for delivering oxygen and neutrition to the tissue of whole body and removes carbon dioxide and the waste products [5], [6], [7], [8]. It is located in front of chest, on the left side and in the thoratic chamber which is anterior to the vertebral column and posterior posterior to the sternum. It is consists of four chamber and the chambers are a) right atrium, b) left atrium, c) right ventricle and d) left ventricle. The heart receives deoxygenated blood by the network of veins. The deoxygenated blood is purified in cardiovascular system and the pure oxygenated blood circulates to the whole body by arteries. Heart is most important organ of human body along with kidney and central nervous system.

Heart is protected in a enclosed sac which is known as pericardium. Pericardium is a cushioned two-walled sac which protect the heart from mechanical damage using the outer layer known as, fibrous pericardium. The heart is consists of three layers: epicardium, myocardium and endocardium. The blood flow in the heart is unidirectional and it is controlled by two types of valves, viz., tricuspid and mitral

valve. The heart is partitioned into right side and left side by a thick wall of muscle which is called as septum.

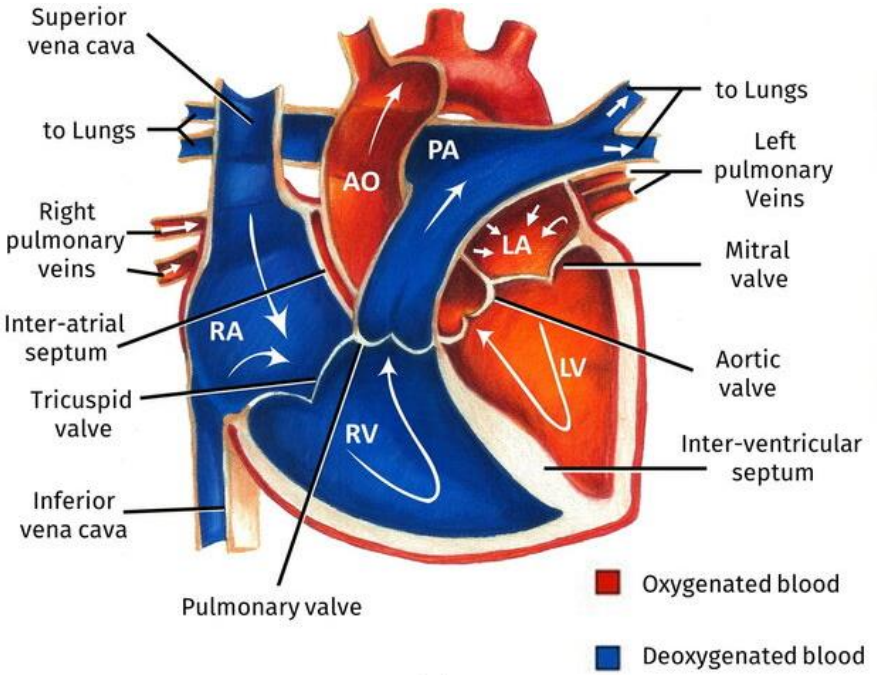

Fig.1.1: Blood flow through the heart [9]

The right atrium and right ventricle receives the oxygen-poor blood from whole body and returning the blood to the lungs for purification. The left chambers of heart, combining with left atrium and left ventricle supply the oxygenated blood to the whole body. The left and right chambers of heart contract and expand at a same instant to recive the impure blood from the body and circulate the pure blood to the whole body.

1.3.1. Blood circulation in the body through heart

A complete cardiac cycle means collection of impure blood from whole body and sending back pure blood to all organs of the body. The superiour vena cava collect the impure bloods from upper organs of body and the inferior vena cava from lower organs of the body to force fill the right atrium. After a certain pressure of deoxygenated blood in right atrium the tricaspid valve is opened to pass the blood to the right ventricle. Then the tricaspid valve is closed to prevent the returning back of blood to the right atrium.

The right ventricle filled up by the blood and start contraction to pump the oxygen-poor blood to the lungs. The pulmonary artery receives the blood through pulmonary valve and carry the blood to lungs using two branches of it. The pulmonary valve is closed after transfering the blood to the artery to restrict the flow back of blood to left ventricle.

In the lungs, the purification of deoxygenated blood takes place by transfering O_2 and expels CO_2. The pure oxygenated blood from lungs supplied to the left atrium of heart by pulmonary vein. Then the mitral valve or biscuspid valve is opened due to the blood pressure of left atrium and the pure blood flows through the left ventricle. After that, the mitral valve is closed to restrict back flow of pure blood. Finally the oxygen rich blood is pumped to the whole body through aortic semilunar valve to the aorta. The blood is supplied to the upper and lower part of the body through major arteries to feed each cell of the body.

1.4 Cardiovascular Disease

The heart beats to circulate blood in whole body and delivering oxygen rich blood to the each of the body and removes waste product like CO_2 from the body [6]. The resting heart rate of an adult is usually 60 - 100 beats per minute. The heart rate is depending on various factors such as, age, gender, illness, fitness, life style, medication etc. The heart rate indicates the condition of a heart. If the resting heart rate incresed than a certain value, the risk of cardiovascular disease will be incresed.

CVDs can be classified into different type on the basis of various factors. CVDs mainly affect one or various part of heart and blood vessels. As per WHO different types of CVDs are as follows:

a) ***Coronary Heart Disease:*** It is also known as coronary artery or ischemic heart disease. The main reason of this type of heart disease is narrowing of coronary arteries who supplies the blood to the heart muscle. This is occurs due to buildup of plaque in the arteries which restricts the blood flow to the heart muscle.

b) ***Arrhythmia:*** This is irregular or abnormal heart beat due to problem in electrical conduction system of heart.

c) ***Cardiomyopathy:*** It is affected the muscle of heart and it becomes difficult for heart to pump the blood.

d) ***Congenital Heart Disease:*** Defect in heart since birth which restrict the development and functioning of heart.

e) ***Cerebrovascular Disease:*** It is also disease of blood vessels which supplies blood to the brain.

f) ***Peripheral Arterial Disease:*** Disease of blood vessels which are responsible for supplying blood to the arms and legs.

g) ***Rheumatic Heart Disease:*** It is caused due to rheumatic fever by streptococcal bacteria which affect the heart muscels and heart valves.

h) ***Deep Vein Thrombosis and Pulmonary Embolism:*** In deep vain thrombosis, blood clot develops in the vein of lower extrimities of the body. Pulmonary embolism occurs when the blood clot dislodge and travel towards the heart and lungs which may tend to life threatening.

Heart attack and stroke both are acute life risk condition which caused due to blockage of blood flow to the heart and brain respectively. The main cause of heart attack and stroke is deposition of fatty substance on the inner wall of blood vessels. Another reason of stroke is bleeding from blood vessels in the brain or from any blood clots.

In our research we are focused on arrhythmia. It is a most prominent cardiovascular disease which can cause heart attack.

1.5 Risk factors of CVDs:

CVD is a complex collection of disease and basically here are two types of risk factors such as behavioral risk factors and environmental risk factors.

1.5.1. Behavioral risk factors:

Behavioral risk factors includes diabeties, obesity, high blood pressure, high LDL (Low density lipoprotein) Cholesterol, smoking, unhealthy diet [10].

a) ***Diabetes:*** Diabetes is a chronic disease which may be caused due to insufficient production of insulin hormone by pancreas or if the blood unable to use the insulin properly to regulate the glucose of blood. The main source of glucose is carbohydrate from food and drinks. The glucose

mainly supply the energy to human body. The level of glucose is controlled by insulin by helping glucose to reach it's final destination from the bloodstream. When the pancreas does not produce sufficient amount of insulin hormone or blood cannot use the hormone, the glucose are bluidup in the bloodstream which increases the sugar level in the blood. It is known as hyperglycemia or high blood sugar. Another reason of high blood sugar is high intake of sugar from unhealthy diet. The high blood sugar is another cause of coronary heart disease, heart attack, stroke.

b) Obesity: Obesity is accumulation of excess fat in the different part of body which has negative impact on the body. It may be cause of differen cronic disease like heart disease, reproduction problem, bone health issues, osteoarthritis, type II diabetis etc. As per WHO basic mass index (BMI) is calculated by the ratio of weight in kg to height in Sq.m. The normal range of BMI of a healthy person should be within 18.5 to 25 kg/m^2. When the range becomes more than 25 to $30kg/m^2$, it is considered as overweight and more than 30 kg/m^2 is considered as obesity. Obesity increase the risk of heart disease like buildup of fatty substance on the arteries, high blood pressure, heart failure, injure the heart muscels, atrial fibrillation, left ventricular hypertrophy, sudden cardiac death etc.

c) High Blood Pressure: High blood pressure is known as hypertension. It causes due to the high pressure on the blood vessels. It is another risk factor of heart disease which may cause heart attack, heart faliur when heart is unable to pump sufficient blood and oxygen to the different organ of the body, chest pain by reducing blood flow to the heart which is known as angina, coronary artery disease, enlarged heart, irregular heartbeat etc.

d) High LDL Cholesterol: High LDL cholesterol means increase the level of bad cholesterol. It can deposite fatty substances on the arteries which in turn narrowing the passage of blow flow. If any clot get blocked in the narrow passage, the chances of heart attack or stroke will be increased.

e) Unhealthy Diet: Unhealthy diet means consumption of saturated fat, excess salt and sugar. It is a major risk factor for different types of chronic disease like obesity, diabeties, cardiovascular diease etc.

f) Smoking: Smoking is an independent risk factor for coronary artery disease which may increase the risk of heart attack 2-3 times more than a non-smoker patient. It damage the heart and blood vessels and increase the probability of death due to CVDs.

1.5.2. Environmental Risk:

According to WHO, environmental risk factors increase the risk of heart disease. Air pollution is most prominent environmental risk factor. Poor air quality increase the probability of cardiac disease, heart attack, stroke. Environmental risk factors also includes noise pollution, season change, increase of arsenic level in drinking water, light pollution etc.

1.6 Symptom of CVDs:

Symptoms of CVDs basically depends on type of cardiac disease but few systomps are common for most of the CVDs. The usual symptoms of CVDs are chest pain, dizziness, shortness of breath, swelling, palpitation, fatigue etc.

1.7 Detection of CVDs:

CVDs can be treated effectively by early diagnosis. The proper diagnosis is possible by detecting the cardiac disease. There are various process to detect CVDs like Electrocardiography (ECG), Echocardiography, Chest X-ray, Heart CT Scan, Doppler Ultrasound, Cardiac magnetic resonance imaging (MRI) etc.

1.7.1. Electrocardiography (ECG):

ECG is simple, non-invasive tool, used to record the tiny electrical signal impulse which is generated in our heart and measure the electrical activity to detect cardiac abnormality for clinical analysis and diagnosis purpose. It is very easy to capture the cardiac rhythm with minimal cooporation of the subject. The recorded cardiac signal is known as Electrocardiogram signal or ECG signal. The signal is recored and print for further analysis.

1.7.2. Echocardiography:

It is also a non-invasive method which provide images of heart and blood vessels in the closest region of heart. It captures the images by ultrasound scan. It shows the structure of heart and heart valves to detect cardiac disease. Though it is a painless and non-invasive method but the patient should not consume any food for four hours prior to the test. The test takes 30 – 60 minutes and the report can be received within few days.

1.7.3. Chest X-Ray:

It is an imaging technique which uses X-ray to capture the image of heart. It is a primary tool and capture the image of heart, lungs and bone of chest.

1.7.4. Heart CT Scan:

It is also a non-invasive imaging method by using X-rays which provides detailed image of heart and blood vessels for diagnosis purpose. This method is safe for adults but it is not recommended for pregnant ladies and patient under radiation therapy. It can be two types, Coronary calcium scan which shows buildup of calcium in the arteries of heart and CT Angiography which detect blockage or narrowing in the arteries which are used to supply the blood to the heart.

1.7.5. Doppler Ultrasound:

This method shows the blood flow to the heart and blockage in the arteries of heart. Usually, it is used for patient of coronary artery disease or atherosclerosis. It is also non-invasive and painless method for cardiac disease detection.

1.7.6. Cardiac magnetic resonance imaging (MRI):

It is a non-invasive method which is used for assessment of cardiac function and heart structure. This method is used for coronary heart disease, cardiomyopathy, congenital heart disease etc.

Among the above mentioned CVD detection method ECG is mostly used method which is recorded cardiac rhythm for disease detection and primary diagnosis purpose.

1.8 Electrocardiography (ECG) :

ECG is a non-invasive tool for monitoring and detecting cardiac abnormality of a patient [5]. It is captured the continuous electrical activity of heart which is originated at the upper region of right atrium from sinoatrial (SA) node. At this node pacemaker cell sponteneously depolarize and repolarize at a rate of 60 – 100 times/minute. The tiny electrical signal is spreaded over the atria at a speed of 4m/sec to contract them together which produces a deflection on the ECG record, known as P-wave. Then the electrical impulse is reached at the lower end of right atria, at atrioventricular (AV) node, through which it can reach at the ventricles. A ring of fibrous tissue seperated the atrial myocardium and ventricles, thus the conduction at AV node produces a pause between atrial conduction and ventricular conduction. The pause is recorded as an equipotential segment on the ECG, known as PR segment. The electrical impulses enter into the bundle of HIS. The bundle of HIS bifurcated into left and right bundle branches. The contraction of ventricles starts together which shows a sharp upward and downward deflection on

the ECG record which is called as QRS Complex. Among the bundle branches the left branch is divided into anterior and posterior fascicle which help in conduction of left ventrical and the right bundle branches prepare the path for conduction of right ventricle. The conduction is distributed over the Purkinji Fibre to spread out in the left and right atria. The atria expands (repolarized) during the ventricular contraction. Though, a feeble electrical impulse is generated but the ventricular activity suppressed the impulse, hence the electrial activity cannot reflected on the ECG and the equipotential segment is recorded as ST segment. Then the ventricles are repolarized together and the wave is noted as T wave. A small deflection is recorded after T wave, known as U wave due to slow repolarization of inter ventricular septum or ventricles. The recorded waveform for a single cycle is known as ECG beat and ECG signal is formed by recording multiple consecutive ECG beats. The clinical pattern of a healthy ECG beat is shown in Figure 2. and the conduction path of ECG signal is shown in Figure 3.

A complete cardiac cycle is consisting of P-wave, QRS complex and T-wave which are connected through equipotential segments. The P wave and QRS complex are connected by PR segment and ST segment connects the QRS segment to T wave. A small positive deflection is recorded after T wave and before P-wave of next consecutive beat which is known as U-wave. These waves and segments are important features of ECG beat. Each feature has range of duration and a specific morphology which indicates the status of heart condition. Among these features R-peak is the most prominent feature of ECG signal. Each feature of ECG has a conventional interpretation which are defined as under:

- Onset: The starting point of an electrical activity such as repolarization or depolarization
- Offset: The terminating point of an electrical activity such as repolarization or depolarization
- Interval : The onset point of one wave to onset/offset point of other wave like PR interval, ST interval, QT interval, R-R interval.
- Segment : The equipotential area between offset of one wave to onset of next wave like PR segment and ST segment.
- Wave duration or width: The time duration between onset and offset of same wave.

For a normal sinus rhythm or healthy cardiac rhythm the each wave, interval and segment has a certain range of time duration. The conventional features and durations are shown in Table I.

P Wave: It is first positive deflection on the ECG recorder and the duration of this wave is 80 ms with range of amplitude from 0.05 mV to 0.25 mV.

PR Segment: This is equipotential space between offset point of P-wave to onset point of QRS complex. The time duration is 50 – 120 ms.

PR Interval : The interval between P-onset to onset of QRS Complex with 120-200ms duration.

QRS Complex: QRS complex is consisting of a negative deflection which is called as Q-point, then prominent a positive deflection with amplitude 0.5mV to 3.0mV and ended with a negative deflection, known as S point. The time duration of QRS complex is 80 – 120 ms.

J-point : J-point is Junction point between QRS Complex and ST segment i.e. end point of QRS complex and starting point of ST segment.

ST Segment : It is a isoelectric segment between offset of S-point and onset of T-wave. The duration of this segment is 80-120ms.

T Wave : The positive deflection after QRS complex is T-wave with 160ms duration.

ST Interval : The interval between S-offset to T-offset is ST interval which has 320 ms time duration.

QT Interval : The interval between Q-onset to T-offset is QT interval. The time duration of this interval is 420ms.

U Wave: The small positive deflection after T wave is known as U-wave.

R-R Interval: It is the interval between peak R-peak point of two consecutive ECG beats. It is another most important feature with duration 0.6 – 1.2 s.

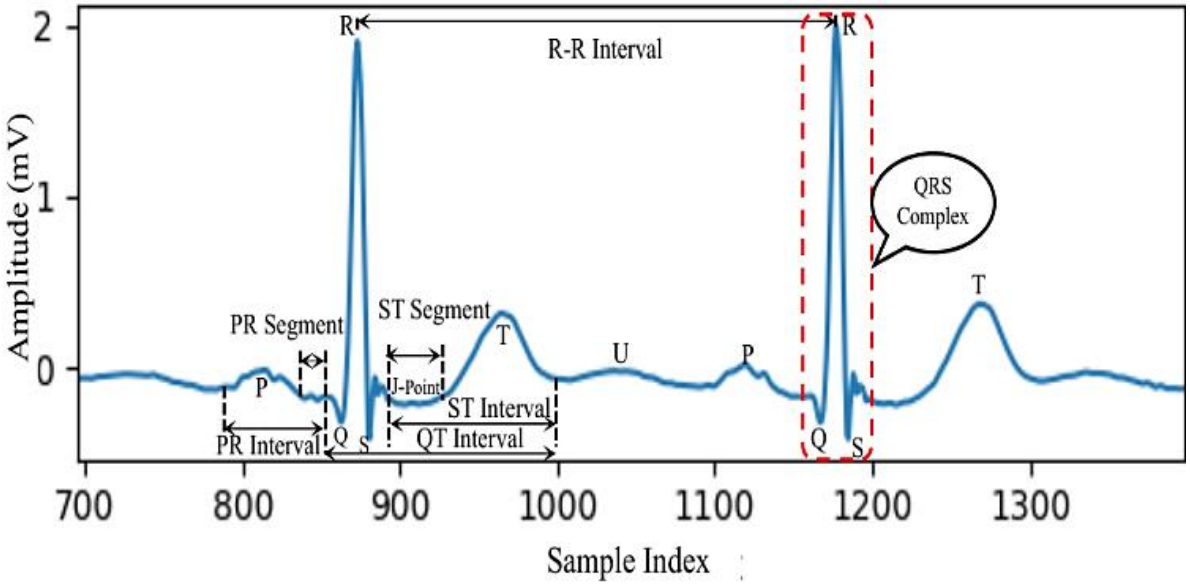

Fig.1.2.: Waves and segments of healthy ECG beat

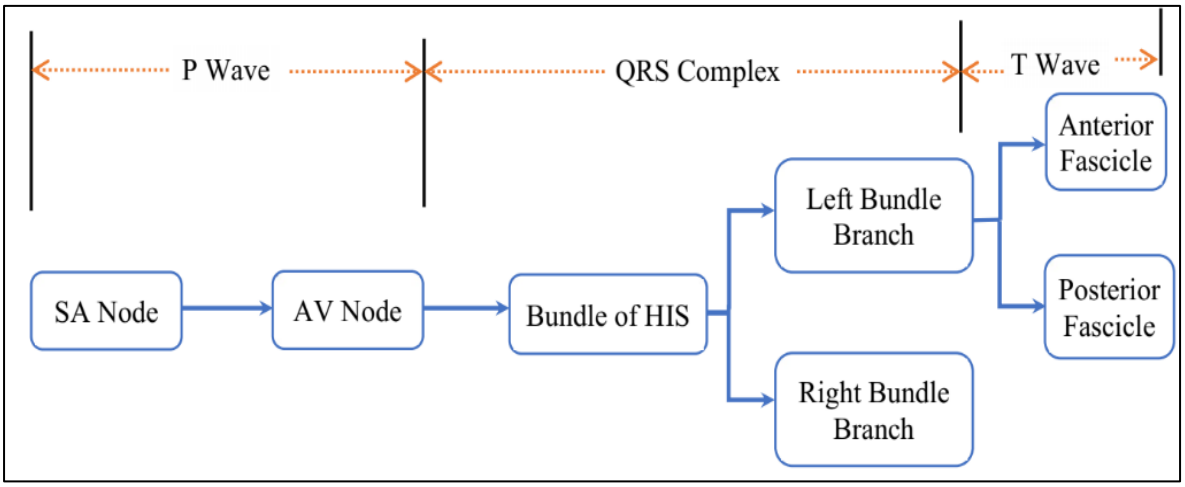

Fig. 1.3.: Conduction pathway of ECG Signal

1.9 Lead System for ECG Acquisition:

ECG is recording of a tiny electrical signal which is generated in heart. ECG acquisition is a non-invasive, painless process and can be captured from a subject with a minimal cooperation. Different lead systems were introduced over the past century and improved day by day. The lead systems are described below.

Table 1.1. Features & Duration of ECG beat

Feature	Description	Duration
P Wave	First positive deflection of ECG beat	80 ms
PR Interval	From the P-onset index to starting index of QRS complex	120-200 ms
PR Segment	From P-offset index to Q-onset index	50-120 ms
QRS Complex	Most prominent feature of ECG beat. Starts from downward deflection of Q and end at downward S deflection including R-peak	80-120 ms
R-R Interval	Interval between two consecutive R-peak index	0.6 – 1.2 s
J-Point	End point of QRS complex	-
ST Segment	From S-offset to T-onset	80-120 ms
ST Interval	From S-offset to T-offset	320 ms
T Wave	The positive deflection ECG after QRS complex	160 ms
QT Interval	From Q-onset index to T-offset index	420 ms
U wave	The small positive deflection after T wave and before P-wave of consecutive beat	-

Einthoven Lead System:

In 1924, W. Einthoven first developed and standardized ECG lead for signal acquisition. According to Einthoven postulates, human body is a perfect sphere with heart at its centre. In this method, three electrods are placed on the skin of left arm, right arm and left leg of a subject, standing with stretched arms. Hence a equilateral triangle is formed inside the sphere. These three leads are call Einthoven's bipolar leads and also known as standard leads. Lead I measures the potential between left arm (V_{LA}) and right arm (V_{RA}), lead II measure the potential between right arm (V_{RA}) and left leg (V_{LL}) and lead III between left arm (V_{LA}) and left leg (V_{LL}) .

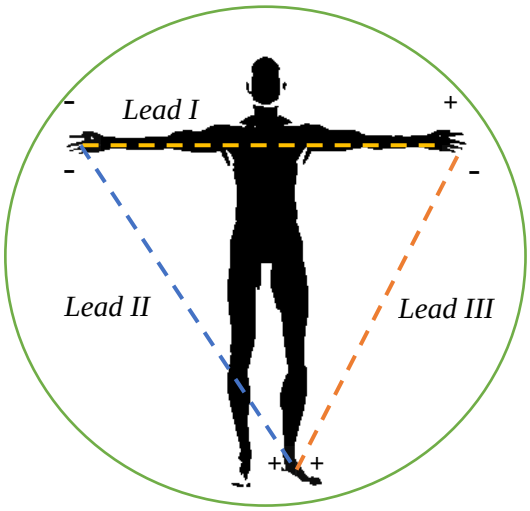

Fig. 1.4. Einthoven's Standard Lead Position

Lead I measures the potential between left arm (V_{LA}) and right arm (V_{RA}), lead II measures the potential between right arm (V_{RA}) and left leg (V_{LL}) and lead III between left arm (V_{LA}) and left leg (V_{LL}) .

Frank Wilson Lead System:

Unipolar lead system was introduced and standardized by Frank Wilson. This method is consisting of three limb lead (Lead VL, LR, VF) and six precordial chest leads (v1, v2, v3, v4, v5, v6). The potentiality is measured with respect to a terminal outside the body. This terminal is called as Wilson Chest Terminal (WCT).

E. Goldberger Lead System

The precordial chest lead was modified by E. Goldberger. He also developed Augmented limb leads (aVR, aVL, aVF). The cardiac potentials were measured by precordial chest leads at specific intercostal spaces of chest with respect to WCT. The six chest (precordial) leads represent the horizontal plane, while leads VL, VR, VF, aVL, aVR, and aVF form six frontal plane leads. Together, they make up the standard 12-lead ECG system, which is the most widely accepted method for recording and interpreting cardiac electrical activity.

1.10 Significance of Modeling of ECG signal:

Modeling of ECG signal plays a crucial role to understand the functionality of heart. Modeling plays a vital role in the analysis, interpretation, and diagnosis of cardiac problems. The main objectives of modeling of ECG signals are as under:

- To develop newer methods of cardiovascular signal modeling and analysis for automated synthesis and interpretation of cardiac abnormalities.
- Modeling of biomedical signals can lead to diseases classification, compression for effective data storage and generation of synthetic waveforms for medical and engineering R&D applications.
- Advanced methods of computational intelligence like deep learning will be utilized for extracting more relevant features from biomedical signals

There are several methods avaiable for modeling of ECG signal [11]. Few of them are described below:

1.10.1. *Polynomial Modeling:*

Each ECG segment is fitted with a polynomial function of an appropriate model order to represent the signal efficiently and compress the signal by preserving all clinical informations [12], [13]. There are different types of polynomial functions such as Jacobi polynomial, Laguerre polynomial, series of orthogonal polynomial, Hermite polynomial etc. Jacobi polynomial can be classified into Legendre polynomial and Chebyshev polynomial. Chebyshev polynomial is very popular for modeling of ECG signal. It can be defined by recurrance relation. It has interesting properties which make it efficient for the design of filter and for the optimal polynomials interpretation.

1.10.2. Wavelet Transform:

Wavelet transform based model are decomposed the ECG signal into time frequency components [14]. The spectral and temporal charateristics of each components are analyzed to extract features of cardiac signal. The valuable features along with QRS complex, P wave, T wave are detected by wavelet transform. The features are used for classification of arrhythmia and compression of ECG signal. It is also used into denoising of ECG signal. The components are analyzed and noisy components are eliminated from the signal to extract denoised ECG.

1.10.3. Fourier Model:

The Fourier model like, Fourier series, Fourier transform model are decomposed the complex ECG into its constituent sinusoidal components [15],[16]. The Fourier series and Fourier transform break downs the electrical activity of heart into frequency components which are sine wave and cosine wave. The frequency contents are analyzed to check the characteristics of each components and used for denoising purpose, feature extraction, class identification of arrhythmia signal.

1.10.4. Gaussian Model:

Gaussian model is a mathematical modeling method which uses Gaussian distribution to extract complex features for class identification of data in the area of signal processing, image processing, statistical modeling and machine learning [17]. Gaussian distribution is suitable for a bell shaped

waveforms. The main parameters of Gaussian model are mean and standard deviation. Gaussian mixture model (GMM) generates data by combining multiple number of Gaussian distribution. GMMs are used for clustering of data and density estimation. GMMs are trained by expectation-maximization algorithm.

1.10.5. Auto regressive (AR) model:

Auto regressive (AR) modeling is a statistical modeling method [18]. It predicts the future trend of a time series based on its past values. The current values are depending on the past values. It is usually analysed the data of time series. The model parameter is denoted by *p* and model with order *p* is known as $AR_{(p)}$ model. The model coefficients are determined the relation between past values and current value to predict the future value.

1.10.6. Moving average (MA) model:

The Moving Average (MA) model is a statistical modeling technique [19]. It predicts future trends of a time series based on past error terms. In this model, future values depend on previous random disturbances rather than on past values of the series itself. MA models are commonly used to analyze data that evolve over time. The model order is denoted by *q*, which represents the number of lagged error terms included in the model. MA model is used to smooth out the irregularities in the data points by considering the random error from previous time step.

1.10.7. Auto regressive moving average model:

Auto regressive moving average (ARMA) model combine the auto regressive model and moving average model for modeling of a stationary time series signal [20]. In this method the AR model used for regression of the variable on its own lagged values and the MA model smooths out irregularities in a time series by incorporating and analyzing lagged error terms.The model order is denoted by *p* and *q* where, *p* is the order for AR model and *q* for MA model. The ARMA model is denoted by $ARMA_{(p,q)}$.

1.10.8. Auto regressive integrated moving average model:

The Auto-Regressive Integrated Moving Average (ARIMA) model is a statistical modeling method primarily used for analyzing and forecasting the future trends of non-stationary time series signals [21]. It differentiates the non-stationary terms one or two times to convert the signal into stationary signal. The AR and MA algorithms are then applied to capture the influence of previous values and past random error terms in order to predict future values. The ARIMA model is defined by three parameters, *p*, *d*, and *q*: where *p* represents the order of the AR component, *d* denotes the degree of differencing (integrated part), and *q* indicates the order of the MA component. An ARIMA model can be defined as $ARIMA_{(p,d,q).}$

1.11 Objective and scope

According to World Health Organization (WHO) Cardiovasucar Disease (CVDs) are the leading cause of mortality across the world. It can be controlled by monitoring, detection of cardiac problems and clinical analysis of ECG signal for proper diagnosis purpose. Modeling and analysis of ECG signal plays a vital role for proper interpretation of ECG signal, computational analysis for disease detection, ECG classification for disease identification, compression of ECG signal for reduction of memory allocation etc. Another aspect of modeling and simulation of ECG signal are education and training of medical student. Hence the main objectives are as follows:

- To develop newer methods of cardiovascular signal modeling and analysis for automated synthesis and interpretation of cardiac abnormalities.
- Advanced methods of computational intelligence like deep learning will be utilized for extracting more relevant features from biomedical signals.

- Modeling of biomedical signals can lead to diseases classification, compression for effective data storage and generation of synthetic waveforms for medical and engineering R&D applications.
- Due to the high population density leading to inadequate medical infrastructure per capita in a developing country like us, thus a self-paced cardio simulator can be used for training of medical students and professionals.

The scope of work are as under:

- Development of cardio simulator for generation of synthetic ECG signal for training of medical professional
- Development of new modeling method for synthesis of ECG signal and minimization of reconstruction error
- Development of deep learning based feature extraction module for modeling, compression and classification of ECG signal
- Development of new compression model for effective storage of ECG signal
- Development of deep learning based ECG classifier to identify disease for clinical analysis and proper diagnosis.

1.12 Organization of the Thesis

Chapter 1: This chapter provides a comprehensive introduction of biomedical signal, class of signal, mechanism of heart for blood circulation, different types of cardiovascular diseases (CVDs), risk factors of CVDs, Symptoms of CVDs, detection of CVDs, brief introduction of ECG, lead system for ECG acquisition. This chapter also covers type of time series signal as biomedical signals are time series signal, significance of modeling for ECG signal and different modeling methods like polynomial, Fourier, Gaussian, wavelet based method, auto regressive (AR) model, moving average (MA) model, auto regressive moving average (ARMA) model and ARIMA model.

Chapter 2: In this chapter, a brief description of need and significance of ECG modeling and analysis. This chapter give a review of literature for denoising and preprocessing of ECG signal, different procedure and literature on feature extraction, modeling of ECG signal and their application like compression and classification of ECG signal. This chapter helps to find out the research gaps from the published work and set a research goal for this thesis.

Chapter 3: This chapter focuses on data acquisition and collection of data from Physionet database. MIT-BIH Arrhythmia database (mitdb) is a popular database of Physionet but in this thesis we have validated our research works using two additional databases of Physionet, namely the PTBDB and MIMIC-III databases. This chapter describe the acquisition of ECG signal from a subject using BSL system. The procedure of denoising and feature extraction from the raw ECG signal are given. Finally, a 2D beat matrix was generated for modeling, analysis, compression and classficiation of ECG signal.

Chapter 4: This chapter illustrates the need and significance of cardiac simulator for training of medical students and professionals. In this chapter the Fourier and Gaussian modeling are described in details. We have used these methods to develop a cardiac simulator, known as Cardio-Sim. The method and results of Cardio-Sim are given in this chapter.

Chapter 5: It presents two novel methods for synthesis of ECG signal to improve the reconstruction error. Segment specific model and adaptive ARIMA model are described in this chapter. Segment specfic model is a new method for ECG modeling where FM and GM are used for specific segments and it is a dynamic error-controlled model. This chapter shows how the adaptive ARIMA model was

developed by optimizing model hyperparameters. Particle swarm optimization (PSO) and Grid search optimization (GSO) methods are used for optimization and which is better to develop adaptive ARIMA model, are described in this chapter.

Chapter 6: The most useful application of modeling and analysis of ECG signal are compression and Classification. This chapter focused into development of lossless compression model and classification model with high accuracy using deep learning method. It describes the development and result of compression model by Multi layer perceptron neural network (MLPNN) and 1D-deep convolution neural network (1D-DCNN) based multiclass ECG classification model.

Chapter 7: In this chapter, the discussion and conclusion of all research works of this thesis are presented. The main contributions of this research thesis are presented in Chapters 4 to 6, while the discussion and conclusion are provided in this chapter. It also highlights the potential research scope for future research to improve the telemedicine based remote diagnostic system.

Chapter 2

Literature Review

2.1. Need and significance of ECG modeling and analysis

Modeling and analysis of ECG signal are plays a significate role for 1) monitoring cardiac activity using wireless wearables, 2) detection of cardiac disease for proper diagnosis purpose, 3) education and training of medical students and professionals. Digital signal processing method had a great contribution for monitoring and analysis of ECG signal. Modeling of signal processing is followed by denoising and preprocessing of ECG signal. There are plethora of methods are available for denoising, preprocessing, modeling and analysis of ECG signal.

2.2. Denoising of ECG signal

ECG signal acquisition is a non-invasive method. The ECG can monitor and measure the electrical activity of our heart surface by placing the electrode in a particular body position and with a minimal cooperation of the subject [5], [6], [7], [8]. But at the time of signal acquisition it may be contaminated by different type of noise such as higher frequency noise, baseline wander, power line interferance, muscle noise etc. It becomes most difficult to extract true ECG signal from the noise. Thus, noise removal is an essential step for clean representation of raw ECG signal for further processing. The common sources of noise are:

a) Power Line Interference: The range of noise is 50 to 60 Hz which comes from power supply

b) Electromyography (EMG) Noise: The noise is very high frequency noise and it is above 100Hz.

c) Muscle Noise: It is caused by movement of other muscle near the heart

d) Electrode motion artifact noise: It is caused due to movement of patient at the time of ECG signal acquisition.

e) Baseline wander noise: It is a lower frequency noise with range 0.5 to 0.6Hz.

A plenty of methods are available for denoising of ECG signal as research on ECG signal is carried out over a decade. The noise removal methods can be classified as under : adaptive filtering, wavelet based method, Fourier methods, statistical method, empirical mode decomposition method etc.

In Adaptive Kalman filter it removes the baseline wander (BW) noise by using a polynomial approximation which is independent with respect to the signal characteristics. A state space model was used alongwith the kalman filter for estimation of state variables and baseline wander approximation of previous values of the ECG signal. The result gives better accuracy than moving average and cubic spline methods [22],[23].

Another noise removal technique is Extended Kalman filter which is also used for compression of ECG signal [24]. Nonlinear Bayesian filtering method also used for removal of noise from raw ECG signal. In this approach a mathematical bayesian framework was developed and compared with the conventinal noise removal methods like Extended Kalman Filter, Kalman smoother etc. It was mainly used to remove noise from single channel noisy ECG signal. It is a dynamic noise reduction method which offered a high resolution ECG [25].

Polynomial spline function decomposes the ECG signal and removes the nosiy level and reconstructs the denoised ECG signal [26]. Piecewise linear model removes baseline wander from noisy ECG signal in two iteration and the noise is subtracted from the noisy signal to offer denoised ECG signal [27].

Another most popular denoising method is wavelet based method. In this method the particular effected wavelet function are removed for denoising. This method is able to remove higher frequency noise (like muscel artifacts, power line interference etc.) as well as lower frequency noise like baseline wander [28],[29],[30],[31].

Empirical mode decomposition (EMD) method can able to remove the higher frequency noise and also the lower frequency BW. EMD is based on data-driven mechanism which decomposes a signal into sum of intrinsic mode functions (IMFs). It is suitable for nonlinear and nonstationary signal like biomedical signals such as ECG, PPG etc.. IMF are consisting of equal number of extrema alongwith zero crossing with its envelops and defined by all local minima and maxima. It gives better result for noise removal as compared to the filtering methods [32],[33],[34].

Component analysis algorithm is an effective technique for denoising of ECG signal. Principal component analysis (PCA) and independent component analysis (ICA) are used for noise reduction from the raw ECG signal. ICA and PCA are basically statistical analysis methods which are used as dimensionality reduction tool. With the dimension reduction of ECG signal it also eliminates the noises with a minimal information loss [35],[36],[37].

Artificial neural network (ANN) based noise reduction approch also used for denoising of ECG signal. In this algorithm the baseline drift is removed by optimizing the hidden layer and coefficient matrix. This method was compared with the tradintional methods like WT method, adaptive filtering methods etc. and found that ANN gives better results in terms of baseline drift removal and distortion of signal at filter output [38].

Apart from the signal processing technique the noise can be reduced by minimizing the patient movement which in turn reduces motion artifacts. The electrode to patient contact can be improved by using electrode gel as it enchances the skin contact and reduces the electricals impedance.

2.3. Feature Extraction of ECG signal

R-peak is the highest peak point in the QRS complex and it is the most prominent features of ECG signal. It is a key part of ECG signal which is very useful for detection of cardiac disease. The QRS complex reflects the activity of heart at the time of ventricular contraction. Hence it is used for heart rate calculation and determination of heart rate variability. The R-peak also used for detection of other features of ECG signal like, P wave, Q-point, S-peak, T wave, ST segment etc. Different algorithms are available for detection of R-peak index.

In derivative based R-peak detection technique second derivative of ECG signal is used with automatic thresholding [39]. Sliding window and moving average (MA) method can be used for this pupose. In this method the steepest windowed gradient is evaluated by using the sliding window and moving average method [40].

The improved Tompkins differential method can detect the R-peak by applying amplitude detection algorithm and differential threshold method. In this method the duration of QRS complex is measured [41]. Hilbert-transform (HT) and moving average (MA) filter are used as R-peak detector. Basically the Shannon energy (SE) envelope is extracted by using zero-phase filter and the SE envelope is used to find out the local maxima by detecting positive zero-crossing point (ZCP). Here Hilterbert transform is applied to find out the positive ZCP of SE envelope. A MA filter also introduces for reduction of positive and negative drift of ZCP. Finally the index of local maxima are used to find out the approximate location of R-peak index [42],[43].

Wavelet based methods are another approach for R-peak detection. In this method the signal is decomposed into multiple level and the R-peak is detected from the predefine wavelets. Discrete

wavelet Transform (DWT) is one of the popular wavelet based R-peak detection method. In case of DWT method a filter bank tree is introduced for decomposition and reconstruction of ECG signal [43],[44],[45],[46].

The morphology of each ECG beat are different. Thus for clinical analysis and detection of cardiac disease, feature extraction plays a important role. Alongwith R-peak point, other features of ECG beat are P-wave, Q-peak, S-peak, T-wave, PR segment, ST segment. The amplitude and duration of these peak points and segments are very important features to indentify and classify a beat whether it is a normal rhythm or a diseased beat.

Apart from these feature many features are available in ECG beat for analysis. These features can be extracted by different feature extraction tools. In wavelet based method like DWT based method where the wavelet coefficients are used as features [47],[48],[49],[50].

Statistical method is based on the criterion of slope and magnitude imposed between the sample data. In this method at first the R-peaks index are detected and on the basis of R-peak position the other feature points are located by upsearch and downsearch method [51]. R-peak can be detected by using double difference and RR interval processing. Here sorting and thresholding are done on the squared double difference ECG signal to locate the approximate QRS position. Then compare the relative magnitude of QRS region and use the RR interval for esuring the exact location of R-peak [52]. PCA also used for extraction of R-peak by normalizing the ECG data to zero mean and unit variance [48],[52],[53].

Neural network (NN) based models are very effective for feature extraction and learning. In NN model each node is fully connected with another node to create a completely dense and complex network. Autoencoder is this type of feature extraction tool. It can be trained by supervised or unsupervised learning method [54],[55]. As each node are interconnected it can extract most important features of ECG signal. These features are used in different type of model such as compression model, classification model, synthesis model etc. for clinical analysis.

Analysis of ECG signal can be divided into three major categories namely synthesis of ECG signal, ECG compression and ECG disease classification.

2.4. ECG Modeling :

ECG signal contains most important information regarding the activity of heart. Thus, modeling is very important tool for information analysis of ECG signal. Mathematical model is very useful for representation of cardiac activity to uderstand the behaviour of signal, thus it can improve the quality of signal. The model parameters are used for compression of ECG signal and classification of ECG signal. A number of methods are available for modeling of ECG signal.

ECG is a nonlinear signal it can be modelled by dynamic nonlinear model. Here masking function is used and modulated by harmonic series. A baseline drift is introduced in this model and the ECG signal is reconstructed by model parameter [56]. In polynomial method for ECG modeling, polynomials of degree 3 was used which includes spline function for interpolation of ECG signal and represent the ECG signal by second order quadratic polynomials [57]. Spectral method also similar to the high degree polynomial. In this method, decomposition of signal is done into a set of orthogonal polynomial [57]. The polynomial spline function are used for morphological modeling using decomposition [13],[37],[58],[59] and development of cardiac simulator [12]. Piecewise nonlinear mixed effect model is very effective to examine the cardiac activity of patient [60].

Fourier model is an old and popular mathematical modeling technique. ECG signal is a periodic signal which is consisting of segmented section like PR segment, QRS region, ST segment. These segments

are represented by Fourier harmonic components [61],[62],[16],[4],[63],[15]. ECG signal consisting of wave like P wave, QRS region, T wave and U wave.

The waveforms can be modelled by Gaussian model [64],[65],[17],[66],[67],[15]. Work also observed where Gaussian combination model (GCM) was used for ECG modeling. In GCM model Gaussian function was fitted around the extrema and local minimum error of ECG signal. The range of Gaussian fittings are measured by Zero crossing and minimum bank method [68].

Recently, few statistical methods like autoregressive (AR) model, Auto regressive moving average model (ARMA), Auto regressive integrated moving average model (ARIMA) are used for synthesis of ECG signal. Among them ARIMA is most suited ECG modeling technique as it is suited for nonlinear time varient signal. AR model used to extract features from ECG signal and further the features are used for classification [69],[70],[71],[72]. Generalised ARMA model extract the features of ECG signal and the features are used for ECG classification [20]. ARIMA model used to model approximate component of decomposed ECG signal and ARMA model used for detail components [21]. ARIMA model is very useful for modeling of ECG signal.

2.5. ECG Compression

ECG signal of critical patients under monitoring are very important to store. Everyday many patients are admitted in the hospital and the data of each patients have to store for pathological analysis and proper diagnosis. Hence a bulk memory is required for this purpose. Practically it is not possible to create a vast memory unit. The only solution is compression of ECG signal [73]. ECG compression also helpful for transmission of clinical information from remote location to the clinical for monitoring and disease detection [74]. Another most important application is efficient storage of data for future clinical study and research. There are many methods available for compression of ECG signal but the desired model is quality-controlled method. The reconstruction quality is an important parameter to preserve clinical information. Wavelet energy based diagnostic distortion (WEDD) localize the error in feature space between the original and reconstructed signal [75].

A wavelet transform based method was published where Huffman coding was applied to improve the compression ratio (CR) [76]. ECG can be compressed by linear or nonlinear method. Slantlet transform (SLT) is a linear transform method lifting wavelet transform (LWT) is a non-linear transform method. Both the methods are transformed coefficient based and thresholded by bisection algorithm to match the predefined user specified percentage root mean square difference (PRD). The LWT method also applied with normalization and found that the CR gives better result than without normalization method [77]. A compression may be lossy or lossless [78]. Lossless ECG compression is desirable to preserved all clinical information as in case of lossy compression technique there is probability of loss of important information. ECG compression using non-recursive WT method is a quality-controlled compression technique. Quality controlled means quality of reconstructed ECG signal after compession. ECG is a non-stationary signal thus the reconstruction quality should be guaranteed for diagnostic use [79].

EMD method was applied with WT method to compress ECG signal. EMD extracts the significant components of ECG signal and the WT coefficients were quantized by dead zone quantization. The transform coefficients were coded by run-length encoding (RLE) method and the reconstructed ECG signal was similar to the original signal. In tunable-Q wavelet (TQWT) method, dead zone quantization was used for quantization of transform coefficients and converted into code by run-length encoding method [80].

Singular value decomposition (SVD) is a efficient method for decomposition of ECG signal. It is a lossy method with high compression ratio [81]. Discrete Anamorphic Stretch Transform (DAST) with DWT method performed as a ECG compression technique [82]. A linear filter was used as phase

recovery unit. But due to recovered phase and high compression ratio the reconstructed signal became inaccurate. Hence an adder with phase recovery unit was applied to fix the problem. QRS segment bank-based compression method is another approach for lossless ECG compression. In this method the QRS and non-QRS region of ECG signal are separated and segment banks were developed. Both segment banks were coded by lossless algorithm to compress the ECG signal. The main aim was lossless but 2% loss present in this work [83].

In 1D DWT based method ECG signal is compressed on the basis of sensing metrics like, percentage root mean squared difference (PRD), root mean square error (RMSE), signal-to-noise ratio (SNR). This method offered better result than the conventional method [84].

2.6. ECG Classification

ECG classification is a basic application of signal processing. It is very useful for clinical analysis and diagnosis purpose. The main objective of ECG classification is detection of different heart condition of cardiac patient for proper treatment. In the beginning of research in this area binary classification were performed where the normal and abnormal beats were identified [85], [86]. But the classifiers are not suitable to identify the different categories of abnormality. But a cardiac cycle may contain different abnormal beat along with normal sinus rhythm (NSR). Hence, multiclass classification plays a vital role to overcome the shortcomings. Multiclass classification is a most challenging job as the classifier have to identify different beat annotation of ECG signal. The classifiers are trained by the feature of ECG signal, hence to achieve the satisfying accuracy, features are most important parameter [87],[88]. Many works are reported in this area.

In a literature, share counter was used for reduction of memory allocation. This algorithm changes the periodical parameter on the basis of morphological change in QRS region [89]. Machine learning method takes a vital place for classification of ECG signal. Support vector machine (SVM), K-nearest neighbor (KNN), random forest, decision tree, Gradient boosting etc. are different types of machine learning based method. Random forest method achieve 79.76% classification accuracy [90],[91]. In conjunction of SVM and Gradient boosting for ECG classification achieved maximum 84.82% [92]. Neural network (NN) method with back propagation yields 96.77% accuracy for binary classification [93].

In a published work the appropriate components of ECG were extracted by independent component analysis (ICA) method. The components were used for calculation of Daubechis wavelet to select the proper features for training of classifier model. Three types of classifier model were trained by these feature and models are KNN, radial basic function (RBF) and multilayer perceptron (MLP). MLP yield the best result among these methods [94]. The most prominent feature of ECG signal is R-peak. Thus, the features related to R-peak are QRS complex and R_R interval [95]. These two features were used with static feature of ECG beat. The skewness and Kurtosis are static features which represent the shape of cardiac signal. These four features were used to train the SVM and MLPNN based classifier and the classification accuracy was 85% [96],[97].

In a multiclass classification approach WT was used with probabilistic neural network (PNN) to classify six ECG beat type. The WT method extract 11 features from each beat of ECG signal and trained the PNN to predict the class of unknown ECG beat. It yields very high accuracy i.e. 99.65% [98]. WT method widely used as a feature extraction tools. It was also used with Kohonen self-organization map to classify six classes of ECG signal [99], [100].

Adaptive wavelet network (AWN) is consisting of two subnetwork architecture. The Morlet wavelets were used to extract the features whereas PNN was employed to identify three classes among ectopic, bundle branch ectopic and ventricular ectopic ECG beat [101], [102].

Multi-objective particle swarm optimization (MOPSO) is a feature extraction method which extract the best fitted features from the signal. It was designed in to add the macro of F1 loss and the normalized dimension. The optimization objectives were calculated as minimum of fitness function. The features were trained different types of classifier model such as KNN, SVM, MLP, extra decision tree and random forest [103], [104], [105],[106], [107]. Among these models, MLP was given best result in terms of class prediction accuracy. It is suitable for single lead ECG signal [108], [109], [110].

In another approach four types of classifiers learning capacity was compared. The classifier models were based on KNN, fuzzy logic based, deterministic analysis and neural network. This work was tested by five types of ventricular complexity: NSR, premature ventricular contraction (PVC), left bundle branch block (LBBB), right bundle branch block (RBBB) and paced (P) beats. They observed that the method assessed by local learning sets achieved higher accuracy than the basic leaning set and as a result the classification accuracy was reduced. While the global learning set was given worst result in terms of ECG class prediction accuracy [111].

In a literature four most used methods were applied for ECG class prediction and the methods are SVM, ANN, Reservoir computing with logistic regression model (RC) and linear discriminant model (LD). In this approach the heart beat was divided into different segment and the features were extracted and develop a learning algorithm for the classifiers. This method classified five types of beats, normal, ventricular ectopic beat (VEB), supraventricular ectopic beat (SVEB), fusion beat and unknown beat (Q) [112],[113].These five beat were classified by another method namely dynamically biased long short term memory (DB-LSTM) and it secured 96.74% accuracy [114],[115].

EMD combined with LD for classification of five types of ECG beat and it obtained 87% accuracy [116]. The shortcomings of machine learning algorithm are improved by deep learning method. MLPNN is deep learning-based method and it was observed that MLPNN gives better result than machine learning methods.

1D convolution neural network (1D-CNN) method is another important deep learning technique which achieve best result than the prior methods. In a study 1D-CNN method was compared with other method like MLPNN, SVM, random forest, gradient boosting and found that 1D-CNN achieve 99.43% accuracy which is very high and acceptable for real time application [117], [118]. 1D-CNN also effective for detection of cardiac morbidities in a ECG-PPG fused signal with 80% accuracy [119],[120].

In our research work, we developed the programs in MATLAB and Python environment. Many books are studied to learn the research methodology [121],[122],[123],[124] coding technique for mathematical modeling [125],[126], time series forecasting [127], hyperparameter tuning [128], machine learning [129], [130],[131] and deep learning [132], [133].

2.7. Objective of the Thesis:

We have done survey on the application of ECG signal processing and studied literature based on modeling, compression and classification of ECG signal. We have focused on the research gap and find the following scope:

1) The above researches were carried out by MIT-BIH arrhythmia database (mitdb). From a decade the research uses same database which may raise a database biasness in the research.

2) ECG modeling was done by various conventional method like polynomial, orthogonal polynomial, spectral method, Gaussian model, Fourier model etc. had been used. We have developed novel method for modeling of ECG signal with negligible reconstruction error.

3) We have developed a cardiac simulator which is very effective to generate 10 different types of synthetic ECG signal. This device is very useful for medical professional and students for training purpose.

4) We have developed an intelligent compression model using ARIMA model which can compress ECG data without any loss of clinical information. In this work deep learning model i.e. MLPNN was employed to predict the best hyperparameters of ARIMA model.

5) We have developed a fused model to classify six ECG signal of mitdb data. In this approach PCA was used with MLPNN for ECG classification. As most of the works are validated by mitdb signal, we have used this database to compare our proposed model with previous published work.

6) We have developed a novel method for classification of a new database i.e. Medical Information Mart for Intensive Care III (MIMIC-III) database under Physionet [134]. The model was designed by deep auto encoder (DAE) and 1D-deep convolution neural network model (1D-DCNN). The work also used for classification of 10 categories of mitdb data. MIMIC-III data along with mitdb ensures the performance of this model. As the model is evaluated by multiple types of database, it becomes more reliable and generalize. The model is free from data biasness. Hence it can be used for real-time application.

Chapter 3

Data Collection/Acquisition and Preprocessing of ECG Signal

ECG signal acquisition and fiducial point extraction are the most important steps for analysis of cardiovascular signal. ECG is a non-invasive tool for monitoring and diagnosis of cardiac problem. It can be captured very easily from the subject with a minimum cooporation. MITBIH arrhythmia database under Physionet database is widely used for analysis of arrhythmia. This database is easily available and a large variety of abnormality are present here thus it is very popular for research. Other than this database, PTB Diagnostic ECG database (ptbdb) and Medical Information Mart for Intensive Care III (MIMIC III) database also available in Physionet. Fiducial extraction is a basic requirement for dimensionality reduction and compaction of data for analysis of ECG signal. Fiducial points are main features of a signal which represent the characteristics of the signal. Each fiducial point has a certain shape and width with a specific duration and amplitude. The duration and amplitude define the range of a healthy waveform. The position of fiducial point helps in analysis and diagnosis of cardiac problem. Thus, fiducial point extraction is very significant for clinical analysis of ECG signal.

3.1. MIT-BIH Arrhythmia Database (mitdb):

Between 1975 and 1979, the Beth Israel Deaconess Medical Center created a database of 48 ECG recordings for the analysis of arrhythmia. This record was developed by collecting ECG data from 47 subjects (22 women and 25 men) which was studied by BIH Arrhythmia Laboratory of aforesaid medical center. This database contains two channels ECG recordings of 48 half excerpts. Among them twenty three recording were collected randomly from a mixed database of 4000 24 hours ambulatory recordings. In these 23 recoding 60% data was captured from inpatients and 40% was collected from outpatients. The balance twenty five recordings were collected from same set but these recording contains less common arrhythmia signal.

The sampling frequency of these signals is 360 Hz. The resolution of the signals are 11 bit with a voltage range of 10mV. These data were annotated by two or more cardiologies. Table 3.1 shows the the represing symbol and meaning of each ECG annotation.

Table 3.1. Symbol and meaning of each ECG annotation

Symbol	*Meaning of ECG annotation*	*Symbol*	*Meaning of ECG annotation*
· *or* N	Normal beat	!	Ventricular flutter wave
L	Left bundle branch block beat	]	End of ventricular flutter/fibrillation
R	Right bundle branch block beat	e	Atrial escape beat
A	Atrial premature beat	j	Nodal (junctional) escape beat
a	Aberrated atrial premature beat	E	Ventricular escape beat
J	Nodal (junctional) premature beat	/	Paced beat
S	Supraventricular premature beat	f	Fusion of paced and normal beat
V	Premature ventricular contraction	x	Non-conducted P-wave (blocked APB)
F	Fusion of ventricular and normal beat	Q	Unclassifiable beat
[	Start of ventricular flutter/fibrillation	|	Isolated QRS-like artifact

In this database fifteen types of ECG beats are available. The most commonly used beats are Normal beat (N), Left bundle branch block beat (L), Right bundle branch block beat (R), Atrial premature beat (A), Premature ventricular contraction beat (V), Paced beat (/). In our research study, we have worked with few less common beats like Aberrated atrial premature beat (a), Nodal (junctional) premature beat (J), Fusion of ventricular and normal beat (F) and Fusion of paced and normal beat (f).

3.2. PTB Diagnostic ECG Database (ptbdb)

PTB Diagnostic ECG database (ptbdb) were collected from 12 standard leads along with Frank XYZ leads. This database contains 549 ECG records of 16-bit resolution with 0.5 μV/LSB. The data were collected from 290 subjects (209 men and 81 women) of age between 17 to 87 years. These signal are 16 channels signal where 14 channels are for ECG, one for respiration and one for line voltage. The signals were collected from 12 conventional leads viz., I, II, III, aVR, aVL, aVF, V1, V2, V3, V4, V5, V6 and three Frank leads viz., vx, vy and vz. The signals are available upto sampling rate of 10 KHz. It contains nine types of cardiac signals from 268 database and 22 records are unidentified. The table 3.2. shows different class of ptbdb database.

Table 3.2. Class of ECG signal under ptbdb database

ECG class	Number of subjects	ECG class	Number of subjects
Myocardial infarction	148	Myocardial hypertrophy	7
Cardiomyopathy/Heart failure	18	Valvular heart disease	6
Bundle branch block	15	Myocarditis	4
Dysrhythmia	14	Miscellaneous	4
Healthy controls	52		

3.3. Medical Information Mart for Intensive Care III (MIMIC III) Database

Beth Israel Deaconess Medical Center developed a new database using the unidentified health issues, known as Medical Information Mart for Intensive Care III (MIMIC III). The data were collected from the patient admitted in the intensive care unit (ICU) of this hospital. The data were collected during 2001-2012. It contains health information of more than forty thousand patients. It is a open nature and widely accessible database and available at PhysioNet. Due to its nature it can be used internationally under a agreement of data use. The open nature allows the database to improve and reproduce the clinical studies.

The data were captured during routine checkup of subjects under hospital care thus the database is not assciated with additional burden on care givers or any interference with the workflow of care givers. The sampling frequency of the data is 125 Hz. The database has data with high temporal resolution and it contains electronic documentation, lab result, result associated with motoring the trend and waveforms.

It contains data of 53,423 adult patients who were admitted in critical care during 2001 to 2012 and 7,870 data from newborns who were admitted during 2001 to 2008. It covers data of 38,597 distinct adult patients and 49,785 data from admitted patients to the hospital. Among the database, 55.9% are male patient, median age of patient i.e. 65.8 years (age between 52.8 – 77.8 years) and 11.5% is inhospital mortality. It was noticed that the median length of stay in ICU is 2.1 days and median length of stay at hospital is 6.9 days. Table 3.3. Shows the class of data available under MIMIC III database.

In our research study, we have considered five categories ECG signal from this database namely, normal (NORMAL), arrhythmia (ARYTH), hypertension (HYPER), dilated cardiomyopathy (DCM) and right bundle branch block (RBBB).

Table 3.3. Class of ECG signal under ptbdb database

Class of data	*Description*	*Class of data*	*Description*
Billing	Coded data recorded primarily for billing and administrative purposes. Includes Current Procedural Terminology (CPT) codes, Diagnosis-Related Group (DRG) codes, and International Classification of Diseases (ICD) codes.	Laboratory	Test result related to blood chemistry, urine analysis, hematology, and microbiology.
Descriptive	Demographic detail, admission and discharge times, and dates of death.	Medications	Administration records of intravenous medications and medication orders.
Dictionary	Look-up tables for cross referencing concept identifiers (for example, International Classification of Diseases (ICD) codes) with associated labels.	Notes	Free text notes such as provider progress notes and hospital discharge summaries.
Interventions	Procedures such as dialysis, imaging studies, and placement of lines.	Physiologic	Nurse-verified vital signs, approximately hourly (e.g., heart rate, blood pressure, respiratory rate).
		Reports	Free text reports of electrocardiogram and imaging studies.

3.4. ECG Signal Acquisition by Biopac® Student Lab (BSL) System:

ECG signal can be acquired from patient by using Biopac® Student Lab (BSL) system. The BSL MP45 System is a simple, 2-channel biomedical data acquisition system that can be configured (acquisition speed, ranging etc.) from the BSL software. It can acquire both ECG and PPG signal from the patient. At a time, ECG signal can be acquired from two subjects. Fig.3.1. shows the accessories of Biopack two-channel Student Lab.

Fig.3.1. Biopack Two-Channel Student Lab (BSL)

Fig. 3.2. : ECG signal acquisition from subject

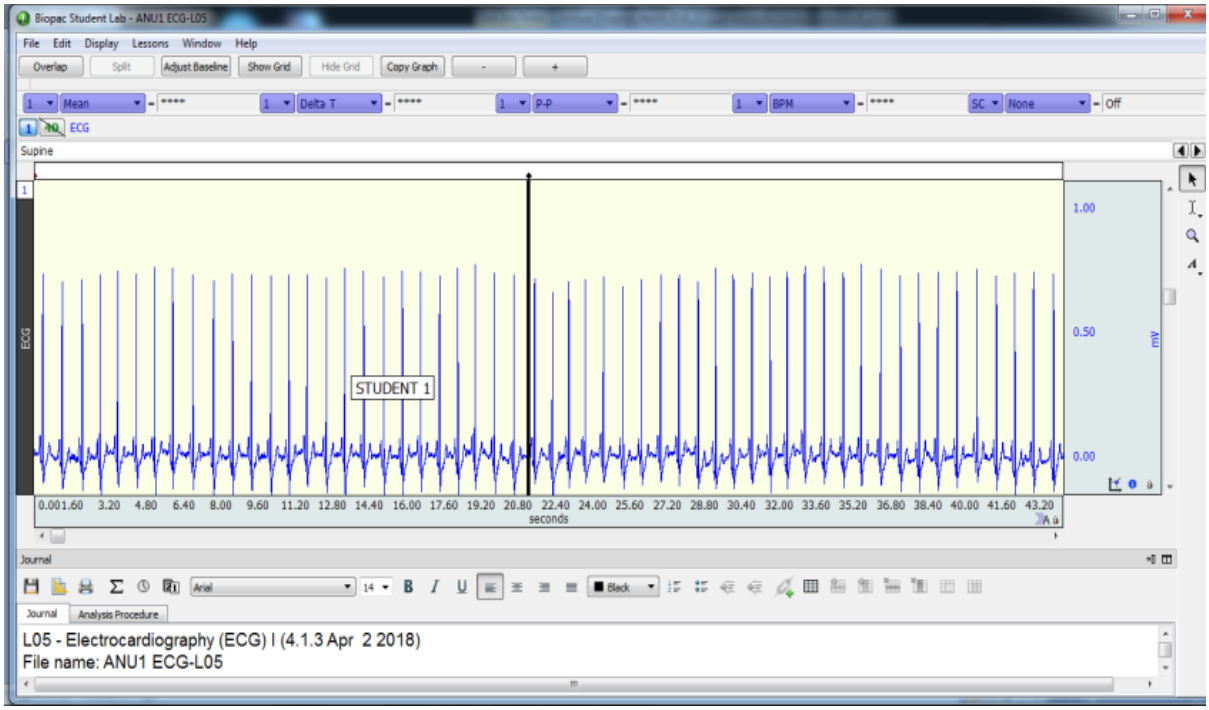

Fig. 3.3.: ECG signal acquired using BSL System

The BSL system includes:

1) MP45 2 channel data acquisition system (USB powered)
2) BSL 4 Software (Lessons and *PRO*) BSL Laboratory Manual MANBSL4

3) Searchable PDF Manuals and Tutorials (BSL *PRO*, Instructor's Guide, Answer Key, etc.)
4) 2 x Electrode Lead Sets – SS2LB
5) Disposable Electrodes, pack of 100- EL503
6) Electrode abrading pads (pack of 10)- ELPAD
7) Headphones (monaural, wide-response) – 40HP

The BSL System includes data acquisition hardware with built-in universal amplifiers to record and condition bioelectric signals. The data acquisition system receives the signals from biomedical sensors. BSL software then displays the numbers as waveforms on the monitor. The data acquisition system connects to a PC running Windows via USB. The MP45 unit has two input channels. Electrodes, transducers, and/or input/output devices connect to the MP data acquisition unit so students can record data from their own heart signals or from other subjects. Fig. 3.2. shows the ECG signal acquisition from the subject using BSL System and Fig. 3.3. shows the collected raw ECG signal from subject and feed into the computer for monitoring and to save for clinical analysis and diagnosis purpose.

3.5. Arrhythmia:

Arrhythmia also called as cardiac arrhythmia. It is occur due to irregular heart beat. It may be life threatning or harm less [135]. The cardiac cycle may be too fast or loo slow. The healthy cardiac signal is known as normal sinus rhythm. The heart beat of more than 100beats per minute in adult at resting condition is known as tachycardia. For adult, the heart at resting condition with heart rate slower than 60 beats per minute is known as bradycardia. Few cardiac arrhythmias have no physiological symptoms. The symptoms of arrhythmia are palpitations or a pause between consecutive hearbeats. In case of serious case the common symptoms are shortness of breath, lightheadness, chest pain, passing out, lack of conciousness. The arrhythmia without any symptoms may become complicated due to stroke or heart failure which may cause of sudden death. The most prominent arrhythmia are as follows:

a) Atrial premature contraction beat (APC)
b) Premature ventricular contraction beat (PVC)
c) Paced beat (P)
d) Left bundle branch block beat (LBBB)
e) Right bundle branch block beat (RBBB)
f) Aberrated atrial premature beat (a)
g) Nodal (junctional) premature beat (J)
h) Fusion of ventricular and normal beat (F)
i) Fusion of paced and normal beat (f)

3.5.1. Normal sinus rhythm or Healthy ECG Signal:

A normal sinus rhythm (NSR) is a healthy and regular cardiac cycle with heart rate between 60 to 100 bpm. It consists of a P wave which preceding every QRS complex with a consistent PR interval. The waveform of a typical NSR signal is shown in Fig. 3.4.

Fig.3.4.: Normal Sinus Rhythm (Images taken from www.physionet.org)

3.5.2. Atrial premature beat (APC):

A atrial premature contraction beat is an extra beat which is generated in the upper chamber of heart i.e. from atria. In that case the premature signals tells the heart to contract but due to the insufficient blood the heart cannot pumped out the blood. It feels like skip of a heart beat. It is most commom in people of all ages. The main cause of this type of beats are as follows:

a) Insufficient blood flow in heart
b) Injury in heart
c) Changes in heart structure such as hypertropic cardiomyopathy, coronary artery disease etc.
d) Consumption of alcohol, tobacco etc.
e) Side effect of certain medication for mental health or cardiac problem
f) Thyroid
g) Intake of caffeine

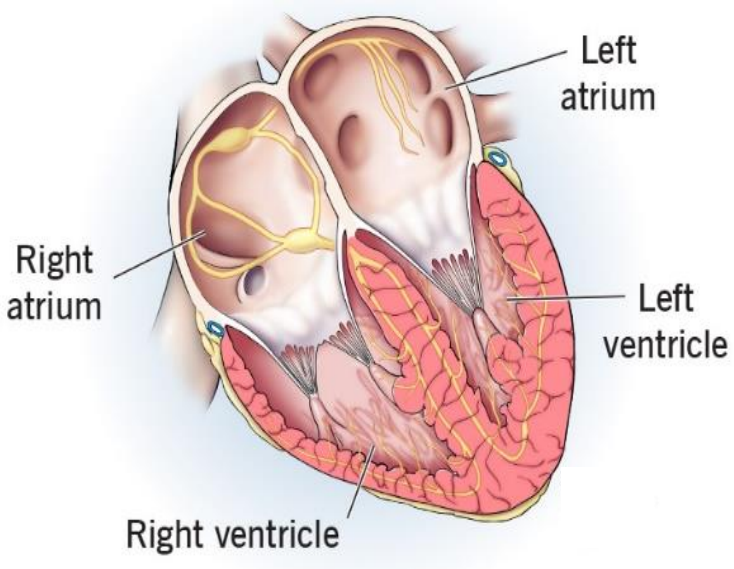

Fig.3.5.: Premature atrial contraction of heart (Images taken from https://my.clevelandclinic.org)

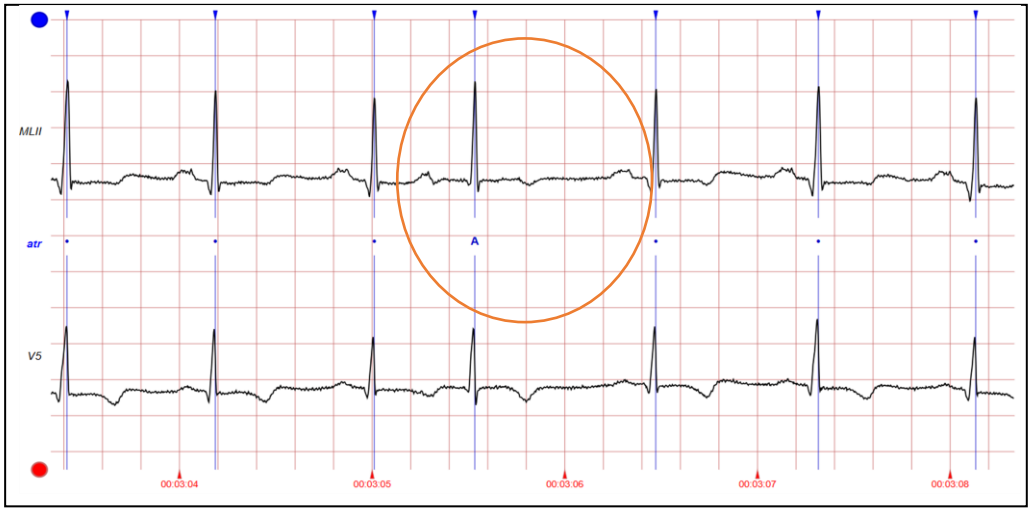

Fig.3.6. Atrial premature contraction beat (Images taken from www.physionet.org)

But basically treatment is not required for this phenomenon. The subject should contact with healthcare provider for precaution. The symptomps of this heart conditions are palpitation, shortness of breath etc. Fig. 3.5 shows the internal condition of heat due to atrial premature contraction and Fig 3.6. shows the typical pattern of atrial premature contraction beat. From this figure it is observable that duration of APC types of beats are more than normal beat. The beat becomes wider than normal.

3.5.3. Premature ventricular contraction beat (PVC):

Premature ventricular contraction (PVC) beat is orginated from ventricle or lower chamber of heart. It is also known as ventricle premature beat. It disrupts the normal cardiac rhythm and causes a pause in regular heart cycle. It casuses sensation of fluttering or skipped beat. It is also a common type of irregular heart beat.

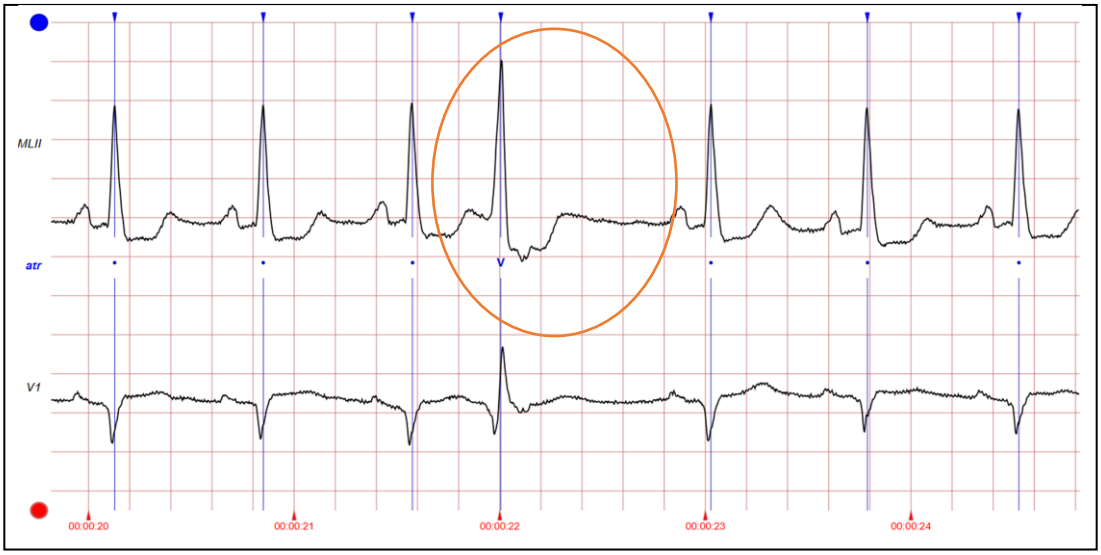

Fig.3.7. Premature ventricular contraction beat (Images taken from www.physionet.org)

The causes of PVC are as follows:

a) Advanced age
b) Hypertension, stress and anxity
c) High blood pressure
d) Associate with other cardiac problem
e) Intake of alcohol, caffaine, smoking
f) Side effect of certain medication

The ocassional premature ventricular beat is not harmful and not required any treatment. But the frequent presence of this beat may underlying serious cardiac problem. It may becomes risk factor for aged people and for cardiac patient like bundle branch block, hypokalemia, ischemic heart disease. It can be either atrial or ventricular. Figure 3.7. shows the typical pattern of PVC types of beat where the QRS complex becomes wider and the duration of beat larger than normal beat.

3.5.4. Paced beat (P):

Pacemaker is a arificial device that perform the task of heart's natural pacemaker. Paced beat is the electrical impulse originated from the pacemaker. In case of paced beat, pacemaker mediated arrhythmia is often seen. In pacemaker mediated arrhythmia, pacemaker plays a vital role. It involves a reentrant circuit where the pathway is formed by pacemaker. The paced beat can be of following types:

a) Atrial Paced (A Paced): In Atrial paced the beat, it is initiated in the atria and the spike of pacing is observed before the P wave on the ECG

b) Ventricular Paced (V Paced): In ventricular paced the beat is initiated in the ventricle and the spike of pacing is observed before the QRS complex on the ECG

c) Atrioventricular Paced (AV Paced): It intitiated by pacemaker in both atria and ventricle and the spike of pacing are observed before P wave and QRS complex on the ECG.

Fig.3.8. shows the arrhythmia due to paced beat. The pattern is different than the normal sinus rhythm.

Fig.3.8. Paced beat (Images taken from www.physionet.org)

3.5.5. Left bundle branch block beat (LBBB):

Left bundle branch block (LBBB) is a cardiac disorder which affect the conduction system of heart related to the left bundle branch. It leads to abnormal electrical impulse or delayed conduction through ventricle. The LBBB beat displays as wider QRS complex than normal i.e. duration of QRS complex is more than 0.12 seconds. Thus the morphology of regular beats of ECG signal is changed. It can be improved by regimented life style. According to the seriousness of heart condition a pacemaker may be needed or resynchronization therapy of heart is required to manage the condition. The usual symptoms are fainting, slow heart rate etc. The LBBB may cause due to different underlying conditions such as heart damage like heart disease such as coronary artary disease, heart attack due to myocardial infarction, heart infection, heart failure, high blood pressure etc.

This type of cardiac abnormality cannot be cured permanently. If the underlying conditions are not persists, medication is not required for only LBBB. The medication is required to control other issues like heart disease, heart attack, blood pressure etc. Fig. 3.9. shows the LBBB beats. It is oberved that QRS complex becomes wider and the T wave is distorted.

Fig.3.9. Left Bundle Branch Block beat (Images taken from www.physionet.org)

3.5.6. Right bundle branch block beat (RBBB):

The right bundle branch block (RBBB) occurs due to the delay or blockage in electrical conduction by the right bundle branch. The electrical signal is running behind the right side instead of both left and right side. As the both ventricles are not working at a same time, irregular heart beat is generated. The main cause of RBBB are as follows:

a) Myocarditis

b) Heart attack due to myocardial infarction

c) Catheterization at right heart or other medical procedures

d) Changes in branch structure like stretching etc.

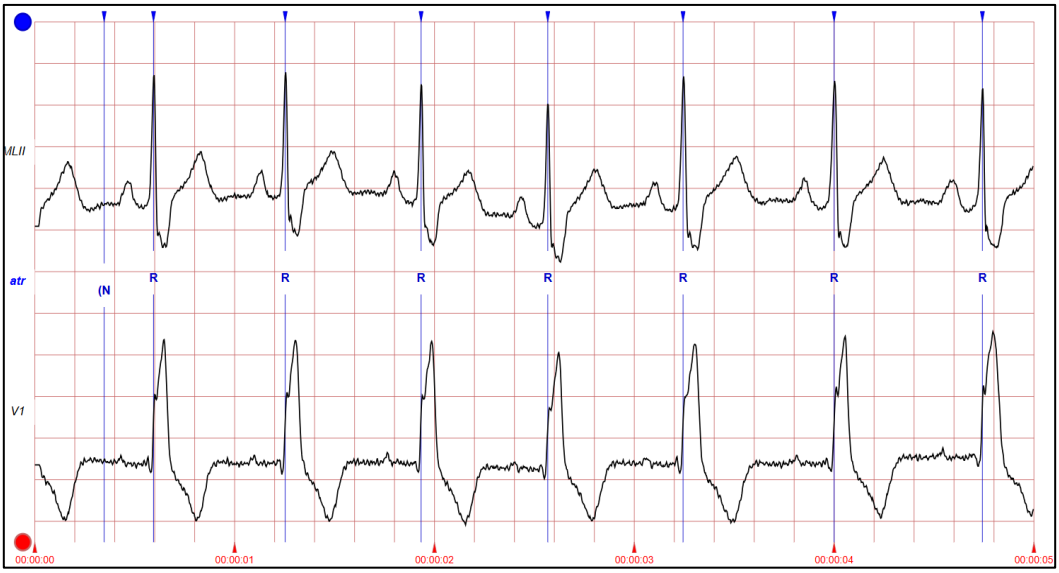

Fig.3.10. Right Bundle Branch Block beat (Images taken from www.physionet.org)

It results in change in shape of QRS and the pattern of ECG signal. The QRS region becomes wider than the regular pattern. It is a effect of mycardial disease and can cause mortality of cardiac patient. Fig. 3.10. shows the pattern of RBBB beats where the T waves becomes wider and the pattern is different than the normal rhythm.

3.5.7. Aberrated atrial premature beat (a):

The aberrated atrial premature (a) beat is originated from upper chamber of heart i.e. from atria and conducted through lower chamber i.e. ventricle of heart. The QRS complex becomes widen due to the abnormal pathway. It is a common cardiac issue and medication is not required. If aberatted atrial premature condition underlying with any other cardiac problem or medication issues, the patient should consult with healthcare provider for proper diagnosis. In Fig. 3.11. the pattern of aberrated atrial beat is shown. From this figure it is noticed that the QRS complex becomes wider.

Fig.3.11. Aberrated atrial premature beat (Images taken from www.physionet.org)

3.5.8. Nodal (junctional) premature beat (J):

Nodal (Junctional) premature beat is an extra beat which is originated at the junction of heart. The junction of heart means from the atrioventricular (AV) node. The AV node is middle point between upper chamber i.e. atria and lower chamber i.e. ventricle of heart. It is irregular heart beat and one type of arrhythmia beat. It is found in individuals who have a history of heart failure or other cardiac problems. Compared with other arrhythmia beat it is less common in people. The common symptoms of nodal junctional premature beats are lightheadness and fatigue.

Usually it does not required any medication but if it associated with other heart condition then proper treatment will be required. In Fig. 3.12. junctional pemature beat is shown along with other beats. The premature beat is marked by a elips. Due to this heart condition a premature peak is observed.

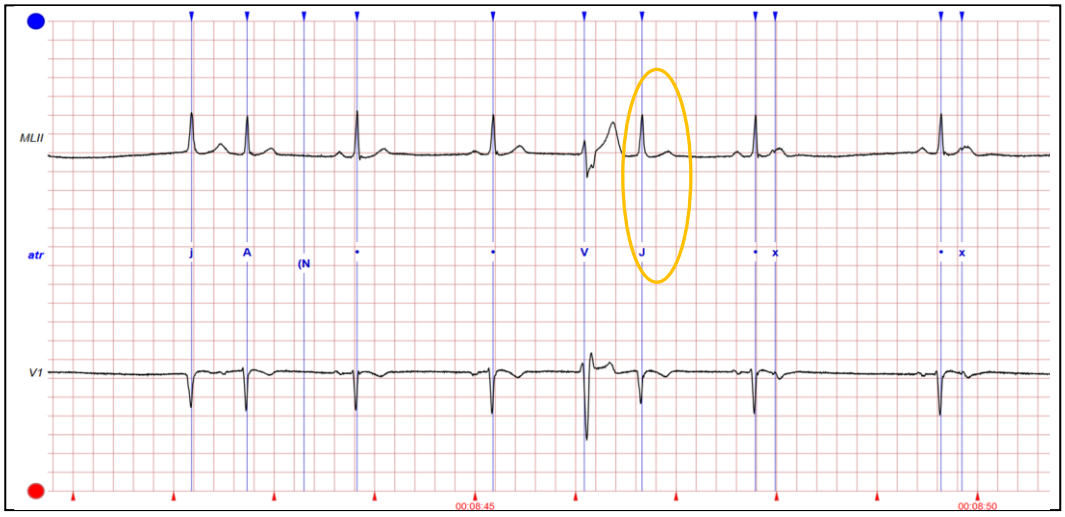

Fig.3.12. Nodal (Junctional) premature beat (Images taken from www.physionet.org)

3.5.9. Fusion of ventricle and normal beat (F):

Fusion of ventricle and normal beat are developed when the ventricles activates simultaneously by supraventricle impuse such as sinus nodel impulse and a ventricle impulse like PVC, as a result a hybrid QRS complex is recorded on ECG. The recorded beat is fusion of QRS morphology of normal sinus rhythm and an abnormal wide QRS morphology of ventricular beat. Fig. 3.13 shows the image of Fusion PVC beat.

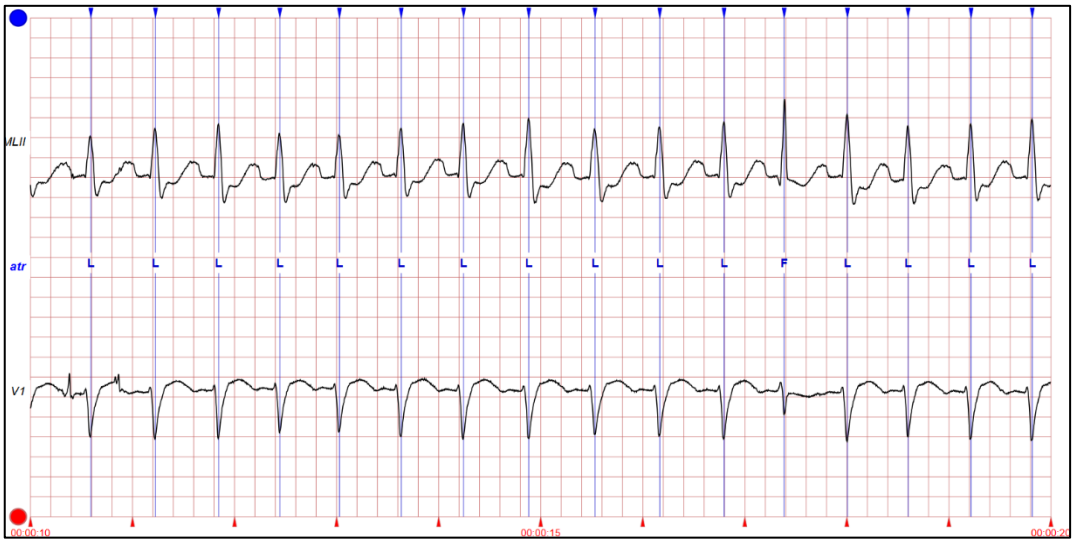

Fig.3.13. Fusion of ventricle and normal beat (Images taken from www.physionet.org)

3.5.10. Fusion of paced and normal beat (f):

Fusion beats are formed by the combination of pacemaker and normal sino atrial node. The both source simultaneously activate the ventricle and as a results hybrid QRS peak is generated. Actually when the impulse generated by the pacemaker coincides with impulse generated by heart's natural pacemaker, a fusion beat is generated. It is sign of dissociation of AV node i.e. when both atria and ventricles are beating independently. This heart condition arises due to malfunction of pacemaker or ventricular tachycardia. In Fig.3.14. the pattern of fusion beats are shown. From this figure it is noticed that the QRS complex is totally distorted and widen. Multiple peaks are observed instead of single R peak.

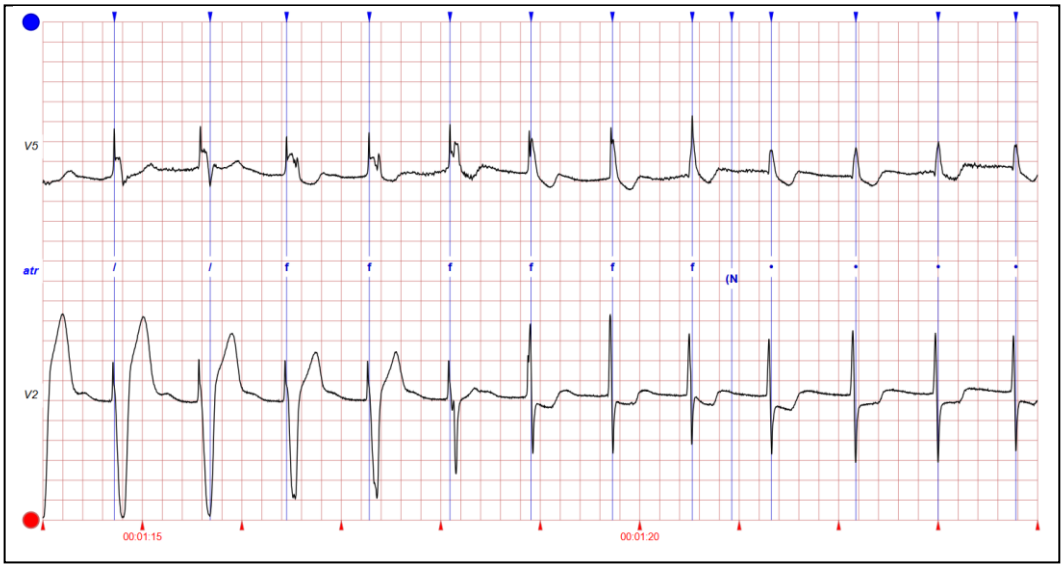

Fig.3.14. Fusion of paced and normal beat (Images taken from www.physionet.org)

3.6. Preprocessing of ECG Signal:

The preprocessing of ECG signal is an essential step before analysis of ECG signal. It can be performed in two steps, 1) denoising of ECG signal and 2) extraction of fiducial points and beat matrix formation.

3.6.1. Denoising of ECG signal:

3.6.1.1. Denoising of mitdb and ptbdb signal

The ECG signal can be contaminated by different types of higher and lower frequency noise. The range of higher frequency noise can be 50 Hz to more than 100 Hz and lower frequency noise is 0.5 to 0.6 Hz. In this approach, discrete wavelet transform (DWT) algorithm was used for denoising of raw ECG signal. DWT is a signal decomposition method which decomposes the signal into various frequency level for detail analysis in time and frequency domain. The mother wavelet is core of DWT method which is scaled and shifted for creating a set of wavelets. Wavelets capture different frequencies at different points in time. The signal was passed through high and low pass filters using wavelets $\psi(t)$ and scaling functions $\phi(t)$. ECG is a time-series signal and it is represented by x(n). The wavelets and scaling functions can be derived from weighted sum of shifted and detailed version of the function itself and can be expressed by :

$$\phi(t) = \sum_n h[n]\phi(2t-n)$$
$$\psi(t) = \sum_n g[n]\psi(2t-n) \quad (3.1)$$

The filtered signal is discretized into x[n] where, n is sample index. The discrete signal decomposition yields an approximation coefficient A (representing low-frequency content) and detail coefficients D (capturing high-frequency components).
The successive decomposition of A makes a pyramidal structure, shown in fig. 3.15:
The decomposed signal $x(n)$ can be expressed as under:

$$\begin{aligned} x(n) &= A_1(n) + D_1(n) \\ &= A_2(n) + D_2(n) + D_1(n) \\ &= A_3(n) + D_3(n) + D_2(n) + D_1(n) \\ &= \ldots\ldots \end{aligned} \tag{3.2}$$

Daubechis 5 (Db5) was used as mother wavelet. The raw ECG signal was decomposed into 12 scales using DWT method. With increase of signal decomposition level, each frequency band becomes narrower which increases the frequency resolution. It becomes easy to identify the superimposed noise in frequency band with higher resolution. The higher frequency noise is present in Level D1, D2 and D3 whereas the lower frequency noises are dominated in D10, D11, D12 levels. The denoised mitdb signals were reconstructed by level D4 to D9 and it is mathematically expressed as:

$$y_{ecg} = D9 + D8 + D7 + D6 + D5 + D4 \tag{3.3}$$

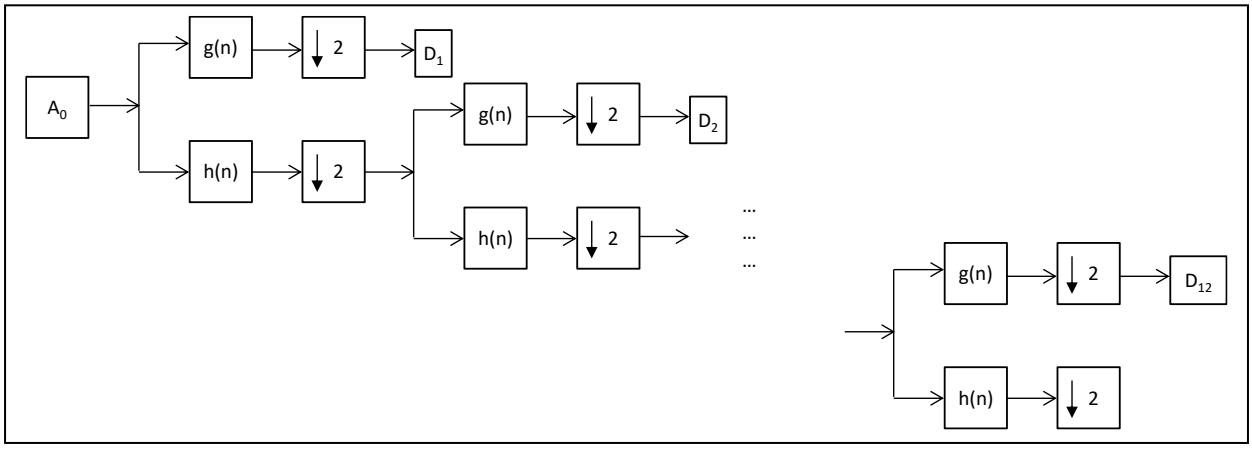

Fig. 3.15.: Signal decomposition using DWT

Figure 3.16. shows the noisy ECG signal, higher frequency noise, lower frequency noise and reconstructed denoised ECG signal. The ECG signal is chosen from mitdb database and the data ID is 106. From this figure we can observe the impact of higher and lower frequency noise. The higher frequency noise totally changes the distorted pattern of signal and the lower frequency noise shifts the baseline. Thus, it is a necessary steps in pre-processing of ECG signal. It is also noticed that the proposed method is able to preserve the important clinical pattern even after removal of those noises.

3.6.1.2. Denoising of MIMIC III signal:

ECG signal may be contaminated by higher or lower frequency noise at the time of signal acquisition. Hence, denoising is the first step of ECG signal processing. DWT method is chosen as noise removal tool. As the sampling frequency of MIMIC-III and mitdb databases are different, two denoising modules had been developed for this purpose. The raw MIMIC III data is distorted by 0.5Hz baseline noise and 50Hz higher frequency noise. It was denoised by 12^{th} level decomposition by DWT method. A biorthogonal Coiflet 3.5 was used as mother wavelet. This type of wavelet can capture both lower and higher frequency noise. It was observed that the higher frequency noise is presents in D1 and D2 level and the lower frequency noise is present in D9 to D12 level. Thus, the denoised ECG signal was reconstructed by combining D3 to D8 level. Fig. 3.17. shows the waveform of raw MIMIC-III signal, denoised ECG signal, higher frequency noise and lower frequency noise of normal ECG signal under

MIMIC III database. The reconstruction error i.e., MSE of denoised signal is in terms of 10^{-4} which is very negligible.

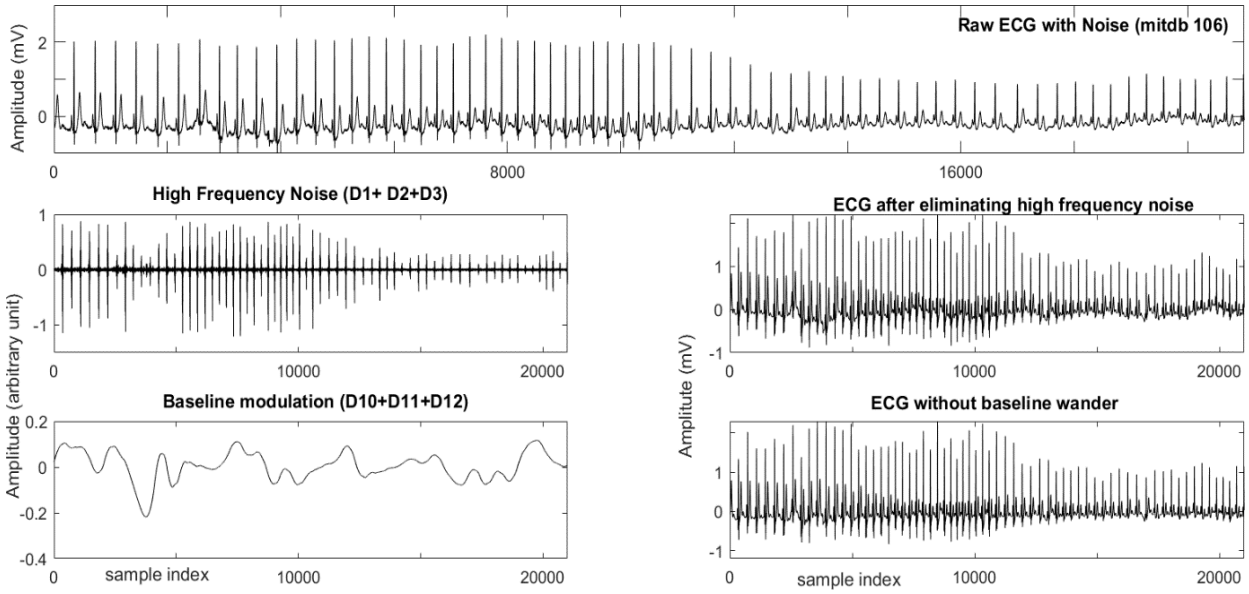

Fig.3.16.: Denoising of mitdb signal using DWT method

Pseudo code 1: ***Denoising of ECG signal by DWT method***

Input: noisyecg_signal.txt
Output: denoisedecg_signal.txt

x_{ij} = Noisy ECG signal, where x_{ij} represent i-th samples of j-th beat. //Load raw ECG signal
W = Discrete Wavelet Transform('db5')
decompose ecg signal= (x_{ij}, 'db5', level =12, mode = symmetric)
Calculate detailed coefficient and approximate coefficients = D1, D2, D3, …, D10, D11, D12 and A12
y_{ij} = waverec(coeffs, wavelet = 'db5') //coeffs = (D5, D6, D7, D8, D9); y_{ij} =Reconstruct denoised ecg signal
y_{ij} = D5 + D6 + D7 + D8 + D9
Save y_{ij} to file: denoisedecg_signal.txt

3.6.2. Extraction of fiducial points & beat matrix formation

3.6.2.1. Fiducial points extraction of ECG signal:

ECG signal is consisting of multiple beats. The morphology of each beat varies due to respiration. The pattern of each beat define the type of ECG. Each beat has few fiducial points. The amplitude, length and position of point define the characteristics of the beat. The basic fiducial point of ECG beat are P-wave, QRS-complex, PR interval, PR segment, R-peak index, R-R interval, J-point, ST-segment, ST interval, T wave, T-interval, U-wave.

P-wave is the first positive deflection in the ECG beat. It represents the electrical depolarization of atria. The duration of this wave is 80ms. The amplitude is maximum 2.5mV in limb node. In lead I and II it is in positive polarity and in aVR it is in inverted direction. Widen or notched P wave indicates abnormality in heart beat. Basically it suggest enlargement of left or right atria. Abnormal P-wave also

help to identify ectopic atrial beat and identify the source of abnormal rhythm other than SA node. The abnormality of P-wave can be identify from lead II, III and aVF.

PR interval is the interval between P-onset index to Q-onset index and it is with duration of 120-200ms. The abnormal PR interval i.e., greater than normal duration indicates delay in conduction through AV node. It can indicates first degree AV block.

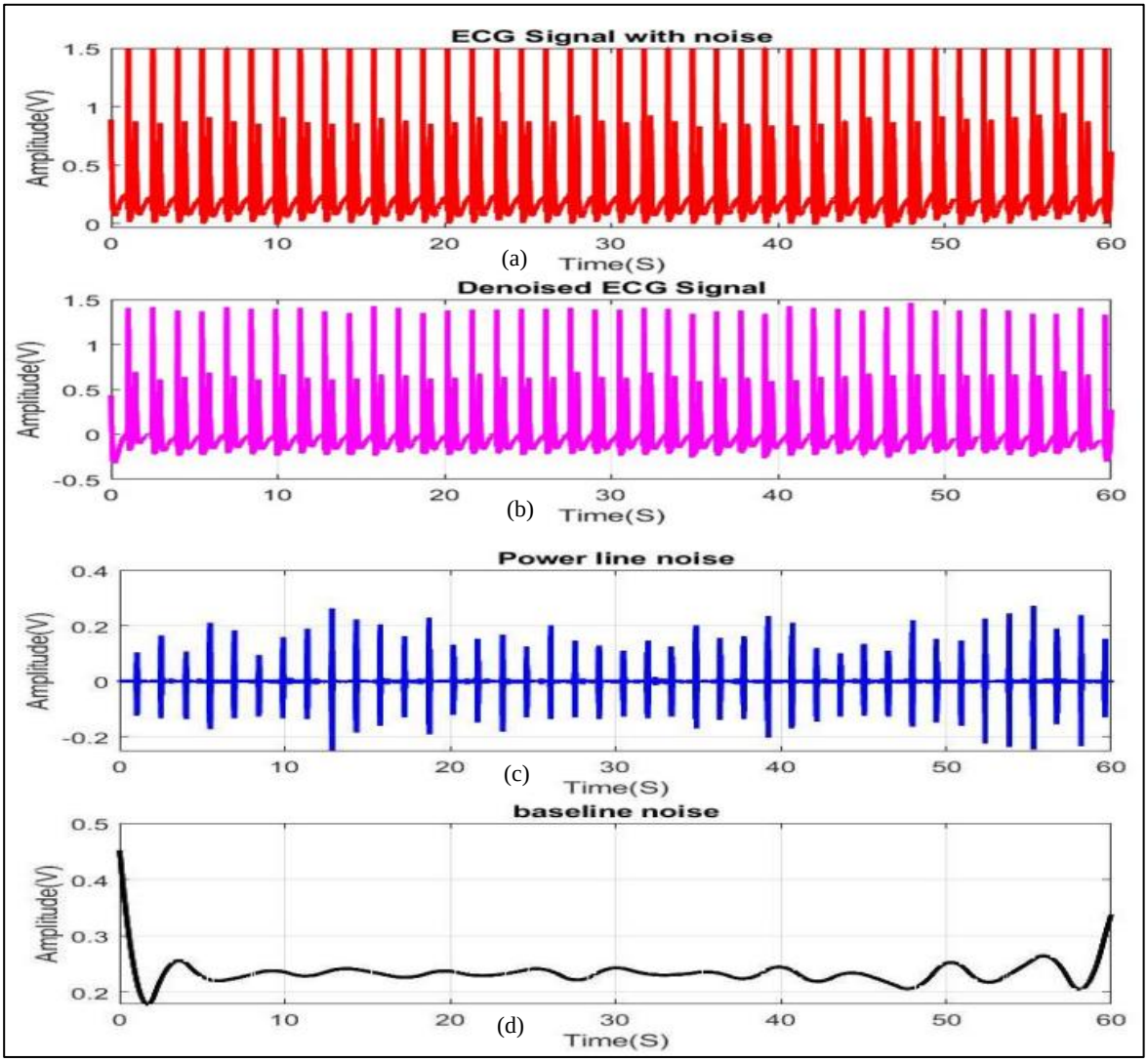

Fig.3.17.: Denoising of MIMIC III Signal using DWT method

PR segment is a flat line between P-offset to Q-onset index with 50-120ms range of duration. It is a delay of the electrical impulse in AV node before travels through the ventricles.

QRS-complex is most important feature of ECG beat. QRS-complex starts with a downward deflection known as Q-peak, a highest poisitive peak in the beat i.e. R-peak and another downward deflection before T-wave known as S-peak. The duration of QRS-complex is between 80-120 ms. The end point of QRS-complex is called as J-point. The QRS complex represents ventricular contraction and depolarization. It indicates different heart condition like, arrhythmia, myocardial infarction, electrolyte imbalance, conduction abnormality etc.

ST segment referred the segment between S-offset to T-onset and its duration is 80-120ms. It represents the intermission between the ventricular depolarization and repolarization. Elevation or depression of ST segment indicates cardiac abnormality like myocardial infarction, electrolyte imbalance etc.

ST interval is a interval between S-offset to T-offset with 320ms duration. It is isoelectrical interval between depolarization and repolarization of ventricle. Abnormality in this interval i.e. either depression or elevation indicates different heart condition like myocardial injury, myocardial infarction or myocardial ischemia.

T-wave is the positive deflection in the beat after QRS-complex with 160 ms duration. Abnormalities in the T-wave - such as prolonged, peaked, flattened, or inverted shapes—indicate various cardiac abnormalities. It basiclly signifies the abnormality like electrolyte imbalance, myocardial infarction, hypokalemia, ischemia, arhythmia etc.

QT-interval is a interval between depolarization and repolarization of ventricle with duration of 420ms. It is measured between Q-onset to T-offset. Basically it measures the electrical systole of ventricle. It is very important feature of ECG as prolonged QT interval may cause sudden cardiac arrest. It is also cause of electrolyte imbalance, arrhythmia, ventricular fibrillation.

U-wave is the small poisitive deflection after T-wave and before P-wave of consecutive beat. It indicates the electrical repolarization of Purkinji fiber and also the certain myocytes of ventricle.

Table 3.4.: Fiducial points of ECG beat

Fiducial Point	**Description**	**Duration**
P Wave	First positive deflection of ECG beat	80 ms
PR Interval	From the P-onset index to starting index of QRS complex	120-200 ms
PR Segment	From P-offset index to Q-onset index	50-120 ms
QRS Complex	Most prominent feature of ECG beat. Starts from downward deflection of Q and end at downward S deflection including R-peak	80-120 ms
R-R Interval	Interval between two consecutive R-peak index	0.6 – 1.2 s
J-Point	End point of QRS complex	-
ST Segment	From S-offset to T-onset	80-120 ms
ST Interval	From S-offset to T-offset	320 ms
T Wave	The positive deflection ECG after QRS complex	160 ms
QT Interval	From Q-onset index to T-offset index	420 ms
U wave	The small positive deflection after T wave and before P-wave of consecutive beat	-

Among the fiducial point R-peak is the most prominent and R-R interval is longest interval of length 0.6 – 1.2 sec. It represents the time between two consecutive R-peaks. It is most significant feature of ECG signal as it represent the duration of ventricular cardiac cycle. It indicates the cardiac health as it is very useful to measure heart rate, cardiac rhythm, heart rate variability etc. This interval helps in diagnosis of various cardiac problems like arrhythmia, atrioventricular (AV) block, ventricular tachycardia, atrial fibrillation.

3.6.2.2. R-peak detection of ECG signal:

R-peaks are the most prominent features of ECG signal. It is a positive deflection in the QRS region. It is used to calculate heart rate and find out the cardiac abnormalities. The morphology of R-peak indicates the ventricular hypertrophy condition. It is very useful for cardiac arrhythmia detection. In case of bundle branch block another upward deflection is noticed after actual R-peak. This deflection is known as R-prime (R'). Several methods are available for detection of R-peak. In this work we had used Pan-Tompkins algorithm and thresholding method. The pseudocode of thresholding method is given in Pseudocode 3.2. It works on the principal of thresholding process by analyzing width of signal, amplitude and slope of ECG signal. Figure 3.18. shows the flow diagram of R-peak detection. The ECG signal is successively passed through band-pass filter unit for ensuring noise minimization. The denoised signal is followed by a differentiator to understand the slope characteristics, an amplitude squaring unit is used for amplification of QRS region and followed by a moving window integrator. The high detection sensitivity was achieved by lower amplitude threshold and determine the R-peak location. Search back algorithm was applied to detect missed beat.

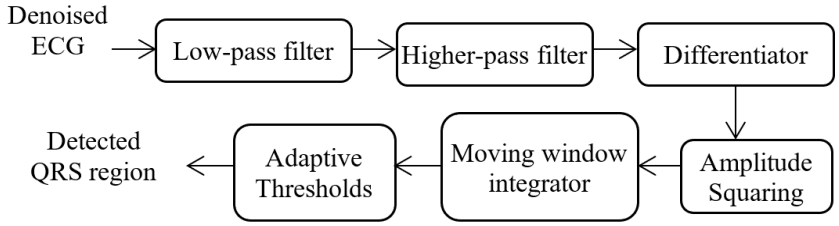

Fig.3.18.: Flow diagram of R-peak detection by Pan-Tompkins algorithm

Pseudo code 3.2.: ***Detection of QRS Index***

Input: denoisedecg_signal.txt (y_{ij})
Output: qrs_index [qrs_i, qrs_j]

```
Load denoisedecg_signal = y_ij
THR_SIG = max(y_ij) * 0.05                                  // Threshold signal
e = max(y_ij[peaks])
a = array(y_ij[peaks])
f = where(a==e)[0]
ss = prominence[f]
s1 = (0.75*ss)[0]
m = peaks
n1 = [j - i for i, j in zip(m[: - 1], m[1:])]
n11 = statistical.mean(n1)
THR_DIS = n11*0.3                                           //Threshold location
peaks, properties = find_peaks(y_ij, height = THR_SIG, distance = THR_DIS,
                                                            prominence = s1)
qrs_x = peaks
qrs_y = y_ij(peaks)
qrs_index = [qrs_x, qrs_y]
rpeak_size = size(qrs_x)
```

3.6.2.3. Beat matrix formation:

Beat matrix was formed by extracting each beat of ECG signal and stored them into a 2D matrix. But it is very significant to identify baseline index. Baseline index (BLI) lies between two consecutive R-peak index. The samples between two consecutive baseline index form a single beat. The R-R interval was divided into 2:1 ratio for detecting the location of TP segment. A 30 sec window was considered as the baseline index is located with minimum slope of absolute10-point around TP. Baseline index is the minimum amplitude between the T-offset and P-onset. A single beat is formed by the samples between two consecutive BLI.

The morphology and length of each beat varies from other, thus a 2-D beat matrix (B) was formed and the stored the beats in this matrix. The R-peak indices of each beat were aligned in a same row of matrix. The k^{th} beat (b^k) of L samples expressed by:

$$b_k = [y_{1k}..y_{1k}y_{2k}y_{3k}\ldots y_{rk}y_{(r+1)k}..y_{Lk}\ldots y_{Lk}]^T$$
$$\Rightarrow \quad b_k = [y_{jk}\ldots y_{rk}y_{(r+1)k}..y_{Lk}\ldots y_{Lk}]^T \qquad (3.4)$$

where, y_{jk} is the j^{th} sample and y_{rk} is the R-peak index of k^{th} beat. The beats are padded on both side to equalize the length of each beat in the matrix. There are p paddings with y_1 on the left side of beat i.e. at the starting of beat ($p=z_l-r$) and q paddings with y_L at the right side of each beat i.e. at the ending of beat ($q= z_r-r$), where, $z_l(z_r)$ is longest beat at left(right) side with respect to the R-peak index for the specific ECG signal under consideration.

Pseudo code 3.3.: ***Detection of Baseline Index for Beat Extraction***

Input: qrs_index [qrs_x, qrs_y]
Output: blp_index[blp_x, blp_y]

```
Calculate the difference between two consecutive R-peak (qrs_diff)
for x in qrs_diff:
{
x  = int ( round (x * 0.6)))
rseg.append(x)
rseg = rseg[0:len(rseg)]
qrs_x = qrs_x [0: rpeak_size - 1]
seg = qrs_x + rseg
seg_size = size(seg)
}
for k in range(0, seg_size - 1):
{
for  k1 in range((seg[k] – 20), (seg[k] + 20)):
{
slp_l = abs(y_ij[k1] - y_ij[k1 – 8])
xl.append(slp_l)
slp_r = abs(y_ij[k1] - y_ij[k1 + 8])
xr.append(slp_r)
mu_slp = (slp_l + slp_r)/2
let mn = 50
}
for  k1 in range((seg[k] – 20), (seg[k] + 20)):
{
if mu_slp <= mn:
{
mn = mu_slp
baseline point : mn_ind = k1
}}}
Append baseline points : blp_x.append(mn_ind)
```

Append location of baseline point: blp_y. append(y_{ij}[mn_ind])
Store the baseline index in a matrix: blp_index = [blp_x, blp_y]
B = [] \\ Blank matrix
B = b_{nxk} \\ Store each beat into the matrix; k represents beat length and Q represents number of beats

3.6.2.4. Fiducial point extraction for beat segmentation:

Fiducial point extraction is an essential step to extract PQ, QRS and ST segments of each beat. The beat vector b_k was divided into two segments, from BLI to R-peak index and from R-peak index to next BLI i.e. upto end of the beat. The P and T peak were labelled as the sample with maximum amplitude in those two segments. The lowest amplitude in PR segment was marked as Q-index and lowest amplitude in RT segment was marked as S-index. For the k^{th} beat (b_k),

$$(P_{peak})_k = \max(y_{1k} : y_{rk})$$
$$Q_k = \min\,[(P_{peak})_k : y_{rk}]$$
$$S_k = \min\,(y_{rk} : y_{Lk})$$
$$(T_{peak})_k = \max\,[S_k : y_{Lk}] \qquad (3.5)$$

The max(min) operator was used to extract the samples with highest(lowest) amplitude from the respective array.

Pseudo code 3.4.: *Fiducial Point Extraction of Beat*

Input: k^{th} Beat
Output: P_{pj}, Q_j, S_j, T_{pj}

B = b_{nxk} // B = beat matrix
F= b_j // j= j^{th} beat of beat matrix
xx=length(F)
TH_loc=xx*0.5
THR_SIG2 = max(F)*0.5
Detect_R_peak = [Rpeaks,Rpeaklocs]

//Divide the beat into two segments

e=length(F (1 : Rpeaklocs)) //Left side sample of R-peak
f=length(F (Rpeaklocs : end)) //Right side samples of R-peak

P_{pj} = max(e (1 : Rpeaklocs)) // P wave detection
Q_j = min(e(P_{pj} : Rpeaklocs) // Q wave detection
S_j = min(f(Rpeaklocs : end) // S wave Detection
T_{pj} = max(f(S_j : end)) // T wave Detection

Pseudocode 3.3. shows the fiducial point extraction process. The algorithm was implemented on lead II data, thus the P wave and T wave are positive. Each beat can be divided in three segments viz., PQ wave, QRS wave and ST wave. For each beat three matrices were formed using the samples of PQ, QRS and ST segment. In these matrices, the respective prominent fiducial points i.e., P, R and T were aligned in a same row of the respective matrix. Each matrix was padded by last samples.

Chapter 4

Development of Cardiac Simulator

4.1. Need and Significance of Cardiac Simulator:

Cardiac simulator is a computer based model which generates synthetic Electro Cardiogram rhythm. In our medical care system the first aim is patient safety and it can be achieved by reducing the medical error. Emerging of simulation software in the training of medical students offers a risk less and quality training. Thus the simulation software is developed to train the medical students and professionals like medical technicians. It can halp medical student and professionals to learn and identify common cardiac rhythms. Cardiac simulator can generates cardiac rhythm with different abnormality which can train student to check variety of cardiac conditions and disease. Emergency medical technicians can learn and sharpen their skills through the simulator. In the rural area, for the remote patient the trainned medical technicians can read and understand the ECG records and identify the cardiac problem for primary analysis. Hence, it becomes an essentical tool for cardiology teaching. The cardiologists are embraced the simulation to understand the complex techniques in interventional cardiac problem, unusual cardiac condition and to build up a medical teamwork. The simulator not only replicates the complex cardiac problem but also used for simple exercise like placing the intervenous lines to complex procedures like cardiac catheterization.

4.2. Significance of ECG Modeling:

ECG modeling plays vital role to understand cardiac function, for diagnosis of cardiac diseases, to develope dignosis tools, for early detection and treatment of various cardiac problem like myocardial infarction, arrhythmia etc. Mathematical model is useful to understand the electrical activity of heart and relation between the model and ECG signal. Researcher can gain knowledge regarding the physiological process of heart like depolarization and repolarization. Mathematical modeling can be used to develope cardiac simulator by the modeling of ECG signal. The simulation technology is of great importance for education and training in medical fields. It can evolve as simulated electrocardiogram (ECG), even as simulated human patients and tutors with detailed simulated animations. The most popular modeling methods are Gaussian modeling, Fourier modeling, Gaussian combination modeling (GCM), Autoregressive modeling, Auto regressive integrated moving average modeling (ARIMA) etc.

4.3. Working principle of Fourier and Gauissian Modeling:

4.3.1. Fourier Model

Fourier analysis decomposed the signal into sum of sinusoidal function with a specific frequency and amplitude. It transforms a time domain data into frequency domian. Fourier model can be mathematically expressed by:

$$z_{pq}(t) = a_0 + \sum_{n=1}^{n} a_n \, Sin(n\omega_0 t) + b_n Cos(n\omega_0 t)$$

$$a_n = \frac{2}{T}\int_0^T e(t)\, Sin(n\omega_0 t)dt$$

$$b_n = \frac{2}{T}\int_0^T e(t)\, Cos(n\omega_0 t)dt \qquad (4.1)$$

where, a_0 represents the average value of zone potential signal, ω_0 represents angular frequency of fundamental component $2\pi/T$, and T represents time period of zone potential wave and *n* represents total number of data points.
By assuming, $A_n = C_n Cos\theta_n$ and $B_n = C_n Sin\theta_n$, Equation (4.1) may be expressed in the following form:

$$z_{pq}(t) = a_0 + \sum_{n=1}^{n} C_n \, Sin(n\omega_0 t + \theta_n)$$
$$C_n = \sqrt{a_n^2 + b_n^2}$$
$$\theta_n = \tan^{-1}\frac{b_n}{a_n} \qquad (4.2)$$

In Fourier modeling method, the model parameters are considered as $\omega_0, a_0,$ and θ_n.

4.3.2. Gaussian Model

The Gaussian model is a normal distribution model or bell curved model. Mathematically it represents the probability distribution of data points which are clustered around the mean value and spread the data determined by standard deviation (SD). It is a continuous distribution method which spread the data symmetrically around the mean value. The key parameters of Gaussian model are mean (μ) and standard deviation (σ).

Mean (μ): It is the centre value of Gaussian distribution.

Standard Deviation (σ): It measures the dispersion or spread of data points around the mean value.

Gaussian model can be Gaussian Mixture model and Gaussian process model.

Gaussian Mixture Model: It is a soft clustering method and a probabilistic model. It is used in unsupervised learning to determine probability of a given data point around a cluster. Multiple Gaussians are used to assume the data points belongs to a cluster.

Gaussian mixture model mathematically expressed by:

$$GC(y_{ecg}) = \sum_{i=1}^{N} a_i e^{-(\frac{y_{ecg}-\mu_i}{2\sigma_i})^2} \qquad (4.3)$$

where, μ_i : mean and σ_i : standard deviation of i^{th} component of Gaussian mixture (combination).

Gaussian Process Model: It is a non-parametric supervised learning model. It is a stochastic process where each finite collection of random variables are distributed. The distribution is a joint distribution of all random variables over continuous time or space domain. It is used for application of regression and probabilistic based classification problem.

4.4. Development of PC based cardiac simulator

Cardiosim is a PC based cardiac simulator which is developed to generate systhetic ECG signal for training of medical student and technitians. It is a user specific module and can generate ten types of ECG annotations. The schematic diagram of Cardiosim is shown in Fig.1. The simulator is developed in two module 1) Database generation module and 2) Synthetic ECG waveform generation module. The raw ECG signal were choosen from MIT-BIH arrhythmia (mitdb) database under Physionet to develop a database. Then a user friendly graphical user interface (GUI) was developed to simulate ECG signal. The ECG waveform is generated in real time and realized by a universal serial interface (USB) which is connected to a data acquisition card (DAC).

4.4.1. Development of ECG database module:

The database was developed using 30 records from mitdb data under Physionet database. The database had been formed to generate 10 types of ECG beats. The ECG morphology are a) normal sinus rhythm or Healthy ECG signal (H), b) ECG signal containing right bundle branch block (R), c) left bundle branch block (L), d) paced beat (P), e) ECG fusion signal consisting of healthy and atrial premature (APC) beat (H-A), f) healthy with premature ventricular contraction (PVC) beat (H-V), g) Left bundle branch block with atrial premature beat (L-A), h) Left bundle branch block with premature ventricular contraction beat (L-V), i) Right bundle branch block with atrial premature beat (R-A), j) Right bundle branch block with premature ventricular contraction beat (R-V). The database generation module formed in two stages, a) preprocessing of raw ECG signal and b) reference dataset generation and database creation.

4.4.1.1. Preprocessing of ECG signal:

The raw ECG signal was denoised by DWT method and the denoised signal was followed by Pan-Tompkins algorithm to detect the R-peak of each beat. A single beat is lies between two consecutive BLI, thus the next step is detection of BLI. The BLI was detected using window method and search back method. Then each beat was extracted and stored into a 2-D matrix to form a beat matrix. After that, the fiducial points (P-peak, Q-peak, S-peak and T-peak) of each beat were extracted by thresholding method to divide the beat into three segments, namely PR, QRS and ST segments. In such way, six types of ECG beats are chosen randomly and preprocessed.

4.4.1.2. Reference dataset generation and database creation:

In this work different age group was considered to collect the data. Three reference segments, $\widehat{PQ}$, $\widehat{QRS}$ and $\widehat{ST}$ were generated from database of different age group within the respective cluster matrices PQ, QRS and ST. Mathematically the segments can be represented by :

$$(z_{seg})_k = \frac{1}{m}\sum y_k \tag{4.9}$$

where, $(z_{seg})_k$: kth sample of reference segment, seg : $\widehat{PQ}$, $\widehat{QRS}$ and $\widehat{ST}$ segments; y_k: kth sample of y number of beats and m: number of samples. Each of the reference segments were modelled separately by Gaussian and Fourier series expansion. The algorithm is based on dynamically error control mechanism i.e., each segment modelled separately by best suited model order on the basis of user defined RMSE for minimization of reconstruction error. The pattern of each segment for each type of ECG beat is different thus the best suited model order also varies. As the model is based on error-controlled mechanism the reconstruction accuracy assured and the chances of overfitting and underfitting possibilities of each segment are decreased.

The database was developed using model order upto 8th level. The coefficient $(c_{k,n})_t^v$ is mathematically represented by:

$$(c_{k,n})_t^v = \begin{vmatrix} a_{01} & a_{11} & b_{11} & 0 & 0 & .. & .. & 0 & \omega_1 & r_1 \\ a_{02} & a_{12} & b_{12} & a_{22} & b_{22} & .. & .. & 0 & \omega_2 & r_2 \\ .. & .. & .. & .. & .. & .. & .. & .. & .. & .. \\ a_{08} & a_{18} & b_{18} & a_{28} & b_{28} & .. & a_{88} & b_{88} & \omega_8 & r_8 \end{vmatrix} \tag{4.10}$$

where, k : the coefficient number; n : the model order; t : 6 types of ECG annotation, like H, A, V, P, L, R; v : ECG segment, like $\widehat{PQ}$, $\widehat{QRS}$ and $\widehat{ST}$ and r : RMSE for different orders of the model. 18 such database were formed to represent three segments of 6 ECG annotation.

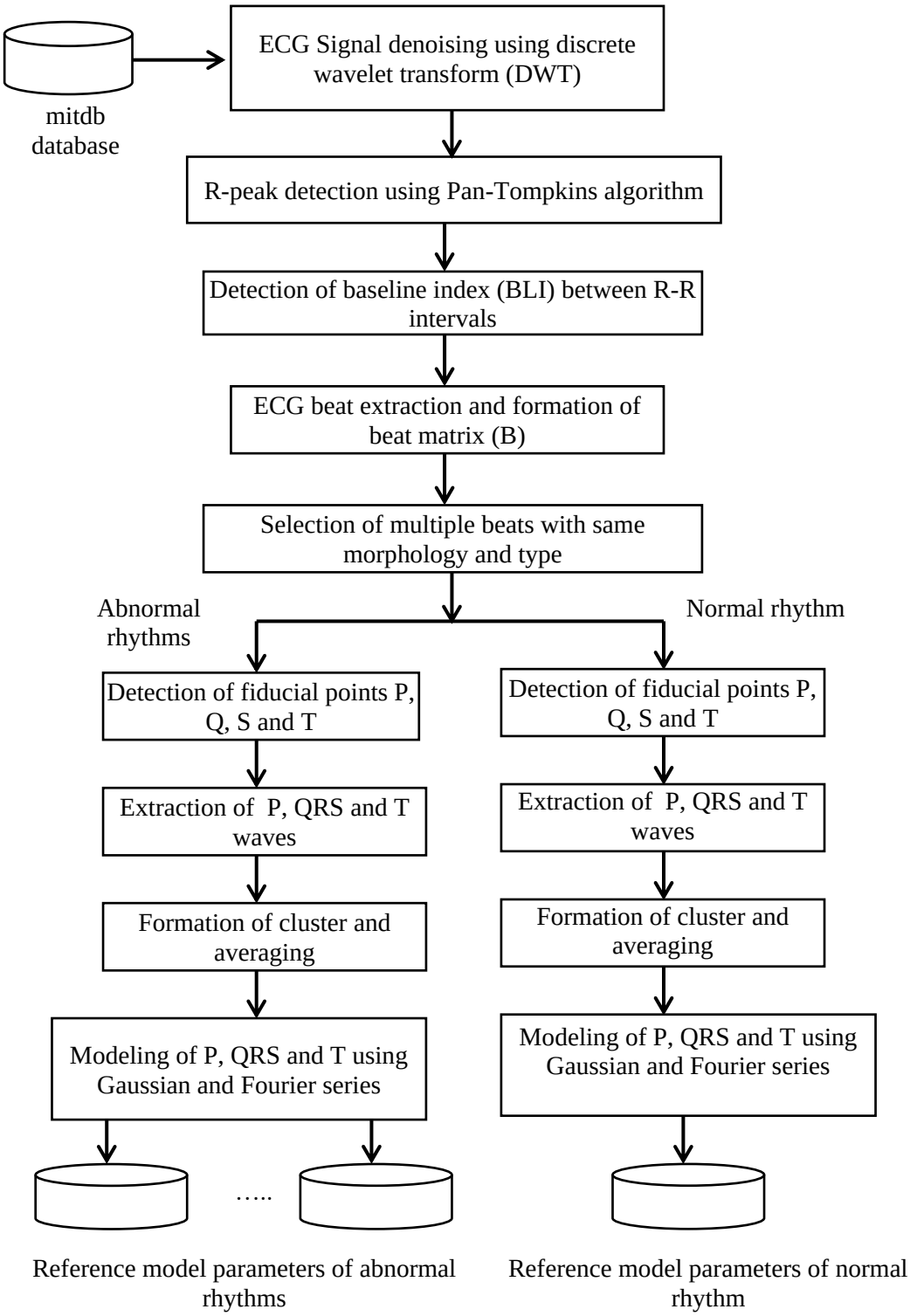

Fig.4.1. Flowchart for development of ECG generating model database

4.4.2. Synthetic ECG waveform generation module:

The segment specific database was formed to develop the cardiac simulator for generation of synthetic ECG signal. It is a user defined ECG simulator which produce ECG signal based on the requirement of user. A GUI was developed with following parameters: age, number of beats to visualize, type of ECG beat, number of abnormal beats in the data, heart rate variability (HRV), RMSE and sampling frequency. The flow diagram of synthetic ECG generation is shown by Fig. 4.2.

After getting the input, the nearest RMSE matched within the coefficient matrix $(c_{k,n})_t^v$ to search respective three reference segments ($\widehat{PQ}$, $\widehat{QRS}$ and $\widehat{ST}$). The synthetic beats are generated according to the sampling frequency. The raw samples of three segments for normal and abnormal rhythms are expressed by: $(x_{\widehat{pq}})_n$, $(x_{\widehat{qrs}})_n$, and $(x_{\widehat{st}})_n$, where n is the type with length of $(l_{\widehat{pq}})_n$, $(l_{\widehat{qrs}})_n$, and $(l_{\widehat{st}})_n$.

The user can add HRV to the individual segments. Hence, the kth modified length of $\widehat{PQ}$, $\widehat{QRS}$ and $\widehat{ST}$ will be:

$$(l_{\widehat{pq}})_n^k = (l_{\widehat{pq}})_n \pm (l_{\widehat{pq}})_n \times HRV\%$$

$$(l_{\widehat{qrs}})_n^k = (l_{\widehat{qrs}})_n \pm (l_{\widehat{qrs}})_n \times HRV\%$$

$$(l_{\widehat{st}})_n^k = (l_{\widehat{st}})_n \pm (l_{\widehat{st}})_n \times HRV\% \qquad (4.11)$$

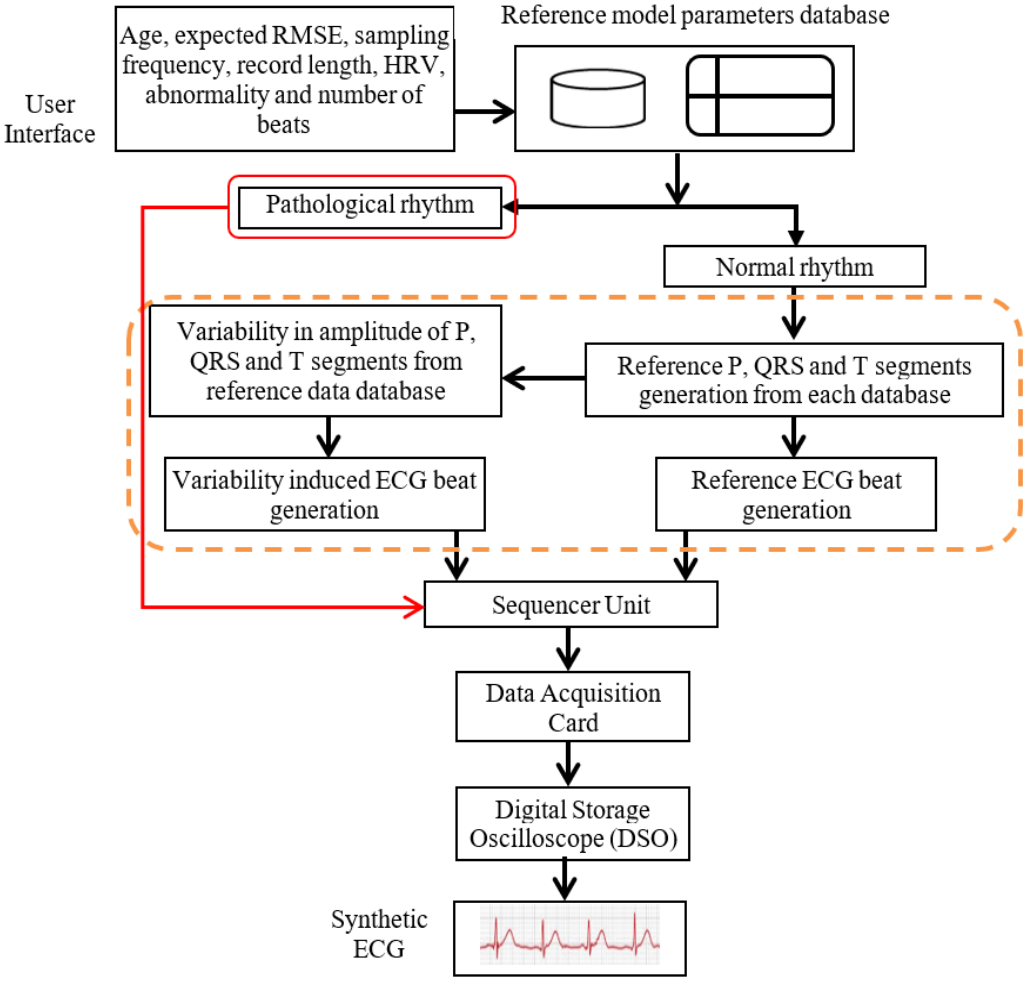

Fig.4.2. Flow diagram of synthetic ECG generation module

In case of $(l_{\widehat{pq}})_n^k > (l_{\widehat{pq}})_n$, half point symmetrical extension was used to add extra samples by extrapolation method. It is given by:

Let,
$$X = [x_1 x_2 x_3]$$
$$X_{new} = [x_2 x_1 x_1 x_2 x_3 x_3 x_2] \quad (4.12)$$

where, X is an array, containing 3 elements and it is extrapolated by 2 samples on both side. X_{new} is the new extrapolated array. In practical case the amplitude of each beat is unique due the effect of respiration. The amplitude variation was done by:

$$a_{new} = a_n \pm a_n \times span \quad (4.13)$$

where, a_n : amplitude of a beat; a_{new} : new amplitude; n: type and span is between 3 to 10 %. Otherwise, $(l_{\widehat{pq}})_n^k < (l_{\widehat{pq}})_n$, the extra samples are truncated from the end to fit in the modified length. The modified complete k^{th} beat is formed by concatenating the reference segments:$(x_{\widehat{pq}})_n^k$: $(x_{\widehat{qrs}})_n^k$: $(x_{\widehat{st}})_n^k$.
For H, L, R and P type ECG annotation the pattern of each beat is same with variable length and amplitude. A sequencer unit was introduced to generate the synthetic signal by combining healthy and diseased beats. The synthetic signals were generated in following manner:

Let, n_{ab} represents the number of abnormal beats, n_k represents the number of healthy beats or paced beats; n_t represents the total number of beats = n_{ab}+ n_k; n_{kL} represents the *L* numbers of H or L or R type beat; n_{k1} represents one H or L or R type beat; *seq*= sequence array of beats;

If n_{ab} = 1;
If n_t = odd, $\frac{(n_k-1)}{2} = n_{kL}$;
$seq = [n_{kL} n_{ab} n_{kL}]$;
If n_t = even ; $\frac{(n_k-2)}{2} = n_{kL}$;
$seq = [n_{kL} n_{ab} n_{kL} n_{k1})]$;
If n_{ab} = 2;
If n_t = odd, $\frac{(n_k-3)}{2} = n_{kL}$;
$seq = [n_{kL} n_{ab1} n_{kL} n_{ab2} n_{k1}]$;
If n_t = even ; $\frac{(n_k-2)}{2} = n_{kL}$;
$seq = [n_{kL} n_{ab1} n_{kL-1} n_{ab2} n_{k1}]$;
If n_{ab} = 3;
If n_t = odd, $\frac{(n_k-3)}{2} = n_{kL}$;
$seq = [n_{kL} n_{ab1} n_{kL-1} n_{ab2} n_{k1} n_{ab3}]$;
If n_t = even ; $\frac{(n_k-4)}{2} = n_{kL}$;
$seq = [n_{kL} n_{ab1} n_{kL} n_{ab2} n_{k1} n_{ab3}]$;

The cardiac simulator can generate 10 types of ECG signal by combining the normal and basic four types of abnormalities: (a) H, (b) L, (c) R, (d) P, (e) H-A, (f) H-V, (g) L-A, (h) L-V, (g) R-A, (h) R-V. For realization of synthetic ECG signal a DAQ is interfaced. In the present work, the sequential array (seq) was delivered to a USB6009 (make:National Instruments) using the analog IO library function of MATLAB®.From the DAQ analog output channel the generated ECG signals are within 0-5V. Fig. 4.3 shows the hardware set-up and generation of synthetic ECG in digital as well as analog mode.

4.5. Results:

A cardiac simulator had been developed, named as CardioSim. It is PC-based Cardiac signal simulator which can generate user defined ECG signal with arrhythmia disease in real time, through a GUI in a personal computer. The salient features of this simulator are : 1) PQ, QRS and ST segments are modelled separately to achieve high performance quality, 2) adaptive error-controlled mechanism through user defined parameters, 3) it is able to generate 10 types of cardiac rhythm including nine types of arrhythmia rhythm, 4) different types of user defined parameters such as age, HRV, RMSE, sampling frequency, disease type etc. make the model dynamic in nature. In addition to that, the GUI can be utilized to generate real-time ECG pattern upto 40 continuous cardiac cycles.

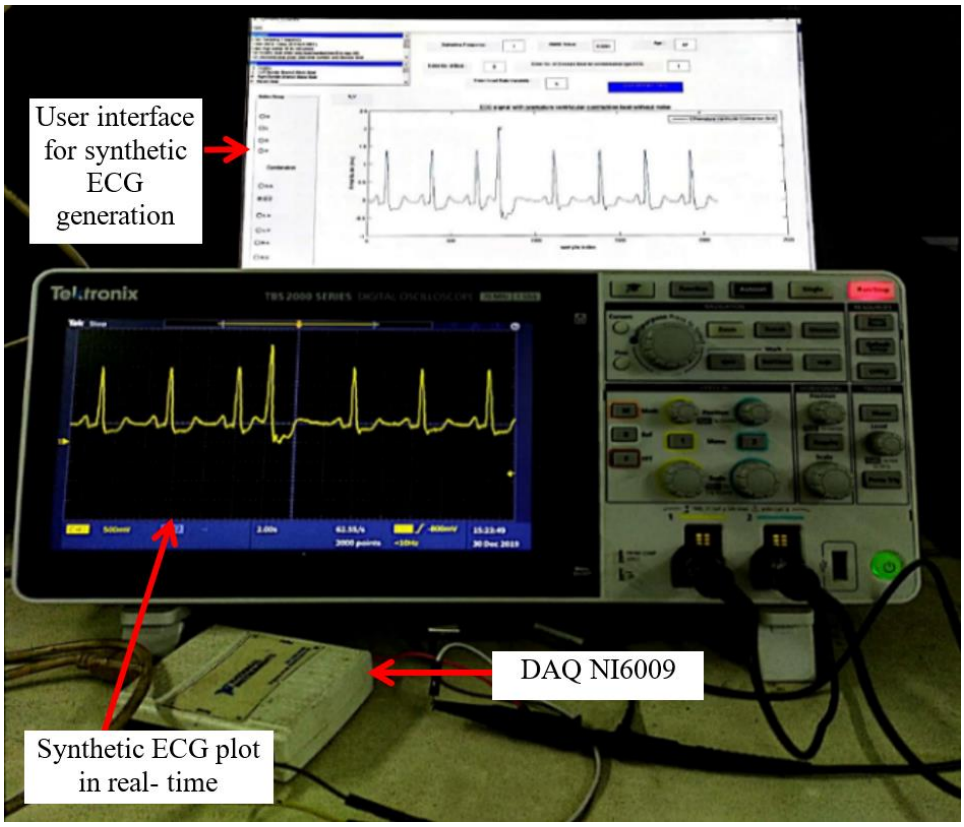

Fig.4.3.: Layout of CardioSim with UI in computer

The model was validated by 30 records from mitdb and few records from ptbdb database under Physionet. The noise reduction was done by DWT method and the value of mother wavelet was selected by trial-and-error method. The denoising performance of different mother wavelet were observed and db5 had been chosen to perform the task of denoising. It was observed from fig.4.4, db4 was unable to discard the baseline wander noise and on the other hand db6 and db7 remove few clinical information along with the noises. The db5 was able to remove both higher and lower frequency noises without losing any clinical information and also preserve the actual pattern of ECG signal.

The ECG signal was decomposed by DWT and reconstructed using different level to achieve denoise ECG signal. Fig. 4.5. shows the decomposed and reconstructed ECG signal at different scale. The 12^{th} level decomposed signal shows better denoising performance after reconstruction using D4 to D9 levels as due to higher level of decomposition each frequency band becomes narrower which increase the resolution. Figure 4.6.(a)-(e) shows the removal of higher frequency and lower frequency noise through different levels of DWT using mitdb 203 data record using 3600 samples. The detected R-peaks and baseline points of denoised ECG signal are shown in Figure 4.6.(f) using mitdb data ID 106.

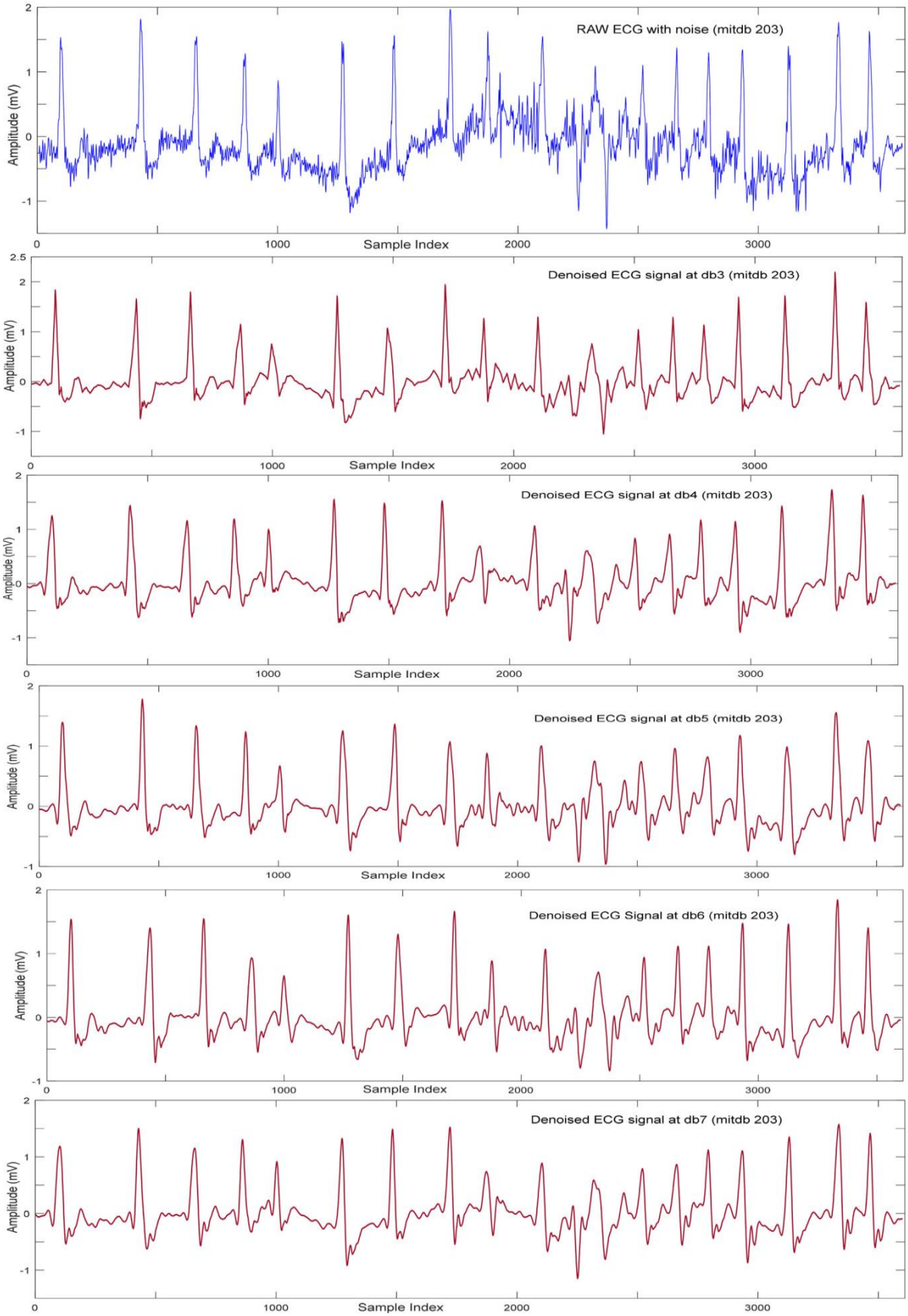

Fig.4.4.: Mother wavelet selection for ECG noise reduction using DWT method

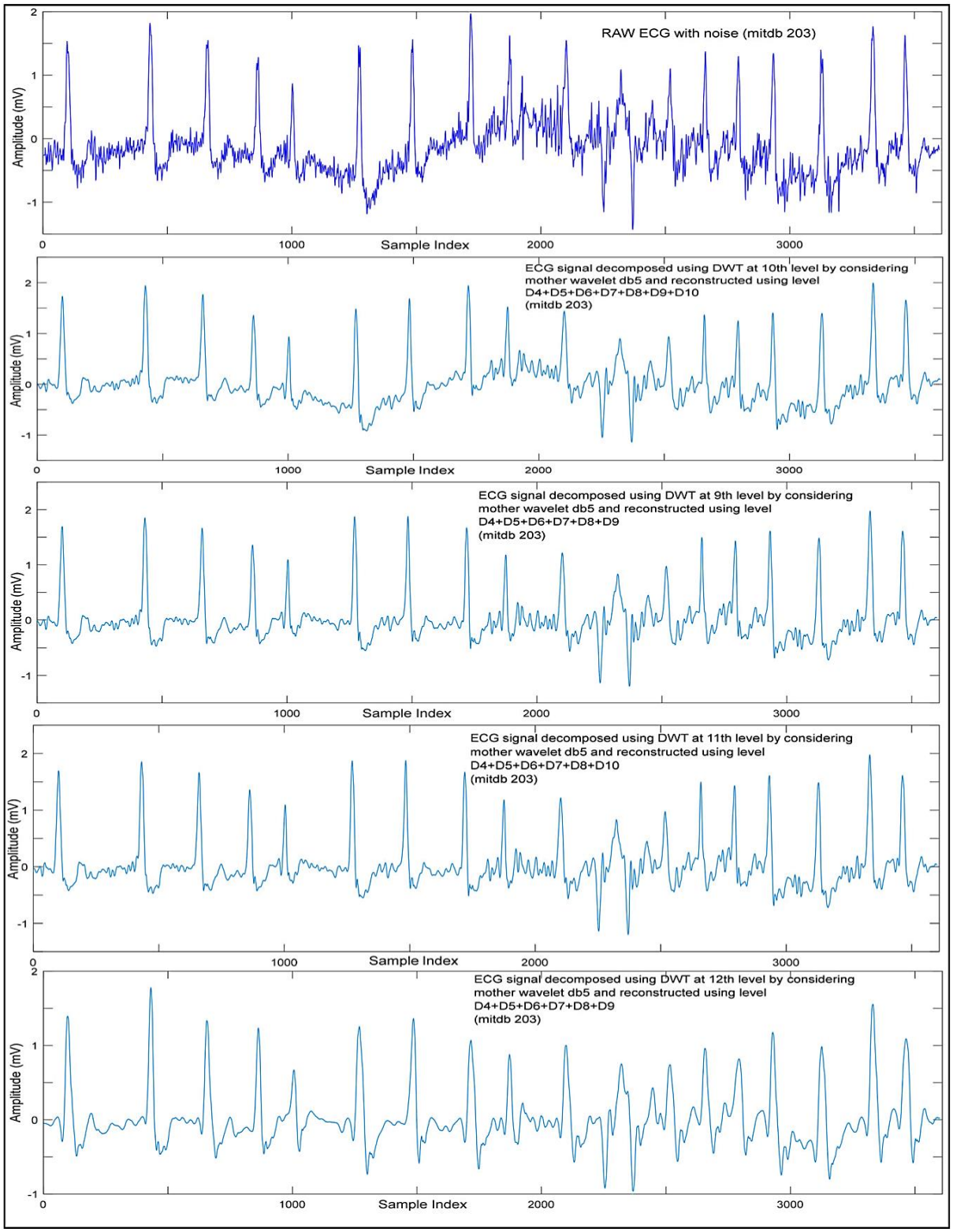

Fig. 4.5.: Raw and reconstructed ECG signal using different decomposition level by DWT method

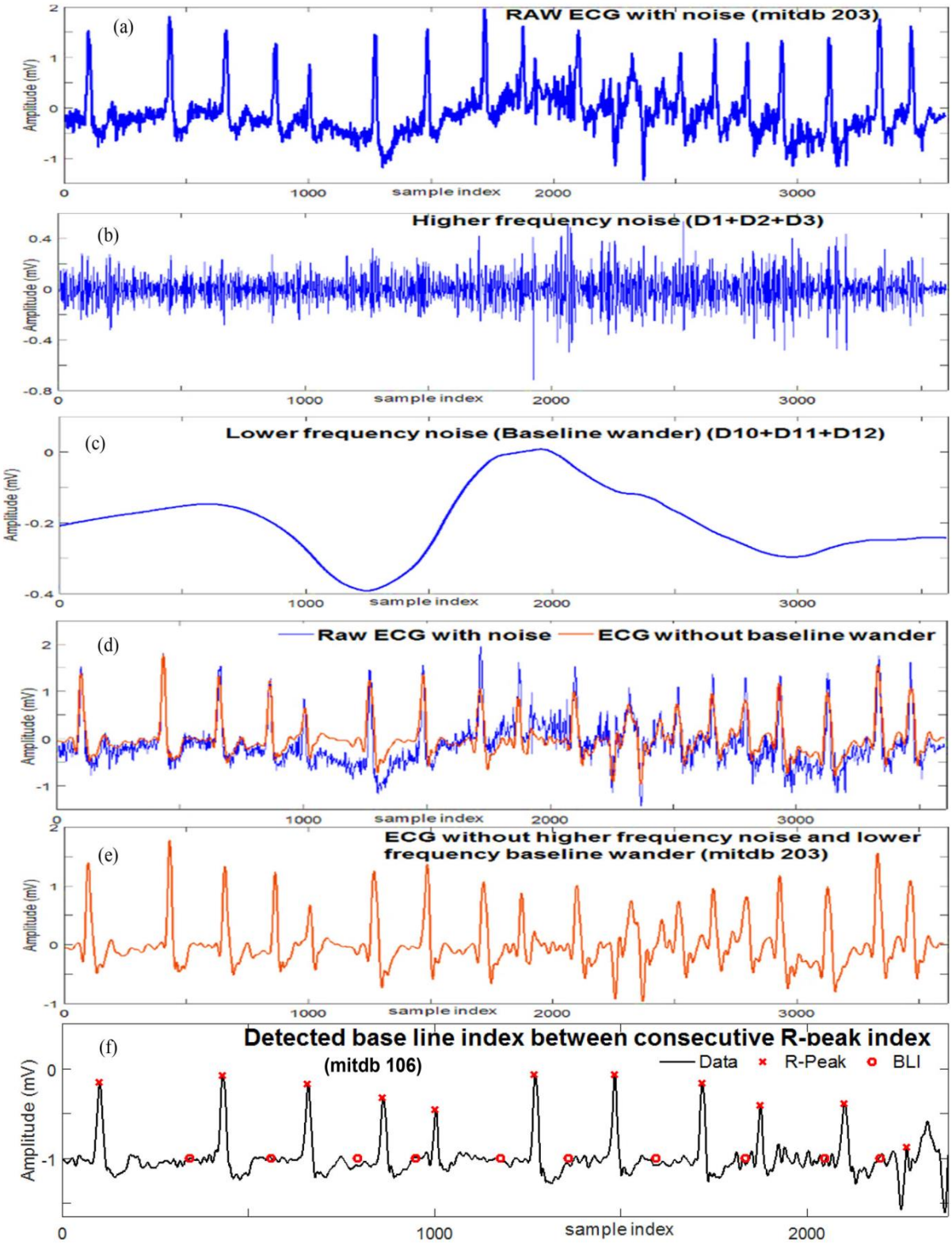

Fig. 4.6.: Noise removal and R-peak detection of ECG signal

Table 4.1.: Reconstruction Performance using Fourier model and Gaussian model

Patient ID record No. with lead and abnormality	Without Segmentation				With Segmentation			
	Fourier Model		Gaussian Model		Fourier Model		Gaussian Model	
mitdb	SNR	MSE $\times 10^{-2}$	SNR	MSE $\times 10^{-2}$	SNR	MSE $\times 10^{-6}$	SNR	MSE $\times 10^{-5}$
H								
100	8.63	0.97	20.66	0.29	87.53	3.26	75.88	1.3
101	14.14	0.75	17.83	0.52	87.77	7.95	73.27	1.71
103	9.72	3.81	25.67	0.77	84.40	0.26	56.9	0.57
106	14.06	3.29	26.89	0.91	88.61	0.23	73.27	1.71
112	18.00	0.58	39.09	0.07	95.13	2.29	62.34	0.06
113	17.34	2.44	12.61	3.92	88.30	0.24	52.15	0.75
115	6.59	4.11	23.72	0.74	87.23	0.18	55.10	0.22
116	18.30	4.29	22.10	2.94	93.34	0.40	60.60	0.77
117	13.22	1.34	7.11	2.73	88.79	0.11	54.53	0.25
121	27.82	0.31	19.45	0.72	89.64	8.19	73.00	2.85
122	36.57	0.26	20.43	1.33	96.45	7.39	71.71	2.95
123	7.24	4.20	26.44	0.61	85.90	0.23	50.15	0.69
124	16.18	2.63	27.07	0.88	84.61	0.44	63.28	0.23
201	25.65	0.26	53.52	0.01	94.17	2.74	61.34	0.13
202	19.46	0.80	23.64	0.52	89.20	0.10	60.22	0.15
205	29.23	0.14	29.31	0.14	85.42	5.32	56.44	0.12
A								
118	27.97	0.71	29.87	0.59	86.45	0.23	74.03	9.77
209	17.56	0.84	17.51	0.85	86.18	8.75	46.03	0.97
V								
105	33.09	0.32	38.11	0.20	99.66	3.30	76.90	6.74
114	20.11	1.29	21.66	1.10	83.80	0.30	72.33	0.09
119	31.20	0.25	25.15	0.31	84.78	0.25	52.11	0.63
200	18.41	0.61	20.42	0.55	88.93	9.87	50.80	0.53
203	40.59	0.28	14.80	3.89	87.80	0.26	71.43	0.23
208	13.51	1.83	36.55	0.18	91.09	7.85	60.71	0.97
210	34.76	0.16	17.27	0.91	82.51	0.13	62.80	9.82
L								
109	60.10	0.021	8.51	3.69	99.68	5.54	89.30	77.5
111	21.81	0.38	16.09	0.69	82.25	0.15	50.00	0.22
207	18.61	1.16	5.25	4.40	74.13	0.13	47.57	0.26
212–R	24.19	0.93	20.94	1.28	83.30	0.25	52.95	0.78
107–P	30.23	0.38	35.58	0.24	97.22	0.43	76.89	0.33
ptbdb								
Healthy(H-II)								
P116_s0302lre	4.44	0.55	26.89	0.05	83.94	2.60	26.60	3.8
P117_s0292lre	8.33	1.06	17.83	0.41	85.80	3.20	57.19	3.4
P121_s0311lre	10.41	0.35	29.58	0.05	90.60	5.15	42.12	5.5
AMI								
P044_s0142lre(v3)	18.97	0.76	15.33	1.10	65.12	0.89	21.50	0.6
P044_s0143lre(v3)	20.83	0.72	17.06	1.05	72.63	0.46	23.42	50.8
P044_s0159lre(v1)	11.12	0.53	14.57	0.37	56.69	0.40	11.34	38.1
P0163_s0034_re(v3)	24.17	0.47	17.43	0.92	92.88	6.10	53.68	3.01
IMI								
P012_s0043lre(II)	10.96	0.07	30.77	0.01	66.51	0.16	45.02	0.17
P012_ s0050lre(II)	10.45	0.11	17.75	0.05	74.65	9.26	32.94	6.37
P021_ s0065lre(III)	11.85	0.16	23.85	0.04	50.41	10.02	45.68	1.21

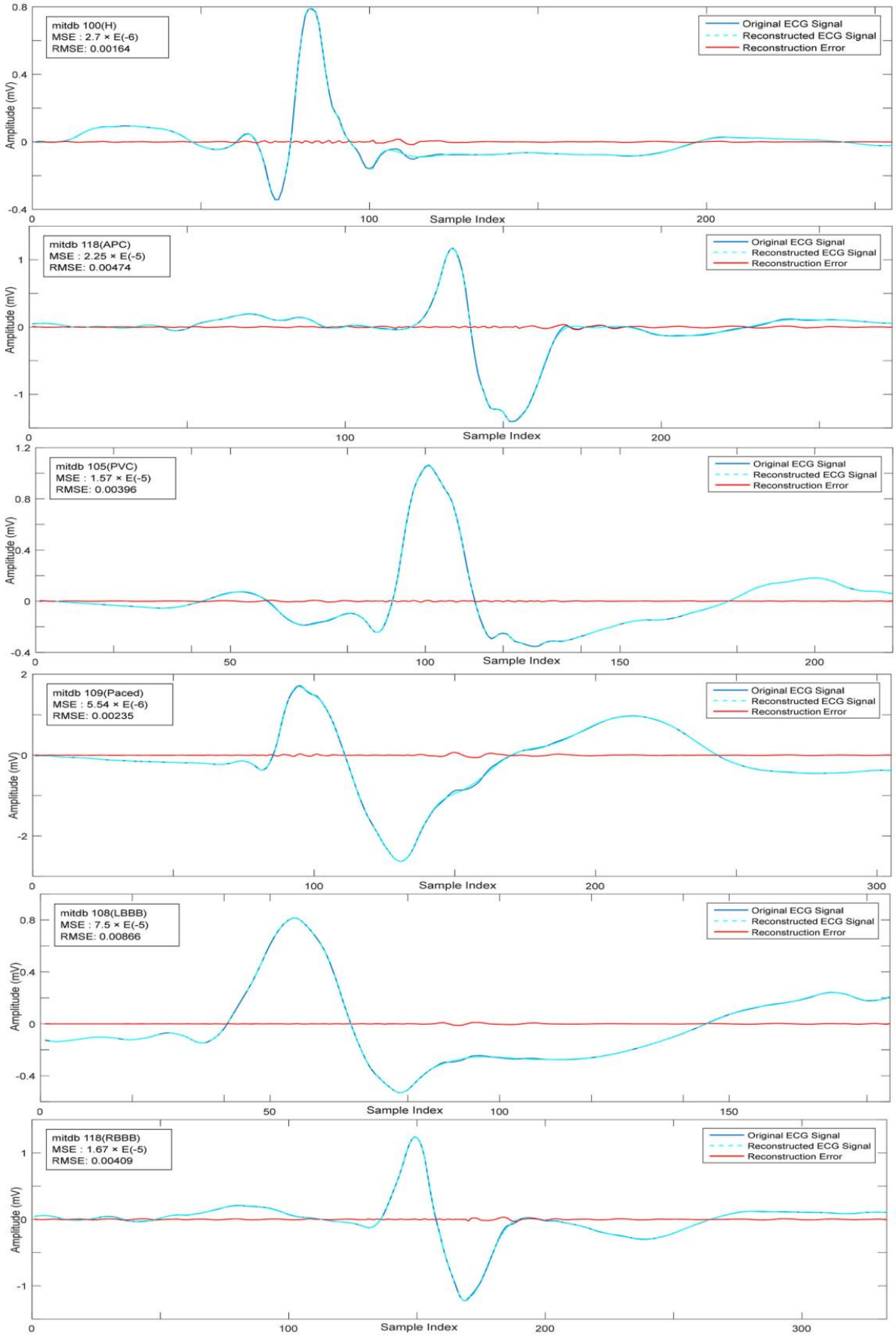

Fig. 4.7.: Reconstruction performance for different beat morphology using Fourier modeling; (a)100-H; (b) 118-APC; (c) 105-PVC; (d) 109-P;(e) 108-LBBB; (f) 118-RBBB

Each beat was synthesised by Gaussian and Fourier model. We have modelled the beat in two ways to understand the reconstruction performance. In first approach the whole beat was modelled using same model order and in other approach each segment of a beat modelled separately using best suited model order. It was observed that segment specific model gives better reconstruction performance than the beat specific model. Also noticed that Fourier model gives higher reconstruction efficiency than Gaussian model. A Gaussian model is appropriate for bell-shaped waveforms, while a Fourier model is better suited for equipotential or periodic waveforms. Table 4.1. shows the Gaussian and Fourier model performance for beat without segment and with segment. The performance of each approach was measured by signal-to-noise ratio (SNR) and mean square error (MSE), defined as:

$$MSE = \frac{\sum_{k=1}^{N}[x(k) - x_r(k)]^2}{N}$$
$$SNR = 10log\frac{\sum_{k=1}^{N}[x(k)-x_m(k)]^2}{\sum_{k=1}^{N}[x(k)-x_r(k)]^2} \quad (4.14)$$

Where, x: original ECG signal and x_r : reconstructed ECG signal.

The average MSE and SNR for 30 mitdb data records and 10 ptbdb data records were computed and given in Table 4.1. The abnormalities are indicated by respective record ID. In most of the cases, Fourier model achieved better performance. The mean SNR for different beat morphology is 89.2(H), 88.37(V), 86.32(A), 85.35(L), 97.22(P) and 83.3(R) and mean MSE is 2.45×10^{-6}(H), 3.14×10^{-6}(V), 8.98×10^{-6}(A), 5.82×10^{-6}(L), 0.43×10^{-6}(P) and 0.25×10^{-6}(R). The table indicates that beat segments modeled with the Fourier approach yield superior results relative to the other methods.

For ptbdb data, healthy (H), myocardial infarction anterior (AMI) and MI inferior (IMI) data were chosen for evaluation. Fourier model shows better performance for ptbdb data also. The average SNR and MSE using Fourier model for different categories are : 86.78 and 3.65×10^{-6}(H), 71.83 and 1.96×10^{-6}(AMI), 63.85 and 6.48×10^{-6}(IMI) respectively. Thus, the reference segments were modelled by Fourier model.

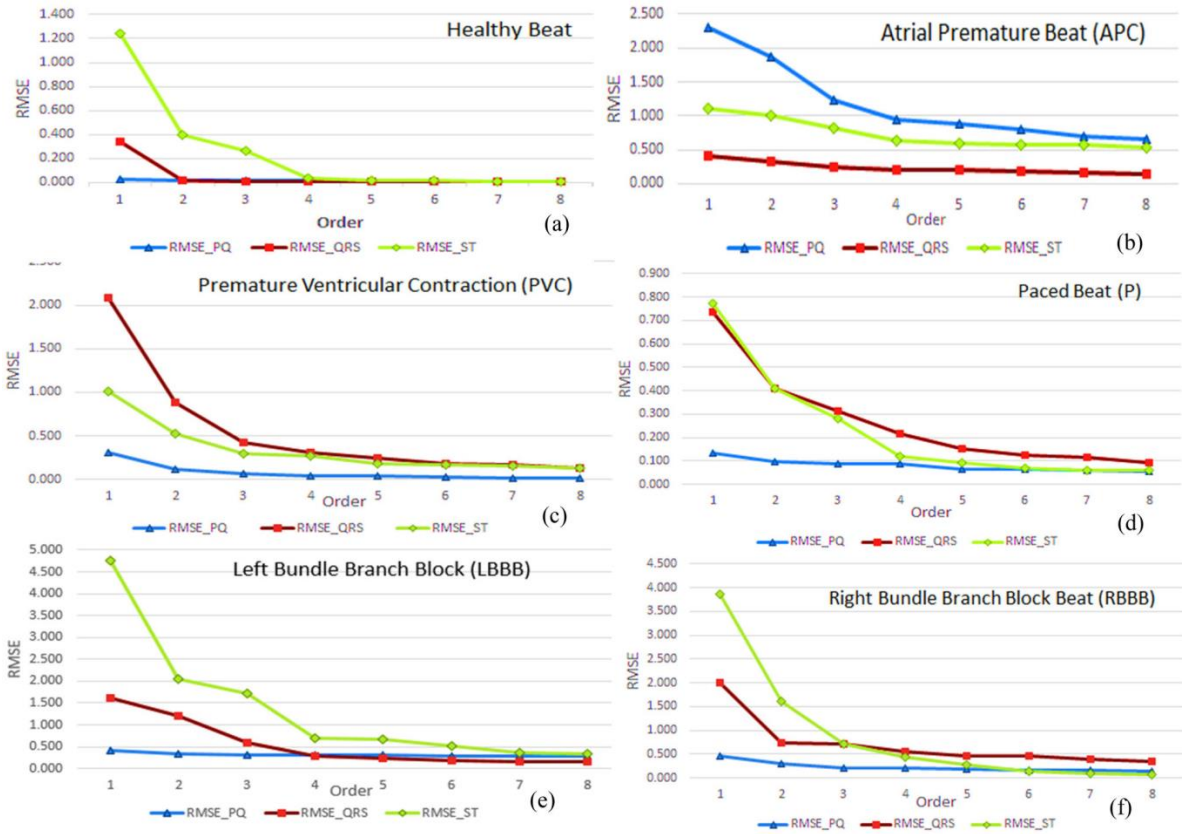

Fig. 4.8.: Segment wise RMSE of six beat morphology: (a) H; (b) APC; (c) PVC; (d) P; (e) LBBB and (f) RBBB

In Fig. 4.7. reconstruction performance of Fourier model for six ECG beat types under mitdb data are shown. In each panel, the original, reconstructed and sample to sample error are shown to understand how close the reconstructed signal follows to the original signal. It indicates high reconstruction efficiency with negligible error.

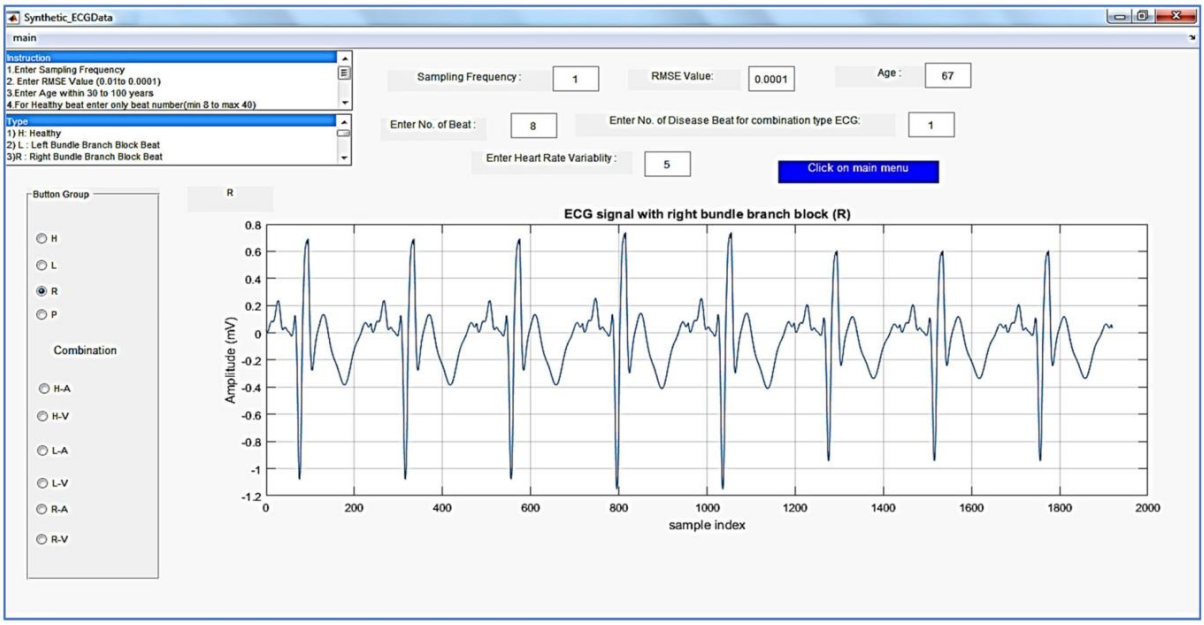

Fig. 4.9.: Layout of graphical user interface of CardioSim

Table 4.2: Comparison of model performance between published research and CardioSim

Work	**Method**	**Dataset and Abnormality**	**RMSE × 10^{-3}**	**MSE × 10^{-5}**	**SNR**	**Computational time**
Billah *et.al.* [136]	Gaussian	mitdb NSR APC PVC LBBB RBBB	 25.69 28.46 59.16 20.02 31.69	-	-	-
Kundu *et.al.* [137]	Gaussian Fourier	ptbdb	-	-	20.71 22.16	-
CardioSim (proposed)	Fourier	mitdb: NSR APC PVC LBBB RBBB Paced	1.8 6.6 1.8 2.7 4.7 6.6	0.32 43.7 0.33 0.75 2.20 4.39	87.53 80.46 99.65 93.54 86.45 97.22	22.22 19.66 21.05 17.41 18.71 19.27
	Gaussian	NSR APC PVC LBBB RBBB Paced	3.6 9.8 8.2 21.5 18.2 14.0	1.30 9.77 6.74 46.0 19.7 33.0	75.87 74.03 76.90 57.46 62.92 76.89	39.22 29.58 34.63 27.14 30.01 33.59

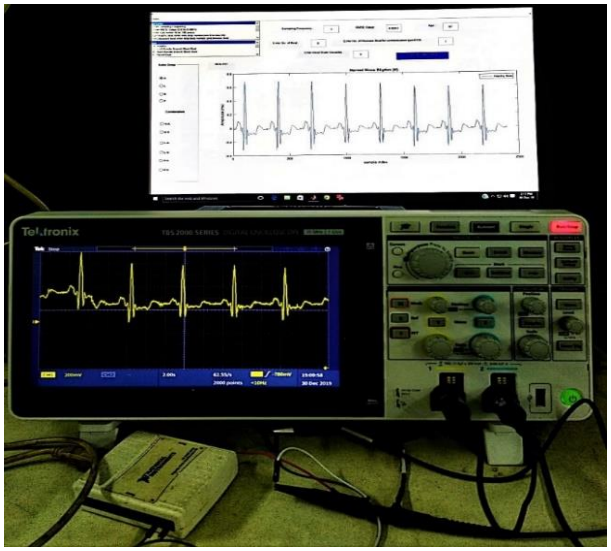
Tektronix

(a)

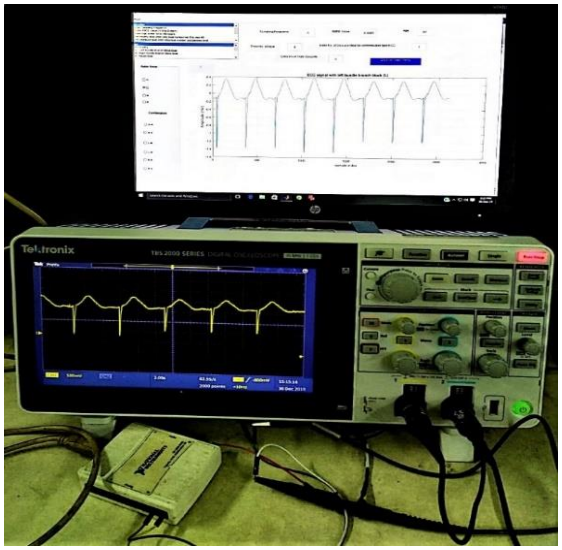
Tektronix

(b)

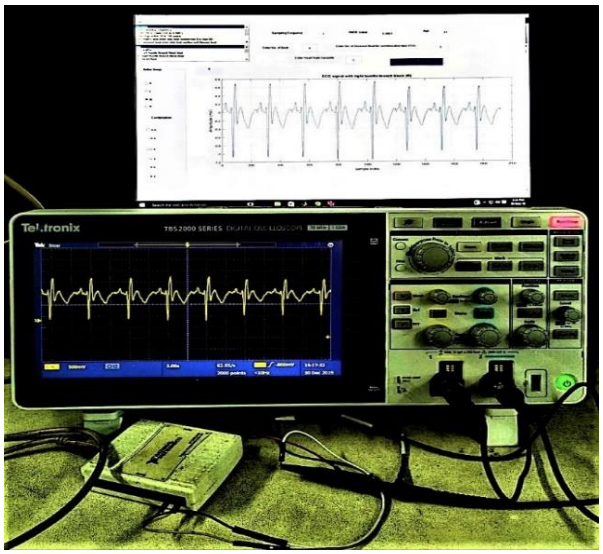
Tektronix

(c)

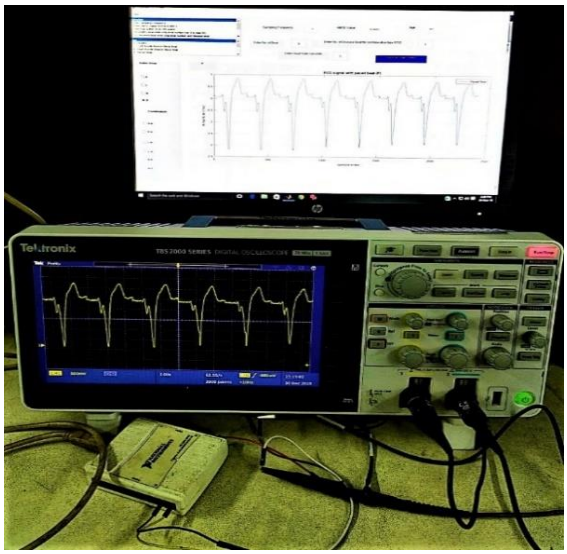
Tektronix

(d)

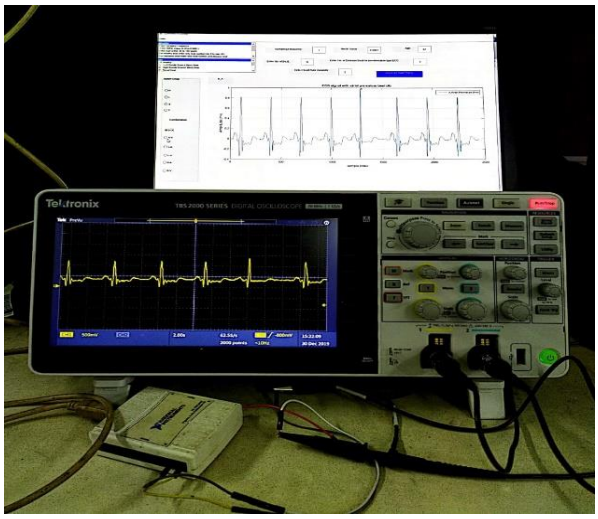
Tektronix

(e)

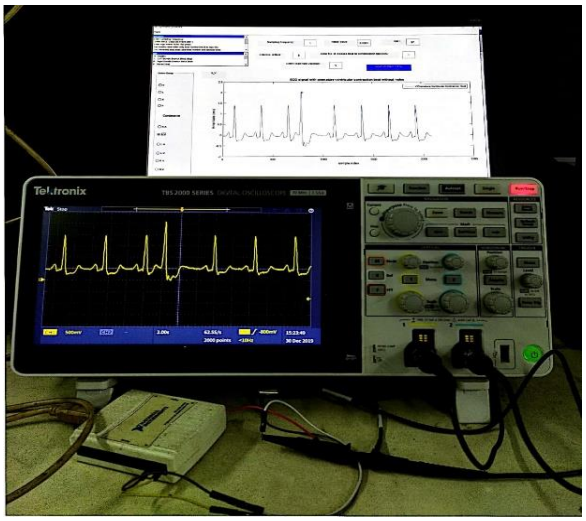
Tektronix

(f)

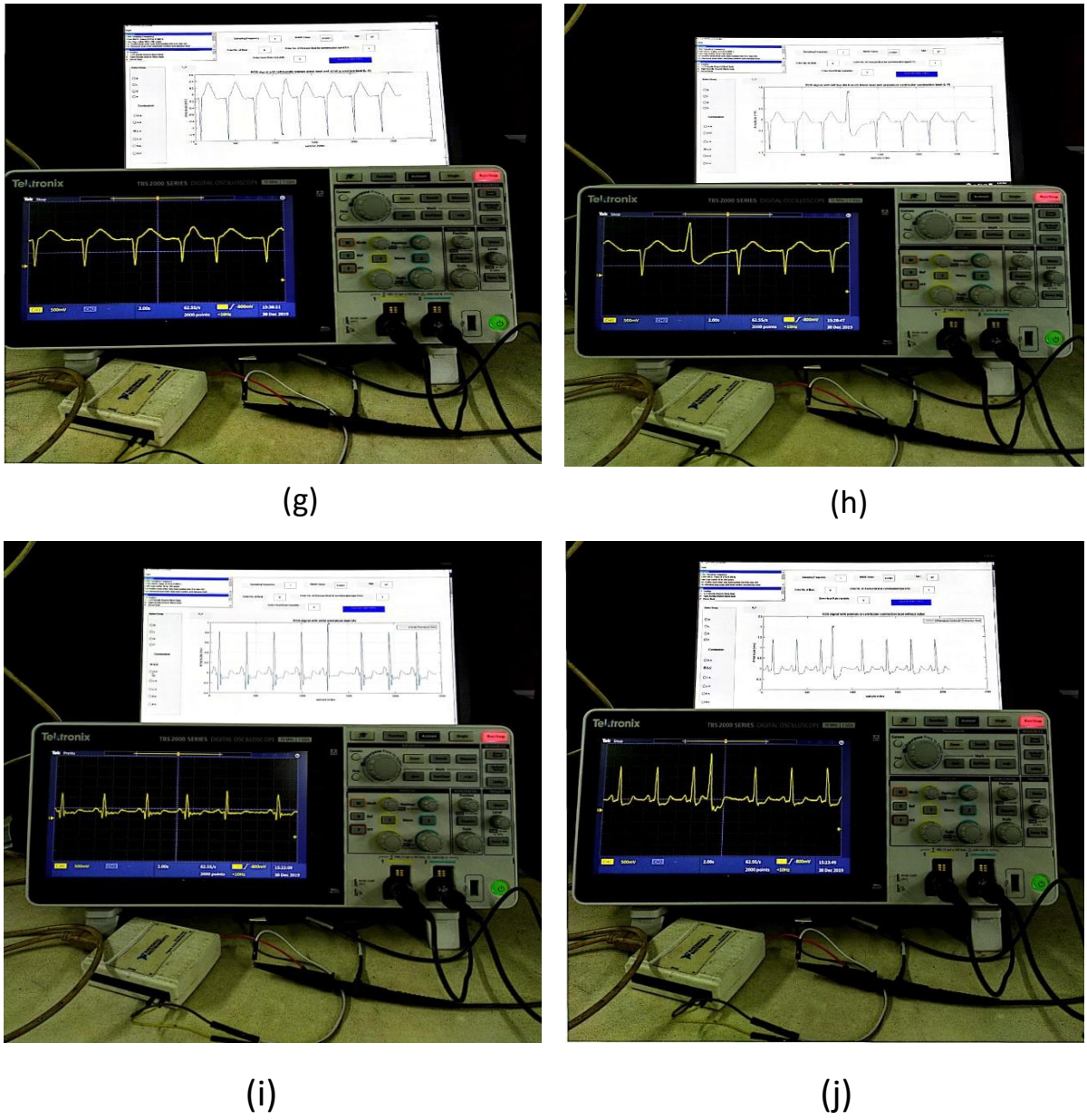

Fig.4.10.: Layout of ECG hardware simulator with UI in computer (a) Normal sinus rhythm (H); (b) LBBB (L); (c) RBBB (R); (d) Paced (P); (e) L and APC (L-A); (f) L and PVC (L-V); (g) R and APC (R-A); (h) R and PVC (R-V); (i) H and APC (H-A); (j) H and PVC (H-V)

The Fig.4.8 shows the variation of RMSE for each segment of ECG (PQ,QRS and ST) for various beat morphology. For each type of morphology, the RMSE sharply falls to the low value upto 3rd model order and after that it becomes flat upto 6th order. Hence, the modeling was performed upto 8th order. The layout of GUI for synthetic ECG signal generation is shown in fig. 4.9. The user can define their required RMSE, sampling frequency, age, HRV, number of beats etc. through the top panel and mix the number and type of abnormalities through the left-hand panel.

Table 4.3: Comparison between published and proposed work on modeling

Work	Model Order	Comparison
Billah *et.al.* [18]	8th Order Gaussian Model	1) Modelled by 8^{th} order thus the computational time is very high. 2) Memory allocation is high to store huge number of model coefficient. 3) Higher computational complexity 4) For many mitdb data better reconstruction performance may achieve in lower order thus unnecessary increase of computational complexity, time and memory usage 5) Modeling done on whole beat of ECG hence reconstruction performance is poor
Kundu *et.al.* [26]	3rd and 4th order Gaussian model 4th order Fourier model	1) ECG beat was divided into three segment and modelled separately using 3rd or 4th order. Reconstruction performance better than Ref.18 but poor than proposed work 2) High MSE so the rate of clinical information loss is high 3) Less complex and lower computational time 4) Lower memory requirement
CardioSim (proposed)	Dynamic model order	1) Reference model parameter database was developed using Fourier method. Each beat divided into three segments and modelled separately using dynamic order, thus minimal reconstruction error (order of 10^{-6}) and high SNR 2) Number of segment is three consequently the computational time is lesser than Ref. 26. 3) Computational complexity is lower than Ref. 26. 4) Smaller memory required to store model coefficients than Ref. 26

Table 4.4: Comparison between CardioSim and other ECG Simulator

Author Name	Dataset used	Comparison
J.C.Edelmann *et.al.* [12]	Healthy	• Generates healthy data and distortion can be added to the ECG template • The adjustable parameters are heart rate and amplitude of ECG waveform
Manju. B.R *et.al.*[16]	Hypokalemia and Hyperkalemia Dextrocardia Angina Pectoris	• Synthetic waveform generates on the basis of theoretical constant • Generates three types of arrhythmia waveform
CardioSim (proposed)	mitdb	• Reference ECG beat generates from mitdb patient database of PhysioNet • It generates ten types of waveform (NSR and nine abnormal rhythms) • Flexible as it generates synthetic ECG on the basis of user defined data such as type, age, number of beats etc. • Real-time realization using DAQ and DSO • User friendly

The CardioSim can generate ten types of synthetic ECG signal using Healthy and five types of arrhythmia disease. These such combinations were verified by qualified cardiologist for clinical validation. The waveforms were resembled by actual ECG of patients with such abnormalities. Fig. 4.11. shows the ten types of synthetic ECG generated by CardioSim.

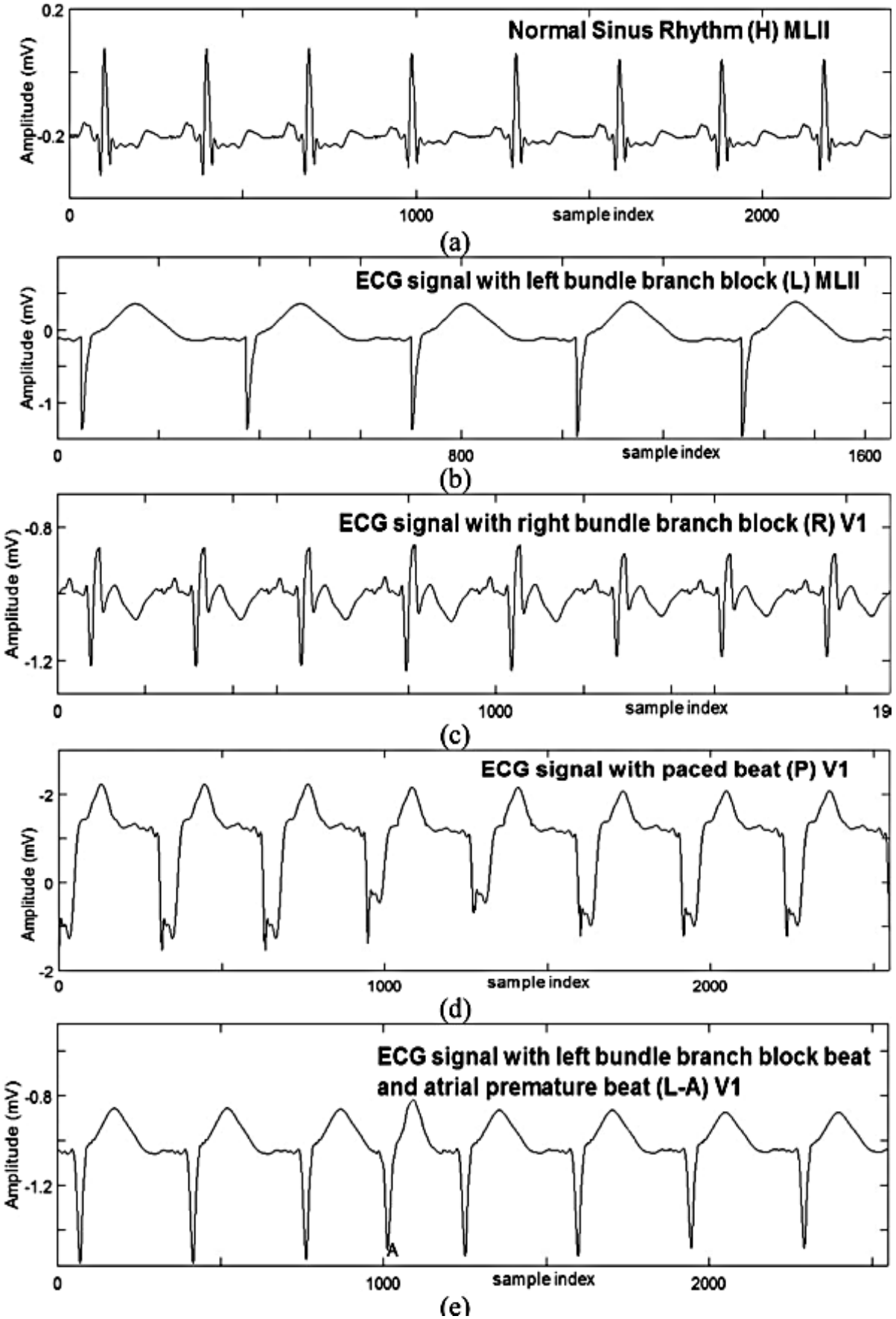
Normal Sinus Rhythm (H) MLII
Amplitude (mV)
0.2
-0.2
0
1000
sample index
2000
(a)
ECG signal with left bundle branch block (L) MLII
Amplitude (mV)
0
-1
0
800
sample index
1600
(b)
ECG signal with right bundle branch block (R) V1
Amplitude (mV)
-0.8
-1.2
0
1000
sample index
19
(c)
ECG signal with paced beat (P) V1
Amplitude (mV)
-2
0
-2
0
1000
sample index
2000
(d)
ECG signal with left bundle branch block beat
and atrial premature beat (L-A) V1
Amplitude (mV)
-0.8
-1.2
A
0
1000
sample index
2000
(e)

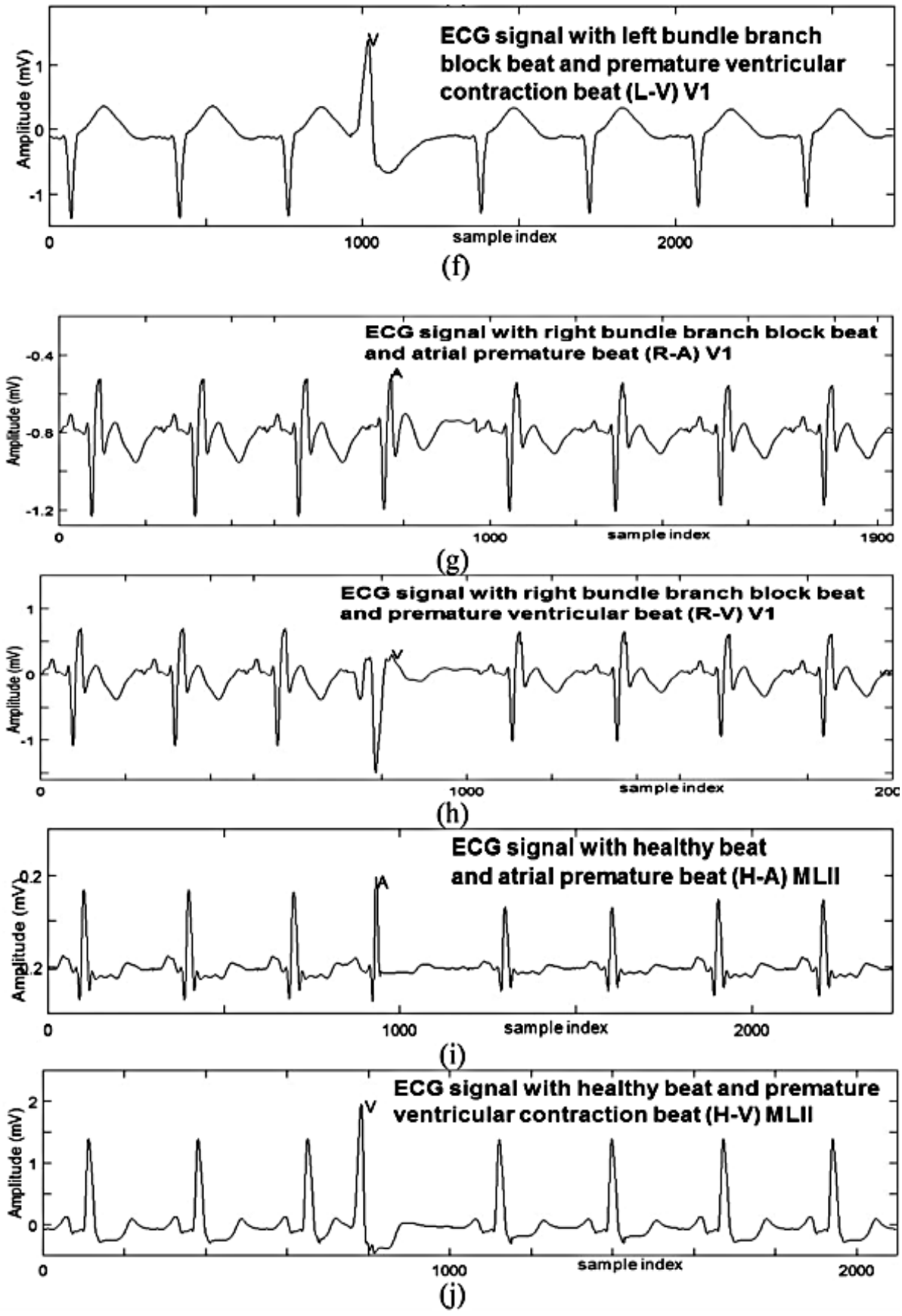

Fig. 4.11.: Synthetic ECG signal generated by CardioSim using different beat morphology

The performance of CardioSim is depends on the modeling method. Thus, the selection of model and the model order is very important to generate synthetic ECG signal. In Table 4.2. and Table 4.3. the model performance was compared with previously published work on modeling where the error parameters are mentioned explicitly. A few works used modeling for compression of ECG data and computed the percentage root mean square difference (PRD), percentage root mean squared difference normalized (PRDN) etc., and thus excluded from comparison. In terms of SNR, which has been cited as common performance index, the proposed work outperforms the published research on ECG modeling. The comparison between published work and proposed work on modeling is shown in Table 4.3. Higher the RMSE and lower SNR means higher reconstruction error. The reconstruction error can be decreased by decreasing RMSE. From the table, it can be observed that the whole ECG beat modelled by Gaussian model which gives higher reconstruction error as compared to Fourier Model. The SNR also very low. The model performance can be improved by dividing the ECG beat into segments. An ECG beat is consisting of different types of waves and equipotential segment. In the proposed work the ECG beat is divided into three segments viz. PQ, QRS and ST and modelled separately by suitable model parameter. For each segment the model order varies according to their shape. Thus, the average reconstruction error becomes negligible. Another advantage of segmented modeling is decreasing of computational time. In case of modeling of a whole beat, the model order may be high as 8^{th} order to achieve lower reconstruction error. It increases the computational time. Whereas in segmental modeling as the accuracy is achieved within 3^{rd} to 6^{th} order the computational time decreases.
Table 4.4. shows the comparison between the published cardiac simulator and CardioSim. A cardiac simulator can generate only the healthy data and only two parameters, HRV and amplitude are associated with the simulator . In another work, the signal are generated on the basis of theoretical constant and can generate only three types of arrhythmia data. On the other hand, in our proposed work the synthetic ECG data are generated from mitdb patient database. It can generate ten types of synthetic signal including healthy signal and nine diseased signals. It is a flexible simulator as it generates ECG signal on the basis of user defined parameters like, age, HRV, RMSE, number of beats, type of abnormality etc. Thus, it becomes a user-friendly simulator. The synthetic signal also realized in real time through DAC and Digital Storage Oscilloscope (DSO).

The cardiac simulator delivers the following:

- e-resource based learning in medical education/Alternative to classroom teaching/medical Internship, which will be vacillated by this development.
- Due to wide variability of the clinical features in ECG with age, gender and other demographic factors, it becomes difficult sometimes to clinically classify a record by visual inspection. Experienced practitioners can only comprehend the records. The simulator thus developed may find itself suitable to help the medical practitioners to a certain degree in complementing their clinical knowledge and judgments.
- In a country like India, where health service and medical amenities/infrastructure is inadequate in view of the total population to be catered, this sort of development is well-timed and a necessary stepping.

4.6. Summary:

CardioSim is a PC-based cardiac simulator which provides dual facility of an interface-based visualization and real hardware-based interface for generation of synthetic waveform by user defined parameters. CardioSim was validated and tested using ten types of cardiac rhythm adopted from 30 numbers of data records from mitdb database. To develop a flexible simulator, a GUI based front panel was introduced so that user can generate ECG signal as per their requirement. It can generate healthy rhythm as well as nine types of diseased rhythm. Moreover, the synthetic signal can be visualized in real-time using a DAQ and DSO. The mean SNR for the modelled beat of six morphologies are: 89.2

(H), 88.37 (V), 86.32 (A), 85.35 (L) and 97.22 (P), and 83.3 (R). CardioSim shows the improved result than the other research work in this area.

The limitation of this cardiac simulator are: it is limited to generate clean ECG of ten types of cardiac morphologies. For realistic ECG appearance, a slow variation of 3-10% was introduced to the reference R-peak. The dynamicity nature of the model can be extended by including more flexibility like user defined muscle noise, respiration effort, baseline wander to the subject. The scope and flexibility of CardioSim was restricted due to the limited variation of data like gender choice, age group etc. The model can be improved by introducing more parameters by collecting good number of ECG records with high variability.

Chapter 5

Segment Specific Modeling and Optimization of ARIMA model Hyperparameters for Improved Reconstruction Error

5.1. Introduction:

Over the past decade, ECG modeling has emerged as a prominent research area, driven by the growing integration of computational techniques in ECG interpretation. Modeling of ECG signal refers to the mathematical representation of cardiac cycle. Modeling of ECG signal is very useful for detection of cardiac abnormality and compression of ECG signal. The retaining of clinical information using minimum number of model coefficient is a challenging job. The main objective of ECG modeling is reduction of reconstruction error. In the cardiac simulator segmental modeling was applied where each segment was modelled separately by Fourier model. The segmental model gives more reconstruction accuracy than the modeling of a whole ECG signal. ECG signal is consisting of different equipotential segments and waveforms with different duration and amplitude. Thus, the model order for each segment should not be same. The segment specific modeling not only improve the reconstruction error but also decreases the memory consumption. Thus, the raw ECG signal are not required for storage of ECG data. The segmented ECG beat is shown in Fig 5.1.

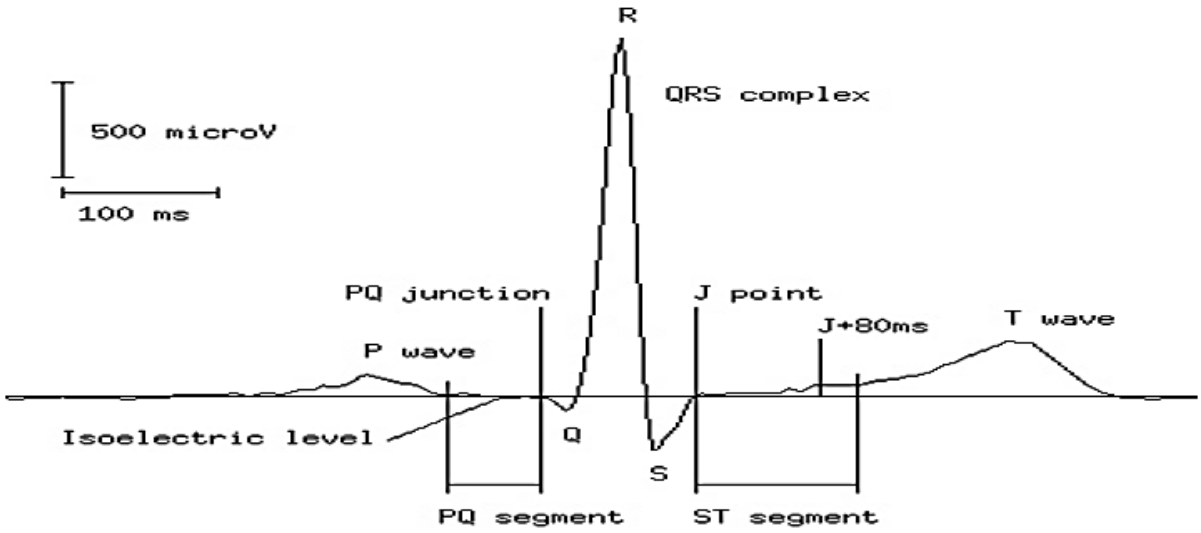

Fig.5.1. A typical lead II ECG cycle showing waves and segments

Fig.5.1. shows the segments of ECG beat. In this figure bell shaped segments are P-wave, QRS Complex and T wave and the segments in isoelectric level are: starting index of beat to P-onset index, PQ segment, ST segments and T-offset index to index of end of the beat. From this figure it can be observed that the characteristics of each segment are different hence the model parameter should be different otherwise the problem of overfitting and underfitting shall be observed and as a result the reconstruction error shall be increased. Over the last decade, the increased use of computers has greatly influenced ECG interpretation. ECG modeling refers to the mathematical representation of an ECG morphological cycle, which means, the raw ECG samples are no more required for storage of ECG data. In one hand,

this provides better structured representation of the signal for cardiac abnormality interpretation. On the other hand, modeling provides a data reduction approach for bulk storage. Thus, the main objective of segmental modeling is minimization of reconstruction error to obtain more accurate model of ECG beat.

5.2. Development of Segment Specific Model for ECG signal

The raw ECG signal was denoised by DWT method and the R-peaks were detected by Pan-Tompkins algorithm. After that the BLI of the ECG signal were detected to extract each beat of ECG signal and the beats were stored into a cell array. User would select the beat of interest for segmentation. The methodology of segment specific modeling of ECG signal is described in the below section. Fig.5.2 shows the flow diagram of segment specific model.

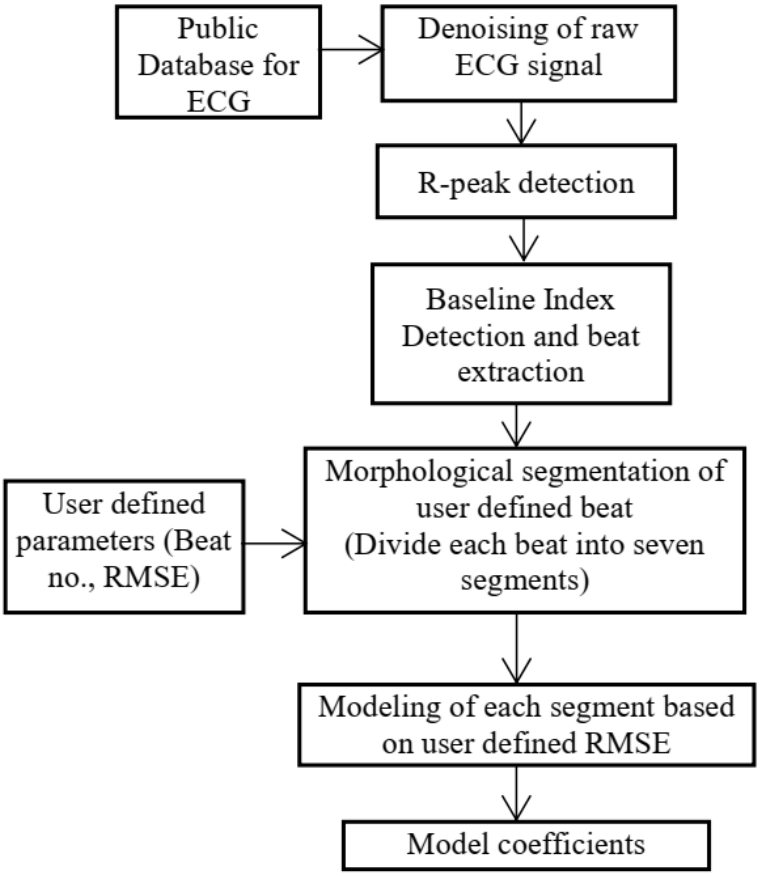

Fig.5.2. Flow diagram of segment specific model

5.2.1. Preprocessing of ECG signal:

The ECG signal was denoised by discrete wavelet transform (DWT) method using Daubechis 5 (Db5) as mother wavelet at 12 level signal decomposition. The higher frequency noise was discarded by eliminating level D1, D2, D3 and D4. The lower frequency noise, i.e., baseline wander was removed by eliminating D10, D11 and D12 level. The denoised ECG signal was formed as given below:

$$y_{ecg} = D5 + D6 + D7 + D8 + D9 \quad (5.1)$$

In the next stage the R-peaks were detected from the denoised ECG signal. The QRS band was selected from the array of (D5 + D6)2 of DWT. The distance between two consecutive QRS region was calculated from the array and also find out the prominence, amplitude and width of the QRS region.

The R-peak was detected using thresholding method based on the parameters such as prominence, amplitude, width and distance between two consecutive QRS complex. Here a window of 10 second was considered for checking the presence of R-peak by considering the thresholding parameters. Each Beat was extracted from the ECG signal by dividing the consecutive R-R interval into 2:1 ratio and the intersecting index is baseline index (BLI). The samples between two consecutive BLI were formed a single beat. Stored the beats into cell array. User would select the beat of interest for segmentation.

5.2.2. Segmentation of ECG beat:

ECG beat was divided into seven segments, namely, a) from the first BLI to P-onset index, b) P-onset to P-offset index (P-wave), c) P-offset index to Q-index, d) QRS-complex, e) S index to T-onset index, f) T-onset to T-offset index (T-wave) and g) T-offset index to next BLI. The user can choose any beat of interest from the cell array. Let consider for k[th] beat (b_k) the fiducia points were detected as follows:

$(P_{peak})_k = \max(y_{1k} : y_{rk})$

$Q_k = \min\,[(P_{peak})_k : y_{rk}]$

$S_k = \min\,(y_{rk} : y_{Lk})$

$(T_{peak})_k = \max\,[S_k : y_{Lk}]$

$(P_{onset})_k = \min\big(y_{1k} : (P_{peak})_k\big)$

$(P_{offset})_k = \min\big((P_{peak})_k : Q_k\big)$

$(T_{onset})_k = \min\big(S_k : (T_{peak})_k\big)$

$(T_{offset})_k = \min\big((T_{peak})_k : y_{Lk}\big)$

where, y_{1k}: first sample of beat; y_{rk} : the sample at R-peak position; y_{Lk}: the last sample of the selected beat and the max (min) operator extracts the highest (lowest) amplitude sample from the respective array. Fig.5.3. indicate the detected fiducial points.

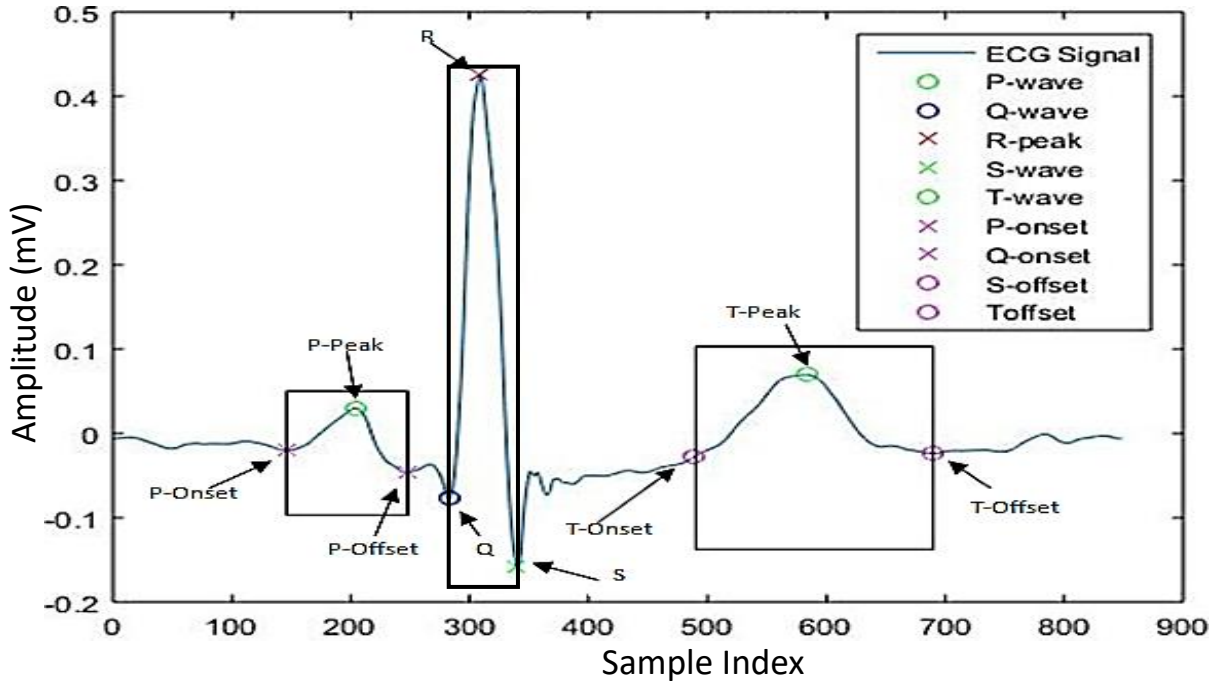

Fig. 5.3.: Detected fiducial points of a beat

5.2.3. Segment specific Modeling of ECG beat:

Gaussian model and Fourier model were used to develop the segment specific model. The modeling method were chosen according to the shape of each segment. Gaussian model is suitable for bell shape in unipolar direction. Thus, the ECG beat was shifted into positive level before segmentation. In ECG beat, P wave, QRS complex and T wave are bell shaped waves. Therefore, Gaussian model was applied in these three segments. Remaining four equipotential segments are modelled by Fourier model. The amplitude and shape of each segment is different. Thus, each segment was modelled by specific modeling method using best suited model order. The model order was adjusted dynamically on the basis of user defined model order.

A graphical user interface was developed to give the input parameter to choose beat randomly from the beat matrix and to define the RMSE. The layout of GUI is shown in Fig.5.4. The GUI layout is consisting of three stages. The Stage 1 is for denoising and beat extraction to form the beat matrix; Stage 2 is for selection of beat and segmentation and Stage 3 is synthesis of specific ECG beat using segment specific model on the basis of user defined RMSE. Fig.5.4.(a) shows the denoising and preprocessing of ECG signal, Fig.5.4.(b) shows the fiducial point extraction and segmentation of user defined beat from the beat matrix and Fig.5.4.(c) shows synthesis of ECG beat on the basis of user defined RMSE. In Fig.5.4.(c) the beat can be modelled by three modeling method viz. Fourier model, Gaussian model and mixed model i.e. segment specific model. Among these three modeling techniques user can choose any method for modeling and also can compare the results using the performance parameter. Here SNR and MSE were used as performance metrics.

Figure 5.4(c) shows the panel that can synthesize ECG signals using three different modeling methods. This feature makes the GUI more flexible, allowing users to compare the results across methods. Fig. 5.5 shows the comparison between these three modeling methods for synthesis of ECG signal. The Fourier model gives SNR:86.7 and MSE: 5.79×10^{-6}; Gaussian model gives SNR: 66.02 and MSE: 6.8×10^{-6} and segment specific model gives SNR: 90.58 and MSE: 3.69×10^{-6}. Hence, among these three models, segment specific model achieved more accuracy in terms of reconstruction efficiency.

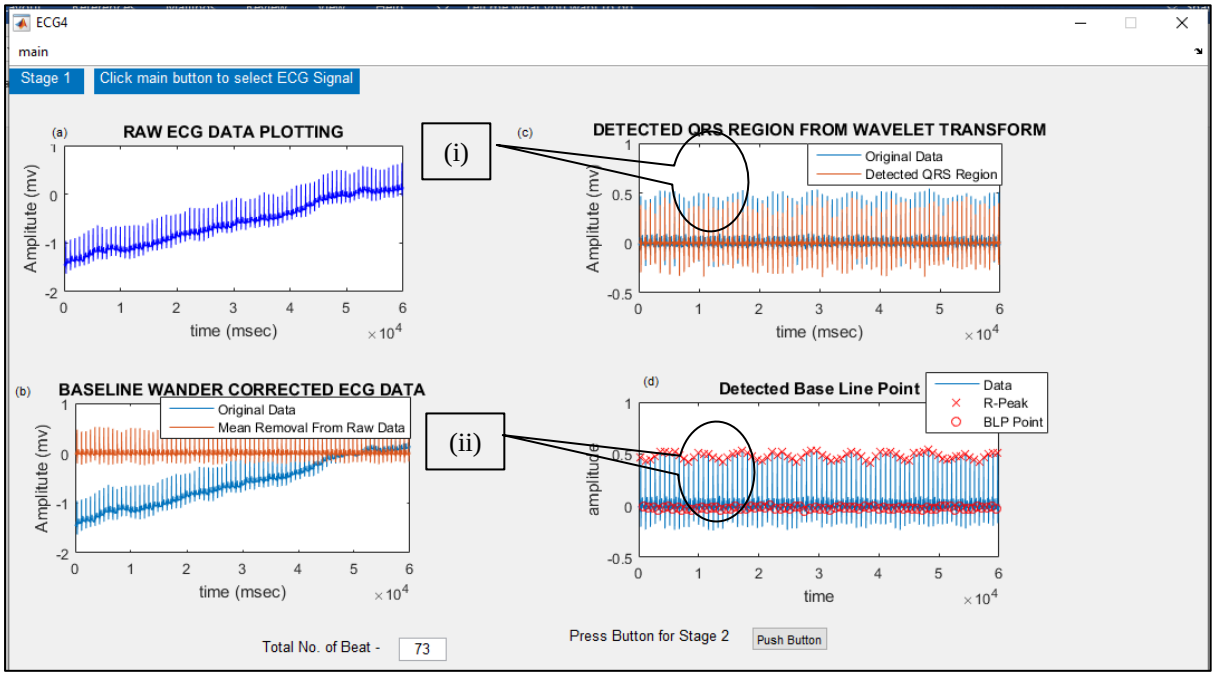

Fig.5.4.(a): Stage 1- Denoising and detection of R-peak index and BLP index of ECG Signal

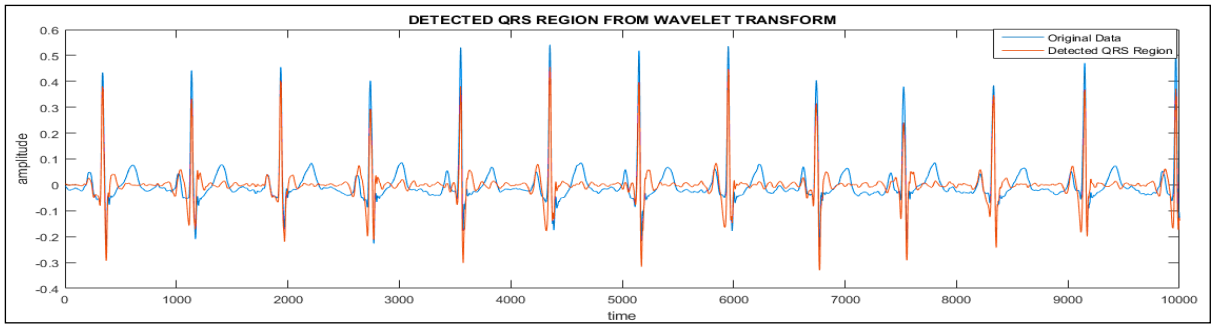

Fig.5.4.(a-i): Panel (c) of Stage 1 showing illustrated view of R-peaks Region

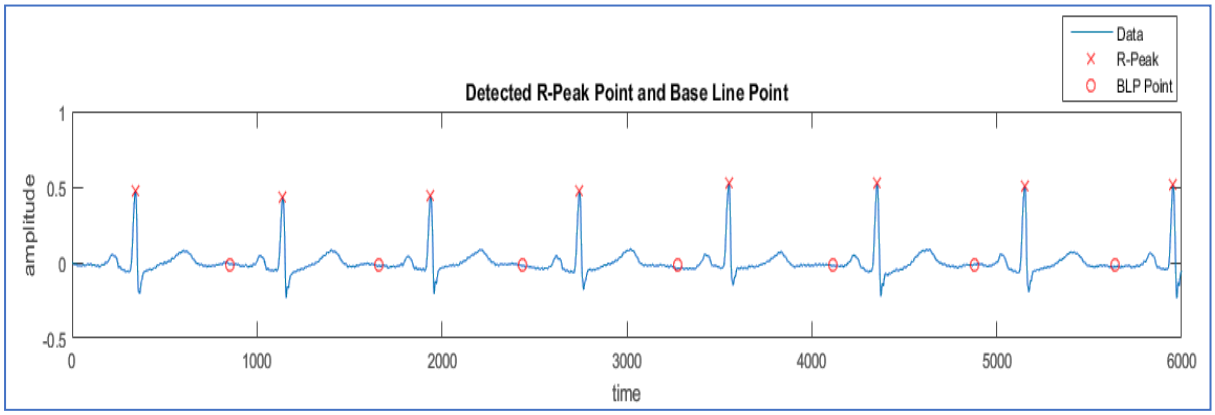

Fig.5.4.(a-ii): Panel (d) of Stage 1 showing illustrated view of R-peaks and baseline index

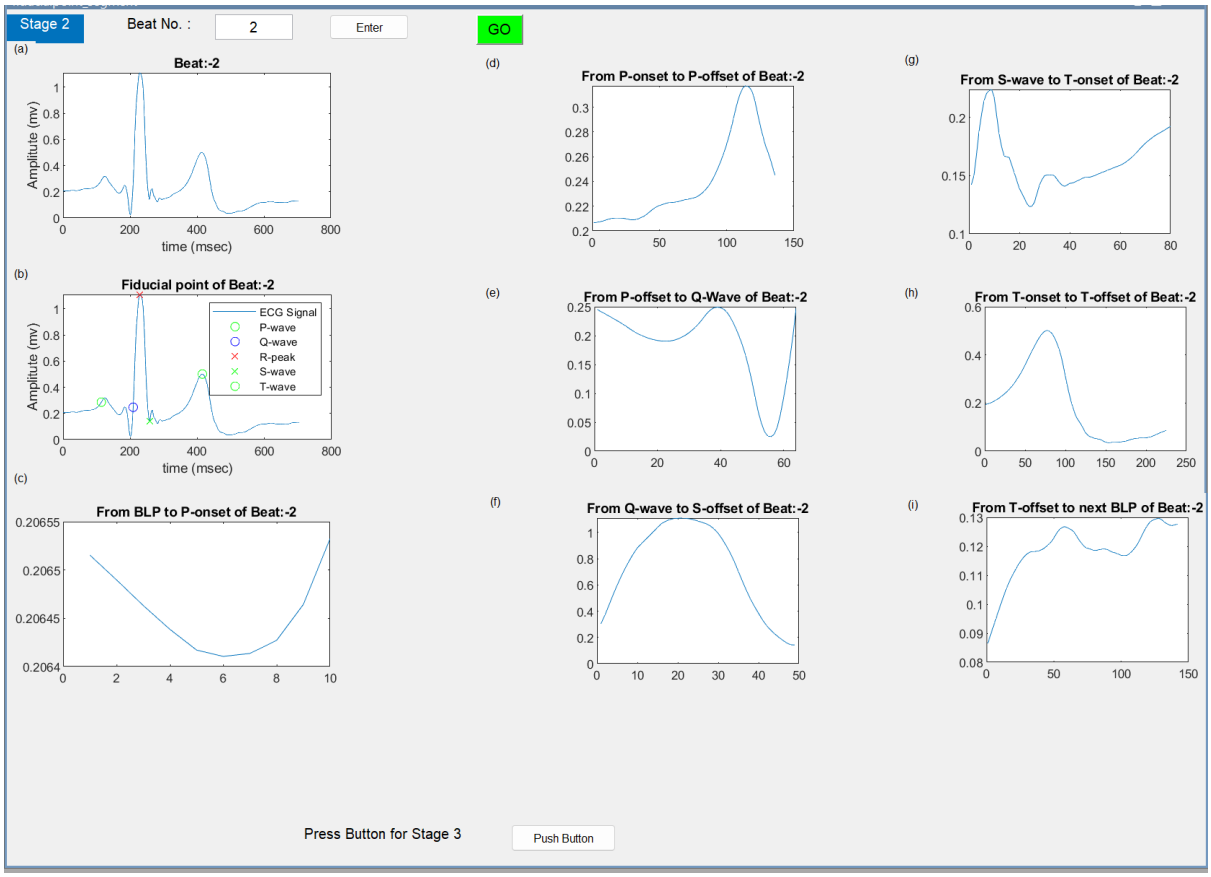

Fig.5.4.(b) Stage 2 – Fiducial Point Extraction and segmentation

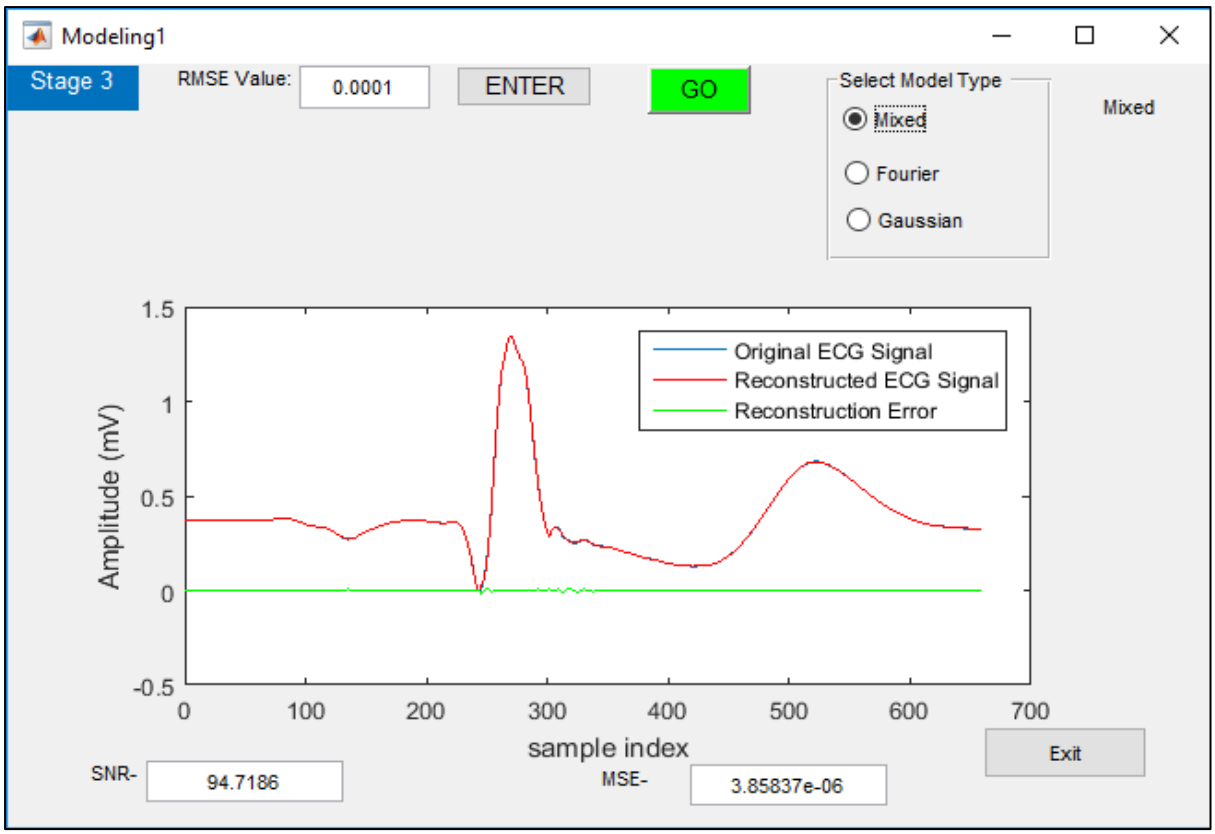

Fig. 5.4.(c): Synthesis of user defined ECG beat by Segment specific model

5.3. Results:

The segment specific model or mixed model was validated by ptbdb and mitdb database under Physionet. Thirty data ID was randomly chosen from mitdb database and the data ID are as follows: 100, 103, 106, 109, 111, 112, 113, 114, 116, 118, 123, 124, 200, 202, 203, 205, 207, 208, 209, 212, 214, 220, 221, 222, 223, 228, 231, 232, 233 and 234. We have considered five types of ECG annotations and among them one type is healthy and four different types of arrhythmia from mitdb and the beat types are: 1) normal sinus rhythm (NSR); 2) atrial premature contraction (APC); 3)premature ventricular contraction (PVC); 4) left bundle branch block (LBBB) and 5) right bundle branch block (RBBB) beat. The mitdb NSR, APC, PVC were obtained from lead MLII and LBBB, RBBB were obtained from lead MLII and V1.

This model was also validated using three types of the ptbdb database including normal sinus rhythm (NSR); anterior myocardial infarction (AMI) and inferior myocardial infarction (IMI). The healthy data were chosen from ptbdb data ID: p104/s0306lre, p117/s0291lre, p116/s0302lre, p121/ s0311lre, p155/s0301lre, p169/s0329lre, p174/s03241lre, p237/s0465re, p245/s0480re, p265/s050lre. The AMI data were randomly selected from data ID: data ID p010/s0036lre, p026/s0095lre, p044/s0046_re,p044/s0142lre, p044/s0143lre, p044/s0146lre, p044/s0159lre,p0163/s0034_re, p081/s0266lre, p081/s0346lre. The IMI beats were chosen from data ID: p012/s0043lre, p012/s0050lre, p021/s0065lre, p021/s0073lre, p021/s0097lre, p100/s0399lre, p100/s0401lre, p100/s0407lre, p139/s0223re, p291/s0554re. The NSR beats were obtained from ECG lead no. I and II. The AMI was taken from ECG lead no. V1, V2, V3 and V4. The IMI beats were taken from ECG lead no. II, III and aVF.

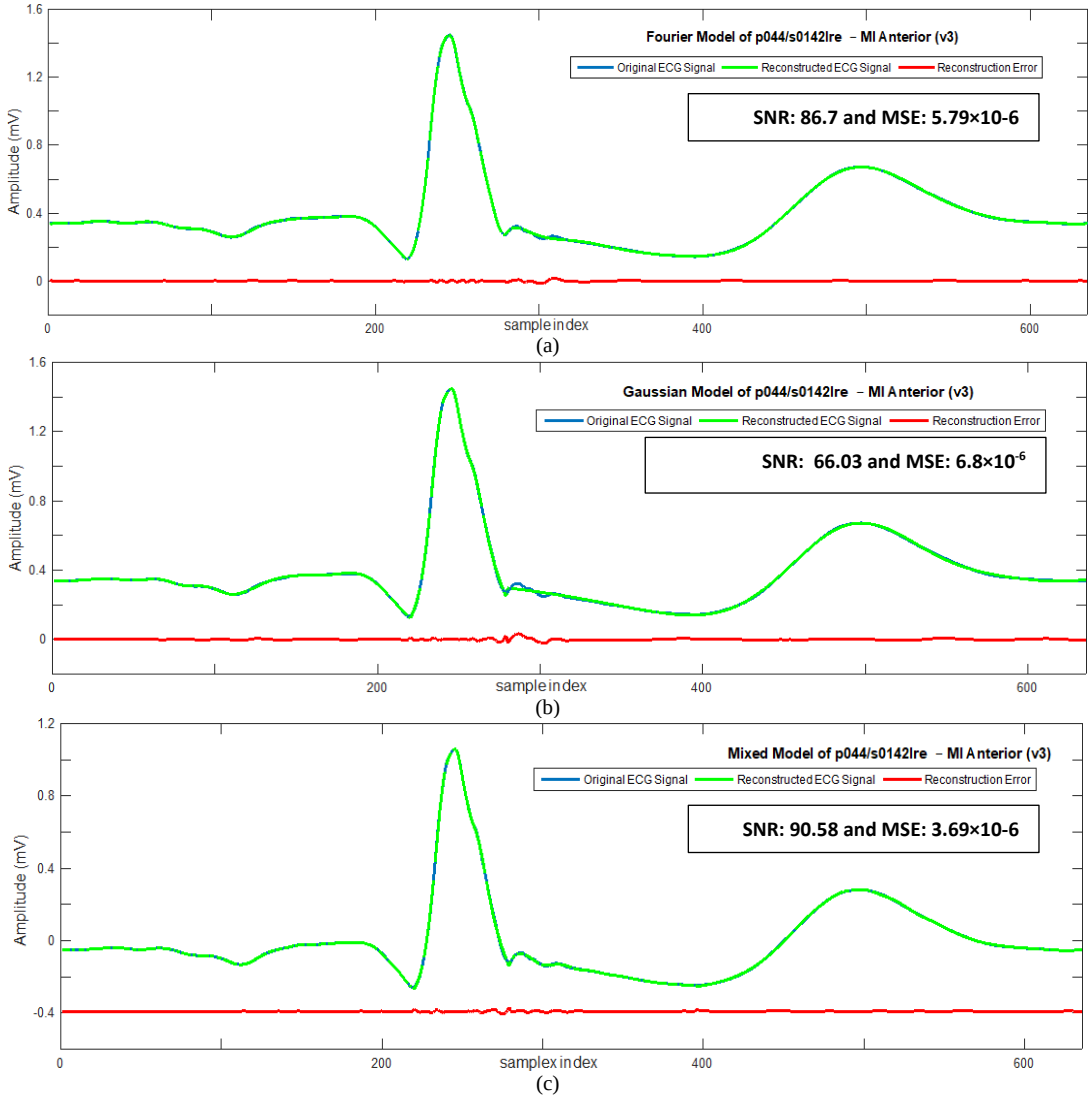

Fig.5.5.Reconstruction of ECG MI Anterior (V3) beat using (a) Fourier model; (b) Gaussian model and (c) Segment specific model

The spegment specific model is a error controlled dynamic model and RMSE was selected to control the error. The model order of each segment depends on the user-defined RMSE and model order for each segment was chosen automatically. The performance of model was evaluated by signal to noise ratio (SNR) and mean square error (MSE). The performance metrics are mathematically expressed as under:

$$RMSE = \sqrt{\frac{\sum_{k=1}^{N}\left[y_{ecg_r}(k) - y_{ecg}(k)\right]^2}{N}}$$

$$E_{max} = max\left[y_{ecg}(k) - y_{ecg_r}(k)\right]$$

$$MSE = \frac{\sum_{k=1}^{N}[y_{ecg}(k) - y_{ecg_r}(k)]^2}{N}$$

$$SNR = 10log\frac{\sum_{k=1}^{N}[y_{ecg}(k) - y_{ecg_m}(k)]^2}{\sum_{k=1}^{N}[y_{ecg}(k) - y_{ecg_r}(k)]^2} \qquad (5.5)$$

where, E_{max} represents maximum reconstruction error; y_{ecg} represents original ECG; y_{ecg_r} represents reconstructed ECG; y_{ecg_m} represents mean of original data; and N is the total number of samples. Table 5.1 shows reconstruction performance of proposed model with few arbitrarily selected data under each category from ptbdb and mitdb database. The average performance metrics i.e., SNR and MSE are given in the table 5.1

The reconstruction performance of mixed model was validated by ptbdb and mitdb data. To evaluate the model performance fifty beats are chosen randomly from each data ID. The average performance metrics are observed and few of them are listed in the Table 5.1. From ptbdb database the average SNR and MSE for NSR is 86.33 and 4.4×10^{-6} respectively, for AMI is 96.18 and 3.7×10^{-6} respectively and for IMI is 80.86 and 1.36×10^{-6} respectively. Hence, it is observed than the SNR for AMI is higher than other two types of beats and the average MSE is in terms of 10^{-6} which is negligible.

Table 5.1. Reconstruction performance of Segment Specific Model using ptbdb and mitdb database

Data ID (Category and lead No.)	***SNR (dB)***	***MSE×10^{-6}***
p169/s0329lre (NSR-I)	88.33	4.03
p174/s03241lre (NSR-I)	86.85	5.27
p237/s0465re (NSR-II)	84.57	4.22
p265/s050lre (NSR-II)	85.52	4.12
Average (NSR)	86.33	4.41
p010/s0036lre (AMI-V1)	99.84	0.12
p081/s0266lre (AMI-V3)	97.83	7.41
p081/s0346lre (AMI-V2)	96.45	3.61
p044/s0159lre (AMI-V1)	90.58	3.69
Average (AMI)	96.18	3.70
p012/s0043lre (IMI-II)	70.14	1.76
p012/s0050lre (IMI-II)	80.87	0.98
p021/s0065lre (IMI-III)	85.54	0.96
p021/s0073lre (IMI-III)	86.9	1.76
Average (IMI)	80.86	1.36
100 (mitdb NSR-MLII)	97.95	0.468
103 (mitdb NSR-MLII)	91.16	7.58
112 (mitdb NSR-MLII)	83.48	1.96
123 (mitdb NSR-MLII)	91.15	4.01
Average (mitdb NSR)	90.94	3.50
202 (APC-MLII)	84.54	4.32
209 (APC-MLII)	91.15	4.01
222 (APC-MLII)	91.58	0.59
232 (APC-MLII)	90.44	0.45
Average (APC)	89.42	2.34
106 (PVC-MLII)	84.09	4.57
208 (PVC-MLII)	92.58	2.17
223 (PVC-MLII)	99.67	3.23
228 (PVC-MLII)	96.81	2.27
Average (PVC)	93.28	3.06
109 (LBBB-V1)	94.11	1.4
111 (LBBB-V1)	97.2	1.23
207 (LBBB-V1)	94.37	6.05
214 (LBBB-V1)	89.4	2.27
Average (LBBB)	93.77	2.74
118 (RBBB-V1)	95.87	1.93
124 (RBBB-MLII)	98.75	5.58
212 (RBBB-V1)	88.35	2.54
231 (RBBB-V1)	88.33	4.03
Average (RBBB)	92.83	3.52

The performance metrics for mitdb data are as follows: for NSR average SNR and MSE is 90.94 and 3.5×10^{-6} respectively, for APC is 89.42 and 2.34×10^{-6} respectively, for PVC is 93.28 and 3.06×10^{-6} respectively, for LBBB is 93.77 and 2.27×10^{-6} respectively and for RBBB is 92.83 and 3.52×10^{-6} respectively. It is observed that the SNR of mitdb data is higher than ptbdb data. As the model is dynamic and error-controlled the reconstruction accuracy becomes high and suitable for both mitdb and ptbdb database.

Fig. 5.6. and 5.7. shows the reconstruction performance of different categories of beats arbitrarily selected from ptbdb data and mitdb data respectively. The original and reconstructed data are superimposed for easy visual comparison, along with the sample-to-sample error plotted. It is observed that the reconstructed plot using model parameters match closely with the corresponding original data plot, and error is negligible.

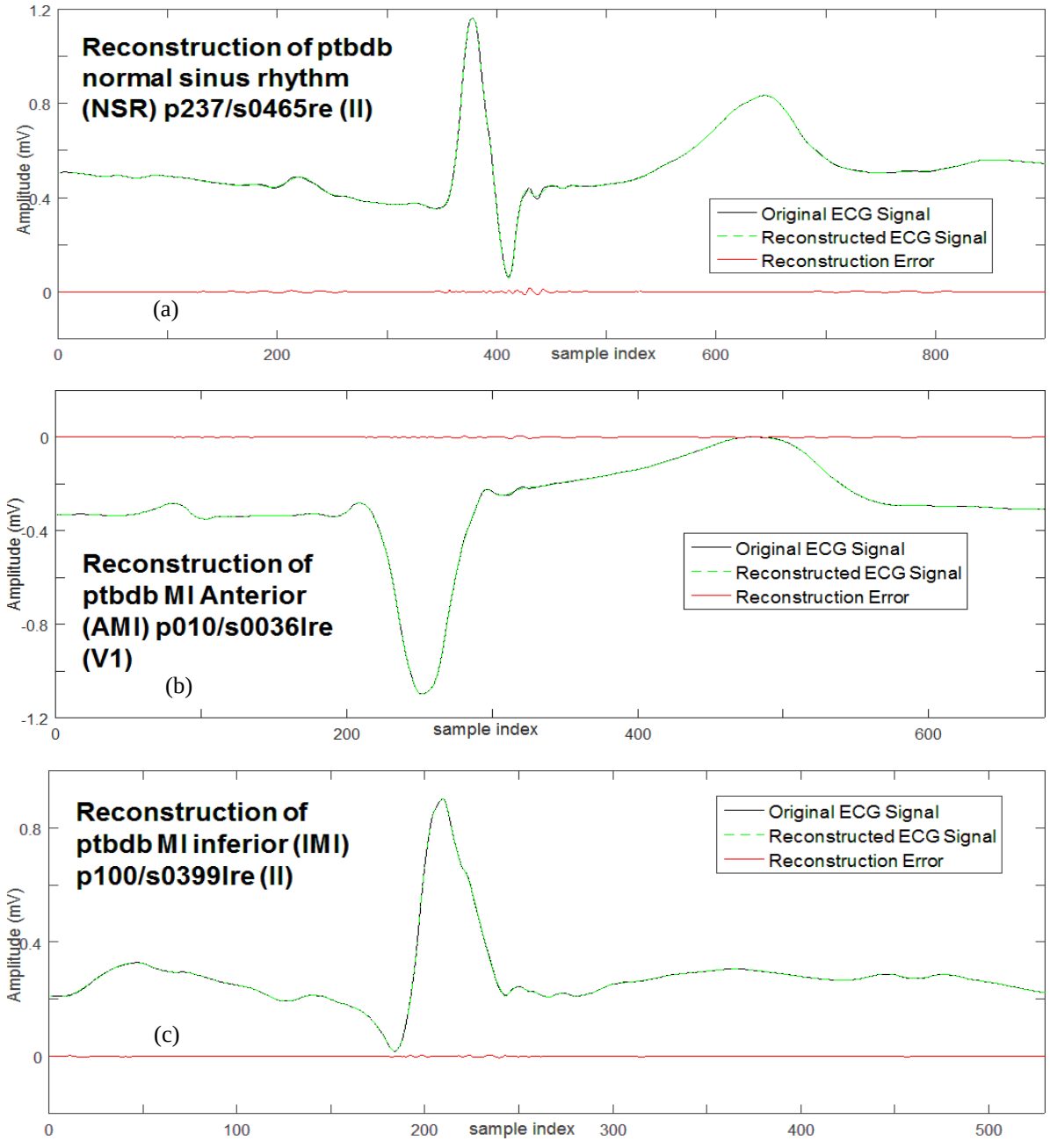

Fig.5.6. Reconstruction of ECG signal from ptbdb database (a) NSR; (b) AMI and (c) IMI

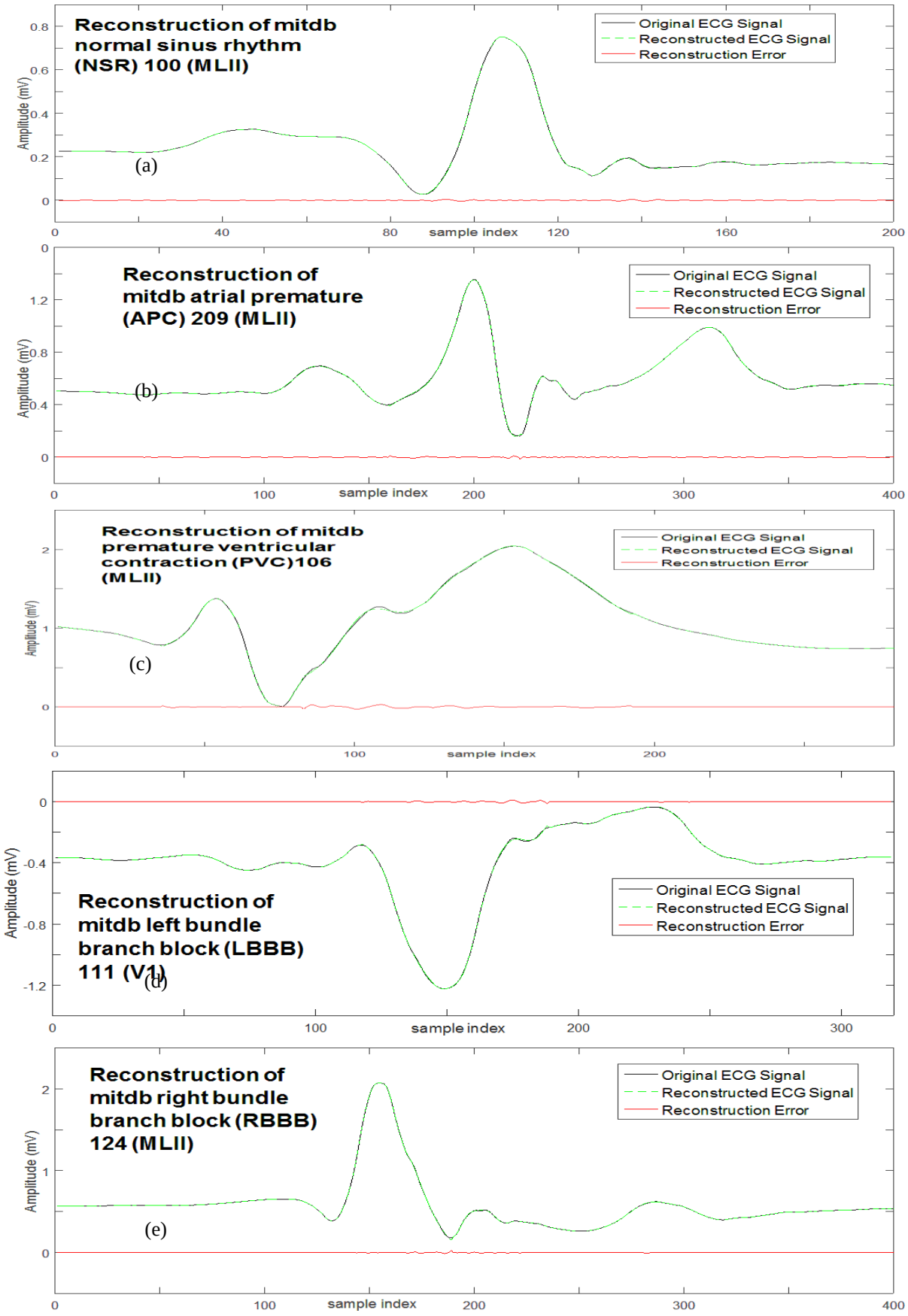

Fig.5.7. Reconstruction of ECG signal from mitdb database (a) NSR; (b) APC; (c) PVC; (d) LBBB and (e) RBBB

Table 5.2. Comparison of reconstruction performance of Segment specific model with published research work

Work	Method	Database and category	SNR	MSE $\times 10^{-6}$	RMSE $\times 10^{-3}$
Kundu [15]	Gaussian	ptbdb (NSR and AMI)	20.71	-	-
	Fourier		22.16	-	-
Bilah [136]	Gaussian	mitdb:			
		NSR	-	-	25.69
		APC			28.46
		PVC			59.16
		LBBB			20.02
		RBBB			31.69
Proposed method	Segment Specific modeling	ptbdb :			
		NSR	86.33	4.41	2.10
		AMI	96.18	3.70	1.72
		IMI	80.86	1.36	1.15
		mitdb:			
		NSR	90.94	3.50	1.70
		APC	89.42	2.34	1.38
		PVC	93.28	3.06	1.73
		LBBB	93.77	2.74	1.56
		RBBB	92.83	3.52	1.83

The performance of segment specific model is compared with the work reported in [15] and [136] where the result is given explicitly. The comparison result is given in Table 5.2. The main objective of ECG modeling is enhancing the reconstruction efficiency by minimizing reconstruction error. The higher SNR value with minimal MSE and RMSE indicates the model accuracy. The high signal-to-noise ratio and low MSE decrease the chance of clinical information loss. It was observed from the previous model methods are not based on error control and dynamic model order, thus the signal was reconstructed by pre-specified model order. As the higher model order may cause overfitting and lower model order may cause under fitting, thus model order selection is very important. In few other works the model performance was evaluated by computing percentage root mean square difference (PRD), PRD normalization etc. These works are excluded to compare with the proposed work. In few works, the model efficiency was evaluated by SNR, MSE, RMSE but the results are not published. From the table 5.2. it can be concluded that mixed model i.e., segment specific model achieves very high reconstruction accuracy as compared with conventional Gaussian and Fourier model.

5.4. Significance of ARIMA model for synthesis of ECG signal:

ECG signal is a time-series signal. The statistical characteristics of ECG is change with time thus it is a non-stationary signal and the behavioral charactictics also change in every instant, hence ECG also a time-variant signal. There are four types of statistical modeling methods available for modeling of time-series signal viz., AR model, MA model, ARMA model and ARIMA model. ARMA model combine the working principal of AR model and MA model. ARMA model is suitable for stationary signal but ECG is a non-stationary signal. Hence ARIMA model is introduced for modeling of ECG signal. Each method is discussed briefly in the below section:

5.4.1. Auto Regressive (AR) Model:

Auto regressive(AR) model is a statistical modeling method which is used to predict future values of a time series signal using the past value. In this method past trend of signal influences the present values to forecast the future trend. The current value is expressed by the linear combination of past trend with a random noise. If, we consider y_t as predicted value and past values are y_{t-1}, y_{t-2}, y_{t-3} etc. The AR model is expressed by:

$$y_t = f(y_{t-1}, y_{t-2}, y_{t-3}, \dots\dots, \varepsilon_t) \quad (5.6)$$

where, ε_t is the random error.

If the model order is *p*, the AR(*p*) model is mathematically expressed by:

$$y_t = (c + \beta_1 y_{t-1} + \beta_2 y_{t-2} + \cdots + \beta_p y_{t-p} + \varepsilon_t) \quad (5.7)$$

where, c is constant, β is the model parameter and p is the order of model.

5.4.2. Moving Average (MA) Model:

Moving average model is a statistical model, used to analyze time series signal. It forecast the future trend by understading the pattern of time series. In this model the present value is depends on the past random error associated with white noise of the time series. The MA model can be expressed by:

$$y_t = f(\varepsilon_{t-1}, \varepsilon_{t-2}, \varepsilon_{t-3}, \dots) \quad (5.8)$$

where, ε_{t-i} are the past random error and i = 1,2,3….q.

MA model depends on q of its past error terms, it is called MA(q) model, is represented by:

$$y_t = (\mu + \varepsilon_t + \theta_1 \varepsilon_{t-1} + \theta_2 \varepsilon_{t-2} + \cdots + \theta_q \varepsilon_{t-q}) \quad (5.9)$$

where, μ : mean of the series, θ : model parameter and q : model order.

5.4.3. Auto Regressive Moving Average (ARMA) Model:

Auto regressive moving average (ARMA) model is best suited for stationary time-series. It works by combining the AR model and MA model for analysis and prediction of time series data. It recognizes the past data and the past random error to forecast the future trend of time-series data. It develops a linear equation by combining past values and error terms to predict future values. The ARMA model has two model parameters *(p,q)*. The model with order *p,q* defined as $ARMA_{(p,q)}$ model ARMA model can be expressed mathematically as under:

$$y_t = \beta_0 + \varepsilon_t + \beta_1 y_{t-1} + \beta_2 y_{t-2} + \dots + \beta_p y_{t-p} + \theta_1 \varepsilon_{t-1} + \theta_2 \varepsilon_{t-2} + \dots + \theta_q \varepsilon_{t-q} \quad (5.10)$$

5.4.4. Auto Regressive Integrated Moving Average (ARIMA) Model:

Auto regressive integrated moving average (ARIMA) model is a statistical model which predict future trend of a time series from the past observations. The AR model and MA model are suitable for stationary time series signal. In stationary time series the trend of signal does not changes over time but in case of non-stationary signal the trend of signal is changed over time. The non-stationary signal are time variant and it is very difficult to predict future trend as it is not constant over time. ARIMA model is the most widely used approach for non-stationary time variant time series. It combines the auto regressive, moving average and integrated approaches. The integrated part convert the non-stationary signal into a stationary signal and then modeling of signal is done by AR and MA approach. ARIMA model mathematically expressed by:

$$y_t = \mu + \varepsilon_t + \beta_1 y_{t-1} + \beta_2 y_{t-2} + \dots + \beta_p y_{t-p} + \theta_1 \varepsilon_{t-1} + \theta_2 \varepsilon_{t-2} + \dots + \theta_q \varepsilon_{t-q} \quad (5.11)$$

The value of hyperparameters are most crucial as it controls the performance of ARIMA model and are defined as follows:

p: The number of lag observations included in the model, known as lag order.
d: The number of times that the raw observations are differenced, known as degree of differencing.
q: The size of the moving average window, known as the order of moving average.

Basically ARIMA model subtracts the past observations from the precedeing one. The values of hyperparameters are $p \geq 0, q \geq 0, d \geq 0$. In case of non-stationary time series, this model differenced the signal two times to convert into a stationary signal. Hence, for most of the cases *d*=2. The values of each parameter is very significant to evaluate model efficiency.

5.5. Significance of optimization of ARIMA model hyperparameters:

Optimization of ARIMA model hyperparameter is very crucial for reduction of model complexity without interrupting the model accuracy. It is very significant to improve computational efficiency of model, to control designs by simplifying the data analysis. It is vital as it finds out the right way to establish a balance among model accuracy and computational cost. The morphology of each ECG beat is different from other. Thus optimization of ARIMA model hyperparameter is important to chose the best suited model order for ECG beats. There are several optimization methods, among them two methods are chosen for ARIMA model hyperparameters viz., grid search method and particle swarm optimization method. The range of hyperparameters are as follows: for *p and q*, the ranege is 0 to 9 and for *d*, the range is 0 to 2. The best suited hyperparameters are chosen from the aforesaid range. The performance of the optimizer was validated using the ptbdb and mitdb database.

5.6. Optimization of ARIMA Model Hyperparameters for synthesis of ECG signal:

In Fig. 5.7. the signal processing flow diagram of ARIMA Model hyperparameter optimization is shown. Each beat of preprocessed ECG signal were stored into a beat matrix. From the beat matrix fifteen data ID were selected from mitdb database and thirty numbers of beats are chosen randomly from the data records to develope a database. The ARIMA model hyperparameters were optimized using the grid search and particle swarm optimization methods. The beat specific optimized paramerters are used for synthsis of those beats by ARIMA model. Model performance was evaluated to identify the most effective optimization method.

5.6.1. Working Principal of Grid Search Optimization (GSO) method:

Grid search optimization (GSO) is a popular method for tunning of model hyperparameter. It is an exhaustive technique which explore all possible combination of hyperparameters within a certain range. In simple word it follows trial-and-error technique to find out the best combination until the desired accuracy is achieved. A model with *N* numbers of hyperparameters, having grid dimension of *N* and the number of trial solution proportinal to L^N where *N* represents the number of trial solution along each dimension of grid. The limit of search grid is defined by the trial solution which are lying in a specific range of values. A three-dimensional grid search is performed as under:

$$p = p_l + (p_u - p_l) \times [0 : L1 - 1]' / (L1 - 1)$$
$$d = d_l + (d_u - d_l) \times [0 : L2 - 1]' / (L2 - 1)$$
$$q = q_l + (q_u - q_l) \times [0 : L3 - 1]' / (L3 - 1) \quad (5.12)$$

The error at each grid point is computed by:

$e = zeros\ (L1, L2, L3)$
for i = [0: L1]
for j = [0: L2]
for k = [0: L3]
$m^{opt} = [p(i), d(j), q(k)]$
$d^{pre} = \mathrm{G}m^{opt}$
$e = d^{obs} - d^{pre} \quad (5.13)$

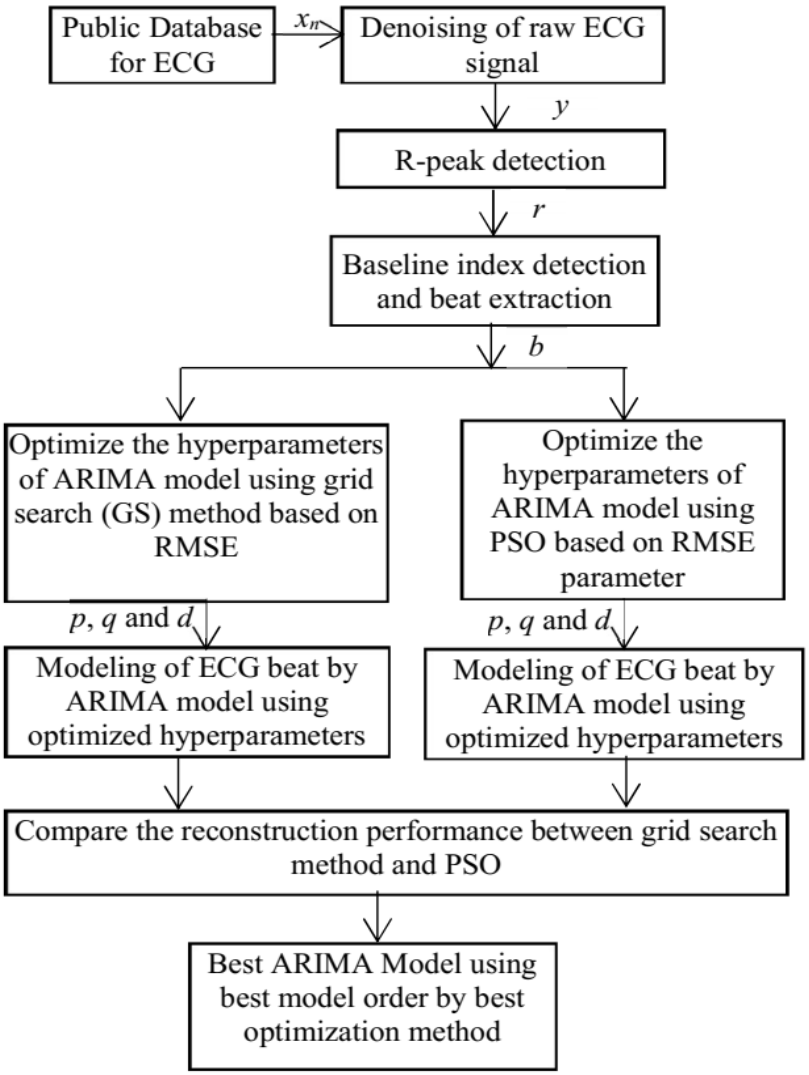

Fig.5.8.: Signal processing flow diagram of ARIMA model hyperparameter optimization

The minimum value of error is computed by:

$e_{temp} = \min(e)$

If, $\min(e_{temp}) \leq e_{min}$

Then, $e_{min} = e_{temp}$

$p^{opt} = p(i)$

$d^{opt} = p(j)$

$q^{opt} = p(k)$

Where, *L1*, *L2* and *L3* are number of trial solutions for model hyperparameters *p*, *d* and *q* respectively for each dimension of grid. The grid of possible values of model parameters are defined by *i, j* and *k*. Here, the lower bound ($p_l, d_l \; and \; q_l$) as 0 and the upper bound ($p_u, d_u \; and \; q_u$) as 9, 2, 9 for p, d and q respectively were considered. Thus, the value of *L1*, *L2* and *L3* and 9, 2 and 9 respectively. Here, $m^{opt}$is the optimized model hyperparameters, d^{obs} is observed data, d^{pre} is predicted data and *e* is the matrix of total error for every point on the grid that is, for every combination of *p, d* and *q*. From the matrix *e*, searches the minimum value e_{min} to determine the corresponding best optimized model hyperparameters, p^{opt}, d^{opt} and q^{opt}. The function $\min(e)$ returns a row vector, e_{temp} which contains the minimum value of e. Now, compare the value of e_{min} and e_{temp}. If e_{temp} is less than or equal to e_{min}, then the value of e_{temp} is stored as e_{min} and the corresponding combination of hyperparameters $[p(i),\ d(j),\ q(k)]$ are the best-optimized model hyperparameters $[p^{opt}, d^{opt}, q^{opt}]$.

5.6.2. Working principle of Particle Swarm Optimization (PSO) Method:

Particle swarm optimization (PSO) is another popular meta-heuristic method for optimization of model hyperparamers. This method working on the principle of interative improvement of the quality of potential solution on the basis of a certain measured value. In this work, PSO was developed to minimize the value of RMSE within 9% which is acceptable for clinical evaluation. The objective function of PSO can be defined as under:

$$min_{h \in U} |r_k - r_{th}| \; where, h = z(t_k) \tag{5.14}$$

where, *h* contains the values of *p, d* and *q* in the global search space *U*; t_k is the optimized values of k^{th} iteration; r_k is the RMSE value calculated in k^{th} iteration using the *p, d* and *q* and r^{th} is the threshold RMSE.

The velocity and position of particles was updated depending on the two best values, *pbest* (personal best or local best) and *gbest* (global best) and it can be mathematically represented as,

$$p_{i+1} = p_i + v_{i+1}$$

$$v_{i+1} = v_i + c1.rand.(pbest - p_i) + c2.rand.(gbest - p_i) \tag{5.15}$$

Where, *p* and *v* represent position and velocity respectively of a particle, and *i* indicates the current step. Here, lower bound is 0 and upper bounds for *p, d* and *q* are of 9, 2, 9 respectively were considered, with 100 numbers of particle in the swarm, 100 numbers of iterations, 0.5 as particle velocity scaling factor, scaling factor 0.5 to search away from the particle's best-known position and 10^{-8} is considered as minimum step size of swarm's best position before the search terminates.

5.7. Results :

The work was validated by mitdb and ptbdb database under PhysioNet. Six classes of ECG beats were chosen from mitdb and the ECG classes are: 1) Normal sinus rhythm (NSR), 2) atrial premature beat, 3) premature ventricular contraction beat, 4) paced beat (P), 5) left bundle brunch block (LBBB), 6) right bundle brunch block (RBBB). The following fifteen data records from mitdb were selected: 100, 101, 102, 103, 106, 109, 111, 114, 115, 118, 124, 205, 207, 212 and 231. The mitdb database were obtained from ECG lead V1, V2, V$ and V5.

Seven classes of ECG beats were selected from ptbdb database and the the ECG classes are as follows: normal sinus rhythm (NSR), anterior myocardial infarction (AMI), MI antero-lateral, MI antero-septal, inferior myocardial infarction (IMI), MI infero lateral, MI infero posterior. From ptbdb database following fifteen data records were selected: p104/s0306lre, p116/s0302lre, p117/s0292lre, p131/s0273lre, p180/s0561re, p002/s0015lre, p005/s0025lre, p010/s0036lre, p0020/s0069lre, p081/s0266lre, p008/s0037lre, p011/s0044lre, p011/s0067lre, p022/s0074lre and p066/s0225lre. The normal sinus rhythm of ptbdb was obtained from lead II. The AMI, MI antero-lateral and MI antero-septal data were obtained from lead V1, V2 and V3. The IMI, MI infero-lateral, MI infero-posterior data were obtained from lead II, III and aVF. The GSO and PSO optimized hyperparameters were used for modeling of ECG signal by ARIMA model. The reconstruction performance were evaluated by maximum reconstruction error (MAX), mean square error (MSE) and mean absolute error (MAE). The MAX and MAE are defined as under:

$$MAX = max\left[y_{ecg}(k) - y_{ecg_r}(k)\right]$$

$$MAE = \frac{1}{N}\left|y_{ecg}(k) - y_{ecg_r}(k)\right| \tag{5.16}$$

where, y_{ecg} denotes original ECG; y_{ecg_r} denotes reconstructed ECG; and N denotes total number of samples.

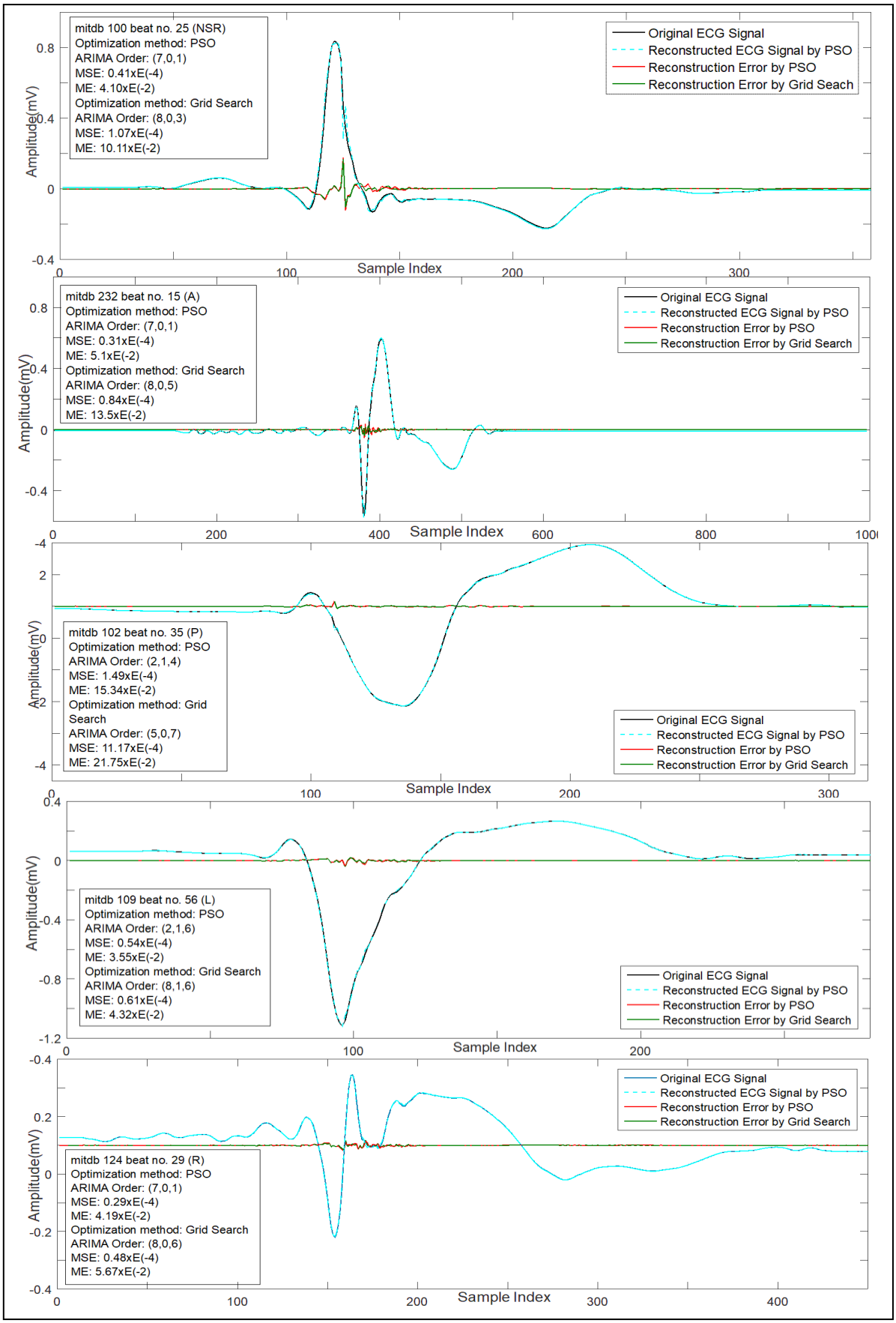

Fig.5.9. Reconstruction of different classes of ECG beat from mitdb database by ARIMA model using optimized hyperparameters; (a) NSR, (b)APC; (c) Paced; (d)LBBB; (e) RBBB

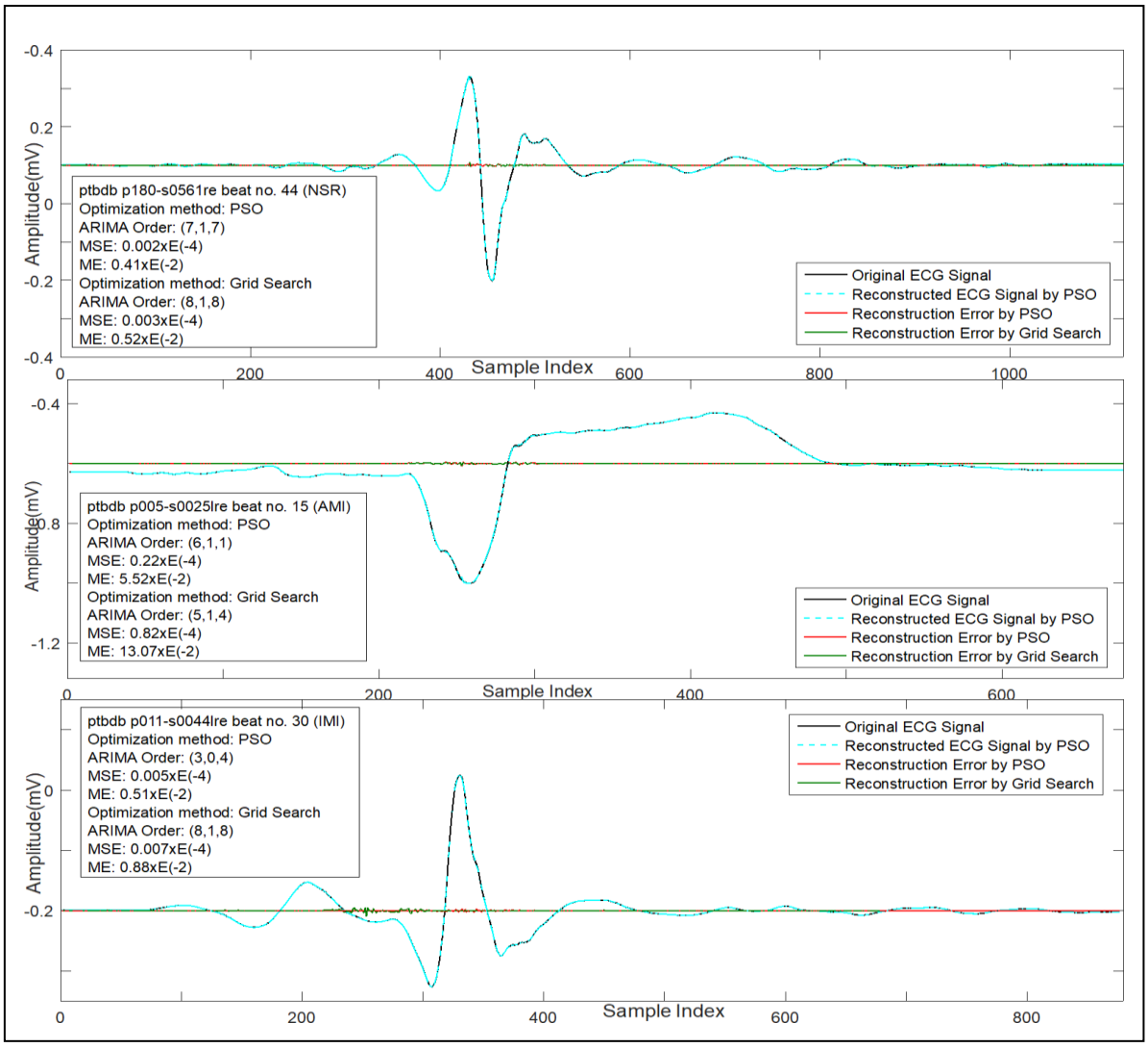

Fig.5.10. Reconstruction of different classes of ECG beat from ptbdb database by ARIMA model using optimized hyperparameters; (a) NSR, (b)AMI; (c) IMI

Fig.5.9. and 5.10. shows original, reconstructed beat and corresponding error signal plot of each type of arrhythmia data as well as pathological beat from mitdb and ptbdb dataset. The corresponding values of MSE, RMSE using the both types of optimization techniques are also indicated in the figure and from this we can observed that both method performs good but PSO achieves better acccuracy in terms of reconstruction performance. The reconstruction error for ARIMA model using PSO optimized hyperparameters are lesser than GSO optimized hyperparameters. It is observed that the reconstructed plot closely follows the original beat and the sample-to-sample error plot is lower using PSO technique. The performance of both methods are compared and tabulated in Table 5.3. for better understading. The table shows the summary of reconstruction performance of ARIMA model using PSO and GSO optimized hyperparameters for different classes of cardiac abnormalities. Table 5.4. shows mean reconstruction performance of the model using ptbdb and mitdb database. From the both table it can be concluded that PSO is better optimization technique for hyperparameter optimization of ARIMA model.

Table.5.3. Comparison of reconstruction performance of ARIMA using PSO and GSO method

Database	Grid search (GS)				Particle warm optimization (PSO)			
	MAX ***($\times 10^{-2}$)***	***MAE*** ***($\times 10^{-2}$)***	***MSE*** ***($\times 10^{-4}$)***	***RMSE*** ***($\times 10^{-2}$)***	***MAX*** ***($\times 10^{-2}$)***	***MAE*** ***($\times 10^{-2}$)***	***MSE*** ***($\times 10^{-4}$)***	***RMSE*** ***($\times 10^{-2}$)***
mitdb Database								
Normal sinus rhythm (NSR)	13.07	1.09	11.31	3.36	5.89	0.46	1.44	1.20
Paced beat (P)	17.71	1.33	4.37	2.09	13.12	0.60	1.43	1.19
Left bundle branch Block (LBBB)	16.37	2.93	44.85	6.69	6.46	0.58	1.53	1.23
Right bundle branch Block (RBBB)	17.52	1.47	12.29	3.51	8.19	0.48	1.16	1.07
Premature ventricular contraction (V)	16.19	1.75	8.51	2.91	8.75	0.50	1.20	1.09
Atrial premature beat (A)	17.22	0.80	2.89	1.70	6.87	0.16	0.27	0.51
ptbdb Database								
Normal sinus rhythm (NSR)	17.14	0.06	0.04	0.20	1.58	0.04	0.01	0.10
Anterior myocardial infarction (AMI)	11.49	0.58	1.14	1.06	6.50	0.45	0.20	0.45
Inferior myocardial infarction (IMI)	3.43	0.24	0.20	0.45	2.07	0.08	0.03	0.17

Table 5.4. Mean Reconstruction performance of ARIMA Model using GSO and GSO optimized hyperparameters

Database	Grid search (GS)				Particle warm optimization (PSO)			
	MAX ***($\times 10^{-2}$)***	***MAE*** ***($\times 10^{-2}$)***	***MSE*** ***($\times 10^{-4}$)***	***RMSE*** ***($\times 10^{-2}$)***	***MAX*** ***($\times 10^{-2}$)***	***MAE*** ***($\times 10^{-2}$)***	***MSE*** ***($\times 10^{-4}$)***	***RMSE*** ***($\times 10^{-2}$)***
mitdb Database	16.35	1.56	14.04	3.38	8.21	0.46	1.17	1.05
ptbdb Database	10.69	0.29	0.46	0.57	3.38	0.19	0.08	0.24

5.8. Summary

The characteristics of each ECG beats are unique. The ECG beat of a single cardiac cycle are different from other. Thus hyperparameters are plays a vital function for modeling of ECG signal. In this approach two methods are described, 1) segment specific model and 2) ARIMA model.

In segment specific model Fourier and Gaussian model were used for synthesis of ECG beat. A single beat was divided into seven segment according to their shape and the modeling methods for each segment were chosen accordingly. The bell shaped waveforms were modelled by Gaussian method and the equipotential segments were modelled by Fourier signal. The model parameters were different for each segment and it was based on user defined RMSE. According to the RMSE value the model parameters were chasen for each segment and modelled seperately by suitable modeling method. As a result the performance of error-controlled and dynamic model was increased by minimizing the reconstruction error . The achieved reconstruction error is in terms of 10^{-6} which is negligible and acceptable for clinical application.

But as the ECG signal is a non-stationary time-series, for realtime application ARIMA model performs more suitably than other published model. But the selection of ARIMA model hyperparameters is a challenging job. ARIMA model has three hyperparameters (p,d and q) and values of each parameter are important to achieve higher model performance. Hence two different types of optimization methods were used to optimize the hyperparameters and compare their performance to chose the best method for hyperparameter tunning. The performance of this work was validated by mitdb and ptbdb database and

observed that reconstruction performance of ARIMA model using PSO optimized hyperparameters offers better result than GSO.

The shortcoming of this model is consumption of higher computational time. The PSO model gives better result than GSO but PSO consume more time than GSO. The average computational time of PSO is 13:28:32 minutes where GSO consumes 5:18:28 minutes. GSO consumes lesser time than PSO but both method are not suitable for realtime application. It can be overcome by development of a hyperparameter prediction model.

Chapter 6

Compression and Classification of ECG signal using Deep Learning based Method

6.1. Introduction

As per the survey of World Health Organization (WHO), Cardiovascular diseases (CVDs) become the most prominent cause of mortality. These can be prevented by early detection and proper diagnosis. CVDs can be detected by constant monitoring an electrocardiogram (ECG). ECG is a non-invasive and economical tool for cardiac signal acquisition. There are various types of heart disease, such as arrhythmia, heart attack, coronary heart disease, and cardiomyopathy. ECGs are also used to investigate cardiac problems, such as chest pain, shortness of breath, and dizziness. From this perspective, ECG modeling becomes very important for clinical analysis, classification, compression and data transmission.

In recent years, telemedicine has become very popular for monitoring and diagnosing cardiac patients in remote locations. A continuous cardiac waveform consumes enormous memory. The compression performs the task of reduction of the link burden and memory utilization of the source device during transmission. The compressed information are decompressed at receiver end for clinical analysis and proper diagnosis. Classification is an important step to identify different heart conditions, interpretation of cardiac rhythm, and disease identification. Automatic ECG classification is very useful for identification of unknown ECG class and saves the valuable time of doctors. Early detection of cardiac disease and proper diagnosis is very helpful to assure survival rate of cardiac patients. It is also useful for research related to CVDs.

Features plays a vital role for lossless compression and effective classification. In compression the features can be stored instead of a whole signal and in classification the complex features carries the clinical trait of each type of heart condition. Thus, before compression and classification feature extraction is a necessary step for denoised and preprocessed ECG signal.

In these work ECG compression and classification were done by deep learning method. The main objectives are lossless ECG compression based on deep-learning method via an adaptive autoregressive integrated moving average(ARIMA) model and 1D-Deep convolution neural network based multiclass ECG classification.

6.2. Development of deep learning based lossless ECG compression model:

The lossless ECG compression model was developed and validated by mitdb data from PhysioNet database. The raw ECG signal was denoised by DWT method. The R-peak detection and baseline index (BLI) detection was done by DWT method. The beats were extracted and stored into a cell for generation of beat cell. The deep learning-based feature extraction module was used to develop a compression module for minimization of compression loss.

A deep autoencoder (DAE) was involved for dimensionality reduction and feature extraction to form a feature matrix (FM). PSO optimizes the ARIMA model hyperparameters of each beat in the beat cell to generate a target matrix (TM). A multilayer perceptron neural network (MLPNN) based automatic hyperparameter prediction model (HPM) was developed and trained/tested by FM and TM. The complex features of each beat were passing through the HPM to predict the best suited ARIMA model hyperparameters for the respective beat. The predicted parameters were used for modeling of beat by ARIMA model and the model coefficients are stored as compressed data. The data are transmitted to

the pathology within a data packet from remote location. At the receiver end the data packets are stored for future use or reconstructed via ARIMA model for pathological analysis.

The compression performance measured by compression ratio (CR) and PRD%. The reconstruction efficiency was evaluated in terms of MSE, MAE and ME. Fig. 6.1. shows a schematic diagram of the lossless compression model, and each block of the diagram is described in sections 6.1.1 to 6.1.6.

The proposed model was developed and evaluated on the basis of ten classes of ECG data from mitdb: 1) normal sinus rhythm (H), 2) atrial premature (A), 3) premature ventricular contraction (V), 4) left bundle branch block (L), 5) right bundle branch block (R), 6) paced (P), 7) aberrated atrial premature (a), 8) nodal (junctional) premature (J), 9) fusion paced (f) and 10) fusion PVC (F) beat. This work was developed in the Python environment using PyCharm, version 3.8, 64 bits.

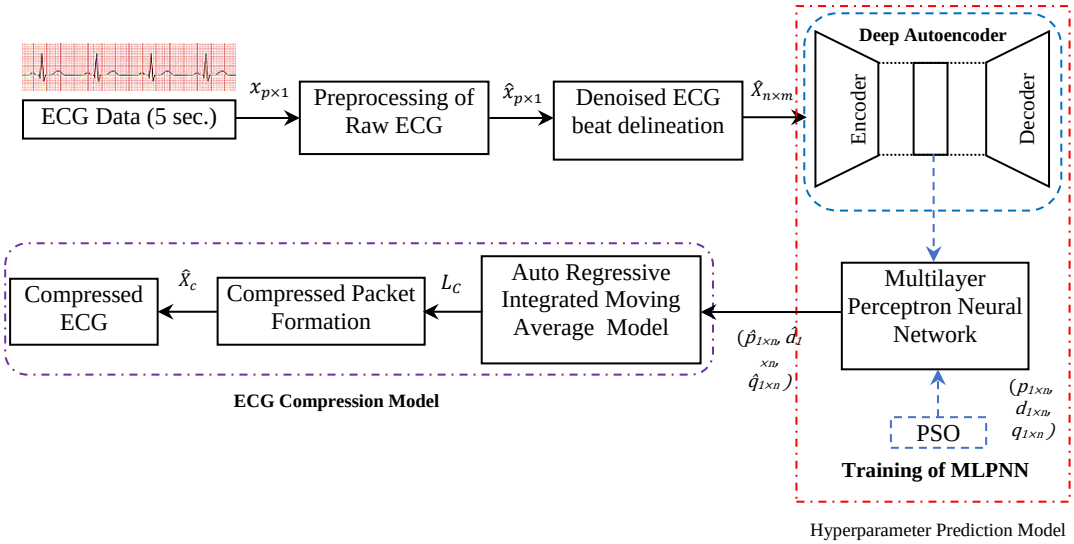

Fig. 6.1. Schematic diagram of the lossless ECG compression model by the adaptive ARIMA model

6.2.1. Feature Matrix Generation via DAE:

The DAE is a nonlinear dimensionality reduction tool based on deep-learning model. It has three layers: one input layer, multiple hidden layers and one output layer. The DAE works in two sections: i) The encoder part encodes data into lower dimensions, and the decoder part decodes the data to its original length. The hidden layer with lower dimensions is the bottleneck layer.

The encoded input layer to the hidden layer is defined as follows:

$$H = g_{\theta 1}(X) = \sigma(W_{ij}X + \varphi_1) \quad (6.1)$$

The hidden layer decoded to the reconstruction layer is defined as follows:

$$X' = g_{\theta 2}(H) = \sigma(W_{jk}H + \varphi_2) \quad (6.2)$$

where, the input data vector $X = (x_1, x_2, \ldots, x_n)$ *and* $(X \in R_n)$, the output data vector $X' = (x'_1, x'_2, \ldots, x'_n)$ and $(X' \in R^n)$, n is the dimension of the input/output vector, $H \in R_m$ (m = the number of hidden units), and H is the reduced dimension from the hidden layer. $W_{ij} \in R_{n \times m}$ defines the weight matrix between the input and hidden layers. $W_{jk} \in R_{m \times n}$ defines the weight matrix between the hidden and output layers. The input and output biased vectors are denoted by φ_1 and φ_2, respectively. The activation functions for the neurons of the hidden and output layers are represented by $g_{\theta 1}$ and $g_{\theta 2}$, respectively. The rectified linear unit (ReLU) is a piecewise linear activation function, that was used here to resolve the vanishing gradient problem and improve model efficiency by fast learning. The adaptive moment estimation (Adam) optimizer optimized the adaptive learning rate to train the DAE.

We observed, that the maximum beat length was 450 samples. Considering the beat length, the DAE was developed using seven hidden layers for feature extraction. The first three hidden layers in the encoder reduce the beat length to achieve 100 features from the latent view layer or bottleneck layer. After the bottleneck, the ECG beat was reconstructed in the decoder part by another four layers. In this manner, the DAE generates a feature matrix ($F_{n\times z}$), where F is the feature matrix with z numbers of features (z=100) for n numbers of beats (n=1500).

Pseudo code 1: ***Data Reduction & Feature Matrix Generation by DAE***

Input : ECG Beat cell ($\hat{X}_{n\times m}$), Sampling Frequency (fs =360Hz),
Output : $F_{n\times z}$ = Feature Matrix

fs =360Hz // Sampling frequency
X = $\hat{X}_{n\times m}$ // Beat cell
N_n =len($\hat{X}_{n\times m}$) // N = length of beat, n = beat number
=1500
$X_{partitioned}$ = Split $\hat{X}_{n\times m}$ into Train and Test //split database for training and testing
$W_{list} = \alpha$
Initializer = *I*
Regularizer = *R*

 # Create DAE Architecture
$X_{train} = (x_1, x_2, \ldots, x_n)$ //Input vector, $X_{train} \in R^{nxm}$ (training dataset with n beats with m samples)
e is the number of epochs to be iterated
b is the number of batches
l is the learning rate

 # Encoding Architecture
dense_layer = Ø
Activation function = ReLU
n = shape($\hat{X}_{n\times m}$)
IL = Input (shape = n) // EL_n= Encoded Layer where n = layer number
EL_1 = (Ø(N – 50), ReLU)(IL)
N_1=N – 50
EL_2 = (Ø(N_1 – 80), ReLU)(EL_1)
N_2=N_1 – 80
M=N_2 – 100
EL_3 = (Ø(N_2 – M), ReLU)(EL_2)

 # Feature Extraction
F_{train} = Latent_view = Ø dense_layer(100, activation = Sigmoid)(EL_3) // F_{train}=Features set of training dataset
 # Decoding Architecture // DL_n= Decoded Layer where n = layer number
DL_1 = (Ø(F_{train} + M), ReLU)(F_{train})
N_2 = F_{train} + M
DL_2 = (Ø(N_2 + 80), ReLU)(DL_1)
N_1 = N_2 + 80
DL_3 = (Ø(N_1 + 50), ReLU)(DL_2)
N = N_1 + 50

 # Output Layer for reconstruction:
OL = Ø(n)(DL_4) // OL = DAE model output layer for reconstruction

Create AE Model
AE Model = *f*(IL, OL)
F = *f*(IL, F_{train})
Compile model, Loss_function = MSE
Train AE model = *f*(*e*,*b*,*l*)

#Test Phase

test_encode = predict($\hat{X}_{ntest\times mtest}$) // $\hat{X}_{ntest\times \text{mtest}}$ = Test dataset

F_{test} = Feature_predict($\hat{X}_{ntest\times mtest}$)

test_decode = predict($\hat{X}_{ntest\times mtest}$)

Reconstruction_Error = $\hat{X}_{ntest\times mtest}$ - test_decode

if MSE < 0.0005

save model

else again train *DAE* model

#Feature Prediction Phase

$F_{n\times z}$ = *predict*($\hat{X}_{n\times m}$)

//$F_{n\times z}$ = Extracted Features for n numbers beat with z samples, here n=1500 & z = 100

6.2.2. Training/Target Optimized Hyperparameter Matrix Generation via PSO:

PSO is a popular computational method for solving optimization problems. It iteratively improves the quality of the potential solution on the basis of a certain measured value. Here, PSO is used to develop the training dataset for the HPM by optimizing the hyperparameters of the ARIMA model. For clinical evaluation, the RMSE of the reconstructed ECG should be less than 9%. Fig.6.2. shows the flowchart of PSO algorithm. The objective function of PSO is defined as follows:

$$min_{h\in U}|r_k - r_{th}|\ where, h = z(t_k) \quad (6.3)$$

where h: observation status, which comprises the value of three hyperparameters (p,d,q) in the global search space U, $z(t_k)$: observation matrix; t_k: optimized values for the k[th] iteration; r_k: calculated RMSE in the k[th] iteration using (p,d,q); and r[th]: threshold value of RMSE.

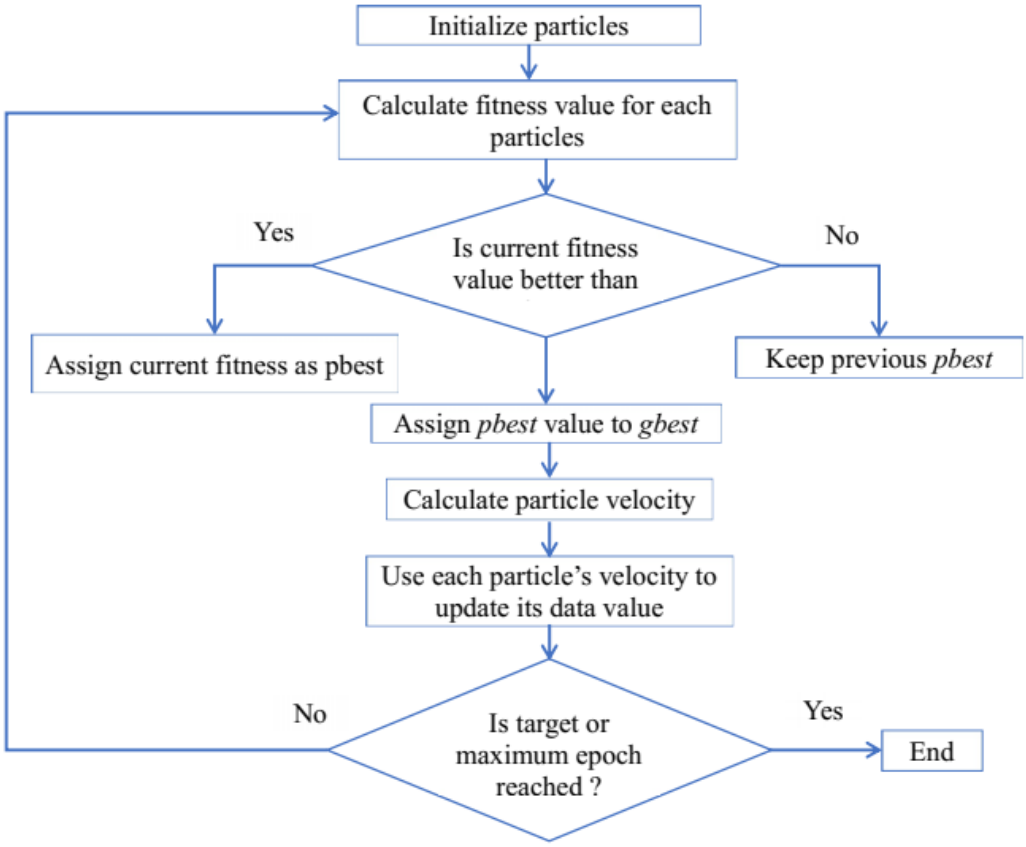

Fig.6.2.: Flowchart of PSO algorithm

The ranges of (*p,d,q)* were considered to be (0:9), (0:2), and (0:9), respectively. Here, we consider 100 particles in the swarm, with 100 iterations, a particle velocity scaling factor = 0.5, and a scaling factor = 0.5 to determine the particle's best-known position. The minimum step size is 1^{-8} to search for the swarm's best position before termination.
The PSOs optimized (*p,d,q)* for each beat-cell were stored in a matrix to train the HPM, called the optimized hyperparameter matrix ($p_{1\times n}, d_{1\times n}, q_{1\times n}$), where *p, d and q* are single row matrices for n=1500 beats of beat-cell.

Pseudo code 2: ***Target Matrix generation by PSO optimized ARIMA model hyperparameters***

Input: $\hat{X}_{n\times \mathrm{m}}$ = denoised beat cell
Output : $(p_{1\times n}, d_{1\times n}, q_{1\times n})$ = Target Matrix

$\hat{X}_{n\times \mathrm{m}}$ = Read input beat cell
(*p,d,q*) = Initialize hyperparameters
Initialize population
sw = 100 // sw = Number of swarm particle
I = 100 // I = number of iteration
v = 0.5 // v =particle velocity scaling factor
step= 1^{-8} // step = minimum step size
while (the measured value: RMSE is not met)
{
for (i=0 to number of particles N)
{
if the fitness of X_i^k > than fitness of p_{i_best}
then update $p_{i\_best} = X_i^k$
if the fitness of X_i^k > than fitness of g_{i_best}
then update $g_{i\_best} = X_i^k$
update velocity vector v_i
$v_{i+1} = v_i + c1.rand.(pbest - p_i) + c2.rand.(gbest - p_i)$
update particle position p_i
$p_{i+1} = p_i + v_{i+1}$
evaluate_arima_model($\hat{X}_{n\times \mathrm{m}}$, optimized hyperparameters)
if
{$RMSE_{cal} < RMSE_{meas}$ // $RMSE_{cal}$ = Calculated RMSE & $RMSE_{meas}$ = Measured RMSE
break
update value of hyperparameters (*p,d,q*)
else
continue
}}
Next iteration
}
 # store value of (p,d,q) for each beat in a matrix
for i = n
TM = append (p_i,d_i,qi) = $(p_{1\times n}, d_{1\times n}, q_{1\times n})$
end

6.2.3. Development of the Hyperparameter Prediction Model (HPM):

In this work, the MLPNN was used for the development of a multioutput hyperparameter prediction model (HPM). It is basically a feedforward deep neural network (DNN) model. It consists of three fully connected layers of nodes namely, one input, one or multiple hidden and one output layer. Except input nodes, each node is known as neuron and uses a nonlinear activation function. The network is trained by supervised learning with backpropagation except the output layer. It learns a function $f(\cdot)$: $R^m \rightarrow R^o$, where m: represents the input dimensions and o: the output dimensions. Each node of the layers are interconnected with a certain weight (wij). The i numbers input transfer the information to the next

layer. Here three hidden layers were used with ReLU. In these layers, the input information is processed to generate the required values at the output nodes.
The HPM model was trained/tested with a DAE-driven feature matrix ($F_{n\times z}$) and a PSO-driven target matrix ($p_{1\times n}, d_{1\times n}, q_{1\times n}$). The Adam was used as optimizer and MAE was considered as loss function. During training of the MLPNN-based HPM, the hyperparameters ($\hat{p}_{1\times n}, \hat{d}_{1\times n}, \hat{q}_{1\times n}$) are predicted for each beat-cell, where *p, d* and *q* are predicted hyperparameters.

Pseudo code 3 ***: ARIMA model hyperparameter Prediction by MLPNN***

Input : $F_{n\times z}$ = Feature Matrix, ($p_{1\times n}, d_{1\times n}, q_{1\times n}$) = Target matrix, PSO optimized hyperparameters for beat cell
Output : ($\hat{p}_{1\times n}, \hat{d}_{1\times n}, \hat{q}_{1\times n}$) = Predicted ARIMA model hyperparameter by MLPNN

IM = $F_{n\times z}$
TM = ($p_{1\times n}, d_{1\times n}, q_{1\times n}$)

n_input = IM_j
n_output = TM_j

 # Define IM and TM to train Regression model
IM,TM = make_regression(data_length=len(IM_i), features=len(IM_j), target_length = len(TM_j))
// i = row of matrix and j = column of matrix
lr = 0.001
activation_function = ReLU
I = Initializer
R = Regularizer

 # Create Dense layer
DL= f(ReLU, I,R)

 # Define MLPNN Regression Model(len(IM_j), len(TM_j))
M = Sequential()
model.add(DL(40, input_dim = len(IM_j), I, ReLU)
model.add(DL(30, I)
model.add(DL(20, I)
model.add(DL(10, I)
model.add(Dense(len(TM_j), I)
compile model(loss = 'MAE', Optimizer = adam)

X = len(IM_j)
Y = len(TM_j)

 # Evaluate Model by Repeated k-fold cross-validation
CV = (k =10, repeats = 3)
CV.split (X,Y)
X = X_{train} + X_{test}
Y = Y_{train} + Y_{test}

 # Define Regression Model
MLPNN_model = f(X,Y)

 # Fit model
MLPNN_Model.fit(X_{train}, Y_{train}, e = 100)

 # Evaluate model on test set
MAE = evaluate_MLPNN_model(X_{test}, Y_{test}, e = 100)

 # Store result
Result.append(MAE)
Predict_hyperparameter = model_predict(X)
($\hat{p}_{1\times n}, \hat{d}_{1\times n}, \hat{q}_{1\times n}$) = MLPNN_model_predict($X_{test}$)

 # Modeling of test_data by ARIMA model using predicted hyperparameter
ARIMA_Model = ARIMA($X_{test}(\hat{p}_{1\times n}, \hat{d}_{1\times n}, \hat{q}_{1\times n})$)
Coefficient = model_fit.parameters
$X_{reconstruct}$ = reconstruct_ARIMA(X_{test})
MSE = mean_square_error(X_{test}, $X_{reconstruct}$)
If MSE <<0.005
fix DAE_MLPNN_model
else train model

6.2.4. ECG compression by the Adaptive ARIMA Model:

In the Chapter 5, the significance of ARIMA model for modeling of ECG signal is already described. ARIMA model is most suitable method for modeling of non-linear, non-stationary and time variant ECG signal. It has three key parameters (p,d,q), which are referred to in the order of autoregressive, integrated and moving average parts of the model, respectively. The values of the hyperparameters are $p \geq 0, q \geq 0, d \geq 0$. In most cases, the signal is differenced two times to convert nonstationary data into stationary data. Thus, the range of d =2. The value of each parameter plays a significant role to achieve model efficiency i.e. synthesis of the signal without any information loss. If the values are greater than the required value, the model can be overfitted; otherwise, it can be underfitted with a lower value. Hence, hyperparameter tuning is very important for the ARIMA model. Here, we focused on lossless ECG compression via the adaptive ARIMA model,. Model performance depends on hyperparameter values. It is a great challenge to develop a beat-specific compression model with an adaptive ARIMA model. The HPM predicts the best-suited combination of hyperparameter $(\hat{p}_{1\times n}, \hat{d}_{1\times n}, \hat{q}_{1\times n})$ for modeling of each beat separately. The model coefficients are stored as compressed data in a packet for future use or transmitted to the clinic for pathological analysis by reconstructing the signal by the model coefficient and model parameter value.

Pseudo code 4: ***ECG Compression by ARIMA Model***

Input : X_{new}=new ECG beat, $(\hat{p}_{1\times n}, \hat{d}_{1\times n}, \hat{q}_{1\times n})_{new}$ = MLPNN predicted hyperparameters
Output : L_c = ARIMA model coefficients, $\hat{X}_{c\_new}$ = Compressed Data

X_{new} = Read new ECG beat as input
$(\hat{p}_{1\times n}, \hat{d}_{1\times n}, \hat{q}_{1\times n})_{new}$ = MLPNN predicted hyperparameters for new input beat
ARIMA_Model = ARIMA($X_{new}(\hat{p}_{1\times n}, \hat{d}_{1\times n}, \hat{q}_{1\times n})_{new}$)
L_c = ARIMA_Coefficient
$\hat{X}_{c\_new}$ = Packet(L_c)
Calculate CR value
Calculate PRD%

6.2.5. Generation of a header structure for encoding of compressed ECG data:

The original file and compressed file size is calculated on the basis of memory allocation size. In python 4byte is required to store a floating point. The first bit i.e., MSB bit define the sign of floating number by Boolean number where positive sign represented by 0 and negative sign represented by 1. After that next 8 bit stores exponential part and 23 bits used to store significant part of floating number.

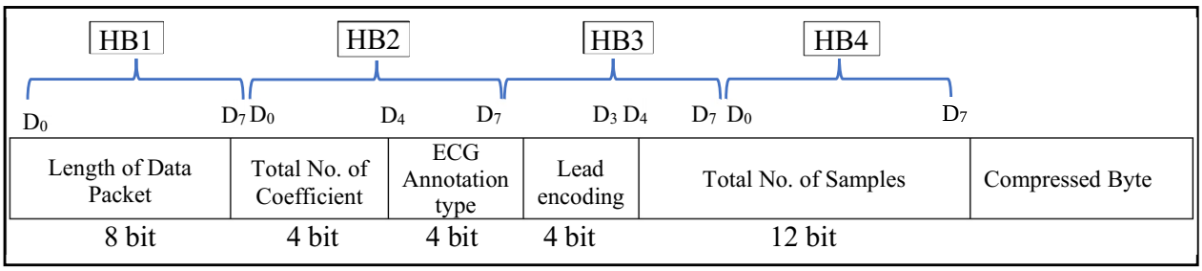

Fig.6.3.: Structure of Encoded Data Packet of Compressed ECG Data

Table 6.1.: Header information of compressed data packet

Header Structure of compressed data packet	
• Total No. of bytes in a packet	8 bits
• Total No. of ARIMA Model coefficient	4 bits
• ECG beat Annotation type	4 bits
• ECG lead type	4 bits
• Number of samples in original data	12 bits

The original ECG beat size is calculated as : [4 bytes to store value of each sample in a beat = (4 × No. of samples in a beat) bytes] and compressed data size is calculated as : [4 × 3 bytes to store value of *p*, *d* and *q* + 4 bytes × No. of coefficients]. The header information of compressed data packet is given in Table 6.1. Fig.6.3. shows the structure of encoded data packet of compressed ECG data shows the header information of compressed ECG data for generation of encoded data packets. The compressed ECG data was encoded using 4 header bytes. The first header byte (D0 to D7) contains the overall length of a data packet. In the second header byte, first 4 bits i.e., D0 to D3 contains total number of ARIMA model coefficients and last 4 bits i.e., D4 to D7 contains ECG annotation type. The third header byte stores ECG lead type in the first 4bit (D0 to D3) and the last 4bit of fourth header byte along with 8 bits of fourth header byte contains the number of samples in original data. After the four header bytes the compressed bytes were stored. In a data packet compressed data were stored after the header bytes.

6.3. Results:

In this work, a novel method for lossless ECG data compression using intelligent ARIMA model was developed. This model is developed and validated using ten classes of cardiac rhythm from mitdb under PhysioNet database and the ECG classes are as follows: 1) normal sinus rhythm (H), 2) atrial premature beat (A), 3) premature ventricular contraction beat (V), 4) left bundle branch block beat (L), 5) right bundle branch block beat (R), 6) paced beat (P), 7) aberrated atrial premature beat (a), 8) Nodal (junctional) premature beat (J) and fusion PVC beat (F). In this work, the hyperparameters prediction has been done for cardiac cycles with 1 minute duration. The compression model performance is evaluated by MSE, MAE, maximum error (ME), PRD and CR Value. The ME mathematically expressed as under:

$$ME = max[\hat{y}_i - y_i] \tag{6.5}$$

where, y_i denotes the true value; $\hat{y}_i$ denotes the predicted value of the hyperparameter and n denotes the number of observations.

The compression performance metrics are defined as follows:

$$CR = \frac{Length\ of\ original\ data}{Length\ of\ compressed\ data\ packet} \tag{6.6.a}$$

$$PRD\ \% = 100 * \sqrt{\frac{\sum_{i=1}^{N}(X_i - Y_i)^2}{\sum_{i=1}^{N}(X_i)^2}} \tag{6.6.b}$$

$$Quality\ Score(QS) = \frac{CR\ Value}{PRD\%} \tag{6.6.c}$$

where X_i: original ECG beat; Y_i: reconstructed ECG beat; and N: number of beat data samples.

DWT based noise removal method was used for denoising of raw ECG signal. In this method, db5 was used as mother wavelet and 12^{th} level decomposition was done to obtain denoised ECG signal with all clinical information. Then the R-peak point and base line index were detected using DWT method to extract each beat from the signal and stored into a beat cell for further process. Then beat delineation has been done and extract each beat of an ECG signal. For each type of ECG signal beats are stored into separate beat matrix for further processing.

The ECG data compression model was developed and validated using 46 mitdb record and the record ID are: 100, 101, 102, 103, 104, 106, 107, 108, 109, 111, 112, 113, 114, 115, 116, 117, 118, 119, 121, 122, 123, 124, 200, 202, 203, 205, 207, 208, 209, 210, 212, 213, 214, 215, 217, 219, 220, 221, 222, 223, 228, 230, 231, 232, 233 and 234. A database of 1500 data was created using ten types of mitdb data beat. The length of each ECG beat is different thus DAE and PCA were used as dimensionality reduction and feature selection tools. The beat length was reduced into 100 using deep auto encoder and the size of DAE and PCA derived input feature matrix is 1500x100 i.e., the length of each beat is 100 and the number of beats in the matrix is 1500.
The K-fold cross validation model was used to validate the train/test dataset. The dataset was partitioned and prediction model efficiency was evaluated by considering 10-fold and 3-repeats to construct a generalized prediction model. The MAE was chosen as the loss function. Finally, error-controlled beat-specific compression was performed via the adaptive ARIMA model. In this method each beat of a cycle was modelled by the best predicted hyperparameters for compression of the ECG signal.

6.3.1. Ablation Study:

We have developed another three model to understand the performance of deep learning-based compression model. Three parallel models are as follows: 1) DAE-SVR model where DAE was performed as feature extraction tool and SVR as HPM to predict ARIMA model parameters; and 2) PCA-MLPNN model where PCA was used as a dimensionality reduction tool and MLPNN as HPM model, 3) PCA-SVR model where SVR predict hyperparameters using PCA driven features.
Table 6.2. shows performance for four types of HPM model using 46 mitdb data with different annotation. From this table it can be observed that a single record can contain different classes of ECG beats. Each beat is different in characteristic from other in a same cardiac cycle. Thus, the ARIMA model hyperparameters combination should be unique for each beat. Table 6.2. shows the maximum and minimum value of each parameter for each data record to understand the difference in values of the parameters predicted by different HPM algorithm. In this table the average number of coefficients required to model ECG beat are given. The table shows DAE-MLPNN based model predicts lowest number of coefficients (8 numbers) for ECG modeling whereas PCA-MLPNN model offered maximum number of coefficients. The coefficients are most significant for compression of ECG beat as it carries the clinical information of the beat. As DAE-MLPNN based HPM model required lowest numbers of coefficient for synthesis of ECG beat, thus it consume lesser time for prediction i.e., only24 seconds for 26 consecutive ECG beats. This model consumes less than one second time to predict the suitable combination of hyperparameters. The aim of this work is lossless ECG compression which was compared with other three model on the basis of compression quality and reconstruction efficiency. Another most important outcome from DAE-MLPNN based ARIMA model is high reconstruction efficiency after decompression.
Once the model is trained it can predict suitable hyperparameters for new ECG data and compress by ARIMA model. The model coefficients were stored in a data packet with header information for future application. The compressed beats were decompressed to validate the reconstruction efficiency of model. Table 6.3. shows the compression and reconstruction performance of adaptive ARIMA model using different types of HPM and Table 6.4. shows the computation time of each model. The compression and reconstruction performance of four models for each class are shown in Table 6.5 and Table 6.6. A high compression quality can be achieved by increasing the CR with decreasing PRD%. CR is the ratio of original file size to compressed file size. The characteristics of lossless model is high compression quality with PRD less than 0.5%.

Table 6.2: Range of Predicted ARIMA Model Hyperparameters by Different Prediction Model

mitdb Data ID	Annotation Type	Lead no.	DAE-MLPNN Model				PCA-MLPNN Model				DAE-SVR Model				PCA-SVR Model			
			Predicted *(p,d,q)* Value		No. of Coefficient		Predicted *(p,d,q)* Value		No. of Coefficient		Predicted *(p,d,q)* Value		No. of Coefficient		Predicted *(p,d,q)* Value		No. of Coefficient	
			Max	Min	Max	Min	Max	Min	Max	Min	Max	Min	Max	Min	Max	Min	Max	Min
100	H	MLII	(3,1,3)	(3,1,2)	7	6	(8,1,6)	(2,1,1)	15	4	(5,1,7)	(3,1,2)	13	6	(8,1,8)	(2,0,1)	17	3
101	H	MLII	(3,1,2)	(2,1,1)	6	4	(8,1,8)	(2,1,1)	17	4	(6,1,7)	(2,1,2)	14	5	(8,1,7)	(2,1,1)	16	4
102	H, P, f	V5	(2,1,4)	(2,1,2)	7	5	(7,2,7)	(2,0,1)	16	3	(4,1,3)	(3,1,2)	8	6	(5,1,3)	(4,1,2)	9	7
103	H	MLII	(4,1,2)	(3,1,1)	7	5	(13,1,6)	(1,1,1)	20	3	(7,1,6)	(2,1,1)	14	4	(4,1,3)	(2,1,2)	8	5
104	H, P, f	V5	(4,1,3)	(3,1,2)	8	6	(11,1,11)	(3,1,1)	23	5	(6,1,5)	(1,1,1)	12	3	(5,1,4)	(3,1,2)	10	6
105	H, V	MLII	(2,1,3)	(2,1,2)	6	5	(10,1,9)	(3,1,4)	20	8	(7,1,7)	(3,1,4)	15	8	(6,1,6)	(2,1,3)	13	6
106	H, V	MLII	(3,1,4)	(2,1,2)	8	5	(11,1,7)	(2,0,1)	19	3	(4,1,5)	(3,1,1)	10	5	(4,1,3)	(2,1,3)	7	6
107	V, P	MLII	(4,1,4)	(3,1,2)	9	6	(7,1,6)	(3,1,2)	14	6	(8,1,3)	(5,0,1)	12	6	(4,1,4)	(2,1,1)	9	4
108	H	MLII	(4,1,3)	(2,1,2)	4	5	(9,1,6)	(2,1,2)	16	5	(4,1,4)	(3,1,3)	9	7	(5,1,4)	(3,1,3)	10	7
109	V, L	V1	(4,1,3)	(3,1,1)	8	5	(7,1,7)	(1,0,1)	15	2	(8,1,6)	(4,1,3)	15	8	(7,2,8)	(2,0,1)	17	3
111	L	V1	(3,1,3)	(3,1,2)	7	6	(10,2,7)	(1,1,2)	19	4	(4,1,3)	(2,1,1)	8	4	(5,1,8)	(3,1,2)	14	6
112	H	MLII	(5,1,3)	(2,1,1)	9	4	(9,1,7)	(2,1,1)	17	4	(5,1,7)	(3,1,2)	13	6	(6,1,6)	(2,1,3)	13	6
113	H, a	MLII	(4,1,3)	(2,1,2)	8	5	(8,2,10)	(2,1,4)	20	7	(6,1,5)	(3,1,1)	12	5	(7,1,7)	(3,1,3)	15	7
114	H, F	MLII	(5,1,2)	(4,1,1)	8	6	(8,1,7)	(3,1,2)	16	6	(8,1,8)	(2,1,1)	17	4	(8,1,9)	(2,1,2)	18	5
115	H	MLII	(3,1,3)	(2,1,1)	7	4	(10,1,8)	(1,1,2)	19	4	(7,1,6)	(3,1,2)	14	6	(7,1,6)	(2,0,1)	14	3
116	H, V	MLII	(4,1,2)	(2,1,2)	7	5	(7,1,9)	(3,1,4)	17	8	(7,1,7)	(2,1,3)	6	6	(8,1,9)	(2,1,2)	18	5
117	H	MLII	(3,1,2)	(2,1,1)	6	4	(9,1,8)	(3,1,3)	18	7	(8,1,6)	(3,1,3)	7	7	(8,1,8)	(2,1,3)	17	6
118	R, A	MLII, V1	(3,1,3)	(2,1,2)	7	5	(8,1,6)	(2,1,2)	15	5	(8,2,7)	(2,1,3)	17	6	(7,1,5)	(3,1,2)	13	3
119	H, V	MLII	(2,1,3)	(3,1,3)	6	7	(8,1,9)	(4,1,5)	18	10	(7,1,8)	(3,1,1)	16	5	(9,1,8)	(3,1,3)	18	7
121	H	MLII	(4,1,4)	(2,1,2)	9	5	(9,2,8)	(1,1,2)	19	4	(6,1,7)	(3,1,3)	14	7	(8,1,8)	(2,1,2)	17	5
122	H	MLII	(4,1,5)	(3,1,1)	10	5	(8,1,9)	(2,1,2)	18	5	(4,1,2)	(3,1,2)	7	6	(6,1,5)	(3,1,3)	12	7
123	H	MLII	(3,1,2)	(2,1,1)	6	4	(7,1,11)	(3,1,2)	19	6	(6,1,4)	(2,1,2)	11	5	(6,1,6)	(2,1,1)	13	4
124	R, F	V4	(3,1,6)	(3,1,2)	10	6	(10,2,6)	(2,1,3)	18	6	(8,1,9)	(2,1,3)	18	6	(7,1,9)	(2,1,2)	17	5
200	H, V, A, j	MLII	(4,1,2)	(1,1,1)	7	3	(9,1,10)	(3,1,4)	20	8	(6,1,5)	(2,1,3)	12	6	(8,1,9)	(3,1,4)	18	8
201	H, V, A, a	MLII	(8,1,8)	(2,1,1)	17	4	(8,1,7)	(3,1,5)	16	9	(4,1,5)	(3,1,2)	10	6	(9,1,8)	(2,1,2)	18	5
202	H, A, a	MLII	(3,1,4)	(2,1,1)	8	4	(8,1,8)	(3,1,4)	17	8	(3,1,4)	(2,1,2)	8	5	(7,1,7)	(3,1,2)	15	6
203	H, V	MLII	(5,1,3)	(2,1,1)	9	4	(10,2,7)	(2,1,2)	19	5	(6,1,5)	(3,1,1)	12	5	(8,1,5)	(2,1,1)	14	4
205	H, V, F	MLII	(7,1,5)	(3,1,1)	8	5	(8,2,7)	(1,0,2)	17	3	(7,1,5)	(2,1,1)	13	4	(6,1,8)	(1,1,1)	15	3
207	L, R, V, A	MLII, V1	(5,1,5)	(2,1,3)	11	6	(7,1,9)	(1,1,3)	17	5	(4,1,7)	(1,1,3)	12	5	(9,1,6)	(1,1,2)	16	4
208	V, F	MLII	(6,1,5)	(2,0,1)	12	3	(8,1,8)	(2,1,4)	17	7	(5,1,8)	(3,1,1)	14	5	(8,1,8)	(2,1,3)	17	6
209	A	MLII	(5,1,3)	(1,1,1)	9	3	(8,1,10)	(3,1,5)	19	9	(8,1,9)	(3,1,1)	18	5	(7,1,8)	(3,1,2)	16	6
210	H, V, a, F	MLII	(4,1,4)	(2,1,3)	9	6	(8,1,8)	(2,1,4)	17	7	(5,1,9)	(2,1,2)	15	5	(9,1,8)	(3,1,3)	18	7
212	R	V1	(5,1,2)	(4,1,1)	8	6	(10,1,7)	(1,0,3)	18	4	(7,1,7)	(1,1,1)	15	3	(6,1,5)	(3,1,3)	12	7
213	V, A, F	MLII	(6,1,4)	(1,1,2)	11	4	(6,1,8)	(3,1,3)	15	7	(5,1,5)	(2,1,2)	11	5	(7,1,6)	(3,1,2)	14	6
214	L, V	V1	(4,1,3)	(1,0,1)	8	2	(7,1,8)	(3,1,2)	16	6	(8,1,5)	(1,1,1)	14	3	(8,1,7)	(2,1,2)	16	5
215	H, V	MLII	(3,1,5)	(3,1,1)	9	5	(9,2,8)	(4,1,3)	19	8	(5,1,6)	(3,1,1)	12	5	(9,1,9)	(3,1,4)	19	8
217	H, V, P, f	MLII	(4,1,4)	(2,1,2)	9	5	(9,1,10)	(1,1,5)	20	7	(5,1,8)	(1,1,1)	14	3	(9,1,9)	(2,1,3)	19	6
219	H, V	MLII	(3,1,4)	(1,1,1)	8	3	(9,1,8)	(3,1,4)	18	8	(9,1,8)	(4,1,3)	18	8	(8,1,8)	(3,1,3)	17	7
220	H, A	MLII	(5,1,4)	(3,1,2)	10	6	(7,2,9)	(3,1,4)	18	8	(4,1,3)	(2,1,1)	4	4	(7,1,8)	(2,1,2)	16	5
221	H, V	MLII	(3,1,3)	(1,1,1)	7	3	(8,1,9)	(4,1,4)	18	9	(5,1,4)	(3,1,2)	10	6	(8,1,9)	(3,1,2)	18	6
222	H, A, j	MLII	(3,1,3)	(2,1,1)	7	4	(10,2,7)	(4,1,5)	19	10	(7,1,10)	(3,1,4)	18	8	(7,1,6)	(3,1,2)	14	6
223	H, V, A, F	MLII	(3,1,5)	(1,1,2)	9	4	(7,1,6)	(3,1,3)	14	7	(4,1,3)	(3,1,1)	8	5	(7,1,7)	(2,1,1)	15	4
228	H, V	MLII	(3,1,2)	(1,1,1)	6	3	(10,2,9)	(4,1,3)	21	8	(5,1,7)	(3,1,3)	13	7	(7,1,8)	(3,1,2)	16	6
230	H	MLII	(4,1,3)	(3,1,2)	8	6	(7,1,9)	(3,1,2)	17	6	(5,1,4)	(3,1,2)	10	6	(7,1,6)	(3,1,3)	14	7
231	R	V1	(5,1,4)	(1,1,1)	10	3	(9,2,6)	(2,0,3)	17	5	(6,1,4)	(2,1,1)	11	4	(6,1,5)	(2,1,2)	12	5
232	A, R	V1	(4,1,3)	(1,1,2)	8	4	(8,2,9)	(2,1,2)	19	5	(7,1,7)	(2,1,2)	15	5	(6,2,8)	(3,1,3)	16	7
233	H, V, F	MLII	(5,1,4)	(2,1,2)	10	5	(9,1,6)	(3,1,3)	16	7	(7,1,4)	(2,1,1)	12	4	(7,1,9)	(2,1,3)	17	6
234	H	MLII	(6,1,4)	(2,1,1)	11	4	(7,1,9)	(2,1,3)	17	6	(7,1,8)	(1,1,1)	16	3	(9,1,8)	(3,1,2)	18	6
Average					**8**	**5**			**18**	6			**12**	5			**15**	**6**

Here 34 mitdb records for H-type beat, 12 records for A-type beat, 22 numbers of mitdb records for V-type beat, 4 mitdb records for L, P, and a type beat, 6 mitdb records for R-type beat, 2 mitdb records for j-type beat, 9 mitdb records for F-type beat and 3 mitdb records for f-type ECG beat were used. Among them 100 records were chosen randomly for evaluation of model performance.

Table 6.5 shows the average compression performance of each model and Fig.6.4. shows the comparison chart of the CR value and PRD% for 10 classes of ECG data. The average compression results obtained from adaptive ARIMA model using the DAE-MLPNN, PCA-MLPNN, DAE-SVR and PCA-SVR prediction models are as follows: CR=43.97 and PRD% = 0.222; CR=33.78 and PRD% = 0.417; and CR=27.64 and PRD% = 0.487 CR=23.50 and PRD% = 0.362, respectively. It can be observed that in Fig.4 the CR value of the DAE-MLPNN model is higher than other models, and the PRD% is negligible.

As the main objective is lossless compression, minimization of reconstruction error is another desirable aspect. Here, ARIMA model was used for the reconstruction of ECG beats, and reconstruction performance was evaluated in terms of MSE, MAE and ME. Table.6.6 presents the average reconstruction performance of ARIMA model using predicted hyperparameters and the results are as follows: for DAE-MLPNN model, MSE=5.26×10-4, MAE=12.54×10-3 and ME=9.96×10-2; for the PCA-MLPNN model MSE=32.66×10-4, MAE=25.82×10-3 and ME=16.74×10-2, for the DAE-SVR model MSE=40.35×10-4, MAE=33.00×10-3 and ME=20.20×10-2 and for the PCA-SVR model MSE=18.23×10-4, MAE=17.32×10-3 and ME=14.67×10-2. Table 6.6 shows that the MSE are in terms of 10-4, the MAEs are in terms of 10-3 and the ME are in terms of 10-2. Hence, the reconstruction error for adaptive ARIMA model is very nominal when the predicted parameters are used. Table 6.5 and 6.6 show that the DAE-MLPNN predicted ARIMA model yields best results for compression and reconstruction. Fig. 6.5 shows a graphical comparison of the compression and reconstruction performance of the four types of compression models. In this figure, the proposed model is represented in blue. Here, the MSE, MAE, ME and PRD% are lower than those of the other three compression models, whereas the CR value is above 40, which is higher than those of the other models. Thus, the proposed model compresses each beat of an ECG cycle without losing clinical information, as the average PRD% is negligible.

Fig.6.6 shows compression of ten classes of ECG beats by adaptive ARIMA model via the DAE-MLPNN-predicted hyperparameters. Table 6.2 shows that a mitdb record may consist of different types of ECG beats. Although the beats belong to the same records the model parameters vary according to their clinical traits. From this figure, we can observe that mitdb 207 record is consisting of three classes of abnormalities, viz., V, L and R; mitdb 201 contains a and j type beats and mitdb 102 contains P and f type abnormalities, but they are modelled separately by a unique set of hyperparameters according to their morphology.

Thus, the novel contributions of the proposed work are as follows: 1) ECG compression based on a quality-controlled intelligent ARIMA model, 2) development of four error-controlled hyperparameter prediction models, 3) beat-by-beat ECG data compression using adaptive hyperparameters, and 4) compression of ten types of ECG beats in the mitdb database using 46 mitdb records

6.3.2. Comparison of ECG compression by the adaptive ARIMA model with published research work:

ECG compression is very important for remote patient monitoring, patient data storage for analysis and diagnosis purposes. Hence numerous algorithms have been published in this area and the main objective is reduction of information loss by improving the compression quality. Table.6.7. shows the comparison of compression performance of the present research with published works where mitdb database was used for validation. ECG compression methods can be classified into a) Direct Data Compression (DDC) methods, b)Transformation domain based (TD) methods and c) Parameter Extraction (PE) methods. AZTEC, turning point, CORTES, and differential pulse code modulation (DPCM) based compression are based on the DDC method.

The DPCM-based method is suitable for real-time telemonitoring but due to fixed thresholding approach, it is unable to provide high compression efficiency [138]. It was validated with mitdb and ptbdb data. The CR values for ptbdb and mitdb data are 6.42, with PRD of 9.77% and 5.92 with PRD of 8.19%, respectively. As the QS is very poor this method cannot be used for ECG compression.

The TD method improves the QS. The WT, Discrete Cosine Transform (DCT), and DAST methods are different algorithms of TD method [139]. In the WT method the ECG signal is transformed from time domain to frequency domain and the transformed coefficient is used to compress the signal. This approach yields average CR, PRD% and QS of 10.63, 4.71 and 2.26 respectively for mitdb data.

Table 6.3.: Compression and reconstruction performance of the adaptive ARIMA model using hyperparameters predicted by different deep learning-based prediction models for 10 types of ECG beats

Disease	Metric	ECG Compression by Adaptive ARIMA model			
		DAE-MLPNN	***PCA-MLPNN***	***DAE-SVR***	***PCA-SVR***
Healthy (H) mitdb 100	MSE	8.49×10^{-5}	2.74×10^{-4}	3.07×10^{-3}	4.54×10^{-3}
	MAE	4.80×10^{-3}	8.09×10^{-3}	3.24×10^{-2}	3.32×10^{-2}
	ME	4.13×10^{-2}	8.17×10^{-2}	2.12×10^{-1}	2.45×10^{-1}
	CR Value	35.36	13.86	12.2	11.29
	PRD%	0.13	0.428	0.8	0.54
	QS	272.00	32.38	15.25	20.91
Atrial Premature Contraction (A) mitdb 201	MSE	1.31×10^{-4}	4.1×10^{-4}	6.91×10^{-4}	6.2×10^{-5}
	MAE	5.74×10^{-3}	1.04×0^{-2}	1.31×10^{-2}	2.78×10^{-3}
	ME	9.13×10^{-2}	1.36×10^{-1}	1.82×10^{-1}	8.26×10^{-2}
	CR Value	34.94	29.42	26.62	20.7
	PRD%	0.17	0.5	0.56	0.38
	QS	205.53	58.84	47.54	54.47
Premature Ventricular Contraction (V) mitdb 106	MSE	4.82×10^{-4}	2.75×10^{-3}	2.28×10^{-3}	3.09×10-4
	MAE	1.63×10^{-2}	3.86×10^{-2}	3.36×10^{-2}	1.31×10^{-2}
	ME	6.88×10^{-2}	1.67×10^{-1}	1.09×10^{-1}	6.12×10^{-2}
	CR Value	40.37	24.3	23.14	21.13
	PRD%	0.25	0.47	0.36	0.34
	QS	161.48	51.70	64.28	62.15
Left Bundle Branch Block (L) mitdb 109	MSE	2.01×10^{-4}	1.46×10^{-3}	4.92×10^{-4}	6.8×10^{-4}
	MAE	8.99×10^{-3}	2.27×10^{-2}	1.25×10^{-2}	1.64×10^{-2}
	ME	5.46×10^{-2}	1.15×10^{-1}	7.07×10^{-2}	8.54×10^{-2}
	CR Value	22.56	15	13.57	11.87
	PRD%	0.22	0.39	0.59	0.2
	QS	102.55	38.46	23.00	59.35
Right Bundle Branch Block (R) mitdb 118	MSE	4.88×10^{-4}	2.16×10^{-4}	7.33×10^{-3}	4.99×10^{-5}
	MAE	1.78×10^{-2}	1.10×10^{-2}	6.62×10^{-2}	$5.39\times x10^{-3}$
	ME	8.78×10^{-2}	6.80×10^{-2}	2.83×10^{-1}	3.86×10^{-2}
	CR Value	38.35	24.3	40.5	18
	PRD%	0.17	0.43	0.36	0.34
	QS	225.59	56.51	112.50	52.94
Paced (P) mitdb 205	MSE	1.51×10^{-4}	2.1×10^{-2}	8.89×10^{-3}	4.44×10^{-4}
	MAE	2.47×10^{-3}	9.37×10^{-2}	6.12×10^{-2}	9.62×10^{-3}
	ME	1.68×10^{-2}	4.11×10^{-1}	2.54×10^{-1}	2.06×10^{-1}
	CR Value	29.28	16.94	12.04	11.48
	PRD%	0.19	0.45	0.35	0.26
	QS	154.11	37.64	34.40	44.15
Aberrated Atrial Premature Beat (a) mitdb 210	MSE	9.45×10^{-5}	$1.21c10^{-4}$	1.13×10^{-3}	5.26×10^{-4}
	MAE	5.08×10^{-3}	5.55×10^{-3}	1.69×10^{-2}	1.20×10^{-2}
	ME	8.8×10^{-2}	9.48×10^{-2}	2.75×10^{-1}	1.66×10^{-1}
	CR Value	41.66	36.76	34.72	32.89
	PRD%	0.24	0.31	0.56	0.42
	QS	173.58	118.58	62.00	78.31
Nodal (Junctional) Premature Beat (j) mitdb 222	MSE	7.22×10^{-5}	1.5×10^{-4}	2.13^{-4}	1.03×10^{-4}
	MAE	4.07×10^{-3}	5.8×10^{-3}	6.68×10^{-3}	4.20×10^{-3}
	ME	7.34×10^{-2}	9.9×10^{-2}	1.10×10^{-1}	8.34×10^{-2}
	CR Value	38.93	36.5	26.54	24.33
	PRD%	0.23	0.32	0.34	0.25
	QS	169.26	114.06	78.06	97.32
PVC Fusion (F) mitdb 208	MSE	3.68×10^{-4}	1.47×10^{-3}	2.65×10^{-3}	10.38×10^{-3}
	MAE	1.25×10^{-2}	2.12×10^{-2}	3.02×10^{-2}	5.52×10^{-2}
	ME	1.01×10^{-1}	1.87×10^{-1}	2.07×10^{-1}	3.37×10^{-1}
	CR Value	25.46	10.85	10.33	9.03
	PRD%	0.24	0.35	0.36	0.47
	QS	106.08	31.00	28.69	19.21
Pacemaker Fusion (f) mitdb 217	MSE	1.83×10^{-3}	4.81×10^{-3}	1.36×10^{-2}	1.14×10^{-3}
	MAE	2.54×10^{-2}	4.12×10^{-2}	5.72×10^{-2}	2.13×10^{-2}
	ME	2.22×10^{-1}	3.14×10^{-1}	3.17×10^{-1}	1.62×10^{-1}
	CR Value	36.62	23.66	22.42	22.42
	PRD%	0.38	0.49	0.56	0.42
	QS	96.37	48.29	40.04	53.38

Table 6.4.: Comparison of computational time between PSO and different methods Hyperparameter Prediction Models

mitdb Data ID	No. of beat in 20sec. window	Execution Time (minute)				
		DAE-MLPNN	PCA-MLPNN	DAE-SVR	PCA-SVR	PSO
100	25	00:22:12	00:38:10	00:35:22	00:40:18	09:42:29
102	24	00:29:00	00:35:00	00:37:18	00:39:20	12:02:23
106	21	00:18:06	00:22:09	00:20:12	00:39:20	14:33:05
109	32	00:32:05	00:29:28	00:37:21	00:58:03	11:35:42
118	24	00:24:11	00:46:17	00:43:12	00:26:14	23:01:12
201	28	00:27:08	00:48:02	00:32:00	00:39:06	09:18:08
205	29	00:20:22	00:34:28	00:34:28	00:33:29	15:11:28
208	32	00:19:07	00:40:00	00:26:46	00:45:25	17:20:16
210	30	00:29:10	00:52:16	00:33:25	00:31:50	05:38:09
217	24	00:24:28	00:39:13	00:25:40	00:28:17	14:12:09
222	24	00:21:15	00:23:50	00:20:08	00:28:22	16:24:00
Average	**26**	**00:24:17**	**00:37:10**	**00:31:27**	**00:37:15**	**13:32:38**

Table 6.5.: Compression performance of the lossless ECG compression model with the adaptive ARIMA model using different hyperparameter prediction algorithms

ECG Annotation type	No. of Data Records	Compression model performance using predicted hyperparameters							
		DAE-MLPNN	PCA-MLPNN	DAE-SVR	PCA-SVR	DAE-MLPNN	PCA-MLPNN	DAE-SVR	PCA-SVR
		CR Value				PRD%			
H	**34**	33.88	19.06	16.05	14.52	0.22	0.42	0.85	0.54
A	**12**	55.9	43	37.26	26.62	0.25	0.56	0.56	0.23
V	**22**	48.6	34.71	32.4	28.58	0.28	0.48	0.42	0.29
L	**4**	31.66	21.92	19	15.83	0.23	0.39	0.56	0.24
R	**6**	48.6	34.71	30.375	23.14	0.21	0.45	0.31	0.38
P	**4**	31.88	23.92	17.94	15.11	0.19	0.42	0.33	0.27
a	**4**	61.22	50.09	45.92	42.38	0.2	0.32	0.59	0.45
j	**2**	38.93	36.5	26.54	24.33	0.25	0.31	0.38	0.26
F	**9**	64.88	58.4	36.5	32.44	0.23	0.33	0.35	0.48
f	**3**	24.12	15.5	14.46	12.05	0.16	0.49	0.52	0.48
Average		**43.97**	**33.7**	**27.64**	**23.5**	**0.222**	**0.417**	**0.487**	**0.362**

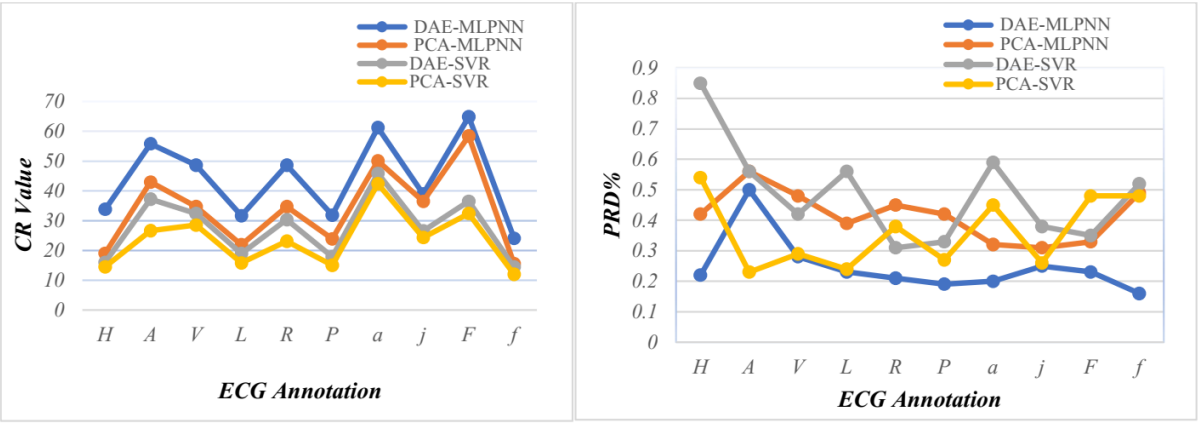

Fig. 6.4.: Comparison graph of the compression performance of the ARIMA model with various HPM algorithms using 10 classes of ECG beats

Table 6.6.: Comparative study of ARIMA based ECG Compression using different HPM Algorithm

ECG Annotation type	No. of Data Records	ARIMA based compression model performance using predicted hyperparameters											
		DAE - MLPNN	PCA - MLPNN	DAE - SVR	PCA-SVR	DAE - MLPNN	PCA - MLPNN	DAE - SVR	PCA - SVR	DAE - MLPNN	PCA - MLPNN	DAE - SVR	PCA - SVR
		MSE (10-4)				MAE (10-3)				ME (10-2)			
H	**34**	0.85	2.74	30.7	45.4	4.8	8.09	32.4	33.2	4.13	8.17	21.2	24.5
A	**12**	1.31	4.1	6.91	0.62	5.74	10.4	13.1	2.78	9.13	13.6	18.2	8.26
V	**22**	4.82	27.5	22.8	3.09	16.3	38.6	33.6	13.1	6.88	16.7	10.9	6.12
L	**4**	2.01	14.6	4.92	6.8	8.99	22.7	12.5	16.4	5.46	11.5	7.07	8.54
R	**6**	4.88	2.16	73.3	0.5	17.8	11	66.2	5.39	8.78	6.8	28.3	3.86
P	**4**	15.1	210	88.9	4.44	24.7	93.7	61.2	9.62	16.8	41.1	25.4	20.6
a	**4**	0.95	1.21	11.3	5.26	5.08	5.55	16.9	12	8.8	9.48	27.5	16.6
j	**2**	0.72	1.5	2.13	1.03	4.07	5.8	6.68	4.2	7.34	9.9	11	8.34
F	**9**	3.68	14.7	26.5	103.8	12.5	21.2	30.2	55.2	10.1	18.7	20.7	33.7
f	**3**	18.3	48.1	136	11.4	25.4	41.2	57.2	21.3	22.2	31.4	31.7	16.2
Average		**5.26**	**32.66**	**40.35**	**18.23**	**12.54**	**25.82**	**33.00**	**17.32**	**9.96**	**16.74**	**20.20**	**14.67**

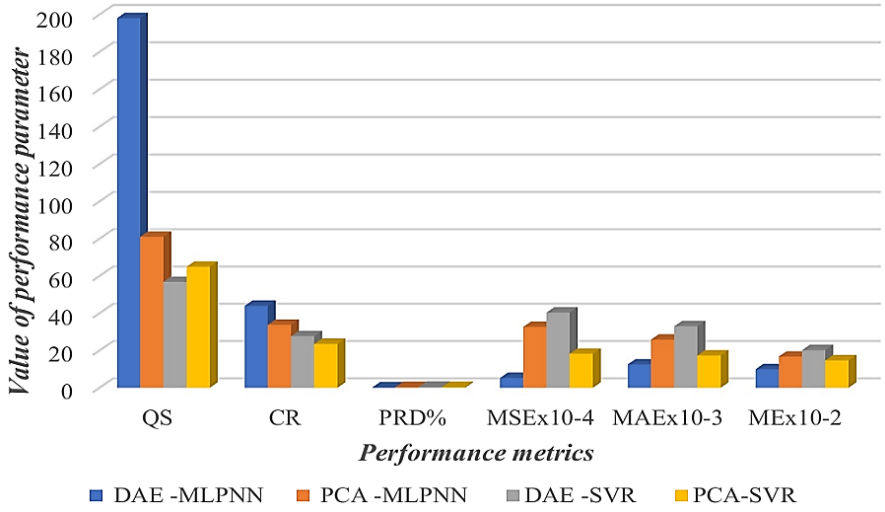

Fig. 6.5.: Comparison chart of compression and reconstruction performance of the ARIMA model by HPM predicted hyperparameters

The DCT method and dual encoding method perform compression by converting the time domain signal into frequency domain. The energy of signal was compacted into a lower frequency coefficient [50]. This method offered a higher compression efficiency than previous methods with CR=16 and PRD%=3.43. Hence the quality score (QS) also improved.

In DAST method, compression was performed via DWT and run length encoding technique, but due to high compression, the loss of information increased [140]. A phase recovery unit was added before the compression unit with a fixed offset to reduce reconstruction loss and average CR was 21.51 which was better than those of the WT and DCT method [82], [141]. However, the average QS was only 4.35 as the PRD% was 4.95. The QS can be improved by decreasing PRD%.

In integer DCT algorithm the QRS-complex and non-QRS region are segregated to develop a subsegment QRS-bank to compress ECG [83]. It offers high QS, i.e. 28.57 with PRD of 0.84% and a CR of 31.51. The 1-D DWT method is another TD-based method in which diverse DWT matrices (Symlets, Battle, Coiflets, Vaidyanathan, and Beylkin wavelets) are examined. This method was

validated on the mitdb arrhythmia database. The Battle1 wavelet-based measurement yields the best performance against db3, coif5 and sym6 in terms of the CR value, PRD%, RMSE and SNR, but values of the performance metrics are not given explicitly.

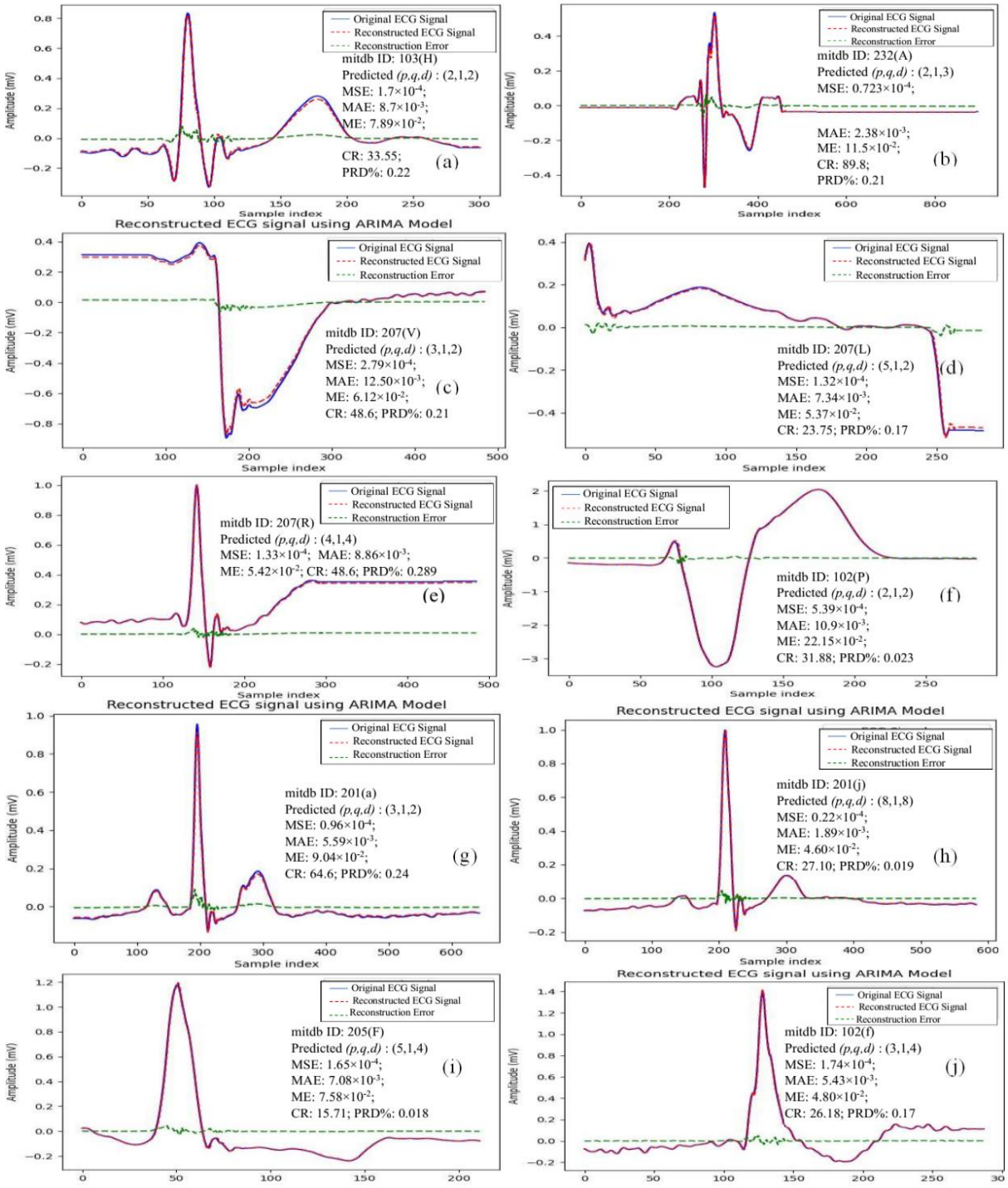

Fig. 6.6.: Compression and reconstruction performance of different types of ECG beat by the intelligent ARIMA model: (a)103–H, (b)232–A, (c)207–V, (d)207–L, (e)207–R, (f)102–P, (g)201–a, (h)201–j, (i) 205–F, (j)102–f

In PE-based compression methods such as CAE, SVD, DE, and Run-Length Encoding (RLE), parameters are extracted to compress ECG signal. The CAE method compresses ECG signal through 27 deep network layers and reconstructs ECG signal [143]. At the encoder side the ECG signal was

reduced into a low-dimensional vector and then reconstructed at decoder part as a result the CR and PRD% were 32.25 and 2.73% respectively.

Table 6.7.: Comparison with previous published work on lossless ECG compression

Work	Method	Database	CR	PRD (%)	QS
(a) Direct data compression methods (DDC)					
Alam *et al.* [138]	DPCM based	ptbdb	6.42	9.77	0.66
		mitdb	5.92	8.19	0.72
(b) Transformation domain-based methods (TD)					
Suresh Patel *et al.* [139]	Wavelet Transform	mitdb	10.63	4.71	2.26
C. K. Jha *et al.* [50]	EMD and DWT method	mitdb	25.74	1.91	13.44
C. K. Jha *et al.* [141]	DCT & Dual encoding technique	mitdb	16	3.43	4.66
A. Pandey [83]	Integer DCT based method	mitdb	31.51	0.84	28.57
Thilagavathy R *et al.* [140]	DAST method	mitdb	20.71	6.12	3.38
R. Thilagavathy *et al.*[82]	DAST method	mitdb	21.51	4.95	4.35
C. K. Jha *et al.* [80]	TQWT and RLE	mitdb	20.61	4.43	5.88
H. S. Pal *et al.* [142]	TQWT	mitdb	13.72	2.89	4.75
(c) Parameter extraction methods (PE)					
Yildirim O *et al.* [143]	CAE Model based	mitdb	32.25	2.73	11.81
L. Zheng, Z. Wang *et al.* [81]	SVD Method	mitdb	53.77	9.23	5.82
S. Banerjee *et al.*[144]	AFD method	ptbdb	48.21	3.88	12.43
S. Banerjee *et al.* [145]	DE and RLE	ptbdb	6.52	Nil	-
		mitdb	3.82	Nil	-
Proposed Method	**Adaptive ARIMA Model**	**mitdb**	**43.97**	**0.222**	**198.06**

In SVD method the ECG signal is divided into segments and a compression algorithm is subsequently applied [146]. The ECG signal was divided into m R–R segments of length n by QRS detection. It offers an average CR of 53.77 with PRD:9.23% and QS:5.82. The CR value of SVD is high but the QS becomes low because of higher reconstruction error.

The AFD method is also a lossless and PE-based compression approach [144]. It was evaluated on the basis of ptbdb data and the QS was better than that of DPCM-based method, delta encoding method and run length encoding method in terms of a better CR, i.e. 48.21 with a PRD% lower than 5% i.e. 3.88%.

The DE and RLE methods are lossless compression methods in which a whole ECG signal is compressed at a time which increases the computational complexity and time consumption [80], [145]. The average CR value is very low for ptbdb the CR is 6.52 and for mitdb the CR is 3.82. A low CR value means more consumption of memory than other methods described for ECG signal compression.

In the previous approach, we observed that in a few methods, such as EMD & DWT, integer DCT, DAST, SVD and AFD, the CR value is high, but the compression quality becomes poor due to PRD%. This signifies that ECG compression should be lossless when developing a quality-controlled compression model. In our proposed algorithm the quality is assured as the average PRD% is only 0.222%, which is lower than that of the previous approaches and the average CR value is 43.97. The CR values of the SVD and AFD-based methods are better than those of our proposed method. However, if we compare the PRD%, our result is negligible compared with the PRD% of the SVD and AFD methods. Therefore, the average quality score becomes very high i.e. 198.06.

6.4. Development of 1D-Deep Convolution Neural Network based Multiclass Classifier :

ECG classification can be either binary or multiclass. In binary classification only healthy and diseased beats are identified. But in multiclass classification different types of diseases are identified along with the healthy data. Many contributions are reported on classification of ECG signal. In this work we focused on multiclass ECG classification. In the previous reported works, we have observed most of the works were validated by five to six class of ECG from mitdb data. But a research should be validated by multiple database to avoid the data biasness and make the model more reliable. We have developed a generalized model for multiclass ECG classification. The model was validated by a new dataset i.e., Medical Information Mart for Intensive Care III (MIMIC III) along with MITBIH. The core contributions are as follows: 1) Development of 1D-DCNN based classifier, 2) Identification of 5 new annotations of MIMIC-III which are not identified in the prior research, 3) Recognition of 10 heart conditions of mitdb among them three new annotation are not considered in the published research.

Denoising and preprocessing of mitdb and MIMIC III database are already discussed in chapter 3. Features of ECG is most important factor for efficient class identification as features of each beat signify the differences in each heart condition. The denoised and preprocessed signal is passed through a DAE for feature extraction. The method of feature extraction is described in Section 6.2.1. A feature bank is developed using the features of different ECG annotation. A target or label matrix also developed by respective label of each beat to train the classifier module. The classifier module is developed using 1D-DCNN algorithm. The model performance is evaluated by accuracy, recall, F1-score, precision and loss using MIMIC-III and mitdb.

In this work five categories were considered from MIMIC III database, namely, normal (NORMAL), arrhythmia (ARYTH), hypertension (HYPER), dilated cardiomyopathy (DCM) and right bundle branch block (RBBB) and from mitdb database ten categories were considered, namely, 1) normal sinus rhythm (H), 2) atrial premature (A), 3) premature ventricular contraction (V), 4) left bundle branch block (L), 5) right bundle branch block (R), 6) paced (P), 7) aberrated atrial premature (a), 8) nodal (junctional) premature (J), 9) fusion paced (f) and 10) fusion PVC (F) beat. Fig. 6.7. shows the flow diagram of 1D-DCNN based multiclass classifier.

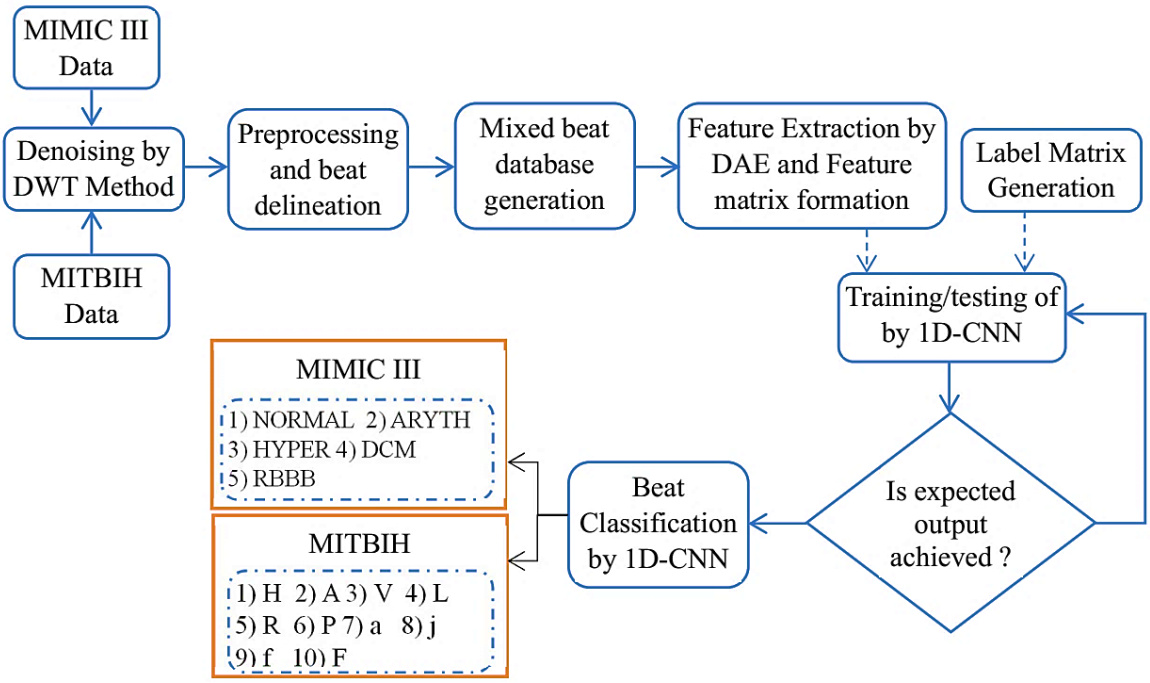

Fig.6.7.: Flow diagram of 1D-DCNN based multiclass classifier

6.4.1. Multiclass classification of ECG beat

A 1D-DCNN is based on deep learning algorithm which is specially designed to process one dimensional (1D) sequential data. It is very useful for sequential data like time-series signal. In 1D-DCNN a sliding convolutional filter or kernel is involved over the input sequence and multiple convolution layers are introduced to improve the learning technique of the model. The learnable weights of the filter are used for training of the network. In this mode it multiplies the filter value i.e. kernel to the original input in a segment of the sequence and the single output is derived by summing up the result of previous stages. It is continuous process to generate the output which is a transformed sequence. The details of DCNN model are discussed below and shown in Fig.6.7.

6.4.1.1. Architecture of 1D DCNN:

In this work, the 1D-DCNN model is developed using two convolution layer followed by a dropout layer. In a conventional 1D-CNN model the learning speed is very high. Here, multiple layers are introduced to slow down the learning speed to increase the identification efficiency of classifier. Then one max pooling layer with pool size 2 is used for down sampling the input value. The layer is performed the task of data reduction. It only considered the important features and reduces the feature size into 1/4th of original size. The next layer is flatten layer which flattened the learned features into one long vector. Then the vector is transferred to the fully connected dense layers prior to the final prediction via output layer. The architecture of 1D-DCNN model is shown in Fig.6.8. In this classifier model 64 parallel features are mapped by considering kernel size=3. ReLU was used as activation function with Adam as optimizer and categorical cross entropy as loss function for learning of multiclass ECG classifier.

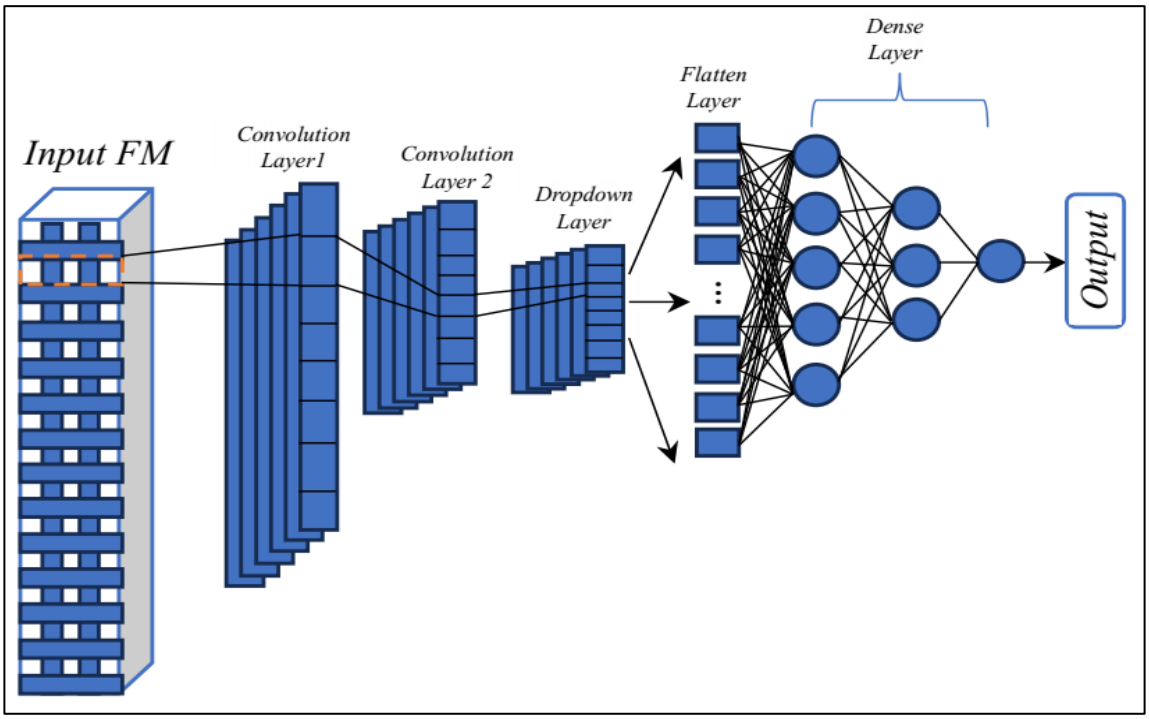

Fig.6.8.: Architecture of 1D-DCNN Model

6.5. Ablation Study:

We have developed another three multiclass classification model using following methods: K-nearest neighbour (KNN), Support vector machine (SVM) and multilayer perceptron neural network (MLPNN) to compare the performance of 1D-DCNN based multiclass classifier.

6.5.1. Working Principle of K-nearest neighbor (KNN)

The k-nearest neighbour is based on supervised machine learning algorithm. It is a non-parametric classifier and used in classification and regression problem. It works on the principal of proximity or similarity index for class recognition of unknown data point. It considers k-nearest neighbours of target to classify new set of data. Here K is number of nearest neighbours. Euclidian distance is used for calculation of distance between each datapoint to find out the k numbers of nearest neighbours. The pair of datapoints with smallest distance are considered. The class which occurred mostly among the neighbour, becomes predicted class of new datapoint. Mathematically Euclidian Distance can be expressed by:

$$dist(x, y) = \sqrt{\sum_{i=1}^{n}(y_i - x_i)^2} \quad (6.7)$$

where, x is new datapoint, x_i is the feature vector of training dataset and y_i is respective target class of training dataset.

It is important to determine the value of k for classification of unknown data. For example, k=1 means the unknown data belongs to same class and it's a single nearest neighbour. The overfitting and underfitting also depends on value k. If the value of k is lower than required one it can have high variance with bias and for high value of k will give low variance with high bias. The choice of k is depended on the input data. The value of k should be odd number to avoid ties in the classification.

6.5.2. Working Principle of Support vector Machine (SVM):

SVM is based on supervised machine learning algorithm and used for classification and regression of both linear signal and non-linear signal. SVM works on the principal of separating different class of data by finding optimal hyperplane on the basis of target features. It is suitable for both binary and multiclass classification. It determines the shape of hyperplane depending on the features of input data. The hyperplane may be a line within a 2-D space for binary classification or a plane in n-dimensional space for multiclass classification. For multiclass classification, it finds out best decision boundary to predict class of unknown data. The line which are aligned adjacently across the hyperplane, known as support vectors. These vectors are gone through the datapoint for determination of the maximal margin. Kernel functions are used for non-linear data set to transform the data into higher dimensional space for linear separation. The kernel function may be of different type on the basis of data characteristics such as linear, redial basis, sigmoid or polynomial kernel. The linear kernel function for non-linear data classification can be expressed as:

$$K(\omega, b) = \omega^T x + b \quad (6.8)$$

where, x reprents input feature vector of the training dataset; ω represents the direction of normal vector to the hyperplane which is perpendicular; b represents the distance of hyperplane from the origin along with the normal vector ω.

6.5.3. Working Principle of Multilayer perceptron neural network (MLPNN):

MLPNN is a deep learning-based model, used to extract feature, for classification and in regression problem. It has one input layer, one or multiple hidden layer and one output layer. For deep network multiple hidden layers are used. These layers are comprising of multiple fully connected nodes. It is a supervised learning method through back-propagation. The node number of input layer depends on the number of features. Hidden layers are the heart of the MLPNN as all computations are done in these layers. The value of each node is multiplied by the weight vector. ReLU used as an activation function to learn the complex pattern or relation of the input-output data. The output layer provides the predicted output based on the number of target value. This model can be represented by n input with m numbers of output and mathematically expressed as:

$$f(\cdot): R^n \rightarrow R^m \quad (6.9)$$

where, n: number of input node; m: number of output node.

6.6. Result

The proposed work is validated by a new dataset i.e. MIMIC-III database under Physionet. It is also validated by mitdb data to compare the performance of this work with previous publish research. Five classes of MIMIC III database and ten classes of mitdb database were considered for performance evaluation.

From the MIMIC-III database five cardiac cycles of each heart conditions are selected and 20 beats are chosen randomly among each cycle. The beats were stored into a cell as each beat is different in length and the cell dimension is 500x1. For each class of mitdb data 100 beats are chosen across the 48 records of mitdb. The dimension of mixed beat cell is 1000x1. The beat cells are called as data banks.

Each beat of data bank was followed by DAE for feature extraction. It extracts 100 complex features from each beat of data bank and stored into a feature matrix (FM). The dimension of FM was 100x500 for MIMIC III data and 100x1000 for mitdb data. The corresponding labels were stored into a separate matrix known as label matrix (LM). The 1D-DCNN classifier model is trained by FM and LM. The predicted result of proposed classifier can be true or false. Thus, the most possible outcome can be of four types, namely,

a) True positive (TP) means prediction of correct positive class

b) True negative (TN) means prediction of actual negative class

c) False positive (FP) means wrongly predicted positive class i.e., actually the class is negative but predict wrongly as positive

d) False negative (FN) means wrongly predicted negative class i.e., actual class is positive but predict wrongly as negative.

A confusion matrix can be defined as a table for performance evaluation of a classifier where the predicted output evaluated against actual output. Fig.6.9. shows a typical confusion matrix for 2x2 classification. In this work, for MIMIC III data the dimension of confusion matrix is 5x5 as it classifies 5 classes of ECG data and for mitdb data the dimension of confusion matrix is 10x10 as it classifies 10 classes of ECG beats. The performance of proposed classifier was evaluated by performance metrics such as accuracy, recall, precision, F1_score,. The performance metrics are defined as under:

		Actual Class	
		Positive	Negative
Predicted class	Positive	True Positive	False Negative
	Negative	False Positive	True Negative

Fig.6.9.: Confusion Matrix

Accuracy: Accuracy measures the percentage of correct prediction by the classification model. It can be expressed by:

$$Accuracy = \frac{TP+TN}{TP+TN+FP+FN} \quad (6.10)$$

Precision: Precision can be defined as the ratio of True positive to all predicted positives by the classifier model. Lower precision proportional to higher false positive prediction by the model. It is expressed by:

$$Precision = \frac{TP}{TP+FP} \tag{6.11}$$

Recall: Recall is the ratio of True positive to all positives in the data. Actually, it is true positive rate. It is defined by:

$$Recall = \frac{TP}{TP+FN} \tag{6.12}$$

F1_score: F1_score measures how well a classifier performs the task of classification. It is expressed by:

$$F1_{Score} = \frac{2}{\frac{1}{Precision}+\frac{1}{Recall}} = \frac{2*TP}{(TP+FP)(TP+FN)} \tag{6.13}$$

We have split the dataset of MIMIC III and mitdb data into three manners: 1) use 60% data for training and 40% data for validation; 2) 65% data for training and 35% for validation and 3) 70% data for training and 30% for validation, to observe the performance of model.

Table 6.8 shows the values of performance metrics for proposed classifier model using three manners of data distributions for MIMIC III and mitdb dataset. From the table 6.8 and Fig. 6.10. & 6.11. it is observable that among three data distribution ratio 70% training and 30% data validation gives highest accuracy for both types of data. As the number of training data are more than other two data distribution, it offered more than 99% class prediction accuracy for MIMIC III and mitdb database.

Table 6.8. Performance of 1D-DCNN based multiclass classification Model of MIMIC III data and mitdb data using different data distribution ratio

Database Distribution ratio (Train : Test)	**Database**	**Performance Metrics**				
		Accuracy	***Precision***	***Recall***	***F1-score***	***Loss***
70:30	MIMIC III	99	99.04	99.00	98.99	0.0800
	mitdb	100	99.87	99.9	99.9	0.0082
65:35	MIMIC III	98.66	98.73	98.66	98.65	0.1200
	mitdb	98.7	98.59	98.7	98.7	0.0091
60:40	MIMIC III	93.99	94	93.99	93.99	0.3120
	mitdb	97.22	97.56	97.22	97.037	0.0570

Table 6.9. Comparison of performance between Different types of Classifier Model

Method	**mitdb Data**				**MIMIC III Data**			
	Accuracy	***Precision***	***Recall***	***F1-score***	***Accuracy***	***Precision***	***Recall***	***F1-score***
KNN	0.91	0.91	0.87	0.89	0.916	0.919	0.869	0.887
SVM	0.952	0.952	0.952	0.951	0.948	0.949	0.977	0.964
MLPNN	0.983	0.979	0.968	0.981	0.966	0.968	0.965	0.9664
1D-DCNN	1.0	0.998	0.999	0.987	0.99	0.9904	0.988	0.989

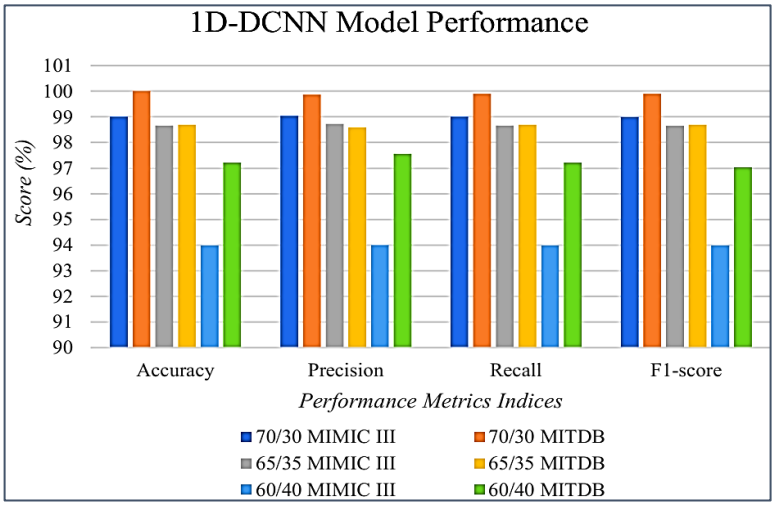

Fig.6.10.:1D-DCNN Classifier Model performance for MIMIC III data and mitdb data using different data distribution manner

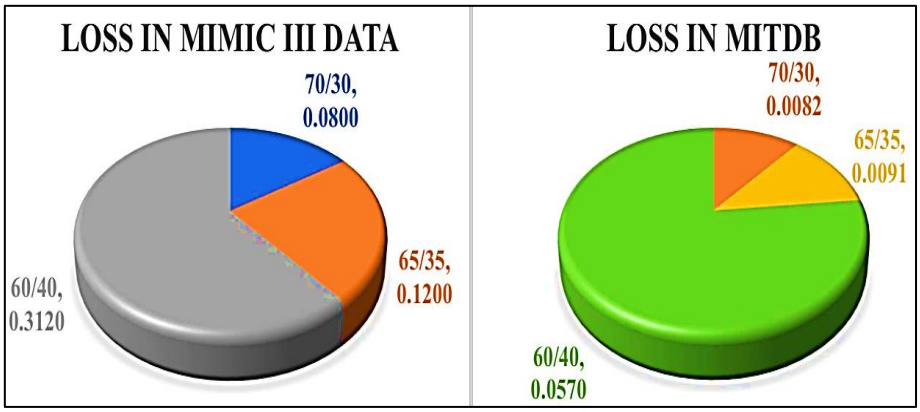

Fig.6.11. Loss in1D- DCNN classifier for different data distribution ratio

In Fig. 6.12. & 6.13. from the accuracy and loss graph of model it is observed that using 70% training data loss of model becomes negligible i.e. only 0.08% with prediction accuracy 99% for MIMIC III and for mitdb data the loss becomes only 0.0082 % with accuracy 100%

Fig. 6.14.(a). and 6.14.(b). are shown the confusion matrix of 1D-DCNN based classifier for mitdb data and MIMIC III data, respectively. From fig. 6.14.(a). it can observe that the 1D-DCNN classifier successfully indetify 10 classes of mitdb data. On the other hand in Fig. 6.14.(b) one instance of MIMIC III data i.e., class 2 was incorrectly predicted as class 3. The ARYTH data was considered as HYPER by the classifier. These figures are assured the class prediction accuracy of 1D-DCNN classifier.

The model performance was compared with other three classifier model based on KNN, SVM and MLPNN. These three models are validated by mitdb and MIMIC III database. KNN and SVM are machine learning based classifier whereas MLPNN and 1D-DCNN are deep learning beased classifier. Table 6.9 and Fig. 6.15 shows that, the KNN method gives 91% class prediction accuracy and precision for both mitdb and MIMIC III but 87% and 89% recall, 86.9% and 88.7% F1-score for mitdb and MIMIC III data respectively. SVM algorithm offers 95.2% accuracy, recall, precision and 95.1% F1-score for mitdb and 94.8% accuracy, 94.9% precision, 97.7% recall and 96.4% F1 score for MIMIC III data. MLPNN offers better performance than machine learning based classifiers. This method yields 98.3% accuracy, 97.9% precision, 96.8% recall, 98.1% F1-score for mitdb and 96.6% accuracy, 96.8%

precision, 96.5% recall, 96.64% F1-score for MIMIC-III data. Whereas, the 1D-DCNN gives 100%, 99.8%, 99.9% and 98.7% accuracy, recall, precision and F1-score respectively for mitdb and 99.0%, 99.04%, 98.8% and 98.9% accuracy, recall, precision and F1-score respectively for MIMIC III.

From Table 6.9 we observed that the proposed 1D-DCNN based classifier gives 100% accuracy for mitdb data and 99.96% for MIMIC III data whereas KNN and SVM based model accuracy are below 96% and highest accuracy obtained by MLPNN model i.e., 98.3% and 96.6% for mitdb and MIMIC-III data respectively . Hence, it is noticed that deep learning model achieves better result than machine learning based method and 1D-DCNN gives best result among them.

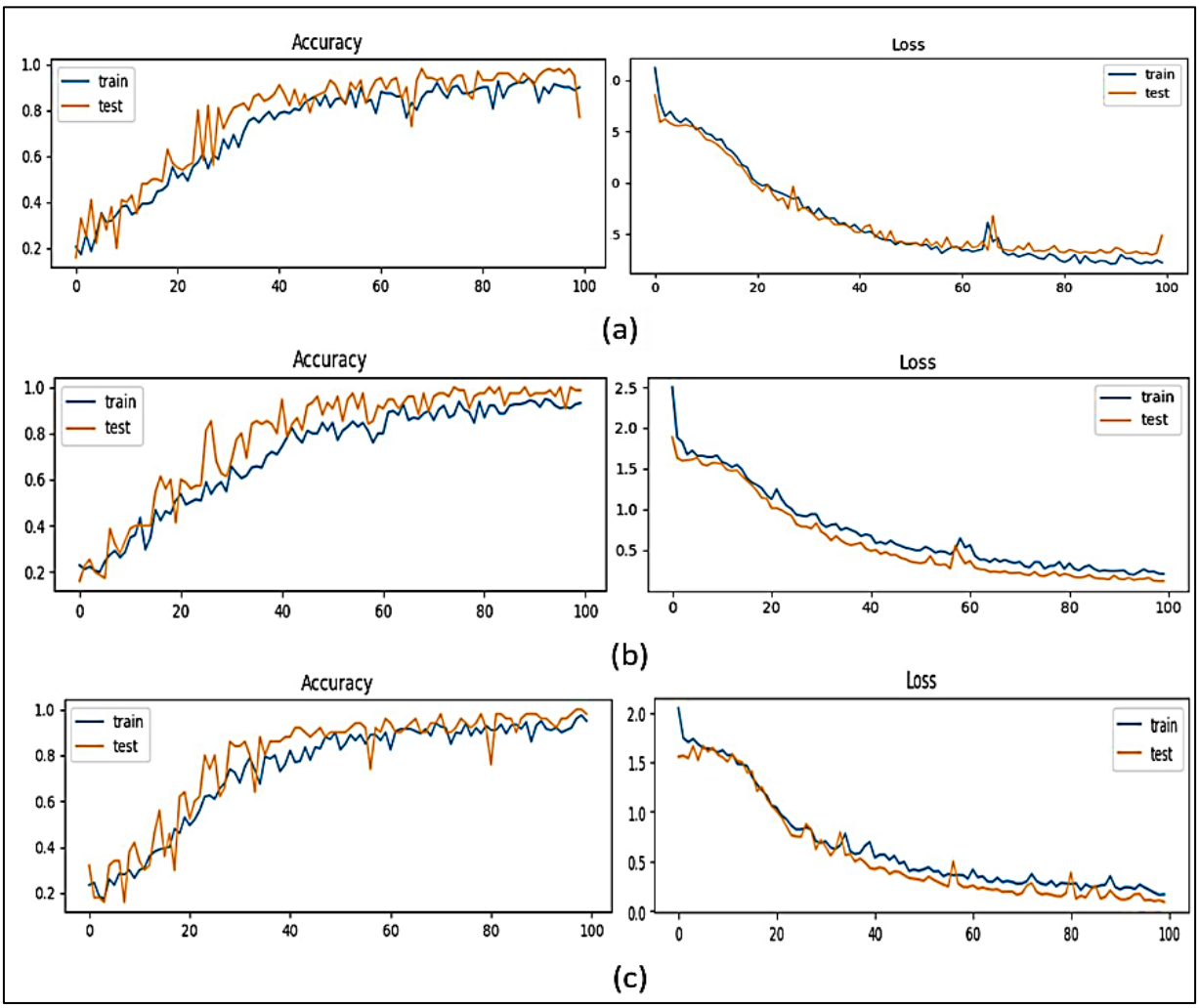

Fig.6.12. Accuracy and Loss of the 1D CNN model for training data and validation data using MIMIC III data: (a) for 60% training data and 40% validation data; (b) 65% training data and 35% validation data; (c) 70% training data and 30% validation data

Plethora of research work are published in this area. The main objective of ECG classification is to achieve higher classification accuracy and to identify multiple cardiac disease for analysis and clinical diagnostic purpose. We have observed in most of the published work of ECG multiclass classification mitdb data under Physionet database were used for validation of the model. We compare the performance of reported work with the proposed algorithm and shown into Table 6.10.

KNN and SVM are most common method used as classification model . These models were trained by features extracted by Burg's method and it can classify two heart conditions, namely, NSR and Atrial fibrillation (AF) [147]. 8th order KNN model offered 100% accuracy for 30 second, 15 second and 5 second record and 8th order KSVM model was achieved 92.3% accuracy for 5 second and 100% accuracy for 15 second and 30 second record. In another work 9th order KNN was applied on the basis of PCA extracted features [70]. It was focused to classify three heart conditions, namely, Atrial Tachycardia (AT), A and Sinus Arrhythmia (SA). It gives better result than 8th order model. This model was achieved approx. 97.14% accuracy on average. It gives maximum 100% accuracy for 15 seconds and maximum duration was considered as 35 second with classification accuracy 85%.

PNN model was developed on the basis of Adaptive wavelet network (AWN) to classify 7 ECG annotations from mitdb data viz., N, A, V, L, R, P and F beats using features extracted by Morlet wavelets [101]. This method offered 94% classification accuracy. In another work , PNN identified six ECG annotation viz. N, A, V, L, R and P beats with 99.65% accuracy [98]. PNN with WT was validated by eight class namely, N, A, V, AF, L, R, supraventricular tachycardia (SVT) and sino-auricular heart block (SHB) with accuracy 92.7%. It is a challenging task to detect eight classes of ECG condition but the accuracy is under 95%.

SVM is another popular method for classification which was used for binary classification on the basis of DAE extracted features [149]. It yields 99.99% accuracy but it identifies whether a beat is normal or abnormal. It unable to recognize different classes. SVM model combined with genetic algorithm (GA) [150] and obtained 97.2% accuracy. 1D-CNN is efficient method which was applied with softmax to recognize 5 heart condition the accuracy is 97.5%.

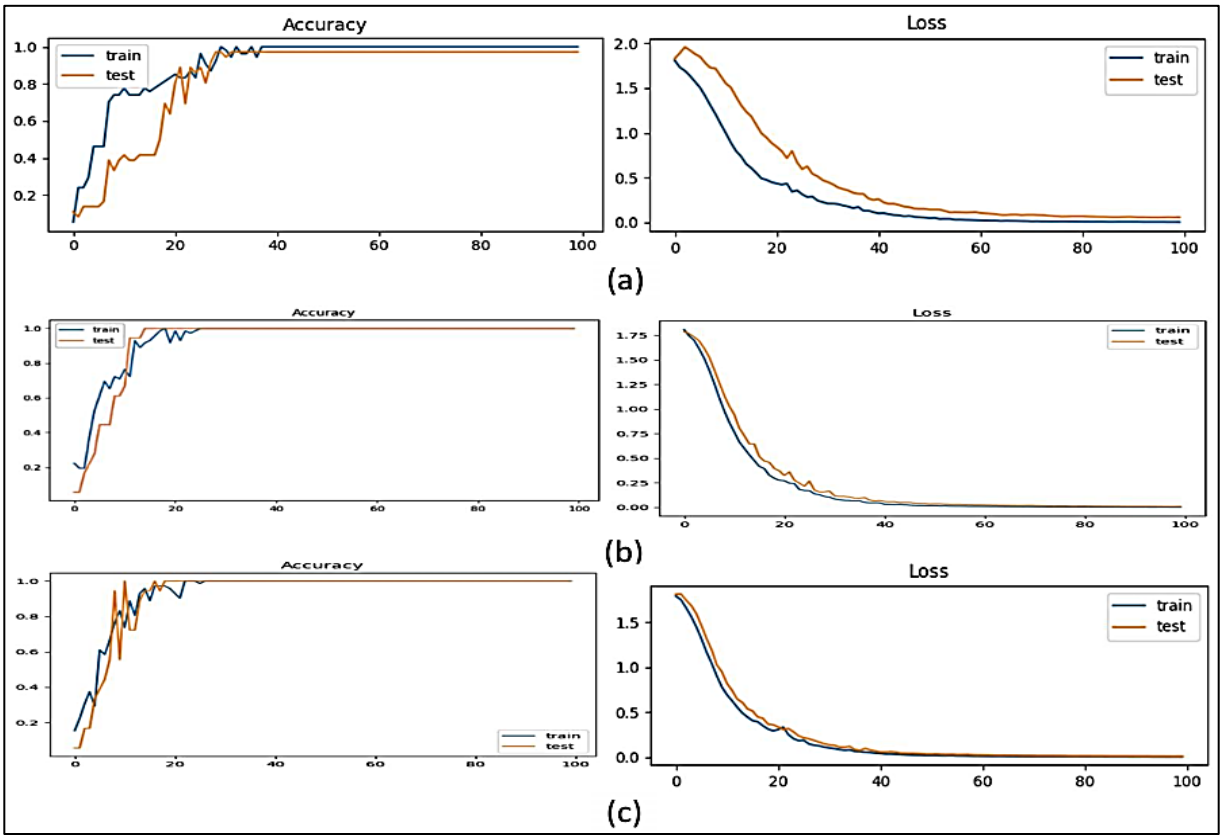

Fig.6.13.: Accuracy and Loss of the 1D CNN model for training data and validation data using mitdb data: (a) for 60% training data and 40% validation; (b) 65% training data and 35% validation data; (c) 70% training data and 30% validation data

	1	2	3	4	5	6	7	8	9	10
1	50	0	0	0	0	0	0	0	0	0
2	0	50	0	0	0	0	0	0	0	0
3	0	0	200	0	0	0	0	0	0	0
4	0	0	0	150	0	0	0	0	0	0
5	0	0	0	0	125	0	0	0	0	0
6	0	0	0	0	0	100	0	0	0	0
7	0	0	0	0	0	0	125	0	0	0
8	0	0	0	0	0	0	0	100	0	0
9	0	0	0	0	0	0	0	0	125	0
10	0	0	0	0	0	0	0	0	0	200

(a)

	1	2	3	4	5
1	56	0	0	0	0
2	0	35	0	0	0
3	0	1	24	0	0
4	0	0	0	28	0
5	0	0	0	0	56

(b)

Fig.: 6.14. Confusion Matrix of (a) mitdb Data and (b) MIMIC III Data

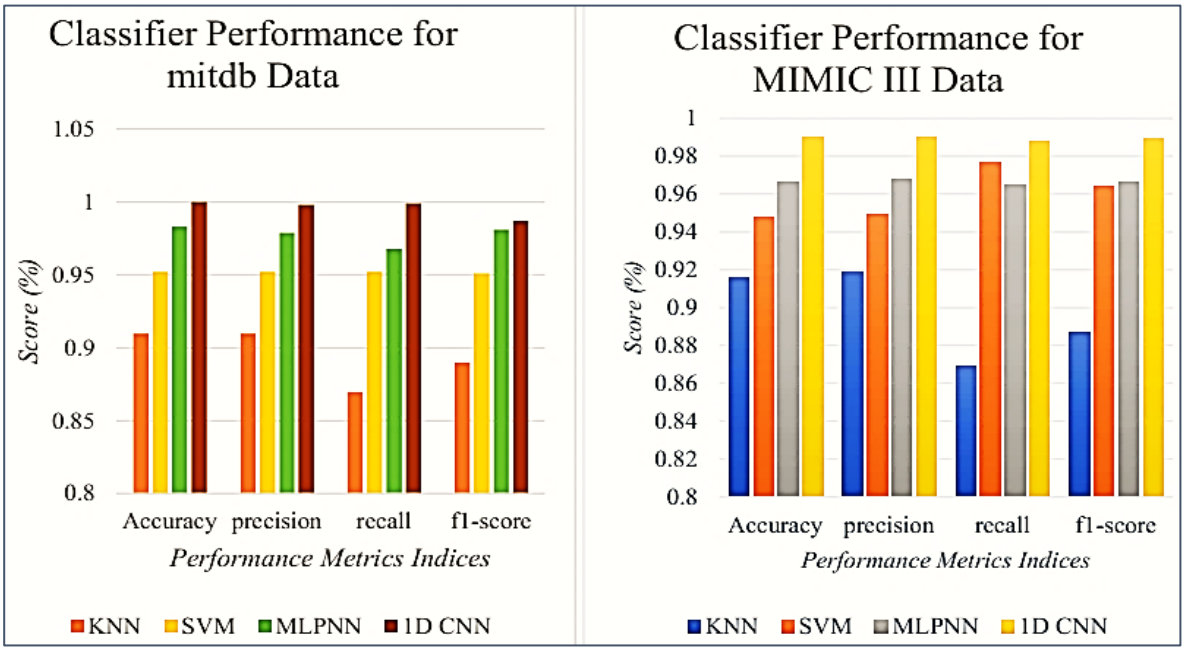

Fig.6.15.: Performance comparison graph of different classifier model for (a) mitdb data and (b) MIMIC III data

In the aforesaid works on classification the model efficiency was evaluated on the basis of mitdb data. But in a recent published work a new database i.e. MIMIC-III data had been used for validation. In this approach 1D-CNN applied with BiLSTM for binary classification. It only detects whether a beat is normal or diseased and achieved accuracy is 95%.

Table 6.10. Comparison of classification performance between proposed work and previous published work

Article	*Feature Extraction*	*Class No.*	*Database*	*ECG Class*	*Classifier*	*Accuracy*
K. Padmavathi *et al*. [147]	Burgs Method	2	mitdb	N, AF	KNN, KSVM	100%, 92.3% &100%
Varun G Gupta *et al*. [70]	PCA & Burges Method	3	Biomedical Lab, NIT, Jalandhar	AT,A, SA	KNN	97.14%
S. Raghav *et al*.[88]	Fractal Feature	5	mitdb	N,A,V, L, R	Template Matching	99.49%
Chia-Hung Lin *et al*. [101]	Morlet wavelets	7	mitdb	N, A, V, L, R, P, F,	PNN	94%
Yu *et al*. [98]	Wavelet Transform	6	mitdb	N, A, V, L, R, P	PNN	99.65%
Jose *et al.* [148]	Wavelet	8	mitdb	N, AF, A, V,L, R, SHB, SVT	PNN	92.70%
P. Bera *et al*.[149]	DAE	2	mitdb	N, A, V, F, L, R and f	SVM	99.9%
Zadeh *et al.* [150]	CWT	5	mitdb	N, A, V, L, R	SVM +GA	97.20%
Elif *et al*.[116]	EMD	6	mitdb	N,A,V,L,R, P	LDA	87%
Dan Li *et al.* [151]	1D-CNN	5	mitdb	N, A, V, L, R	Softmax	97.50%
Qingshan Liu *et al*.[114]	Combined Feature	2	mitdb	N, Arrhythmia	LSTM	97.74%
Jiuqiang Xu *et al*. [118]	LSTM	2	mitdb	N, Diseased	1D-CNN	95.96%
Abhinav Vishwa *et al*. [93]	ANN	2	mitdb	N, Diseased	ANN	96.21%
Aldughayfiq *et al.* [120]	1D-CNN	2	MIMIC III	N, AF	1D CNN + BiLSTM	95%
Proposed Method	DAE	5	MIMIC III	N, ARYTH, HYPER, RBBB, DCM	1D CNN	99.96%
		10	mitdb	N, A, V, P, L, R, a, f, F, j	1D CNN	100%

We have studied the published papers in this area and find out the research gap and work on this area. we observed that all research were done on the basis of one database i.e. mitdb which introduce risk of database bias. A research should be validated by multiple database to mitigate the risk of database biasness. Different database ensures comprehensive and accurate analysis and make the research finding more reliable and generalized. It ensures true result for various database not for a specific database. In this research we developed multiclass classification module for MIMIC-III database along with mitdb database.

6.7. Summary:

In this chapter we focused on two most important application of ECG signal processing and modeling i.e., compression and classification of ECG signal. ECG compression is very useful in telemedicine for transmission of bulk clinical data from remote location to the pathology for analysis, detection of heart condition and diagnosis. The main aim was to develop a lossless compression model and deep-learning method was applied for lossless ECG compression by ARIMA model. It is a novel method for compression where a hyperparameter prediction model was developed using DAE-MLPNN hybrid model to predict hyperparameters *(p,d,q)* of ARIMA model for compression of new ECG signal. The ARIMA model coefficients are stored in a data packet alongwith a header file and the data packet is transmitted for clinical analysis. The method was compared with another three models based on PCA-

SVM, DAE-SVM and PCA-MLPNN model. The models were validated by ten classes of mitdb data. The DAE-MLPNN model gives highest accuracy in terms of compression quality and reconstruction efficiency. DAE-MLPNN model yields 198.06 as average quality score.

Classification is the preliminary steps for ECG anomaly detection and for proper diagnosis. As observed in ECG compression work DAE driven complex features increase the efficiency of MLPNN based compression model. For ECG classification DAE driven complex features were used to train the classifier model. The classifier model was based on 1D-DCNN model. The model performance was validated using ten classes of mitdb and five classes of MIMIC III database. The model performance was compared with another three models based on KNN, SVM and MLPNN. We observed that deep learning model gives better accuracy than machine learning model. MLPNN based classifier gives higher performance than KNN and SVM based classifier. Whereas, 1D-DCNN based model classification efficiency is better than MLPNN based model. The proposed model yield 99.96% class identification accuracy for MIMIC III data and 100% accuracy for mitdb data.

Chapter 7

Discussion, Conclusion and Future Scope

7.1. Discussion and Conclusion:

As per World Health Organization (WHO) cardiovascular diseases is one of the prominent causes of mortality rates all over the world. Computerized analysis and interpretation of cardiovascular signals has been one of the focused areas of research for electrical and electronic engineering. Modeling of cardiovascular signals can lead to diseases classification, compression for effective data storage and generation of synthetic waveforms for medical and engineering R&D applications. The research study concludes the development of newer methods of cardiovascular signal modeling and analysis for automated synthetics and interpretation of cardiac abnormalities. Advanced methods of computational intelligence like machine learning, deep learning were utilized for extracting more relevant features for developing robust models for synthesis, compression and classification of cardiovascular signals. The contributions of thesis are enlisted as under:

7.1.1. Discussion and Conclusion of Chapter 3:

In chapter 3 we discussed about the type of database used in our research work and the database are mitdb, ptbdb and MIMIC III database. The main purpose of using different types of data is to develop model for synthesis, compression and classification without any data biasness. It will enhance the reliability and make a generalize model. For processing of cardiovascular signals, the preliminary steps are denoising and pre-processing of data. The main outcome of this chapters are as under:

a) In chapter 2 we have discussed different methods of denoising of ECG signal. The most popular methods are Kalman Filter, digital filter, wavelet-based method, EMD method, component analysis method, neural network methods etc. In our work we have used digital filter and DWT method for denoising of mitdb, ptbdb and MIMIC III data. We have observed that as the sampling frequency of each type of signal are different, the mother wavelet and reconstruction levels are different. After noise removal the reconstruction efficiency was high and the clinical signature of signals remain same.

b) After denoising the next important step is R-peak detection and baseline index detection for extraction of beats from the signal. R-peak is most prominent feature of ECG beat thus for further processing of ECG signal, it is desirable to detect the accurate location of R-peak index. The R-peak detection was done by DWT method and baseline detection was done by window method. We have observed that the R-peak detection and baseline detection was done properly thus the number of extracted beats was matched with the total number of beats in a record.

c) The duration and amplitude of fiducial point are described the heart condition. For healthy ECG beat there are some significant duration and amplitude of each fiducial points. Thus, any difference from this range defines the abnormalities in the heart function. In our work we have used min-max search operation to extract the fiducial points and the result was satisfying for further processing of ECG signal.

We can conclude that for any biomedical signal denoising and feature extraction plays a vital role for successful development of any signal processing model. In our work, the preprocessing of ECG signal was accurate thus it helps to achieve accuracy in synthesis, compression and classification of ECG signal.

7.1.2. Discussion and Conclusion of Chapter 4:

In chapter 4 we have develop a cardiac simulator. The base of this simulator is modeling of ECG signal. We have used two types of models, namely, Fourier and Gaussian model to develop a database. Two methods were chosen to compare the performance of the models and selection of best model for development of cardiac simulator. The outcome of this chapter are as follows:

a) Development of segment specific database according to their shape. We have divided an ECG beat into three segments i.e., PR, QRS and ST segments. Each segment was modelled by suitable model order on the basis of pre-defined RMSE. The coefficients were stored for each segment to develop a database for further process. The database was prepared for six types of data from mitdb and the ECG classes are NSR or H, APC, PVC, P, LBBB, RBBB.

b) We have developed a user defined cardiac simulator using the database. The cardiac simulator can generate 10 types of ECG signal on the basis of user defined sex, age, type of abnormality, sampling frequency, number of beats and desirable RMSE. The user will enter their required criterion via a GUI in desktop..

c) The cardiac simulator also realized by DAQ. The sequential array (seq) was fetched to a USB6009 using the analog IO library function of MATLAB®. The DAQ analog output channel generates the user desired ECG signal within 0-5 V.

d) We have compared the proposed cardiac simulator with other work and observed that in a published work on cardiac simulator, the simulator can generate only healthy ECG beat and the variation of pattern depends on two parameters i.e. heart rate and amplitude. In another work the simulator can generate three types of cardiac rhythm but the rhythms are generated on the basis of theoretical values.

We can conclude that it is very useful for medical student to understand different type of cardiac rhythm and to train medical professionals without presence of any subject. As it can generate ten types data by combining six class of ECG signal for different age and sex of people and the rhythms are more realistic as it was developed using mitdb database. It will clear the concept of medical student and professionals.

7.1.3. Discussion and Conclusion of Chapter 5:

In this chapter we focused into developments of new algorithm for improvement of reconstruction performance. We discussed about two algorithms for synthesis of ECG signal, namely, 1) Segment specific model and 2) ARIMA model.

In this first approach we have divided the ECG beat into seven segments and modelled each segment by Fourier or Gaussian modeling according to their shape. The equipotential segments are modelled by Fourier model and the bell-shaped waveforms are modelled by Gaussian model. The model is dynamic in nature and error controlled. The model order selection is depended on the user defined value of RMSE. The method was validated by ptbdb and mitdb database. The average reconstruction results of ptbdb data and mitdb data are as follows: SNR = 87.8; RMSE = 1.65×10^{-3} and SNR = 92.05; RMSE = 1.64×10^{-3}, respectively. We have compared the result in Table 5.2 with Fourier and Gaussian model and found that average SNR for two classes of data from mitdb are 20.71 and 22.16. In another work, five classes of data from mitdb was modelled by Gaussian model and the average RMSE is 33×10^{-3}. Thus, from the result we conclude that the segment specific model ensured the better synthesis of ECG signal with higher reconstruction performance.

In another approach we have used ARIMA model but in this approach the reconstruction efficiency was improved by optimizing hyperparameters of ARIMA model. This model is used as it is more suitable in real time application as it is used for modeling of non-stationary time variant signal. We have developed two types of hyperparameter optimizer based on PSO and GSO. We observed that PSO consumes more computational time than GSO but PSO optimizes more suitable hyperparameters of ARIMA model for modeling of ECG signal. The ECG signal modelled by PSO optimized hyperparameters achieved higher model accuracy than GSO. The main drawbacks of these two optimizers are slow in execution, high computation time and higher memory consumption. It can be overcome by developing a deep learning based hyperparameter prediction model.

From this chapter we can conclude that segment specific model is better than modeling of a whole beat by a particular modeling method. The ARIMA model is better than segment specific model. But the model accuracy depends on model hyperparameters thus optimization of model hyperparameter is a necessary step before modeling. PSO gives better result than GSO for optimization of hyperparameters but PSO consumes enormous time. Hence, development of hyperparameter prediction model can overcome these shortcomings of PSO.

7.1.4. Discussion and Conclusion of Chapter 6:

In this chapter we developed ECG compression model and classification model. In the chapter 4 and 5 we discussed different types of modeling method. But the main application of ECG modeling are compression and classification of ECG signal.

n chapter 5, we observed that ARIMA model is best method for ECG modeling but the model accuracy is depended upon the model hyperparameters. PSO is very efficient hyperparameter optimizer but the drawback is high computational time. To overcome this problem, we have developed a deep learning based hyperparameter prediction model using MLPNN. The ECG beat are modelled by predicted hyperparameters using ARIMA model and compressed by storing the model coefficient in a data packet. We compare our work with other work on compression and found our work propose average compression quality 198.06 which is higher than other previous published work. The result is achieved for 10 different classes of ECG. We conclude that the compression method is more reliable than other methods as it validated by highest class of ECG signal and achieve a high compression quality.

In this chapter we focused on another important application of ECG signal processing and i.e., ECG classification. The work was validated by two types of databases, mitdb and MIMIC III. It can classify ten classes of mitdb data and five classes of MIMIC III data. Deep learning method was applied for feature extraction and classification. 1D-DCNN model was developed to achieve high classification accuracy. We observe that in the previous published work, mitdb data was used for validation which create a data biasness. In our work, we introduce MIMIC III data to make a generalize, non-bias and reliable model. From Table 6.10 we observed that for both mitdb and MIMIC III data the classification model yields class identification accuracy of 99.96% and 100% respectively which are very high.

7.2. Future Scope:

In This dissertation we develop new methods and algorithm for signal processing and modeling of cardiovascular signal. Nowadays, remote monitoring of cardiac patients becomes very common for quick diagnosis and treatment of the patients. The application of ECG signal processing and modeling like representation of signal of interest, compression, classification are very useful for remote monitoring and treatment of the subject. Although in our work we developed various machine learning and deep learning-based approach for modeling, compression and classification but research can be done to develop wearables for early detection of CVDs.

We can enlist the following future scope:

a) ECG Data acquisition from cardiovascular patient using ECG signal acquisition unit and modeling of the data to create synthetic ECG which may develop a large unbiased dataset with a large variation like age, sex, abnormalities etc. The dataset may use for AI training.

b) In future the cardiac simulator can be converted into a stand-alone simulator real for time cardiac application using hardware components like Raspberry –Pi embedded controller, Touch screen etc.

c) The deep learning based compression model and classification model can be used for developing for IoT devices and wearables for personal healthcare.

References:

[1] S. E. E. Profile, “Biomedical Signal Processing and Analysis I,” no. September, pp. 101–101, 2019, doi: 10.1109/iwssip.2019.8787308.

[2] S. Mihandoost, M. Chehel, and A. Ieee, “Biomedical Signal Processing and Control Cyclic spectral analysis of electrocardiogram signals based on GARCH model,” *Biomedical Signal Processing and Control*, vol. 31, pp. 79–88, 2017, doi: 10.1016/j.bspc.2016.07.012.

[3] A. Naït-Ali, “Advanced biosignal processing,” *Advanced Biosignal Processing*, pp. 1–378, 2009, doi: 10.1007/978-3-540-89506-0.

[4] T. Ferenti, “Biomedical applications of time series analysis,” pp. 000083–000084, 2018, doi: 10.1109/nc.2017.8263256.

[5] R. Gupta, M. Mitra, and J. Bera, *ECG acquisition and automated remote processing*. Springer India, 2014.

[6] F. Morris, W. J. Brady, and J. Camm, Eds., *ABC of Clinical electrocardiography*, Second Edi. Blackwell Publishing, 2014.

[7] A. Houghton, D. Gray, and A. R. Houghton, “Making Sense of the ECG: Cases for Self Assessment,” *Making Sense of the ECG: Cases for Self Assessment*, 2014, doi: 10.1201/b16922.

[8] J. G. Webster, *Medical Instrumentation application and design Webster*, Fourth. .

[9] “www.pediatricheartspecialists.com.” .

[10] D. Adhikary, S. Barman, R. Ranjan, and H. Stone, “A Systematic Review of Major Cardiovascular Risk Factors: A Growing Global Health Concern,” *Cureus*, vol. 14, no. Mi, 2022, doi: 10.7759/cureus.30119.

[11] S. Palani, “Representation of Signals and Systems,” *Basic System Analysis*, pp. 1–173, 2023, doi: 10.1007/978-3-031-28280-5_1.

[12] J. C. Edelmann, D. Mair, D. Ziesel, M. Burtscher, and T. Ussmueller, “An ECG simulator with a novel ECG profile for physiological signals,” *Journal of Medical Engineering and Technology*, vol. 42, no. 7, pp. 501–509, 2018, doi: 10.1080/03091902.2019.1576788.

[13] E. K. Roonizi and R. Sameni, “Morphological modeling of cardiac signals based on signal decomposition,” *Computers in Biology and Medicine*, vol. 43, no. 10, pp. 1453–1461, 2013, doi: 10.1016/j.compbiomed.2013.06.017.

[14] P. E. Tikkanen, “Nonlinear wavelet and wavelet packet denoising of electrocardiogram signal,” *Biological Cybernetics*, vol. 80, no. 4, pp. 259–267, 1999, doi: 10.1007/s004220050523.

[15] P. Kundu and R. Gupta, “Electrocardiogram synthesis using Gaussian and fourier models,” in *Proceedings of 2015 IEEE International Conference on Research in Computational Intelligence and Communication Networks, ICRCICN 2015*, 2016, pp. 312–317, doi: 10.1109/ICRCICN.2015.7434256.

[16] B. R. Manju and B. Akshaya, “Simulation of Pathological ECG Signal Using Transform Method,” *Procedia Computer Science*, vol. 171, no. 2019, pp. 2121–2127, 2020, doi: 10.1016/j.procs.2020.04.229.

[17] M. Tlili, A. Maalej, M. Ben Romdhane, F. Rivet, D. Dallet, and C. Rebai, “Mathematical modeling of clean and noisy ECG signals in a level-crossing sampling context,” *2016 International Symposium on Signal, Image, Video and Communications, ISIVC 2016*, pp. 359–363, 2017, doi: 10.1109/ISIVC.2016.7894015.

[18] J. Wang and S. Tang, “Time series classification based on arima and adaboost,” *MATEC Web of Conferences*, vol. 309, p. 03024, 2020, doi: 10.1051/matecconf/202030903024.

[19] J. J. Águila, E. Arias, M. M. Artigao, and J. J. Miralles, “A prediction of electrocardiography signals by combining ARMA model with nonlinear analysis methods,” 2011.

[20] O. Raach, T. R. Pillai, and A. Abdullah, “GARMA modeling of ECG and classification of arrhythmia,” *Proceedings - International Conference on Intelligent Systems, Modelling and Simulation, ISMS*, vol. 2018-May, pp. 26–31, 2018, doi: 10.1109/ISMS.2018.00015.

[21] F. Huang, T. Qin, L. Wang, H. Wan, and J. Ren, “An ECG Signal Prediction Method Based on ARIMA Model and DWT,” *Proceedings of 2019 IEEE 4th Advanced Information Technology, Electronic and Automation Control Conference, IAEAC 2019*, no. Iaeac, pp. 1298–1304, 2019, doi:

10.1109/IAEAC47372.2019.8997620.

[22] N. V. Thakor and Y. S. Zhu, “Applications of Adaptive Filtering to ECG Analysis: Noise Cancellation and Arrhythmia Detection,” *IEEE Transactions on Biomedical Engineering*, vol. 38, no. 8, pp. 785–794, 1991, doi: 10.1109/10.83591.

[23] M. A. Mneimneh, E. E. Yaz, M. T. Johnson, and R. J. Povinelli, “An adaptive kalman filter for removing baseline wandering in ECG,” *Computers in Cardiology*, vol. 33, pp. 253–256, 2006.

[24] O. Sayadi and M. B. Shamsollahi, “ECG denoising and compression using a modified extended Kalman filter structure,” *IEEE Transactions on Biomedical Engineering*, vol. 55, no. 9, pp. 2240–2248, 2008, doi: 10.1109/TBME.2008.921150.

[25] R. Sameni, M. B. Shamsollahi, C. Jutten, and G. D. Clifford, “A Nonlinear Bayesian Filtering Framework for ECG Denoising,” *IEEE Trans Biomed Eng*, vol. 54, no. 12, pp. 2172–2185, 2007.

[26] M. F. Hutchinson and F. R. de Hoog, “Smoothing noisy data with spline functions,” *Numerische Mathematik*, vol. 47, no. 1, pp. 99–106, 1985, doi: 10.1007/BF01389878.

[27] B. Boucheham, Y. Ferdi, and M. C. Batouche, “Piecewise linear correction of ECG baseline wander: A curve simplification approach,” *Computer Methods and Programs in Biomedicine*, vol. 78, no. 1, pp. 1–10, 2005, doi: 10.1016/j.cmpb.2004.10.008.

[28] M. A. Tinati and B. Mozaffary, “A wavelet packets approach to electrocardiograph baseline drift cancellation,” *International Journal of Biomedical Imaging*, vol. 2006, pp. 1–9, 2006, doi: 10.1155/IJBI/2006/97157.

[29] V. K. Pandey and P. C. Pandey, “Wavelet based cancellation of respiratory artifacts in impedance cardiography,” *2007 15th International Conference on Digital Signal Processing, DSP 2007*, pp. 191–194, 2007, doi: 10.1109/ICDSP.2007.4288551.

[30] M. Kania, M. Fereniec, and R. Maniewski, “Wavelet denoising for multi-lead high resolution ECG signals,” *6th International Conference on Measurement, MEASUREMENT 2007 - Proceedings*, vol. 7, no. 4, pp. 400–403, 2007.

[31] O. Sayadi and M. B. Shamsollahi, “Multiadaptive bionic wavelet transform: Application to ECG denoising and baseline wandering reduction,” *Eurasip Journal on Advances in Signal Processing*, vol. 2007, no. c, 2007, doi: 10.1155/2007/41274.

[32] M. Blanco-Velasco, B. Weng, and K. E. Barner, “ECG signal denoising and baseline wander correction based on the empirical mode decomposition,” *Computers in Biology and Medicine*, vol. 38, no. 1, pp. 1–13, 2008, doi: 10.1016/j.compbiomed.2007.06.003.

[33] Y. Lu, J. Yan, and Y. Yam, “Model-based ECG denoising using empirical mode decomposition,” *2009 IEEE International Conference on Bioinformatics and Biomedicine, BIBM 2009*, pp. 191–196, 2009, doi: 10.1109/BIBM.2009.14.

[34] S. Pal and M. Mitra, “Empirical mode decomposition based ECG enhancement and QRS detection,” *Computers in Biology and Medicine*, vol. 42, no. 1, pp. 83–92, 2012, doi: 10.1016/j.compbiomed.2011.10.012.

[35] W. Zhou and J. Gotman, “Removal of EMG and ECG artifacts from EEC based on wavelet transform and ICA,” *Annual International Conference of the IEEE Engineering in Medicine and Biology - Proceedings*, vol. 26 I, pp. 392–395, 2004, doi: 10.1109/iembs.2004.1403176.

[36] I. Romero, “PCA and ICA applied to noise reduction in multi-lead ECG,” *Computing in Cardiology*, vol. 38, pp. 613–616, 2011.

[37] S. Pal and M. Mitra, “Increasing the accuracy of ECG based biometric analysis by data modelling,” *Measurement*, vol. 45, no. 7, pp. 1927–1932, 2012, doi: 10.1016/j.measurement.2012.03.005.

[38] J. S. Mateo, C. Sanchez, R. Alcaraz, C. Vaya, and J. J. Rieta, “Neural networks based approach to remove baseline drift in biomedical signals,” *IFMBE Proceedings*, vol. 16, no. 1, pp. 90–93, 2007, doi: 10.1007/978-3-540-73044-6_24.

[39] N. M. Arzeno, Z. Deng, and C. Poon, “Analysis of First-Derivative Based QRS Detection Algorithms,” vol. 55, no. 2, pp. 478–484, 2008.

[40] E. Zeraatkar, “Improving QRS Detection for Artifacts Reduction,” no. November, pp. 3–4, 2010.

[41] G. Zhengzhong, K. Fanxue, and Z. Xu, "Accurate and Rapid QRS Detection for Intelligent ECG Monitor," pp. 2–5, 2011, doi: 10.1109/ICMTMA.2011.76.

[42] M. S. Manikandan and K. P. Soman, "A novel method for detecting R-peaks in electrocardiogram (ECG) signal," *Biomed. Signal Process. Control*, vol. 7, no. 2, pp. 118–128, 2012, doi: 10.1016/j.bspc.2011.03.004.

[43] M. Rakshit and S. Das, "An efficient wavelet-based automated R-peaks detection method using Hilbert transform," *Biocybern. Biomed. Eng.*, vol. 37, no. 3, pp. 566–577, 2017, doi: 10.1016/j.bbe.2017.02.002.

[44] F. Paper, "Comparative Study of QRS Complex Detection in ECG Based on Discrete Wavelet Transform," vol. 2, no. 5, 2009.

[45] K. V. L. N. Corresponding, "Wavelet based QRS detection in ECG using MATLAB," *Innovative Systems Design and Engineering*, vol. 2, no. 7, pp. 60–69, 2011.

[46] T. Sharma and K. K. Sharma, "QRS Complex Detection in ECG Signals Using the Synchrosqueezed Wavelet Transform," vol. 2063, no. September, 2016, doi: 10.1080/03772063.2016.1221744.

[47] J. Xue, W. He, X. Yan, and C. Zheng, "Feature extraction and classification of EEG for mental tasks based on wavelet packet analysis," *Sheng wu yi xue gong cheng xue za zhi = Journal of biomedical engineering = Shengwu yixue gongchengxue zazhi*, vol. 21, no. 3, 2004.

[48] R. J. Martis, C. Chakraborty, and A. K. Ray, "An integrated ECG feature extraction scheme using PCA and wavelet transform," *Proceedings of INDICON 2009 - An IEEE India Council Conference*, no. Chazal 2004, pp. 1–4, 2009, doi: 10.1109/INDCON.2009.5409439.

[49] S. Banerjee, R. Gupta, and M. Mitra, "Delineation of ECG characteristic features using multiresolution wavelet analysis method," *Meas. J. Int. Meas. Confed.*, vol. 45, no. 3, pp. 474–487, 2012, doi: 10.1016/j.measurement.2011.10.025.

[50] C. K. Jha and M. H. Kolekar, "Empirical Mode Decomposition and Wavelet Transform Based ECG Data Compression Scheme," *Irbm*, vol. 42, no. 1, pp. 65–72, 2021, doi: 10.1016/j.irbm.2020.05.008.

[51] H. K. Chatterjee, R. Gupta, and M. Mitra, "A statistical approach for determination of time plane features from digitized ECG," *Comput. Biol. Med.*, vol. 41, no. 5, pp. 278–284, 2011, doi: 10.1016/j.compbiomed.2011.03.003.

[52] D. Sadhukhan and M. Mitra, "R-Peak Detection Algorithm for Ecg using Double Difference And RR Interval Processing," *Procedia Technology*, vol. 4, pp. 873–877, 2012, doi: 10.1016/j.protcy.2012.05.143.

[53] P. Bera and R. Gupta, "Disease-aware Compression of Multi-lead Electrocardiogram Using Intelligent Hybrid Encoder," *IETE Technical Review (Institution of Electronics and Telecommunication Engineers, India)*, vol. 39, no. 1, pp. 207–218, 2022, doi: 10.1080/02564602.2020.1831971.

[54] V. Kazak, *Unsupervised feature extraction with autoencoder: for the representation of parkinson' s disease patients*. 2018.

[55] T. Wen and Z. Zhang, "Deep Convolution Neural Network and Autoencoders-Based Unsupervised Feature Learning of EEG Signals," *IEEE Access*, vol. 6, pp. 25399–25410, 2018, doi: 10.1109/ACCESS.2018.2833746.

[56] D. N. Dutt, S. M. Krishnan, and N. Srinivasan, "A dynamic nonlinear time domain model for reconstruction and compression of cardiovascular signals with application to telemedicine," *Comput. Biol. Med.*, vol. 33, no. 1, pp. 45–63, 2003, doi: 10.1016/S0010-4825(02)00058-6.

[57] F. Guendouzi and M. Attari, "Polynomial modeling of the ECG signals," *International Conference on Computer Medical Applications, ICCMA 2013*, no. 3, pp. 0–4, 2013, doi: 10.1109/ICCMA.2013.6506177.

[58] W. Philips, "tive Noise Removal from Biome s Using ed Polynomials," pp. 480–492, 1996.

[59] D. Tchiotsop, D. Wolf, V. Louis-Dorr, and R. Husson, "ECG data compression using Jacobi polynomials," *Annual International Conference of the IEEE Engineering in Medicine and Biology - Proceedings*, no. 2, pp. 1863–1867, 2007, doi: 10.1109/IEMBS.2007.4352678.

[60] H. Jang, D. J. Conklin, and M. Kong, "Piecewise nonlinear mixed-effects models for modeling cardiac function and assessing treatment effects," *Computer Methods and Programs in Biomedicine*, vol. 110, no. 3, pp. 240–252, 2013, doi: 10.1016/j.cmpb.2012.11.007.

[61] S. C. Bera, B. Chakraborty, and J. K. Ray, "A mathematical model for analysis of ECG waves in a normal

subject," *Measurement*, vol. 38, pp. 53–60, 2005, doi: 10.1016/j.measurement.2005.01.003.

[62] Z. Wang, F. Wan, C. M. Wong, and L. Zhang, "Adaptive Fourier decomposition based ECG denoising," *Computers in Biology and Medicine*, vol. 77, pp. 195–205, 2016, doi: 10.1016/j.compbiomed.2016.08.013.

[63] A. Mitra, P. Kundu, and R. Gupta, "Segment Specific Modeling of Electrocardiogram for Improved Reconstruction Error," in *Proceedings of 2020 IEEE Applied Signal Processing Conference, ASPCON 2020*, 2020, pp. 16–20, doi: 10.1109/ASPCON49795.2020.9276731.

[64] S. Islam and N. Alajlan, "A morphology alignment method for resampled heartbeat signals," *Biomedical Signal Processing and Control*, 2012, doi: 10.1016/j.bspc.2012.11.006.

[65] R. M. Evaristo, A. M. Batista, R. L. Viana, K. C. Iarosz, J. D. Szezech, and M. F. d. Godoy, "Mathematical model with autoregressive process for electrocardiogram signals," *Commun. Nonlinear Sci. Numer. Simul.*, vol. 57, pp. 415–421, 2018, doi: 10.1016/j.cnsns.2017.10.018.

[66] T. Peng, M. L. Trew, and A. Malik, "Predictive modeling of drug effects on electrocardiograms," *Computers in Biology and Medicine*, vol. 108, pp. 332–344, 2019, doi: 10.1016/j.compbiomed.2019.03.027.

[67] C. Qian, H. Su, and H. Yu, "Local means denoising of ECG signal," *Biomedical Signal Processing and Control*, vol. 53, p. 101571, 2019, doi: 10.1016/j.bspc.2019.101571.

[68] S. Parvaneh and M. Pashna, "Electrocardiogram synthesis using a gaussian combination model (GCM)," *Comput. Cardiol.*, vol. 34, no. 1, pp. 621–624, 2007, doi: 10.1109/CIC.2007.4745562.

[69] D. F. Ge, B. P. Hou, and X. J. Xiang, "Study of feature extraction based on autoregressive modeling in ECG automatic diagnosis," *Zidonghua Xuebao/Acta Automatica Sinica*, vol. 33, no. 5, pp. 462–466, 2007, doi: 10.1360/aas-007-0462.

[70] V. Gupta and M. Mittal, "KNN and PCA classifier with Autoregressive modelling during different ECG signal interpretation," *Procedia Computer Science*, vol. 125, pp. 18–24, 2018, doi: 10.1016/j.procs.2017.12.005.

[71] A. Staffini, T. Svensson, U. Il Chung, and A. K. Svensson, "Heart rate modeling and prediction using autoregressive models and deep learning," *Sensors*, vol. 22, no. 1, pp. 1–13, 2022, doi: 10.3390/s22010034.

[72] N. Srinivasan, D. F. Ge, and S. M. Krishnan, "Autoregressive modeling and classification of cardiac arrhythmias," *Annual International Conference of the IEEE Engineering in Medicine and Biology - Proceedings*, vol. 2, pp. 1405–1406, 2002, doi: 10.1109/IEMBS.2002.1106452.

[73] L. Famiglini, A. Campagner, A. Carobene, and F. Cabitza, "A robust and parsimonious machine learning method to predict ICU admission of COVID-19 patients," *Medical and Biological Engineering and Computing*, no. 0123456789, 2022, doi: 10.1007/s11517-022-02543-x.

[74] I. S. Fathi, M. A. A. Makhlouf, E. Osman, and M. A. Ahmed, "An Energy-Efficient Compression Algorithm of ECG Signals in Remote Healthcare Monitoring Systems," *IEEE Access*, vol. 10, pp. 39129–39144, 2022, doi: 10.1109/ACCESS.2022.3166476.

[75] M. S. Manikandan and S. Dandapat, "Quality Controlled Wavelet Compression of ECG Signals by WEDD," pp. 581–586, 2008, doi: 10.1109/iccima.2007.333.

[76] A. Alshamali, "Wavelet based ECG compression with adaptive thresholding and efficient coding," *Journal of Medical Engineering and Technology*, vol. 34, no. 5–6, pp. 335–339, 2010, doi: 10.3109/03091902.2010.486469.

[77] V. Aggarwal and M. S. Patterh, "ECG compression using Slantlet and lifting wavelet transform with and without normalisation," *International Journal of Electronics*, vol. 100, no. 5, pp. 626–636, 2013, doi: 10.1080/00207217.2012.720941.

[78] S. K. Mukhopadhyay, S. Mitra, and M. Mitra, "A combined application of lossless and lossy compression in ECG processing and transmission via GSM-based SMS," *Journal of Medical Engineering and Technology*, vol. 39, no. 2, pp. 105–122, 2015, doi: 10.3109/03091902.2014.990159.

[79] M. Elgendi, A. Mohamed, and R. Ward, "Efficient ECG Compression and QRS Detection for E-Health Applications," *Scientific Reports*, vol. 7, no. 1, pp. 1–15, 2017, doi: 10.1038/s41598-017-00540-x.

[80] C. K. Jha and M. H. Kolekar, “Tunable Q-wavelet based ECG data compression with validation using cardiac arrhythmia patterns,” *Biomedical Signal Processing and Control*, vol. 66, no. April 2020, p. 102464, 2021, doi: 10.1016/j.bspc.2021.102464.

[81] L. Zheng, Z. Wang, J. Liang, S. Luo, and S. Tian, “Effective compression and classification of ECG arrhythmia by singular value decomposition,” *Biomedical Engineering Advances*, vol. 2, p. 100013, 2021, doi: 10.1016/j.bea.2021.100013.

[82] R. Thilagavathy and B. Venkataramani, “Optimization of Discrete Anamorphic Stretch Transform and Phase Recovery for ECG Signal Compression,” *IETE Journal of Research*, vol. 69, no. 10, pp. 7106–7120, 2023, doi: 10.1080/03772063.2021.2012281.

[83] A. Pandey, “ECG data compression using the formation of QRS-complex segment bank and integer DCT-based plateau region processing,” *Biomedical Signal Processing and Control*, vol. 85, no. March, p. 104823, 2023, doi: 10.1016/j.bspc.2023.104823.

[84] Y. V. Parkale and S. L. Nalbalwar, “Compressed sensing for ECG signal compression using DWT based sensing matrices,” *Smart Science*, vol. 11, no. 4, pp. 759–773, 2023, doi: 10.1080/23080477.2023.2258643.

[85] O. Valenzuela *et al.*, “Intelligent Classifier for Atrial Fibrillation (ECG),” *Encyclopedia of Artificial Intelligence*, pp. 910–912, 2011, doi: 10.4018/9781599048499.ch134.

[86] A. Ukil, L. Marin, S. C. Mukhopadhyay, and A. J. Jara, “AFSense-ECG: Atrial Fibrillation Condition Sensing from Single Lead Electrocardiogram (ECG) Signals,” *IEEE Sensors Journal*, vol. 22, no. 12, 2022, doi: 10.1109/JSEN.2022.3162691.

[87] P. Khandait, N. Bawane, and S. Limaye, “Features Extraction of ECG signal for Detection of Cardiac Arrhythmias,” *International Journal of Computer Applications*. pp. 6–10, 2012.

[88] S. Raghav and A. K. Mishra, “Fractal feature based ECG arrhythmia classification,” 2008, doi: 10.1109/TENCON.2008.4766475.

[89] C. Chandrakar and M. Sharma, “A Real Time Approach of Cardiac Profiling Scheme for ECG Beat Classification using Shared Counters Chinmay,” in *2015 International Conference on Computing, Communication and Control, IC4 2015*, 2015, pp. 1–6, doi: 10.1109/IC4.2015.7375735.

[90] S. H. Jambukia, V. K. Dabhi, and H. B. Prajapati, “Classification of ECG signals using machine learning techniques: A survey,” *Conference Proceeding - 2015 International Conference on Advances in Computer Engineering and Applications, ICACEA 2015*, pp. 714–721, 2015, doi: 10.1109/ICACEA.2015.7164783.

[91] S. S. and A. P. V. Hiremani, R. M. Devadas, H. L, “Heart Arrhythmia Classification Using Machine Learning Algorithms,” in *2023 2nd International Conference on Ambient Intelligence in Health Care (ICAIHC), Bhubaneswar, India*, 2023, pp. 1–4, doi: 10.1109/ICAIHC59020.2023.10431441.

[92] A. Batra and V. Jawa, “Classification of Arrhythmia Using Conjunction of Machine Learning Algorithms and ECG Diagnostic Criteria,” *International Journal of Biology and Biomedicine*, vol. 1, pp. 1–7, 2016.

[93] A. Vishwa, M. K. Lal, S. Dixit, and P. Vardwaj, “Clasification Of Arrhythmic ECG Data Using Machine Learning Techniques,” *International Journal of Interactive Multimedia and Artificial Intelligence*, vol. 1, no. 4, p. 67, 2011, doi: 10.9781/ijimai.2011.1411.

[94] D. S. Z. Sabzevari Vahid R., Azemi Asad, Khademi Morteza, Gholizade Hossein, “Arrhythmia Detection and Classification Using Wavelet and ICA,” *Encyclopedia of Healthcare Information Systems*, vol. Vol. 3, pp. 115–121, 2008, doi: 10.4018/978-1-59904-889-5.ch016.

[95] and C. L. Tony Basil, “AUTOMATIC CLASSIFICATION OF HEARTBEATS,” in *22nd European Signal Processing Conference (EUSIPCO), Lisbon, Portugal*, 2014, pp. 1542–1546.

[96] H. Li and P. Boulanger, “A model-based approach for arrhythmia detection and classification,” *Lecture Notes in Computer Science (including subseries Lecture Notes in Artificial Intelligence and Lecture Notes in Bioinformatics)*, vol. 11010 LNCS, pp. 429–436, 2018, doi: 10.1007/978-3-030-04375-9_37.

[97] M. G. Tsipouras, C. Voglis, I. E. Lagaris, and D. I. Fotiadis, “Cardiac arrhythmia classification using support vector machines,” *The 3rd European Medical and Biological Engineering Conference*, pp. 2–7, 2005.

[98] S. N. Yu and Y. H. Chen, “Electrocardiogram beat classification based on wavelet transformation and

probabilistic neural network," *Pattern Recognition Letters*, vol. 28, no. 10, pp. 1142–1150, 2007, doi: 10.1016/j.patrec.2007.01.017.

[99] F. Belhachat and N. Izeboudjen, "Conception of intelligent classifiers for cardiac arrhythmias detection," 1956.

[100] E. N. Hadji Salah, "Cardiac Arrhythmia Classification by Wavelet Transform," *International Journal of Advanced Research in Artificial Intelligence*, vol. Vol. 4, No, 2015.

[101] C. H. Lin, Y. C. Du, and T. Chen, "Adaptive wavelet network for multiple cardiac arrhythmias recognition," *Expert Systems with Applications*, vol. 34, no. 4, pp. 2601–2611, 2008, doi: 10.1016/j.eswa.2007.05.008.

[102] F. A. Elhaj, N. Salim, A. R. Harris, T. T. Swee, and T. Ahmed, "Arrhythmia recognition and classification using combined linear and nonlinear features of ECG signals," *Computer Methods and Programs in Biomedicine*, vol. 127, pp. 52–63, 2016, doi: 10.1016/j.cmpb.2015.12.024.

[103] O. Valenzuela *et al.*, "Intelligent systems to autonomously classify several arrhythmia using information from ECG," *Proceedings - SocialCom/PASSAT/BigData/EconCom/BioMedCom 2013*, pp. 1038–1045, 2013, doi: 10.1109/SocialCom.2013.168.

[104] S. G. N. C. Gurudas Nayak, G. Seshikala, Usha Desai, "Identification of Arrhythmia Classes Using Machine-Learning.pdf," *International Journal of Biology and Biomedicine*, vol. 1, pp. 48–53, 2016.

[105] V. Gliner and Y. Yaniv, "Identification of features for machine learning analysis for automatic arrhythmogenic event classification," *Computing in Cardiology*, vol. 44, pp. 1–4, 2017, doi: 10.22489/CinC.2017.170-101.

[106] Y. T G, D. R. K. G K, and M. S. D, "Robust Classification of Cardiac Arrhythmia Using Machine Learning," *International Journal for Research in Applied Science and Engineering Technology*, vol. 10, no. 6, pp. 1536–1542, 2022, doi: 10.22214/ijraset.2022.44095.

[107] M. Ramkumar, M. Alagarsamy, A. Balakumar, and S. Pradeep, "Ensemble classifier fostered detection of arrhythmia using ECG data," *Medical and Biological Engineering and Computing*, vol. 61, no. 9, 2023, doi: 10.1007/s11517-023-02839-6.

[108] A. Nasim, D. C. Nchekwube, F. Munir, and Y. S. Kim, "An Evolutionary-Neural Mechanism for Arrhythmia Classification With Optimum Features Using Single-Lead Electrocardiogram," *IEEE Access*, vol. 10, no. August, pp. 99050–99065, 2022, doi: 10.1109/ACCESS.2022.3203586.

[109] S. A. Bellegdi, S. Mohandes, O. M. Soufan, and S. Arafat, "Computational intelligence for cardiac arrhythmia classification," *UKCI 2011 - Proceedings of the 11th UK Workshop on Computational Intelligence*. pp. 93–97, 2011.

[110] E. J. D. S. Luz, T. M. Nunes, V. H. C. De Albuquerque, J. P. Papa, and D. Menotti, "ECG arrhythmia classification based on optimum-path forest," *Expert Systems with Applications*, vol. 40, no. 9, pp. 3561–3573, 2013, doi: 10.1016/j.eswa.2012.12.063.

[111] I. Jekova, G. Bortolan, and I. Christov, "Assessment and comparison of different methods for heartbeat classification," *Medical Engineering and Physics*, vol. 30, no. 2, pp. 248–257, 2008, doi: 10.1016/j.medengphy.2007.02.003.

[112] E. J. da S. Luz, W. R. Schwartz, G. Cámara-Chávez, and D. Menotti, "ECG-based heartbeat classification for arrhythmia detection: A survey," *Computer Methods and Programs in Biomedicine*, vol. 127, pp. 144–164, 2016, doi: 10.1016/j.cmpb.2015.12.008.

[113] M. Sansone, R. Fusco, A. Pepino, and C. Sansone, "Electrocardiogram pattern recognition and analysis based on artificial neural networks and support vector machines: A review," *Journal of Healthcare Engineering*, vol. 4, no. 4, pp. 465–504, 2013, doi: 10.1260/2040-2295.4.4.465.

[114] Q. Liu, C. Gao, Y. Zhao, S. Huang, Y. Zhang, and Z. Lu, "ECG abnormality detection Based on Multi-domain combination features and LSTM," 2023, doi: 10.1109/ICCEA58433.2023.10135380.

[115] J. Hu, W. L. Goh, and Y. Gao, "Classification of ECG Anomaly with Dynamically-biased LSTM for Continuous Cardiac Monitoring," in *Proceedings - IEEE International Symposium on Circuits and Systems*, 2023, vol. 2023-May, doi: 10.1109/ISCAS46773.2023.10181690.

[116] E. Izci, M. A. Özdemir, R. Sadighzadeh, and A. Akan, "Arrhythmia Detection on ECG Signals by Using Empirical Mode Decomposition," 2018, doi: 10.1109/TIPTEKNO.2018.8597094.

[117] K. S. Jaisinghani, "ECG-Based Heartbeat Classification using Machine Learning: Survey," *Bioscience Biotechnology Research Communications*, vol. 13, no. 14, pp. 415–418, 2020, doi: 10.21786/bbrc/13.14/94.

[118] J. Xu and J. Zhang, "An Heterogeneous Ensemble Learning based Method for ECG Classification," 2019, doi: 10.1109/IAEAC47372.2019.8997701.

[119] P. Pal and M. Mahadevappa, "Adaptive Multidimensional Dual Attentive DCNN for Detecting Cardiac Morbidities Using Fused ECG-PPG Signals," *IEEE Transactions on Artificial Intelligence*, vol. 4, no. 5, pp. 1225–1235, 2023, doi: 10.1109/TAI.2022.3184656.

[120] B. Aldughayfiq, F. Ashfaq, N. Z. Jhanjhi, and M. Humayun, "A Deep Learning Approach for Atrial Fibrillation Classification Using Multi-Feature Time Series Data from ECG and PPG," *Diagnostics*, vol. 13, no. 14, pp. 1–25, 2023, doi: 10.3390/diagnostics13142442.

[121] M. S. Ummah, *Research Methodology*, vol. 11, no. 1. 2019.

[122] L. Hoang, "Research methodology," pp. 1–41, 2005, [Online]. Available: https://www.academia.edu/8400464/RESEARCH_METHODOLOGY_For_Private_Circulation_Only.

[123] Ranjit Kumar, *Research Methodology*, 3rd ed. Sage, 2011.

[124] C.R.Kothari, *Research Methodology*, Second rev. New Age International Publishers, 2004.

[125] S. Talukder, *Mathematical Modelling and Applications of Particle Swarm Optimization*, vol. 488, no. February. 2014.

[126] A. Rosenblad, "Multivariate Statistical Methods: A Primer (4th Edition)," *Journal of Statistical Software*, vol. 78, no. Book Review 3, 2017, doi: 10.18637/jss.v078.b03.

[127] R. Adhikari K. and A. R.K., "An Introductory Study on Time Series Modeling and Forecasting Ratnadip Adhikari R. K. Agrawal," *arXiv preprint arXiv:1302.6613*, 2013.

[128] T. Bartz-Beielstein, "Hyperparameter Tuning," no. August, pp. 125–140, 2024, doi: 10.1007/978-981-99-7007-0_10.

[129] F. Hutter, *Automated Machine Learning*, vol. 19. Springer, 2017.

[130] S. Raschka, *Python_Machine_Learning_Sebastian_Raschka*, vol. 36, no. 10. 2015.

[131] A. Geron, *Hands-On Machine Learning with Scikit-Learn & tensorflow: O'Reilly Media, Inc.* 2017.

[132] N. Buduma and N. Locascio, *Fundamentals of deep learning: designing next-generation machine intelligence algorithms.* 2017.

[133] D. Y. Li Deng., "Deep Learning: Methods and Applications," *Experimental Physiology*, vol. 75, no. 2, pp. 280–281, 1990, doi: 10.1113/expphysiol.1998.sp004170.

[134] "Physionet database. [Online]. Available: www.physionet.org. [Accessed: 10-Jan-2020]." .

[135] C. J. Zhang, Yuan-Lu, F. Q. Tang, H. P. Cai, Y. F. Qian, and Chao-Wang, "Heart failure classification using deep learning to extract spatiotemporal features from ECG," *BMC Medical Informatics and Decision Making*, vol. 24, no. 1, pp. 1–18, 2024, doi: 10.1186/s12911-024-02415-4.

[136] M. S. Billah, T. B. Mahmud, F. S. Snigdha, and M. A. Arafat, "A novel method to model ECG beats using Gaussian functions," *Proceedings - 2011 4th International Conference on Biomedical Engineering and Informatics, BMEI 2011*, vol. 2, no. ii, pp. 612–616, 2011, doi: 10.1109/BMEI.2011.6098409.

[137] P. Kundu and R. Gupta, "Electrocardiogram synthesis using Gaussian and fourier models," in *Proceedings of 2015 IEEE International Conference on Research in Computational Intelligence and Communication Networks, ICRCICN 2015*, 2016, pp. 312–317, doi: 10.1109/ICRCICN.2015.7434256.

[138] S. Alam and R. Gupta, "A DPCM based Electrocardiogram coder with thresholding for real time telemonitoring applications," *International Conference on Communication and Signal Processing, ICCSP 2014 - Proceedings*, pp. 176–180, 2014, doi: 10.1109/ICCSP.2014.6949823.

[139] Patel S.Datar D. A., "ECG Data Compression using Wavelet Transform," *International Journal of Engineering Trends and Technology*, 2014, doi: 10.14445/22315381/ijett-v9p346.

[140] T. R and V. B, "A novel ECG signal compression using wavelet and discrete anamorphic stretch transforms," *Biomedical Signal Processing and Control*, vol. 71, no. PB, p. 102773, 2022, doi:

10.1016/j.bspc.2021.102773.

[141] C. K. Jha and M. H. Kolekar, "ECG data compression algorithm for tele-monitoring of cardiac patients," *International Journal of Telemedicine and Clinical Practices*, vol. 2, no. 1, p. 31, 2017, doi: 10.1504/ijtmcp.2017.10003014.

[142] G. K. S. & Hardev Singh Pal, A. Kumar, Amit Vishwakarma and Heung-No Lee, "An effective ECG signal compression algorithm with selfcontrolled reconstruction quality," *Computer Methods in Biomechanics and Biomedical Engineering*, vol. 27 (7), pp. 849–859, doi: 10.1080/10255842.2023.2206933.

[143] O. Yildirim, R. S. Tan, and U. R. Acharya, "An efficient compression of ECG signals using deep convolutional autoencoders," *Cognitive Systems Research*, vol. 52, no. July, pp. 198–211, 2018, doi: 10.1016/j.cogsys.2018.07.004.

[144] S. Banerjee and G. K. Singh, "Agent-based beat-by-beat compression of 12-lead electrocardiogram signal using adaptive Fourier decomposition," *Biomedical Signal Processing and Control*, vol. 75, no. July 2021, p. 103628, 2022, doi: 10.1016/j.bspc.2022.103628.

[145] S. Banerjee and G. K. Singh, "A new real-time lossless data compression algorithm for ECG and PPG signals," *Biomedical Signal Processing and Control*, vol. 79, no. P1, p. 104127, 2022, doi: 10.1016/j.bspc.2022.104127.

[146] Y. Chen *et al.*, "An Optimizing and Differentially Private Clustering Algorithm for Mixed Data in SDN-Based Smart Grid," *IEEE Access*, vol. 6, 2018, doi: 10.1109/ACCESS.2019.2893624.

[147] K. Padmavathi and K. Sri Ramakrishna, "Classification of ECG signal during Atrial Fibrillation using Autoregressive modeling," *Procedia Computer Science*, vol. 46, no. Icict 2014, pp. 53–59, 2015, doi: 10.1016/j.procs.2015.01.053.

[148] J. A. Gutiérrez-Gnecchi *et al.*, "DSP-based arrhythmia classification using wavelet transform and probabilistic neural network," *Biomedical Signal Processing and Control*, vol. 32, pp. 44–56, 2017, doi: 10.1016/j.bspc.2016.10.005.

[149] P. Bera and R. Gupta, "Improved Arrhythmia Detection from Electrocardiogram," *Proceedings of 2019 IEEE Region 10 Symposium, TENSYMP 2019*, pp. 547–552, 2019, doi: 10.1109/TENSYMP46218.2019.8971240.

[150] A. E. Zadeh and A. Khazaee, "High efficient system for automatic classification of the electrocardiogram beats," *Annals of Biomedical Engineering*, vol. 39, no. 3, pp. 996–1011, 2011, doi: 10.1007/s10439-010-0229-6.

[151] D. Li, J. Zhang, Q. Zhang, and X. Wei, "Classification of ECG signals based on 1D convolution neural network," *2017 IEEE 19th International Conference on e-Health Networking, Applications and Services, Healthcom 2017*, vol. 2017-Decem, pp. 1–6, 2017, doi: 10.1109/HealthCom.2017.8210784.

Review Compliance Report

Review Compliance against the advice by Prof. Jitendra Nath Bera

1. The references must appear in sequence of their serial no. But in some portions of the thesis has not been followed. For example, In section 2.1 under chapter 2,, [22] comes after [8].
Kindly check all such citations for this sort of mistakes.

Response: Complied. The reference no. from 1-21 are given in Chapter 1.

2. In page 22, it is mentioned that "Table 3. Shows the class of data available under MIMIC III database.". I think it should be Table 3.3.

Response: Complied. The Table No. has been corrected in Pg.22.

3. What is yk in equation 4.9 is not mentioned.

Response: Complied. y_k is mentioned in Pg. 42

Review Compliance against the advice by Prof. Tarikul Islam

According to his advice I have correct the spelling and grammar in following pages of final thesis. The pages are as follows:

Page No. xiii, 6, 9 – 13, 21, 22, 25, 28, 30-36, 40, 41, 52, 61,62, 64, 66 – 68, 73-75, 78 & 79.

Anumita Mitra
Signature of Candidate:

Date:

Certified by Supervisor(s):
(Signature with date, seal)

1. 10/12/2025
Professor
Electrical Engineering Department
JADAVPUR UNIVERSITY
Kolkata - 700 032

2. 10/12/25
Professor
Electrical Engg. Deptt.
Jadavpur University
Kolkata - 700 032